

172458

**PRENATAL DEVELOPMENT OF BRAIN  
IN GOATS (*Capra hircus*)**

By  
**K. M. LUCY**

**Thesis submitted in partial fulfilment of the  
requirement for the degree of**

**Doctor of Philosophy  
in  
Veterinary Anatomy**

**Faculty of Veterinary and Animal Sciences  
Kerala Agricultural University, Thrissur**

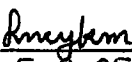
**2005**

**Department of Anatomy  
COLLEGE OF VETERINARY AND ANIMAL SCIENCES  
MANNUTHY, THRISSUR-680651  
KERALA, INDIA**

## DECLARATION

I hereby declare that the thesis entitled “**PRENATAL DEVELOPMENT OF BRAIN IN GOATS (*Capra hircus*)**” is a bonafide record of research work done by me during the course of research and that the thesis has not previously formed the basis for the award to me of any degree, diploma, fellowship, associateship or other similar title, of any other University or Society.

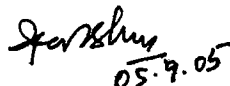
Mannuthy  
5-9-05

  
5-9-05  
K.M. LUCY  
(2000-23-01)

**CERTIFICATE**

Certified that the thesis entitled "**PRENATAL DEVELOPMENT OF BRAIN IN GOATS (*Capra hircus*)**" is a record of research work done independently by **Smt. K. M. Lucy**, under my guidance and supervision and that it has not previously formed the basis for the award of any degree, diploma, fellowship or associateship to her.

Mannuthy  
05.9.2005

  
05.9.05  
**Dr. K.R. Harshan**  
(Chairman, Advisory Committee)  
Associate Professor & Head  
Department of Anatomy  
College of Veterinary & Animal Sciences  
Mannuthy

## CERTIFICATE

We, the undersigned members of the Advisory Committee of **Smt. K.M. Lucy** (2000-23-01), a candidate for the degree of **Doctor of Philosophy in Veterinary Anatomy**, agree that the thesis entitled "**PRENATAL DEVELOPMENT OF BRAIN IN GOATS (*Capra hircus*)**" may be submitted by **Smt. K.M. Lucy**, in partial fulfilment of the requirement for the degree.

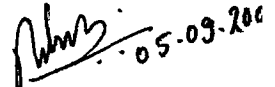


**Dr. K.R. Harshan**

(Chairman, Advisory Committee)  
Associate Professor & Head  
Department of Anatomy  
College of Veterinary & Animal Sciences  
Mannuthy



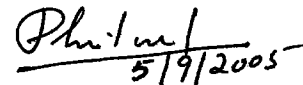
**Dr. Jose John Chungath**  
Associate Professor  
Department of Anatomy  
(Member)



**Dr. N. Ashok**  
Assistant Professor (SS)  
Department of Anatomy  
(Member)



**Dr. T. Sreekumaran**  
Professor and Head  
Department of Pathology  
(Member)



**Dr. P.T. Philomina**  
Associate Professor & Head  
Department of Physiology  
(Member)



**Dr. GEETHA RAMESH**  
External Examiner

## ACKNOWLEDGEMENTS

*I, with immense pleasure, express my deep sense of gratitude to **Dr. K.R. Harshan**, Associate Professor and Head, Department of Anatomy and Chairman of the Advisory Committee for his inspiring advice, precious guidance and constant encouragement throughout the period of the study.*

*My sincere thanks are due to **Dr. Jose John Chungath**, Associate Professor, Department of Anatomy and member of the Advisory Committee for his stable support, help and valuable suggestions offered from time to time.*

*I am deeply indebted to **Dr. N. Ashok**, Assistant Professor (SS), Department of Anatomy for his sustained encouragement, timely help and constructive suggestions as member of the Advisory Committee throughout the course of the research work.*

*I sincerely thank **Dr. T Sreekumaran**, Professor and Head, Department of Pathology and **Dr. P.T. Philomina**, Associate Professor and Head, Department of Physiology, members of the Advisory Committee, who gracefully bore the pain of critically and meticulously analysing the research work and offered valuable comments during the period of study.*

*I am pleased to express my sincere gratitude to **Dr. C. K. Sreedharan Unni**, Associate Professor, Department of Anatomy for his support and encouragement. I also appreciate the inspiration given by **Dr. Lucy Paily**, Professor and Head (retired) and **Dr. Shyla Prakash**, Assistant Professor, Department of Anatomy, during the period of my research work.*

*I wish to place on record my sincere thanks to **Dr. S. Maya**, Assistant Professor, Department of Anatomy for her remarkable co-operation, timely help and unfailing support for the completion of this work.*

*I express my extreme sense of gratitude to **Dr. E. Nanu**, Dean, College of Veterinary and Animal sciences, Mannuthy, for providing the necessary facilities to carry out this work.*

*I owe a word of sincere thanks to **Dr. P.P. Balakrishnan**, Associate Dean, College of Veterinary and Animal Sciences, Pookot for his timely support.*

*I am deeply indebted to **Dr. G. Krishnan Nair**, Associate Professor, Department of Microbiology for the unstinting help rendered in photomicrography. The help extended by **Dr. V. Jayaprakasan**, Associate Professor and Head,*

*Dr. M. Mini, Assistant Professor (SS) and Dr. Chinthu Ravisankar, Assistant Professor, Department of Microbiology, deserve special mention.*

*I am thankful to Smt. K.S. Sujatha, Assistant Professor (SG) and Head and Dr. K.A. Mercy, Assistant Professor, Department of Statistics for the valuable help offered in analysing the data.*

*I am grateful to Dr. P. Kuttinarayanan, Associate Professor and Head, Department of Livestock Products Technology, Dr. K. Devada, Assistant Professor (SS), Department of Parasitology, Dr. K.S. Anil, Assistant Professor, Department of Livestock Production and Management, Dr. A.M. Vahida, Assistant Professor, Department of Animal Reproduction, Dr. K.D. John Martin and Dr. M.K. Narayanan, Assistant Professors, Department of Surgery, Dr. K. Karthiyini, Assistant Professor, Department of Physiology and all my friends for the help rendered at various stages of the research programme.*

*The sincere help and assistance extended by Dr. S. Rajathi, Dr. K. B. Sumena, Dr. Preethy John and the staff of the Department of Anatomy are gratefully acknowledged.*

*My heartfelt appreciation goes to Smt. Rema Nair and staff of Yescom for their efforts in formatting the manuscript.*

*I am thankful to Kerala Agricultural University for granting me study leave and part-time registration for the study.*

*Finally, I express my deep sense of indebtedness to my parents, husband and children for their constant encouragement and earnest help for the successful completion of this work.*

*Above all, I thank God for His guidance and blessings.*

Mannuthy

K. M. Lucy

**CONTENTS**

---

| <b>Chapter No.</b> | <b>Title</b>          | <b>Page No.</b> |
|--------------------|-----------------------|-----------------|
| 1.                 | INTRODUCTION          | 1               |
| 2.                 | REVIEW OF LITERATURE  | 3               |
| 3.                 | MATERIALS AND METHODS | 52              |
| 4.                 | RESULTS               | 58              |
| 5.                 | DISCUSSION            | 252             |
| 6.                 | SUMMARY               | 327             |
|                    | REFERENCES            | 338             |

---

## LIST OF TABLES

| Table No. | Title  | Page No. |
|-----------|--|----------|
| 1.        | Body weight, age and straight CRL of goat foetuses at different stages of gestation                        | 123      |
| 2.        | Age, body weight, straight CRL and number of goat foetuses used for the study                              | 125      |
| 3.        | Micrometrical parameters of telencephalon in the first month of gestation in goat foetuses, $\mu\text{m}$  | 126      |
| 4.        | Micrometrical parameters of diencephalon in the first month of gestation in goat foetuses, $\mu\text{m}$   | 127      |
| 5.        | Micrometrical parameters of mesencephalon in the first month of gestation in goat foetuses, $\mu\text{m}$  | 128      |
| 6.        | Micrometrical parameters of metencephalon in the first month of gestation in goat foetuses, $\mu\text{m}$  | 129      |
| 7.        | Micrometrical parameters of myelencephalon in the first month of gestation in goat foetuses, $\mu\text{m}$ | 130      |
| 8.        | Correlation and regression coefficients of brain vesicle parameters in the first month of gestation        | 131      |
| 9.        | Body parameters of goat foetuses at different ages   | 132      |
| 10.       | Head parameters of goat foetuses at different ages   | 134      |
| 11.       | Skull parameters of goat foetuses at different ages  | 135      |
| 12.       | Craniometry of goat foetuses at different ages, cm   | 136      |
| 13.       | Encephalometry of goat foetuses at different ages  | 137      |
| 14.       | Measurements of cerebral hemispheres of goat foetuses at different ages, cm                                | 139      |
| 15.       | Measurements of cerebellum of goat foetuses at different ages  | 141      |
| 16.       | Measurements of diencephalon of goat foetuses at different ages  | 142      |
| 17.       | Measurements of mesencephalon of goat foetuses at different ages   | 143      |
| 18.       | Measurements of pons of goat foetuses at different ages  | 144      |



| Table No. | Title  | Page No. |
|-----------|--|----------|
| 19.       | Measurements of medulla oblongata (MO) of goat foetuses at different ages  | 145      |
| 20.       | Measurements of ventricles of brain of goat foetuses at different ages   | 146      |
| 21.       | Length of some of the cerebral fissures in goat foetuses during fourth and fifth months of gestation                             | 148      |
| 22.       | Micrometrical parameters of cerebral wall of goat foetuses during second, third and fourth months of gestation, $\mu\text{m}$    | 149      |
| 23.       | Micrometrical parameters of cerebral hemispheres of goat foetuses in the fifth month of gestation, $\mu\text{m}$                 | 150      |
| 24.       | Micrometrical parameters of basal nuclei at different ages in goat foetuses, $\mu\text{m}$                                       | 151      |
| 25.       | Micrometrical parameters of cerebellar folia in goat foetuses at different ages, $\mu\text{m}$                                   | 152      |
| 26.       | Micrometrical parameters of diencephalon of goat foetuses at different ages, $\mu\text{m}$                                       | 153      |
| 27.       | Micrometrical parameters of mesencephalon of goat foetuses at different ages, $\mu\text{m}$                                      | 154      |
| 28.       | Micrometrical parameters of choroid plexus epithelium in the ventricles of brain at different stages of gestation, $\mu\text{m}$ | 155      |
| 29.       | Correlation coefficients (r) of whole brain parameters on body parameters  | 156      |
| 30.       | Correlation coefficients (r) of head parameters on selected brain and body parameters  | 157      |
| 31.       | Correlation coefficients (r) of skull parameters on selected brain and body parameters   | 158      |
| 32.       | Correlation coefficients (r) of parameters of bones forming the roof of the skull on those forming the base                      | 159      |
| 33.       | Correlation coefficients (r) of craniometric parameters on whole brain parameters  | 160      |
| 34.       | Correlation coefficients (r) of encephalometric parameters on body weight, age and CRL (straight)                                | 161      |

| Table No. | Title  | Page No. |
|-----------|--|----------|
| 35.       | Correlation coefficients (r) of craniometric parameters on encephalometric parameters  | 162      |
| 36.       | Correlation coefficients (r) of cerebral parameters on selected whole brain parameters and body parameters                           | 163      |
| 37.       | Correlation coefficients (r) of cerebellar parameters on selected whole brain and body parameters                                    | 164      |
| 38.       | Correlation coefficients (r) of brainstem and diencephalic parameters on selected whole brain and body parameters                    | 165      |
| 39.       | Correlation coefficients (r) of mesencephalic parameters on selected whole brain, body and brainstem parameters                      | 166      |
| 40.       | Correlation coefficients (r) of parameters of pons and medulla oblongata (MO) on selected whole brain, body and brainstem parameters | 167      |
| 41.       | Regression coefficients of brain parameters on body and skull parameters of goat fetuses   | 168      |
| 42.       | Regression coefficients of individual values among brain parameters  | 169      |
| 43.       | Regression equations for prediction of unknown brain parameters in goat fetuses  | 170      |

## LIST OF FIGURES

| Figure No. | Title   | Page No. |
|------------|---|----------|
| 1.         | C.S. of the telencephalon (24 days of gestation). H&E. x 100  | 171      |
| 2.         | C.S. of the neural tube wall at the junction between telencephalon and diencephalon (27 days). H&E. x 100               | 171      |
| 3.         | C.S. of the telencephalon (27 days). H&E. x 100   | 171      |
| 4.         | C.S. of the cephalic end of goat embryo at the cephalic end of telencephalon (24 days). H&E. x 100                      | 172      |
| 5.         | C.S. of the cephalic end of goat embryo at the level of telencephalon showing open olfactory pits (24 days). H&E. x 100 | 172      |
| 6.         | C.S. of the diencephalon (26 days). H&E. x 100  | 172      |
| 7.         | C.S. of the neural tube at the junction between telencephalon and diencephalon (27 days). H&E. x 100                    | 173      |
| 8.         | Section of the diencephalon at the level of Rathke's pouch (27 days). H&E. x 100  | 173      |
| 9.         | C.S. of the neural tube at the level of optic cup (27 days). H&E. x 100   | 173      |
| 10.        | C.S. of the optic cup (26 days). H&E. x 100   | 174      |
| 11.        | C.S. of the dorsal half of mesencephalon (26 days). H&E. x 100  | 174      |
| 12.        | C.S. of the ventral half of the mesencephalon (26 days). H&E. x 100   | 174      |
| 13.        | Frontal section of the metencephalon (24 days). H&E. x 100  | 175      |
| 14.        | C.S. of the metencephalon (27 days). H&E. x 100   | 175      |
| 15.        | C.S. of the metencephalon (27 days). H&E. x 100   | 175      |
| 16.        | C.S. of the semilunar ganglion (24 days). H&E. x 100  | 176      |
| 17.        | C.S. of the cephalic end of the goat embryo at the level of otocyst (27 days). H&E. 100                                 | 176      |
| 18.        | C.S. of the hind brain at the level of facial nerve (27 days). H&E. x 100   | 176      |
| 19.        | C.S. of the cephalic part of goat foetus showing ganglia and nerves in the mesenchyme (27 days). H&E. x 100             | 177.     |

| Figure No. | Title  | Page No. |
|------------|--|----------|
| 20.        | L.S. of the myelencephalon (24 days). H&E. x 100                                     | 177      |
| 21.        | Section of goat foetus through myelencephalon and pharynx (26 days). H&E. x 100      | 177      |
| 22.        | C.S. of the myelencephalon (24 days). H&E. x 100                                     | 178      |
| 23.        | C.S. of the myelencephalon (26 days). H&E. x 100                                     | 178      |
| 24.        | C.S. of the myelencephalon (27 days). H&E. x 100                                     | 178      |
| 25.        | C.S. of the wall of telencephalon (24 days). H&E. x 100                              | 179      |
| 26.        | C.S. of the telencephalic wall showing a blood channel (24 days). H&E. x 100         | 179      |
| 27.        | C.S. of the wall of telencephalon (27 days). H&E. x 400                              | 179      |
| 28.        | C.S. of the wall of telencephalon (26 days). H&E. x 400                              | 180      |
| 29.        | C.S. of the metencephalic floor (26 days). H&E. x 100                                | 180      |
| 30.        | C.S. of the telencephalon showing double layer of pia mater (27 days). H&E. x 100    | 180      |
| 31.        | L.S. of the cephalic end of the embryo showing pontine flexure (40 days). H&E. x 100 | 181      |
| 32.        | Relation between body weight and age   | 181      |
| 33.        | Relation between age and body parameters   | 181      |
| 34.        | Relation between age and brain weight  | 182      |
| 35.        | Relation between age and brain parameters  | 182      |
| 36.        | Relation between age and weight of cerebrum, cerebellum and brainstem                | 182      |
| 37.        | Relation between age and parameters of right cerebral hemisphere                     | 183      |
| 38.        | Relation between age and parameters of left cerebral hemisphere                      | 183      |
| 39.        | Relation between age and cerebellar parameters                                       | 183      |
| 40.        | Relation between age and weight of brainstem components                              | 184      |
| 41.        | Relation between body weight and brain weight  | 184      |

| Figure No. | Title   | Page No. |
|------------|---|----------|
| 42.        | Relation between body weight and brain parameters   | 184      |
| 43.        | Relation between body weight and weights of cerebrum, cerebellum and brainstem  | 185      |
| 44.        | Relation between body weight and parameters right cerebral hemisphere   | 185      |
| 45.        | Relation between body weight and parameters of left cerebral hemisphere   | 185      |
| 46.        | Relation between body weight and cerebellar parameters  | 186      |
| 47.        | Relation between body weight and weight of brainstem components   | 186      |
| 48.        | Relation between CRL (straight) and brain weight  | 186      |
| 49.        | Relation between age and head parameters  | 187      |
| 50.        | Relation between age and parameters of head and body at different stages of gestation   | 187      |
| 51.        | Percentage contributions of brain components to the total brain weight during gestation   | 187      |
| 52.        | Mean length, width and thickness of whole brain(B), cerebrum (C), cerebellum (Ce) and brainstem (BS) at different stages of gestation | 188      |
| 53.        | Percentage contributions of components of brainstem to the total brainstem weight during gestation                                    | 189      |
| 54.        | Comparison between weight of left and right cerebral hemispheres during gestation   | 189      |
| 55.        | Comparison between skull parameters at different stages of gestation  | 189      |
| 56.        | Comparison between cranial height and brain thickness during gestation  | 190      |
| 57.        | Comparison between brain length and length of skull bones during gestation  | 190      |
| 58.        | Dorsal surface of the brain (55 days)   | 191      |
| 59.        | C.S. of the cerebral hemisphere showing the lateral ventricle (48 days). H&E. x 100   | 191      |
| 60.        | C.S. of the cerebrum and diencephalon (48 days). H&E. x 100   | 191      |
| 61.        | C.S. of the cerebrum (48 days). H&E. x 100  | 192      |

| <b>Figure No.</b> | <b>Title</b>   | <b>Page No.</b> |
|-------------------|--|-----------------|
| 62.               | Ventral surface of brain showing Sylvian sulcus (69 days)  | 192             |
| 63.               | C.S. of cerebrum showing the hippocampal fissure (81 days). H&E. x 100   | 192             |
| 64.               | Dorsal surface of brain showing developing sulci on the cerebral surface (76 days)                                   | 193             |
| 65.               | Ventral surface of brain showing circle of Willis (76 days)  | 193             |
| 66.               | Dorsal surface of brain (83 days)  | 193             |
| 67.               | Dorsal surface of the brain showing developing sulci on the cerebral surface (93 days)                               | 194             |
| 68.               | Dorsal surface of brain (124 days)   | 194             |
| 69.               | Lateral view of cerebral hemisphere (124 days)   | 194             |
| 70.               | Medial surface of cerebral hemisphere (124 days)   | 195             |
| 71.               | Dorsal surface of foetal brain (full term)   | 195             |
| 72.               | C.S. of the cerebrum and diencephalon showing caudate nucleus (48 days). H&E. x 100                                  | 195             |
| 73.               | C.S. of the brain showing septum pellucidum and thalamus (58 days). H&E. x 100                                       | 196             |
| 74.               | C.S. of the cerebral hemispheres showing the thin medial walls of both sides (48 days). H&E. x 100                   | 196             |
| 75.               | C.S. of the lateral cerebral wall showing cortical migration of cells (48 days). H&E. x 100                          | 196             |
| 76.               | C.S. of the cerebral wall showing wavy lines of migrating neuroblasts through the white matter (58 days). H&E. x 100 | 197             |
| 77.               | C.S. of the lateral cerebral wall showing different layers (58 days). H&E. x 100                                     | 197             |
| 78.               | C.S. of the cerebral wall showing stratification of cerebral cortex (76 days). H&E. x 100                            | 197             |

| <b>Figure No.</b> | <b>Title</b>   | <b>Page No.</b> |
|-------------------|--|-----------------|
| 79.               | White matter of the cerebrum (76 days). H&E. x 400   | 198             |
| 80.               | C.S. of the cerebrum showing choroid plexus in the lateral ventricle (61 days). H&E. x 100                       | 198             |
| 81.               | C.S. of the corpus callosum forming the roof of the lateral ventricle (61 days). H&E. x 100                      | 198             |
| 82.               | C.S. of the cerebral cortex (101 days). H&E. x 100   | 199             |
| 83.               | T.S. of the cerebral cortex showing layers of cerebral cortex at the bottom of the sulcus (124 days). H&E. x 100 | 199             |
| 84.               | T.S. of the cerebral cortex showing layers of cerebral cortex on the top of the gyrus (144 days). H&E. x 100     | 199             |
| 85.               | T.S. of the cerebral cortex showing the superficial layers (144 days). H&E. x 400                                | 200             |
| 86.               | T.S. of the cerebral cortex showing external pyramidal layer (144 days). H&E. x 400                              | 200             |
| 87.               | T.S. of the cerebral cortex showing deeper layers of cerebral cortex (144 days). H&E. x 400                      | 200             |
| 88.               | T.S. of the cerebral cortex showing inner layers of cerebral cortex and white matter (144 days). H&E. x 100      | 201             |
| 89.               | White matter of the cerebrum (144 days). H&E. x 400  | 201             |
| 90.               | T.S. of the cerebral cortex showing corpus callosum (144 days). H&E. x 100                                       | 201             |
| 91.               | L.S. of the olfactory bulb and the cerebrum (48 days). H&E. x 100  | 202             |
| 92.               | L.S. of the olfactory bulb and olfactory nerve fibres (48 days). H&E. x 100                                      | 202             |
| 93.               | Section of the olfactory peduncle (81 days). H&E. x 100  | 202             |
| 94.               | Section of the lateral olfactory stria (81 days). H&E. x 100   | 203             |
| 95.               | Ventral surface of the brain (101 days)  | 203             |
| 96.               | Ventral surface of the brain (Full term)   | 203             |

| <b>Figure No.</b> | <b>Title</b>   | <b>Page No.</b> |
|-------------------|--|-----------------|
| 97.               | L.S. of the olfactory bulb (144 days). H&E. 100  | 204             |
| 98.               | L.S. of the hippocampus (48 days). H&E. x 100  | 204             |
| 99.               | C.S. of the fimbria and thalamus (62 days). H&E. x 100   | 204             |
| 100.              | Layers of the hippocampus (48 days). H&E. x 400  | 205             |
| 101.              | C.S. of the fimbria and thalamus (58 days). H&E. x 100   | 205             |
| 102.              | C.S. of the hippocampus (144 days). H&E. x 100   | 205             |
| 103.              | C.S. of the hippocampus showing stratum pyramidale (144 days).<br>H&E. x 400                                     | 206             |
| 104.              | C.S. of the hippocampus through the superior fold (144 days).<br>H&E. x 100                                      | 206             |
| 105.              | C.S. of the hippocampus through the dentate gyrus (124 days).<br>H&E. x 400                                      | 206             |
| 106.              | C.S. of the hippocampus through the dentate gyrus (124 days).<br>H&E. x 100                                      | 207             |
| 107.              | C.S. of the hippocampus showing fimbria (144 days). H&E. x 100   | 207             |
| 108.              | C.S. of the corpus striatum (58 days). H&E. x 100  | 207             |
| 109.              | C.S. of the basal nuclei (48 days). H&E. x 100   | 208             |
| 110.              | C.S. of the caudate nucleus and internal capsule (76 days). H&E. x 100   | 208             |
| 111.              | C.S. of the putamen, external capsule and insular cortex (62 days).<br>H&E. x 100                                | 208             |
| 112.              | T.S. of the corpus striatum showing the junction between internal and<br>external capsule (144 days). H&E. x 100 | 209             |
| 113.              | T.S. of the basal nuclei showing claustrum, extreme capsule and<br>amygdaloid body (144 days). H&E. x 100        | 209             |
| 114.              | C.S. of the caudate nucleus (58 days). H&E. x 400  | 209             |
| 115.              | C.S. of the caudate nucleus (144 days). H&E. x 400   | 210             |



| <b>Figure No.</b> | <b>Title</b>  | <b>Page No.</b> |
|-------------------|---|-----------------|
| 116.              | C.S. of the globus pallidus (144 days) H&E. x 100   | 210             |
| 117.              | C.S. of the putamen (144 days). H&E. x 100  | 210             |
| 118.              | C.S. of the cerebellum (48 days). H&E. x 100  | 211             |
| 119.              | C.S. of the medulla oblongata at the level of rostral medullary velum (48 days). H&E. x 100                                   | 211             |
| 120.              | C.S. of the medulla oblongata showing caudal medullary velum and choroid plexus of the fourth ventricle (48 days). H&E. x 100 | 211             |
| 121.              | C.S. of the cerebellum showing the vermis and lateral hemisphere (58 days). H&E. x 100  | 212             |
| 122.              | T.S. of the cerebellar folium (62 days). H&E. x 100   | 212             |
| 123.              | Midsagittal section of the brain (Full term foetus)   | 212             |
| 124.              | C.S. of the cerebellum showing external granular layer and primitive Purkinje cells (58 days). H&E. x 400                     | 213             |
| 125.              | L.S. of the metencephalon showing layers of dura mater (48 days). H&E. x 100  | 213             |
| 126.              | C.S. of the cerebellum and fourth ventricle (48 days). H&E. x 100   | 213             |
| 127.              | Neurons of the deep cerebellar nucleus (76 days). H&E. x 400  | 214             |
| 128.              | L.S. of the cerebellar folium (101 days). Sevier-Munger silver impregnation method x 100                                      | 214             |
| 129.              | C.S. of the cerebellum showing layers of the cerebellar cortex (101 days). H&E. x 400   | 214             |
| 130.              | Sagittal section of cerebellum (124 days). H&E. x 100   | 215             |
| 131.              | Section of the cerebellar folium (144 days). H&E. x 100   | 215             |
| 132.              | L.S. of the cerebellar folium (124 days). PTAH. X 400   | 215             |
| 133.              | L.S. of the cerebellar folium (124 days). H&E. x 400  | 216             |
| 134.              | L.S. of the cerebellar folium (144 days). PTAH. X 400   | 216             |
| 135.              | L.S. of the cerebellar folium (144 days). H&E. x 400  | 216             |

| Figure No. | Title   | Page No. |
|------------|---|----------|
| 136.       | Section of cerebellar folium (144 days). Holme's silver nitrate luxol fast blue method x 400    | 217      |
| 137.       | Section of cerebellar folium (144 days). H&E. x 400   | 217      |
| 138.       | C.S. of the thalamus showing third ventricle and massa intermedia (48 days). H&E. x 100         | 217      |
| 139.       | C.S. through the dorsal portion of third ventricle showing choroid plexus (58 days). H&E. x 100 | 218      |
| 140.       | L.S. of the diencephalons and mesencephalon showing pineal evagination (48 days). H&E. x 100    | 218      |
| 141.       | C.S. of the hypothalamus showing trough-like floor (58 days). H&E. x 100                        | 218      |
| 142.       | C.S. of the hypothalamus and pituitary (48 days). H&E. x 100                                    | 219      |
| 143.       | L.S. of the hypothalamus and pituitary (48 days). H&E. x 100                                    | 219      |
| 144.       | C.S. of the hypothalamus showing optic chiasma and optic nerve (48 days).                       | 219      |
| 145.       | C.S. of the optic nerve emerging through the optic foramen (48 days). H&E. x 100                | 220      |
| 146.       | Section of hypothalamus showing optic recess of third ventricle (48 days). H&E. x 100           | 220      |
| 147.       | C.S. of optic chiasma and supraoptic nucleus (58 days). H&E. x 100                              | 220      |
| 148.       | Choroid plexus of the fourth ventricle (80 days). Best's carmine x 100                          | 221      |
| 149.       | Dorsal view of the brainstem (124 days)   | 221      |
| 150.       | L.S. of thalamus showing internal capsule (48 days). H&E. x 100                                 | 221      |
| 151.       | C.S. of the eye ball (48 days). H&E. x 100  | 222      |
| 152.       | C.S. of eye ball showing cornea sclera, lens and retina (48 days). H&E. x 100                   | 222      |
| 153.       | C.S. of the subcommissural organ lined by tanocytes (58 days). H&E. x 100                       | 222      |

| Figure No. | Title   | Page No. |
|------------|---|----------|
| 154.       | Neuronal aggregations in the thalamus (62 days). H&E. x 100   | 223      |
| 155.       | C.S.of the thalamus showing ciliated ependymal cells lining the third ventricle (76 days). H&E. x 400 | 223      |
| 156.       | C.S.of the pineal gland (76 days). H&E. x 100   | 223      |
| 157.       | C.S.of the pineal gland showing pinealocytes and glial cells (76 days). H&E. x 400                    | 224      |
| 158.       | C.S.of the hypothalamus showing the trough-like floor (81 days). H&E. x 100                           | 224      |
| 159.       | C.S.of the hypothalamus showing optic tract and supraoptic nucleus (81 days). H&E. 100                | 224      |
| 160.       | C.S.of the posterior commissure showing subcommissural organ (76 days). H&E. x 100                    | 225      |
| 161.       | C.S.of the diencephalon showing two parts of supraoptic nucleus (101 days). H&E. x 100                | 225      |
| 162.       | C.S.of the supraoptic nucleus of hypothalamus (101 days). H&E. x 400                                  | 225      |
| 163.       | C.S.of the thalamus showing anterior nucleus (144 days). H&E. x 100                                   | 226      |
| 164.       | C.S.of the thalamus showing dorsomedial nucleus (144 days). H&E. x 100                                | 226      |
| 165.       | C.S.of the thalamus showing reticular nucleus (144 days). H&E. x 100                                  | 226      |
| 166.       | C.S.of the hypothalamus showing mamillothalamic tract (144 days). x 100                               | 227      |
| 167.       | C.S.of the hypothalamic nucleus showing supraoptic nucleus (144 days). H&E. x 100                     | 227      |
| 168.       | C.S.of the pineal gland (144 days). H&E. x 100  | 227      |
| 169.       | C.S.of the pineal gland (144 days). x 400   | 228      |
| 170.       | L.S.of the mesencephalon (48 days). H&E. x 100  | 228      |
| 171.       | C.S.of the aqueduct of Sylvius (76 days). H&E. x 100  | 228      |

| Figure No. | Title  | Page No. |
|------------|--|----------|
| 172.       | C.S.of the aqueduct showing pseudostratified ciliated ependymal cells (76 days). H&E. x 400  | 229      |
| 173.       | C.S.of the mesencephalon showing mesencephalic nuclei of trigeminal nerve (81 days). H&E. x 100  | 229      |
| 174.       | C.S.of the red nucleus (76 days). H&E. x 400   | 229      |
| 175.       | C.S.of the red nucleus showing magnocellular part (81 days). H&E. x 400  | 230      |
| 176.       | C.S.of the red nucleus showing parvocellular part (81 days). H&E. x 400  | 230      |
| 177.       | C.S.of the red nucleus showing the oculomotor nerve traversing through it (81 days). Holme's silver nitrate luxol fast blue method x 400 | 230      |
| 178.       | C.S.of the crura cerebri showing the substantia nigra (81 days). H&E. x 100  | 231      |
| 179.       | C.S.of the tegmentum of mesencephalon showing mesencephalic nucleus of trigeminal nerve (101 days). H&E. x 400                           | 231      |
| 180.       | C.S.of the red nucleus showing large multipolar neurons (101 days). H&E. x 400   | 231      |
| 181.       | C.S.of the mesencephalon (144 days). H&E. x 100  | 232      |
| 182.       | C.S.of the rostral colliculus (144 days). H&E. x 100   | 232      |
| 183.       | C.S.of the mesencephalic tegmentum showing red nucleus (144 days). H&E. x 100  | 232      |
| 184.       | C.S.of the mesencephalic tegmentum showing interpeduncular nucleus (144 days) x 100  | 233      |
| 185.       | C.S.of the mesencephalon showing corticospinal tract (144 days). H&E. x 100  | 233      |
| 186.       | L.S.of the pons showing the emergence of trigeminal nerve and semilunar ganglion (48 days). H&E. x 100                                   | 233      |
| 187.       | C.S.of the pons showing the sulcus limitans (76 days). H&E. x 100  | 234      |

| Figure No. | Title   | Page No. |
|------------|---|----------|
| 188.       | C.S.of the pons showing trigeminal nerve fibres emerging from lateral aspect (81 days). Holme's silver nitrate luxol fast blue method x 100 | 234      |
| 189.       | C.S.of the pons showing pontine nucleus (48 days). H&E. x 100   | 234      |
| 190.       | C.S.of the pons showing migrating alar plate neurons (48 days). H&E. x 100  | 235      |
| 191.       | C.S.of the pons showing a multipolar motor neuron of trigeminal nerve (76 days). H&E. x 400   | 235      |
| 192.       | C.S.of the ventral portion of the pons showing the pontine nuclei (81 days). H&E. x 100   | 235      |
| 193.       | C.S.of the pons showing pontine nuclei (144 days). H&E. x 100   | 236      |
| 194.       | C.S.of the pons showing median raphe (144 days). H&E. x 100   | 236      |
| 195.       | C.S.of the medulla oblongata showing trapezoid body and reticular formation (48 days). H&E. x 100 .   | 236      |
| 196.       | C.S.of the medulla oblongata showing the facial nerve and endolymph duct (48 days). H&E. x 100  | 237      |
| 197.       | Choroid plexus of fourth ventricle (40 days). H&E. x 400  | 237      |
| 198.       | L.S.of the medulla oblongata showing the fourth ventricle and circumventricular organ (48 days). H&E. x 100                                 | 237      |
| 199.       | C.S.of the medulla oblongata showing medullary pyramids (81 days). H&E. x 100   | 238      |
| 200.       | C.S.of the medulla oblongata showing foramen of Lushcka and caudal medullary velum (76 days). H&E. x 100                                    | 238      |
| 201.       | C.S.of the caudal part of medulla oblongata (76 days). H&E. x 100   | 238      |
| 202.       | C.S.of the reticular formation of medulla oblongata showing a large neuron of nucleus reticularis gigantocellularis (81 days). H&E. x 400   | 239      |
| 203.       | C.S.of the medulla oblongata showing single layered ependyma (101 days). H&E. x 400   | 239      |
| 204.       | C.S.of the medulla oblongata showing chief olivary nucleus (101 days). H&E. x 100   | 239      |

| <b>Figure No.</b> | <b>Title</b>  | <b>Page No.</b> |
|-------------------|---|-----------------|
| 205.              | C.S.of the mesencephalon (101 days). PTAH. x 400  | 240             |
| 206.              | C.S.of the medulla oblongata showing vagal nucleus and vagus nerve (144 days). H&E. x 100   | 240             |
| 207.              | C.S.of the medulla oblongata showing hypoglossal nerve (144 days). H&E. x 100   | 240             |
| 208.              | Mean length, width and height of Lateral Ventricle (LV), Third Ventricle (IIIv), Aqueduct of Sylvius (AS) and Fourth Ventricle (4th V) at different stages of gestation | 241             |
| 209.              | Section of the brain showing choroid fissure and the stalk of choroid plexus of lateral ventricle (48 days). H&E. x 100   | 242             |
| 210.              | Stalk portion of the choroid plexus of lateral ventricle (48 days). H&E. x 400  | 242             |
| 211.              | Choroid plexus of lateral ventricle (48 days). H&E. x 400   | 242             |
| 212.              | T.S.of the brainstem through the fourth ventricle (48 days). H&E. x 100   | 243             |
| 213.              | T.S.of the brainstem through the fourth ventricle (76 days). H&E. x 100   | 243             |
| 214.              | Choroid plexus of the lateral ventricle (76 days). H&E. x 100   | 243             |
| 215.              | Choroid plexus of the lateral ventricle (80 days). Sevier-Munger silver impregnation method x 100   | 244             |
| 216.              | Section of the medulla oblongata (48days). H&E. x 400   | 244             |
| 217.              | Section of the semilunar ganglion (76 days). H&E. x 400   | 244             |
| 218.              | C.S. of the mesencephalon showing corticospinal tract (144 days). Holme's silver nitrate luxol fast blue method x 400   | 245             |
| 219.              | Ependymal lining of lateral ventricle (124 days). Best's carmine method x 400   | 245             |
| 220.              | C.S. of the medullary reticular formation (144 days). Holme's silver nitrate luxol fast blue method x 100   | 245             |
| 221.              | L.S. of cerebellum showing glial cells (101 days). PTAH. x 400  | 246             |
| 222.              | Section of the cerebrum showing glial cells in the subependymal region (144 days). H&E. x 400   | 246             |

| <b>Figure No.</b> | <b>Title</b>  | <b>Page No.</b> |
|-------------------|---|-----------------|
| 223.              | Section through the meninges (58 days). H&E. x 100  | 246             |
| 224.              | C.S. of the cranial vault showing venous sinus of the cranial dura (58 days). H&E. x 100          | 247             |
| 225.              | Section through the meninges (58 days). Aldehyde-thionine PAS method x 100                        | 247             |
| 226.              | Section through the meninges and cerebral cortex (144 days). H&E. x 100                           | 247             |
| 227.              | Section through the meninges and cerebral cortex (124 days). H&E. x 100                           | 248             |
| 228.              | Section of cerebral cortex showing pia mater extending into the sulcus (124 days). H&E. x 100     | 248             |
| 229.              | Section of cerebellum showing myelination of the white matter (Full term). Oil Red O method x 100 | 248             |
| 230.              | L.S. of the pineal gland (Full term). Oil Red O method x 100                                      | 249             |
| 231.              | L.S. of the habenular commissure and pineal gland (Full term). Oil Red O method x 100             | 249             |
| 232.              | Section of the cerebral cortex (144 days). PAS. x 100   | 249             |
| 233.              | C.S. of the cerebral cortex (Full term). Gomori's method for alkaline phosphatase x 100           | 250             |
| 234.              | Sagittal section of cerebellum (Full term). Gomori's method for alkaline phosphatase x 100        | 250             |
| 235.              | Section of cerebral cortex (Full term). Gomori's method for alkaline phosphatase x 100            | 250             |
| 236.              | Sagittal section of cerebellum (Full term). Gomori's method for acid phosphatase x 400            | 251             |
| 237.              | Sagittal section of cerebellum (Full term). Gomori's method for acid phosphatase x 400            | 251             |
| 238.              | L.S. of pineal gland (Full term). Gomori's method for acid phosphatase x 400                      | 251             |

# *Introduction*

---



# 1. INTRODUCTION

Nervous system is a highly differentiated and the most complex system in the body and is the first to begin and the last to complete its development. The survival of an organism depends on its ability to adapt successfully to the environment. Active neuronal integration plays the primary role in adaptation. Depending on the type of adaptation to the environment, specific anatomic peculiarities are observed in the nervous system of different species of animals.

Brain and spinal cord, comprising the central nervous system, develop from an elongated and thickened portion of ectoderm called the neural plate. This appears at the late presomite stage of the embryo in the mid-dorsal region. The plate invaginates along its long axis until the neural folds fuse over the neural groove to form a neural tube. Rapid unequal growth of the cephalic end of the neural tube results in the formation of three brain vesicles, which subsequently give rise to five secondary vesicles. Further differentiation involves extensive thickening of the walls and evagination or invagination in various locations until the brain takes its definitive shape.

Embryonic pattern is the blue print for understanding the structure of the adult brain. The most characteristic feature of mammalian brain is the large size of the forebrain. The brain of goat provides an excellent example of the highly developed type of mammalian brain. Cerebral gyri appear to have evolved independently in different mammalian lineages, and there is no general model of gyrogenesis. Different species arrived at a gyral configuration in different ways and foldings have been related to various patterns of organisational changes within the evolving nervous systems (Jenkins, 1978).

Foetal brain is most vulnerable during the period of rapid growth. The spectacular growth spurt of brain is interesting in its teratological implications. A comprehension of the cellular mechanisms has significant importance in the understanding of the neural tube defects.

Goats, by virtue of their size and reproductive efficiency have biological as well as managerial advantage over other farm animals. Brain disorders due to cysts and tumors have been frequently reported in Indian goats (Sharma *et al.*, 1978). Polioencephalomalacia or cerebrocortical necrosis is a neurodegenerative disease in

goats, which leads to serious economic losses to farmers. Animals having good ability for movement in more than one plane have a large cerebellum (Mc Intosh *et al.*, 1979). Normal cerebellum: brain ratio can be used to assess cases of suspected cerebellar hypoplasia.

Managemental and environmental factors affect the brain development to a great extent. Since brain grows at a much faster rate than the body, its growth rate depends critically on the proper supply of nutrients; deficiencies during the period of growth can cause permanent damage.

The relative maturity of the brain in goats at birth justifies the classification of goat along with the sheep as a prenatal brain developer. In most part of the brain, the full complement of neurons is established at birth itself (Mc Intosh *et al.*, 1979). The study of anatomical organisation of brain in goat may be of great value in investigating varied functional entities including the neuroendocrinological role of the organ in the species.

Though extensive research has been done on mammalian brain, information regarding the developmental aspects of the organ in ruminants is scanty. Therefore, a comprehensive study on the histomorphogenesis of the brain in goats seems to be a relevant area of research. It is contributory to the existing anatomical knowledge and will form a basis for further physiological, pathological and neuroendocrinological studies. Hence, the present study was undertaken with the following objectives:

1. To trace the morphogenesis and histogenesis of the brain in goats at different stages of prenatal life.
2. To study the morphology, topography and cytoarchitecture of anatomical divisions of brain, viz., cerebrum, cerebellum and brainstem.
3. To determine the relationship if any, between the size of the cranium and the brain.
4. To establish a standard to compare normal and abnormal brain development.

# *Review of Literature*

---

## 2. REVIEW OF LITERATURE

Neurulation in vertebrates involves thickening of the dorsal ectoderm into a neural plate, elevation of margins of the neural plate as neural folds on either side of a neural groove and fusion of the neural folds to form a neural tube. Neural tube formed the primordium for the whole central nervous system (CNS). Excepting few neuroglial components and the dura mater, the nervous system as a whole developed from the ectoderm (Ghosh, 2002).

### 2.1 DEVELOPMENT OF THE NEURAL TUBE

Major morphogenetic event in the development of CNS was the transformation of the neural plate into the neural tube. Soon after the three embryonic germ layers were established, the ectoderm began to thicken in the area of the future embryo as the first indication of CNS. This thickened area of ectoderm; the neural plate appeared at three weeks of gestation in human embryos (Arey, 1957) and at ten days in pig embryos (Wischnitzer, 1975). At first, the neural plate was flat and single layered, but it rapidly became thick and stratified. The plate folded into a neural groove by the time somites appeared and its lateral edges soon became elevated to form the neural folds. With further development, the neural folds approached each other in the midline, and finally fused to form the neural tube. The fusion began in the cervical region and proceeded in an irregular fashion in cephalic and caudal directions. In pig embryos, the neural plate started to transform into neural tube at about 14 days of gestation. At about the 16<sup>th</sup> day, the primordia of the eyes and ears appeared in the form of optic protuberances and otic pits, respectively (Wischnitzer, 1975).

Geelen and Langman (1977) reported that in mouse embryos of nine to twenty somites, first closure of the neural groove occurred in the cervical region. The fusion process gradually proceeded in rhombencephalic direction until it reached a level just caudal to the otic pits. Shortly afterwards, the prosencephalic walls fused together independent of the rhombencephalic closure. This prosencephalic fusion process proceeded caudally in the direction of the mesencephalon until it reached the rostral portion of the rhombencephalon. Anterior neuropore was the last part of the brain vesicles to close.

Dyce *et al.* (1996) stated that in vertebrates, even before the neural plate became a closed tube, its anterior end had expanded considerably in preparation for the development of the brain. At the cranial and caudal ends of the embryo, the neuropores temporarily formed open connections between the lumen of the neural tube and the amniotic cavity, and for a short period amniotic fluid circulated through the lumen to nourish the cells of the tube (Ghosh, 2002). Sadler (2004) reported that the signals for segregation of brain into forebrain, midbrain and hindbrain regions were derived from homeobox genes expressed in the notochord, prechordal plate and neural plate. He also found that the final closure of the cranial neuropore occurred at 18-20 somite stage (25<sup>th</sup> day) in human embryo and closure of the caudal neuropore approximately two days later.

### **2.1.1 Brain Vesicles**

Jenkins (1978) concluded from studies on canine brain that embryonic growth and development were inherently influenced by a phenomenon called cephalization, which meant that the cephalic portion of the embryo possessed greater powers of proliferation and differentiation than did the caudal region. Thus the rapid proliferation of the neural tube in the cephalic region occurred in an intracranial space that was inadequate to contain the linear tubular growth. The neural tube area from which the brain was derived exhibited three primary brain vesicles. The lumen of the neural tube continued into these regions and modified to form the ventricles of brain.

#### ***2.1.1.1 Morphogenesis***

Development of brain vesicles has been explained by Patten (1948) in fig. Primarily three vesicles were formed, viz., the prosencephalon or forebrain, the mesencephalon or midbrain and the rhombencephalon or hindbrain. The prosencephalon again divided into a rostral telencephalon and a caudal diencephalon; the midbrain remained undivided as the mesencephalon and the rhombencephalon divided into a rostral metencephalon and a caudal myelencephalon. These five vesicles started to differentiate in 7mm pig embryo and well established in embryos of 9 to 12mm stage. The optic recess marked the point of junction of the telencephalon and diencephalon. The metencephalon was distinguished from the more posterior myelencephalon by its much thicker roof. Telencephalon formed the most rostral part of the neural tube together with the paired dorsolateral outgrowths called the lateral

telencephalic vesicles. These were regarded to be evolved from the alar plates. The most conspicuous features of diencephalon were the paired lateral outgrowths from which formed the optic vesicles and the median ventral diverticulum, the infundibulum.

Arey (1957) reported that in human embryos of about 3mm (early fourth week), the forebrain showed indication of a groove that subdivided it into the telencephalon and diencephalon. At 8mm stage, the hindbrain specialized into the metencephalon and the myelencephalon. According to him the moulding of brain was aided by the turgor of the distending fluid actively secreted by the ependymal layer of the neural tube, which bulged the thinner regions while the more resistant parts remained as relative constrictions. The spinal cord was more easily influenced by external environmental factors than the brain, in which the intrinsic factors apparently played a major role.

Further, he noticed that the diencephalon in vertebrates developed from alar and roof plates. Neither the basal plate nor the floor plate of lower levels of the neural tube extended this far rostrad. Rathke's pouch could be distinguished close to the ventral wall of diencephalon in 10mm pig embryo and the optic vesicles developed into optic cup comprising the retina and pigmented epithelium. Lens was in the form of a closed vesicle at this stage.

Milart (1964) studied morphogenesis of brain in cattle and found that in foetuses up to 40mm, the rate of growth of mesencephalon and telencephalon was considerably higher than that of the diencephalon. The hemispheres grew most intensively up to the middle of the foetal life. Quadrigeminal bodies were discernible in foetuses of 36mm, thalamic tubercles at 65 to 68mm, peduncles at 40mm, pituitary at 20mm and the epiphysis at 36 to 40mm. The optic chiasma was recognizable at a foetal size of 45mm, the olfactory bulb at 40mm and the piriform lobe at 49 to 68mm.

Huettner (1967) noticed that in 7mm pig embryos, the sides of the diencephalon were moderately thick but the roof was thin for the later accommodation of the choroid plexus of the third ventricle. The wall of the mesencephalon was thick throughout.

Harper and Maser (1975) in their study on the brain development in American plain buffalo found that the cephalization was based on lateral expansion of brain.

Shrivastava *et al.* (1987) studied morphogenesis of cerebrum in early, middle and late stages of foetal development in goats. The transverse distance of cerebrum was found to be greater than its vertical distance in all the three stages.

Gilbert (1997) observed that in chick embryos, the ballooning of the early embryonic brain was marked in the rate and extent and was primarily due to an increase in the cavity size and not because of tissue growth. The volume expanded 30 fold between three and five days of development. This rapid expansion was caused by positive fluid pressure applied against the walls of the neural tube by the fluid contained in it.

Hypophysis developed from two completely different parts namely, an ectodermal outpocketing of the stomodeum immediately in front of the buccopharyngeal membrane, known as Rathke's pouch, and a downward extension of the diencephalon, the infundibulum (Arey, 1957). Sadler (2004) reported that when human embryo was three weeks old, Rathke's pouch appeared as an evagination of the oral cavity and subsequently grew dorsally towards the infundibulum. By the end of second month, it lost its connection with the oral cavity and was then in close contact with the infundibulum.

### ***2.1.1.2 Histogenesis***

#### **2.1.1.2.1 Neural Plate**

Moore *et al.* (1987) described the cytological changes during neurulation in vertebrates. The first indication was a change in cell shape. Midline ectodermal cells became elongated, while the cells destined to form the epidermis became more flattened. The elongation of dorsal ectodermal cells caused these regions to rise above the surrounding ectoderm, thereby creating the neural plate. As much as 50 percent of the ectoderm was included in this plate. Cells of neuroepithelium were classified according to the shapes of their profiles as rectangular, round or tapered. Calcium appeared to be important in neurulation. Supplementation of calcium in the medium in which mammalian embryos were cultured accelerated certain phases of neurulation.

#### 2.1.1.2.2 Neural Tube

According to Arey (1957), wall of the developing neural tube at first consisted of a few layers of columnar cells, in human beings. Their rapid proliferation soon gave rise to many layers and later differentiated into three fairly distinct layers, the ependymal, mantle and marginal layers. The innermost ependymal zone lined the neural tube and composed of considerably tall cells with elongated nuclei. Some of them remained to form the ependyma that lined the ventricles of brain. Others formed germinal cells which mitotically proliferated and migrated outwards into the middle layer, the mantle layer. This zone was richly cellular and formed the gray matter. The germinal cells differentiated into neuroblasts and spongioblasts. Toward the end of the first month, neuroblasts separated from the ependymal layer to lie in the mantle layer of the ventrolateral wall of the neural tube. The neuroblasts were characterized by their early assumption of a pyriform shape, due to incipient outgrowth of an axonal process. The spongioblasts developed a series of branching protoplasmic processes, which interlaced freely to form a closed meshed network.

Further, he stated that in vertebrates the brain moulded its shape as a result of differential growth rates. However, the local rate was influenced by the ingrowth of sensory nerve fibres that brought about the cell division and differentiation in the centres penetrated. Moreover, the presence and abundance of nerve cells in various centres and levels influenced the quantitative development of neurons in other regions.

De Lahunta (1983) reported that in vertebrates, in the first stage of development within the wall of the neural tube, the neuroepithelial cells were organised in a pseudostratified arrangement. The cell membrane of each cell was connected to both sides of the wall of the neural tube, but the nuclei were at different levels. These cells were actively mitotic and the nuclei migrated within the wall of the tube whose position varied at different stages of mitosis. During interphase, the nuclei were located on the external surface of the tube. Chromosomal duplication occurred in that position. As the nucleus entered mitosis it migrated through its cytoplasm to the luminal surface. The cytoplasm also retracted to that position. The two new daughter cells extended their cell membrane to the periphery and the nucleus



migrated to the external surface again. In a short time, differentiated cells appeared on the external surface of the actively mitotic layer.

According to Ulinski (1997) the differences in size and shape of the brain in vertebrates resulted from the dynamics of cell division within the neural tube. Neuronal processes were generated during the early life of the neural tube. They migrated radially into the walls of the neural tube, leading to an increase in its width. Hence, the shape of the adult brain was determined by the spatial and temporal pattern of cell divisions in the neural tube.

Sadler (2004) opined that the neuroblasts initially had a central process extending to the lumen (transient dendrite), but when they migrated into the mantle layer, this process disappeared, and neuroblasts were temporarily round and apolar. With further differentiation, two new cytoplasmic processes appeared on opposite sides of the cell body forming a bipolar neuroblast. The process at one end elongated rapidly to form the primitive axon, and the process at the other end formed primitive dendrites. The cell was then known as a multipolar neuroblast and with further development became the adult neuron. The distinctive cytological characters of nerve cells began to appear very early. In the human embryo, neurofibrillar differentiation first occurred before the end of the fifth week of development. The marginal layer was the outer layer of the neural tube. At the beginning, cytoplasmic processes of the primitive ependymal cells occupied this layer. Subsequently neuroglia and processes of neurons from the mantle layer invaded the marginal layer, which later became the white matter. Neurons migrated from the mantle layer through the marginal layer to form the peripheral layers of gray matter of the cerebrum and cerebellum.

#### 2.1.1.2.3 Cerebral Vesicle

Todd (1982) described the gross morphology and geometry of cell production in the early development of the mouse cerebral vesicle. At nine days post-conception, the neural tube comprised a simple cylinder of epithelial tissue. The onset of differentiation of neural precursor cells to form protoneurons, and their aggregation into the cortical plate started at the pole and spread radially over the vesicle in the order of a single cell cycle.

Smart (1985) noticed that in mouse embryos of 10 days of age, the cerebral vesicle formed an approximately hemispherical dilatation of the lateral wall of the

neural tube. By 11 days the medial wall also formed and neuron release had commenced rostrally in the basal region of the telencephalon and in the adjacent lateral wall. Further, studies on the interrelation between the three proliferative systems in the lateral wall of the developing telencephalon were also conducted. Morphologically they were evident as the medial and lateral ventricular elevations and the surrounding area of pallium: the latter part was crescentic in outline and concerned with the generation of isocortical cells.

Trautwein *et al.* (1994) reported that in bovine foetuses, the cortical plate was first noticed in the wall of telencephalic vesicle at 3.2cm CRL (Crown Rump Length) stage. The other zones could be distinguished from 4.5cm CRL onwards.

### **2.1.2 Brain Flexures**

While several divisions of the brain were differentiating, certain flexures appeared in its roof and floor due to unequal growth processes (Arey, 1957). The first, or cephalic flexure occurred in the midbrain region of the embryos and the primitive head made a sharp bend ventrad. A second bending, the cervical flexure occurred at the junction of the brain and spinal cord. The cephalic flexure occurred in the midbrain region of human embryos at 3 to 4mm CRL stage. At about the same stage, the cervical flexure appeared. The pontine flexure began to gain prominence at 10mm stage. Eventually the two caudal flexures straightened and disappeared, but the cephalic flexure was set permanently.

Mc Ewen (1957) observed that in pig embryos, the cephalic flexure made its appearance at 13-somite stage and shortly thereafter, the cervical and pontine flexures were also underway. Houston (1968) and Jenkins (1978) reported that in the canine embryos, the cephalic flexure appeared at 17<sup>th</sup> day and the cervical flexure at 18<sup>th</sup> day of development while the pontine flexure was visible at 21<sup>st</sup> day.

The cervical flexure was less pronounced in quadrupeds, where the spinal cord extended more horizontally compared with that in bipedal animals. Between these two flexures was a bending of the neural tube in an opposite direction in the rostral area of the rhombencephalon, which was named as the pontine flexure (Jenkins, 1978).

Jacobson and Tam (1982) analysed cephalic neurulation in the mouse embryo and found that cranial flexures developed well before the neural tube formation and

early appearance of this flexure imposed a mechanical impediment to tube closure in forebrain and midbrain regions.

## 2.2 DEVELOPMENT OF PARTS OF BRAIN FROM SECOND MONTH TO TERM

### 2.2.1 Encephalometry

#### 2.2.1.1 *Relationship Between Body Weight and Brain Weight*

Studies in foetal pigs revealed that brain increased in weight faster than the spinal cord (Tumbleson, 1973). The percentage contribution of brain to the body weight, decreased from 12 weeks of gestation to four weeks after birth. However, the brain weight increased in a linear fashion from eight weeks of gestation until 13 weeks after birth. Thereafter, the rate of increase declined.

The changes in the weight of the whole brain, rhombencephalon and eye lens were studied by Hubbert *et al.* (1974) in the developing bovine foetuses. Percentage weight of the brain increased from 10.1 percent to 12.4 percent from a foetal weight of 300g to 384g. Smith and Jansen (1977) studied the development of brain in cats ranging from six weeks post conception to adulthood. Brain weight at birth was 20 percent of that of the adult and reached the adult level at three months post partum. It was found that maximum rate of gain of brain weight, DNA and cholesterol occurred postnatally.

Brain development in foetal sheep was recorded by Mc Intosh *et al.* (1979). The weight of brain increased from 40 days to 150 days of gestation with a decrease in the brain-body weight ratios.

In the foetal goat, between four and six weeks of gestation, the embryo recorded 145.0 percent increase in body weight and 171.5 percent in brain weight. From sixth to eighth week, both the embryo and brain recorded much higher rates of development of 237.7 and 165.7 percent, respectively while at 10<sup>th</sup> week, the rate of growth had sharply reduced to 16.2 and 47.7 percent, respectively. Between 10<sup>th</sup> and 14<sup>th</sup> week, a significant and massive spurt in the growth of these parameters was noticed as 159.4 and 109.2 percent, respectively. From 14<sup>th</sup> to 18<sup>th</sup> week, the increase was 113.6 and 68.7 percent, respectively (Adejumo, 1992).

In sheep, Turley *et al.* (1996) observed that the weight of brain increased 32-fold between 90 days of gestational age and 17 days after birth. Increase in brain weight occurred in two phases, one up to 90 days and a more rapid and larger increase thereafter, which continued until birth. These two phases appeared to reflect an increase in neuroblast multiplication followed by neuroglial multiplication and myelination respectively. At birth, weight of the brain was 50 percent of that of the adult, while the cerebral hemispheres, the cerebellum and spinal cord recorded 52 percent, 40 percent and 40 percent of the adult size, respectively. They opined that the relative maturity of the brain at birth justified the classification of the sheep as a prenatal brain developer.

Ulinski (1997) established a relationship between the size of an animal's brain and the size of its body. Mammals and birds possessed larger brains per unit body weight than other groups of vertebrates. It was also reported that bigger animals had bigger brains.

#### ***2.2.1.2 Relationship Between Age and Brain Weight***

Fox (1963) and Pampiglione (1963) studied the structure and postnatal development of brain in dog. By two weeks of age, the superficial flexures of the cerebral hemispheres resembled the adult brain. The relative size of different lobes of the cortex and the ratio between the length and width of these lobes were adult like by six weeks of age. Adult brain weight was attained by 12 weeks.

No sex difference was noticed in the rate of growth for the developing murine brain by Blinderman and Brown (1966). Monterde *et al.* (1998) assessed the effects of age, gender and body weight on brain morphometric variables during the early postnatal life in kids. These variables increased over the age-range studied. The age exerted a significant influence on brain weight and length only whereas, the live weight was the main factor of variation for all morphometric parameters except hemisphere width and height. Between sexes, females had a significant influence on brain weight, hemisphere weight and length.

#### ***2.2.1.3 Morphometry of Brain***

Kappers *et al.* (1967) reported that the white matter increased as the cube while the gray matter increased as the square in the central nervous system of animals. Large brain had relatively more white substance than the small one. They also found

that there was relatively small increase in thickness of the cerebral cortex in comparison with the brain weight. Gray substance was about six times more vascular than the white substance, but the blood vessels did not play any role in the localisation of the fissures.

A biometrical study on the brain of the Indian buffalo was made by Khatra and Roy (1980). The gross morphology conformed to the general pattern of large ungulates. The forebrain was smaller than that in cattle, wisent or bison. The mean weight of the brain of the buffaloes was 483.9g.

Encephalometry of Asian elephant has been reported by Malik *et al.* (2000). The brain of eight-year-old female elephant measured 36cm, 30cm and 11cm its greatest length, width and thickness, respectively. The brain was much heavier (3675g) in comparison to the brain of the horse (650g), ox (500g), pigs (125g) and dogs (60 to 70g). Morphometry of the brain in calves has been recorded by Parmar *et al.* (2000) and found that the brain weighed approximately 2.5 times the weight of the spinal cord.

## **2.2.2 Craniometry**

### **2.2.2.1 Prenatal Period**

Langman (1981) reported that the head constituted approximately one-half of the crown rump length in human foetus at the beginning of the third month of gestation. At first the face was comparatively smaller than the neurocranium. This was caused by the virtual absence of the paranasal sinuses and the small size of jawbones. Parmar *et al.* (1997) investigated the growth dynamics of head in the foetal goat and concluded that all the measurements of head revealed greater increase in early gestation than in late gestation. The maximum symmetry of the body especially of the head was attained in mid-gestation period.

### **2.2.2.2 Postnatal Period**

Young (1959) studied the influence of cranial contents on postnatal growth of the skull in the rat. Changes in cranial contents led to compensatory modifications in size and spatial arrangement of functionally related tissues. The cranial vault was highly influenced; the cranial base was affected to a lesser degree and facial skull remained unaltered. It was suggested that intracranial pressure resulting from expansion of cranial contents was translated into tensile forces in surrounding tissues,

influencing their orientation, and stimulating their proliferation, thereby producing compensatory expansion of the cerebral capsule.

Pampiglione (1963) described the main changes in cranio-cerebral relationship in the growing dog. It was reported that the position of the brain in relation to the coronal plane through the centre of the eyeballs appeared as if displaced backwards. This was suggested to be due to several factors like increase in the volume of cavity of the skull, increase in the size of the facial bones and growth of the frontal sinuses.

The sutural system of the mammalian braincase was arranged in three planes, viz., coronal, transverse and sagittal (Moore, 1981). Thus, increments at the sutures produced enlargement in the length, breadth and height of the braincase. The greatest growth increments were generally noticed in the coronal plane.

Sandhu and Dhingra (1986) explored the possibility of predicting cranial capacity from skull parameters in camels. Cranial capacity showed a significant positive correlation with the width, length and base length of skull and also with cranial length, cranial width, length of cranial cavity, orbital capacity and interorbital distance, mandibular length and weight. Thus the external appearance of the skull, especially that of the cranial part in camel, appeared to be closely related to its cranial capacity. A similar observation was made by Malik *et al.* (1989) in adult goats. In the goat, posterior cranial height influenced the endocranial volume more than the intersupraorbital foramina distance and orbital circumference. The influence of intercornual distance on the endocranial volume was found to be less.

Gupta and Sharma (1990) noticed that the length of skull in bovine had a significant positive linear relationship with the cranial length and skull width. The facial length had no significant relationship with either of these parameters. Thus the cranial length could be used precisely to determine the length and width of skulls. They also noticed that the cranial capacity and brain size were not affected by any of the parameters of the bovine skull or orbit.

Towe and Mann (1992a) examined the relationship between the cranial volume and body length in myomorph rodents. Within species, cranial capacity was directly proportional to the body length and to the cube root of body weight. Across species cranial capacity was directly proportional to the square of body length and to two-thirds power of body weight. They found that cranial capacity could be estimated

accurately from body weight and that body length was better if any differences in habitus were involved.

Dyce *et al.* (1996) found that the closest agreement between the external contours and the cranial cavity was found in the newborn of all species. Among adults this agreement was best retained in cats and dogs. In adult animals, the form and extent of the cranial cavity could not be easily predicted from the external inspection since the paranasal sinuses, horns, bony ridges and other projections of the skull, and the temporal muscles contributed significantly to the conformation of this part of the head. The rostral limit of the cranial cavity showed considerable variation among species; it extended up to the caudal margin of the zygomatic processes of the frontal bones in dogs and cats, with the rostral level of these processes in horses and cattle, but extended to the middle of the orbit in pigs and small ruminants.

Archana *et al.* (1998) found that the length of the skull in yak reflected the length of the cranial cavity but not the cranial capacity. However width of the skull and the intercornual distance influenced the length as well as the cranial capacity.

Sarma *et al.* (2004) conducted craniometrical studies on the skull of New Zealand White rabbit. He noticed that the cranium was much longer than the facial part. The cranial height was more than double the cranial width. The length of the cranial cavity was much lesser than cranial length indicating a roomy cranial cavity in the rabbit.

### **2.2.3 Cerebrum**

Cerebral hemispheres were subdivided into basal and dorsal parts. The basal part consisted of a medially located septal nuclei and a more lateral one with the basal nuclei. The dorsal part surrounded the basal part like a coat, the pallium or cortex, which constituted the relatively thin gray layer forming the outer surface (Jenkins, 1978).

#### **2.2.3.1 Morphogenesis**

June (1978) investigated quantitative changes in the foetal brain of the human beings with special reference to cytoarchitecture of insular cortex. Insular cortical thickness at five month was 0.6 mm, which increased to 1.7mm at the end of foetal life. The absolute cortical cell densities were progressively lowered at fifth and ninth month of foetal life. Differentiation of the insular cortical lamination was completed

within sixth month. No sexual difference was found in the cortical thickness and the relative or absolute cell densities.

Smart (1982) studied the development of cerebral convolutions in postnatal ferret. At birth, cerebral hemispheres were smooth. The sulci were initially shallow depressions on the surface. By the end of third week, they formed closed folds. Smart and Mc Sherry (1986) correlated external features of gyrus formation with certain internal changes. The gyri were formed by longitudinal and radial expansion of the cortical component occurring between relatively fixed areas, which formed the sulcal floors. Ferrer *et al.* (1987) revealed the plastic capabilities related to cortical folding of Layer VI neurons in cat. On gestational day 50, the cerebral surface was smooth and the thickness of the cortex was similar throughout the lateral wall. The molecular layer occupied about 15-17 percent of the cortex. At the end of gestation, sulcus cinguli and median suprasylvian sulcus were well defined. At the end of third postnatal week, the convolution pattern resembled that of adult in appearance.

Shrivastava *et al.* (1987) studied morphogenesis of cerebrum in foetal goats. Foetuses up to 10.0cm CRL possessed agyric cerebrum. Between 10.2 to 19.5cm CRL, the cerebrum showed convolutions separated by sulci of varying depth and extent, and these became identical to those of adults in foetuses with CRL above 20.0cm. Rhinal sulcus was the earliest to appear. Sylvian sulcus was one of the most prominent features of the lateral surface. Suprasylvian, marginal and coronal sulci appeared in the cerebrum of foetuses of CRL 10.0 to 12.0cm.

Louw (1989) described the development of sulci and gyri in the cerebrum of bovine foetuses. Until day 58, the cerebrum was smooth. Then an indentation appeared which marked the position of Fissura Sylvania. Lateral rhinal sulcus appeared at day 68. In general, gyri were developed only after the appearance of grooves. By 160 days of foetal age, most of the sulci were developed. The final groove to form was the sulcus rhinalis medialis.

Danko (1999) reported that in foetal sheep, the hippocampal and Sylvian fissures were observed at 42 to 43 days and 60 to 61 days, respectively.



### 2.2.3.2 Morphology

Kappers *et al.* (1967) observed that in larger ungulates such as the giraffe and camel, the retrosplenial sulcus of the medial cortex formed a branch, the ramus horizontalis posterior. This was always lacking in small ungulates except sheep.

Brain of buffalo was similar to that of ox and horse (Ommer *et al.*, 1971; Rao and Sharma, 1974). Considerable variation in the sulcal pattern was observed between specimens and also between two halves of the same organ. Yeh *et al.* (1981) observed that in Chinese buffalo, the cerebrum was longer and the ratio of the length to width as well as the length of corpus callosum was greater than in cattle. The middle branch of the Sylvian fissure was much shorter and narrower than in cattle and other ruminants.

Dellmann and Mc Clure (1975) found that the most prominent fissure on the lateral surface of brain in small ruminants was the Sylvian fissure with a very deep middle branch and a long ventrolaterally running rostral branch parallel to the lateral rhinal sulcus. Unlike in large ruminants, an ectomarginal sulcus was absent in small ruminants.

Jenkins (1978) opined that the pattern of gyri and sulci of the cerebral cortex is species specific and therefore the names of most of the gyri and sulci were not easily transferable from the brain of one animal to that of another. Based on the bones of the calvaria under which specific areas of cerebral hemispheres were situated, the cortex was conveniently subdivided into four lobes, the frontal, occipital, temporal and parietal lobes. He also noticed that the brain of dogs had a poorly developed temporal lobe in comparison with the brain of primate and it did not extend much ventrorostrally.

Chrisman (1991) reported that the intellectual activities and learning in animals were processed in the frontal lobe. Fine motor abilities such as those tested by hopping and placing reactions during the neurological examination depended on the frontal lobe. However, gross motor activities did not depend on the frontal lobe in animals unlike in human beings. The parietal lobe processed sensory information such as pain, touch and proprioception. The occipital lobe processed visual informations and the temporal lobe aided processing of auditory information.

### 2.2.3.3 Histogenesis

Richard and Angevine (1962) conducted autoradiographic analysis of time of origin of various components of telencephalon of mouse. Neurons destined for amygdaloid nuclei were noticed on day 10. Basal and cortical nuclei and claustrum began to develop on day 11. The neurons of globus pallidus appeared on 10<sup>th</sup> and 11<sup>th</sup> days of foetal life. First neurons for caudate-putamen appeared on day 12. Hippocampus and dentate gyrus developed between 13 and 17 days.

In human foetuses, Kappers *et al.* (1967) found that, during fifth month, undifferentiated neopallium started arrangement of the neuroblasts into cell layers. By sixth month, neurons of deeper subgranular layers showed some migration and differentiated into two layers, which were lying close together. The cell masses overlying the subgranular layer formed an undifferentiated lamina granularis interna, which, subdivided further, so that in the eighth month of intrauterine life, all the six layers of neocortex could be differentiated. In the beginning, these six layers were alike over the whole neocortex. Later a regional differentiation appeared. The neocortex showed differences in structure on the top of convolutions and at the base of sulci. These variations were explained as being due to differences in the compression or stretching of the various layers. The outer layer was compressed at the base of the fissure and the inner layer stretched, while at the top of the gyrus it was just the reverse. The vascularisation of the superficial layers (I to IV) was independent of that of the deeper layers. The blood supply to the deep granular layer VI was especially rich. They suggested that this layer was the chief matrix in which proliferation occurred in the organization of the cortex.

According to Stanley (1968), the molecular layer in the cerebral cortex of an immature mammal contained many neurons in a confined area. In the adult, he opined that the number of cells might be the same but they were distributed over a greater area.

Sinha (1970) made an ontogenic study of the occipital lobe of puppy less than a month old, which showed that with increasing age, there was an increase in the laminar thickness. At one month of age there was arborization of apical and basal dendrites and their collaterals.

Harrison (1978) studied the histogenesis of the wall of the cerebral hemisphere in the human foetus. In the primitive neural tube, the neuroblasts were congregated in the mantle zone of the tube. Later these neuroblasts migrated to the periphery of the tube and so formed the gray matter which lay on the external aspect of the cerebrum. Hence the gray matter occupied the marginal zone of the neural tube and the nerve fibres to which its cells gave origin passed centripetally. A similar process occurred in the cerebellum also. Similar observations were made in domestic animals by Ghosh (2002).

#### ***2.2.3.4 Histology***

Histologically the cerebral hemisphere consisted of gray matter and white matter. The gray matter was divided into the cerebral cortex, rhinencephalon and basal nuclei. The white matter was composed of association fibres, projection fibres and commissural fibres (King, 1987).

##### ***2.2.3.4.1 Gray Matter***

###### ***2.2.3.4.1.1 Cerebral Cortex***

Patten (1948) stated that in mammals, the whole cerebral cortex except its ventral part was designated as neocortex, due to its recent phylogenetic origin. Bell and Lawn (1956) noticed that in goats, the region of cerebral cortex regulating the somatic motor activity was restricted to a small area of the medial anterodorsal aspect of the hemisphere. This embraced a part of the superior and middle longitudinal gyri. Ipsilateral fibres from the middle longitudinal gyrus controlled fine and highly skilled movements at the periphery. In goat, prehension is affected by fine and delicate movement of lips, comparable to the fine movement of thumb and index fingers in the primates.

Brizzee and Jacobs (1959) studied the glia to neuron index in the submolecular layers of the motor cortex in kittens and adult cats in order to determine the relationship between the index and brain weight. The results suggested that the glia index was determined by the functional complexity of the cortex as well as the brain weight.

Moliner (1960) made a statistical analysis of dendritic distribution in the cerebral cortex of cat and the results showed that the distribution of dendrites was

trimodel. In the subpial layers, the dendrites were considerably more abundant than in any of other layers.

Deutsch (1973) observed that the ultrastructure of the cerebral cortex in ox was similar to that reported for other species. Fleischhauer and Angelika (1979) determined the number of nerve cells and glial cells and total number of cells per unit volume of various layers of striate area of brain, in adult rabbits. Cell densities represented depth of cerebral cortex. Nerve cell density was below 10 cells per unit volume in layer I, reached greater than 80 in layer II and III, a maximum of about 120 in layer IV and just below 70 in layer VI. Glial cell density decreased from more than 30 cells at layer V and in layer VI, it increased steeply to reach a maximum of more than 90 cells per unit volume.

Ferrer *et al.* (1986) compared the sixth layer of cerebral cortex in carnivores, Artiodactyla and primates. They observed a basic structural uniformity in all these species. When compared with lissencephalic species, a horizontal fibrillary system of cerebral cortex, which was vertically arranged in gyral region, was observed in convoluted brains. The great development of this cortico-cortical association system in gyrencephalic species was considered to be a major step in neocortical evolution.

Shrivastava *et al.* (1987) described the cerebral cortex of foetal goat as heterogenetic type that did not reveal all the six distinct layers. Four layers, viz., molecular, superficial, intermediate and deep granular layers were identified. Fletcher (1993) reported that in domestic animals this layering was evident in only thick sections and the prominence of individual layers varied from region to region. From peripheral to deep, the layers were named as molecular or plexiform, external granular, external pyramidal, internal granular, internal pyramidal and fusiform.

#### 2.2.3.4.1.2 *Rhinencephalon*

##### 2.2.3.4.1.2.1 Olfactory Pathways

Bradley (1948) reported that the olfactory lobe in the brain of dogs consisted of the olfactory bulb from which arose a flattened white band, the olfactory tract. At its posterior extremity the tract divided into medial and lateral striae, the former disappeared into the fissure between the hemispheres and the lateral stria coursed as a white band across the surface of the anterior prolongation of the piriform lobe and finally disappeared in this. Between the two striae was a gray eminence, the olfactory

trigone, greater part of which was pitted with holes and thus constituted the anterior perforated substance. Jenkins (1978) observed that olfactory bulbs in dogs were very large when compared with those in human beings. In foetal elephant, the olfactory bulbs were flat, oval and large (Mariappa, 1985). Smuts and Bezuidenhout (1987) found that in the adult dromedary, olfactory bulb was exceptionally small.

Crosby and Schnitzlein (1982) noticed that the rhinencephalon in all ungulates was well developed and occupied a good proportion of the ventral part of the brain. The olfactory bulbs and stalks were short and stocky, extending slightly beyond the frontal pole of the brain. A conspicuous accessory bulb was located on the dorsomedial angle of the olfactory bulb. Structurally the olfactory bulb presented the same concentric lamination as in other mammals.

Padmanabhan and Singh (1982) studied the postnatal development of the olfactory bulb in rat. At birth, the bulbs were ovoid. Overall increase in size and cytoarchitectural elaboration was rapid in the first two weeks of postnatal period and the adult structure was attained by the end of third week.

Wischnitzer (1993) found that the olfactory bulb was ovoid and compressed rostrocaudally and was obliquely oriented rostroventral to the cerebrum, in cats and sheep. In sheep, lateral olfactory tracts were more distinct than the medial tracts and were demarcated laterally by prominent rhinal fissures.

#### 2.2.3.4.1.2.2 Piriform Lobe and Hippocampus

Lakomy (1970) studied cytoarchitecture of the piriform lobe in cow and noticed that the lobe was divided into three regions, which in turn subdivided into 11 areas. Ryszard (1979) found that the piriform lobe in sheep was triangular in shape with a distinct convexity, whose base was directed rostrally and the apex caudally. Cortex of the lobe was divided into three regions: the regio praepiformis, periamygdalioidea and entorhinalis. The regio praepiformis and periamygdalioidea were composed of two layers namely marginal and cellular layers. In regio entorhinalis four layers were distinguished namely marginal, external cellular, central cellular and internal cellular.

Larsell (1951) reported that the cerebral cortex showed its earliest differentiation in the hippocampus. In human embryos at 12mm stage, cells were found to migrate in the dorsomedial walls of the hemisphere from the mantle zone

into the marginal zone. These became the cells of the hippocampal cortex, which being the first to appear and was designated as the archicortex. According to Ghosh (2002), hippocampal cortex in domestic animals developed from the medial wall of the telencephalic vesicle and remained in close association with choroid fissure. Due to elongation of the posterior part of the lateral ventricle and formation of the horn, the hippocampal cortex developed a curve.

Postnatal development of dentate gyrus of the hippocampal formation was studied in mouse by Lavail and Wolf (1973). In the newborn, it was distinctly wedge shaped. The granule cells of the suprapyramidal limb were positioned in a small well-defined lamina, while the granule cells of the infrapyramidal limb were more dispersed. By fifth day, both supra- and infrapyramidal limbs of the dentate gyrus became larger with all the three cortical layers, viz., a molecular layer extending from the hippocampal fissure to the granule cell layer, a granule cell layer whose central region was packed with small neurons, and the polymorphic layer in the hilus between the two limbs.

Baer *et al.* (1985) examined the ultrastructure of the hippocampus of cattle, sheep and goats. Three layers and 13 cell types were distinguished in this region. Rao (1991) reported that the hippocampus in sheep was located in the floor of the inferior horn of the lateral ventricle. It was made up of the interlocked dentate gyrus, cornu ammonis and related structures. The cornu ammonis revealed five layers from exterior to the interior namely, ventricular ependymal layer, stratum alveus, stratum oriens, stratum pyramidale and stratum lacunosum-moleculare.

According to Eustachiewicz and Luszczywska (1999), hippocampus in polar fox extended from the splenium of corpus callosum to the ventromedial angle of the cerebral hemisphere.

#### 2.2.3.4.1.3 *Basal Nuclei*

Basal nuclei are the gray areas of the cerebral medullary substance. Four gray bodies constituted the basal nuclei, viz., the caudate nucleus, lenticular nucleus, claustrum and amygdaloid body. The alternation of these nuclei with the fibre aggregations in which they were embedded gave this region the name corpus striatum (Arey, 1957).

Stromston (1947) found that the corpora striata in cat were the anterior most of the basal nuclei and pear shaped. A thin layer of white matter, the stria terminalis separated the optic thalamus from the caudate nucleus. Rangelov (1966) studied the amygdaloid nucleus in pigs, which appeared as a large nuclear mass deep within the piriform area at the rostral tip of the ventral horn of the lateral ventricle. It was 12 to 13mm long and 9 to 11mm wide at 10 to 12 months of age.

Truex and Carpenter (1969) reported that the cells of neostriatum in man were of two types, small round, or spindle shaped cells and large multipolar cells. The ratio between the small and large neurons was 20:1. The lenticular nucleus in man appeared wedge shaped whose broad, convex base directed laterally while its blade medially. It was separated from the caudate nucleus by internal capsule. A vertical plate of white matter, the lateral medullary lamina, divided the nucleus into an outer putamen and inner globus pallidus. Nin *et al.* (1978) determined the neuronal distribution in the caudate nucleus of the cat and found that large neurons were more frequent in the infero-external region.

Jenkins (1978) reported that the claustrum in dog appeared as a layer of gray matter lateral to the lenticular nucleus from which the external capsule separated it. Crosby and Schnitzlein (1982) found that the claustrum in ungulates consisted of dorsal and ventral parts. In sheep, the two parts were connected by a slender band of loosely arranged cells that was absent in goats. Large and medium sized polymorphic cells were more loosely arranged in the ventral part than in the dorsal. Medium sized cells were less in cattle than in small ruminants.

Tanaka and Alexander (1978) conducted electron microscopic study on the caudate nucleus in the neonatal dog. The immature synapses and the axonal and dendritic growth cones indicated the dynamic state of both pre and post-synaptic components of the caudate neuropil at early postnatal stage.

Victor *et al.* (1979) studied the prenatal development of neostriatum (caudate nucleus and putamen) in the rabbit. Cellular components originated between 15 and 18 days of intrauterine life from a layer of proliferating matrix cells that lay on the floor of the anterior part of the lateral ventricle. From this proliferating layer, precursor cells sequentially migrated outwards to reach the developing neostriatum according to two gradients of histogenesis. Neurons formed at early stages occupied a

ventromedial position in the neostriatum, while those formed at later stages occupied a dorsolateral position. The rostral regions of the neostriatum arose somewhat later than the caudal ones, demonstrating the existence of a caudo-cephalic gradient of cytogenesis. Crosby and Schnitzlein (1982) opined that in ungulates the basal nuclei showed only minor variations from one species to another and resembled those of higher mammals.

King (1987) opined that most of the activities of basal nuclei were applied to the cerebral cortex and brought about the complicated automatic actions which an animal performs every day of its life whilst changing its posture, walking, feeding and defending itself. The young one of Equidae and other fleet-footed herbivores run with their mother within a few hours of birth and rely on this to escape predators. He opined that their basal nuclei would be fully programmed genetically at birth.

#### 2.2.3.4.2 White Matter

There are three types of cerebral fibres based on distribution such as association fibres, projection fibres and commissural fibres. The commissural fibres connected the left and right cerebral hemispheres across the midline. The largest commissure, the corpus callosum formed the most important pathway by which the cortical areas of one hemisphere were connected to those of the other. Stromston (1947) reported that corpus callosum that joined the two cerebral hemispheres was about 1mm in thickness and 3cm in width in cats. Bell and Variend (1985) detected sex differences in the shape of splenium of corpus callosum only in adult human beings but not in children. The association fibres comprised of a vast network of interneurons joining different areas of the same hemisphere while each hemisphere was linked to other parts of the CNS by projection fibres (King, 1987).

### 2.2.4 Cerebellum

#### 2.2.4.1 Morphogenesis

Done and Hebert (1968) studied growth of cerebellum in foetal pig. Absolute and relative growth curves were determined for whole brain and the cerebellum from 45 days of gestation to term. The growth curves were curvilinear, but could be expressed as linear by considering each curve as two straight segments with a sharp change in the rate of growth between nine and ten weeks. The increase in cerebellar weight and whole brain weight with increasing age was little, but linear between sixth



and ninth week. After nine weeks there was a sharp and linear increase in the rate of brain growth. This acceleration was most marked for cerebellum.

Shrivastava *et al.* (1986) investigated prenatal morphogenesis of cerebellum in goat. In foetuses having 3.7 to 7.5cm CRL, the cerebellum was plain and transversely elongated. It showed fissures of variable depth at 8.5cm CRL. In the foetus of 10.0cm CRL primary caudolateral fissure separated rostral and caudal divisions of the cerebellum. At 20.0cm and above, secondary and tertiary branching and foliation of cerebellar cortex were prolific and attained surface globular configuration. Length and width of the cerebellum increased more compared to the corresponding parameters of cerebrum.

#### **2.2.4.2 Morphology**

Takeda *et al.* (1960) made phylogenetic and ontogenetic studies of cerebellum of birds and mammals. By the measurement of the volumes of various nuclei, a dimensional relationship was found. The volume ratio of cerebellar nuclei became smaller during the phylogenetic or ontogenetic development.

Dellmann and Mc Clure (1975) found that in small ruminants, the vermis was more prominent than in large ruminants and was more clearly separated from the lateral hemispheres. The hemispheres were flat and smooth on their rostral surfaces as against the irregular and subdivided lobes and lobules on the caudal surface.

Inouye and Ichi (1980) did not notice any sex related differences in the cerebellar foliate pattern, in mouse.

Khatra and Roy (1980) found that cerebellum in buffalo was much larger than in bison but smaller than that in cattle and wisent. The cerebellar percentage of whole brain was 8.62. Cerebellum contributed 10 percent of the brain mass in adult goat (Roy and Khatra, 1982). Yeh *et al.* (1982) found that the average weight of cerebellum in Chinese buffalo was  $44.917 \pm 1.950$ g. They also observed that the posterior part of the culmen of the vermis was more developed. Malik *et al.* (2000) noticed that the cerebellum in Asian elephant was compressed rostrocaudally and formed the highest part (11.00cm) of the brain. It was about two-third in width to that of the cerebrum or brain. The vermis was narrower and lower in level than the lateral lobes. Parmar *et al.* (2000) reported that the percentage length and width of

cerebellum in male calves of one to two months of age was 31.86 and 57.05 percent of the length and width of the brain, respectively.

#### **2.2.4.3 Histogenesis**

Postnatal development of cerebellar cortex in rabbit was studied by Smith (1960). At birth the external granular layer was 8 to 10 cell thick, and composed of closely packed, uniform cells with dense ovoid nuclei, prominent nucleoli and sparse cytoplasm. Mitotic figures were numerous. The molecular layer was thin, consisting of only a few nerve fibres and astrocytic processes. The Purkinje cells were present in a definite layer but had not attained the size or number of processes of adult. Small uniform densely packed cells with a few processes formed the internal granular layer. The cerebellar cortex attained its mature form by the age of two months. Glial cells were few in number in early stages.

Histological differentiation of the cerebellum of cats was reported by Beery (1962) and Smith and Downs (1978). There was a parallel relationship between the differentiation of the cerebellar cortex and development of co-ordination. Lamina granularis externa was well developed in the newborn. Changes in the external granular layer thickness and in the morphology of the granule cell neurons as they migrated through the molecular layer into the granular layer occurred within the first two weeks postnatally. These changes occurred earlier in the cat than in birds, but the sequence was the same (Smith and Downs, 1978). In calves, foals and other species that walk within an hour after birth, the cerebellum was better developed. In foetal calves, the external granular layer appeared at around 57 days of gestation and reached maximum thickness at around 183 days (De Lahunta, 1983).

Bujak (1967) studied the development of the nucleus interpositus of the cerebellum in pigs. There were two nuclei, nuclei interpositus anterior and posterior. Both developed from the same cell group and the cell bridges connected the two. Together they formed the nucleus lateralis.

Andreoli *et al.* (1973) determined the time of origin of Purkinje cells and their final location in various lobes of the cerebellum in mice. Cells formed on 11 and 12 days of gestation appeared in all the lobes of vermis but those formed on day 13 became restricted mainly in the anterior lobe.

Choi and Lowell (1980) examined astrogliogenesis in the human foetal cerebellum between nine and twenty weeks of gestation. Ontogenesis of cerebellar astroglia, in particular Bergmann fibres, was identified. These fibres were the final stage of the development of a definite group of radial glia in the cerebellum. Radial fibers were present at nine weeks of gestation, with features of astroglial differentiation. Those arising near the ventricular zone did not reach all the way to the pial surface but terminated in vascular walls of the intermediate zone. A second set of glial cells located in the intermediate zone gave rise to long, tapering processes oriented radially to the pia, a few of them reaching the surface and terminating there in conical swellings. Radial glia with these features were observed in cerebella at all foetal stages, indicating their availability for guidance of the external granular layer as they migrated outward.

Shrivastava *et al.* (1986) reported that in the goat embryos of 2.7cm to 44.0cm CRL, the cerebellar cortex showed four layers, viz., outer granular layer, molecular layer, Purkinje cell layer and inner granular layer. Gabr *et al.* (1991) studied histogenesis of the cerebellar cortex in camel. The external granular layer reached its maximum thickness at 51cm CRL, and then it decreased to about one to two cells in thickness at 125cm CRL. The molecular and internal granular layers increased in thickness at 125cm CRL. The increase in thickness of the molecular and internal granular layers was at the expense of external granular layer. The Purkinje cell layer was formed of three to four cells in thickness up to 100cm CRL. At 125cm CRL, the Purkinje cells increased in size but did not attain their mature form.

Moustafa (1996) traced the histogenesis of cerebellar cortex of dog during prenatal life and suckling period. In canine embryos of 10 to 15mm CRL, the dorsolateral parts of alar plates of the metencephalon bent medially and formed the rhombic lips; the primordium of cerebellum. As the development progressed, the neuroblasts migrated from the mantle zone to the marginal zone. The neuroblasts of the mantle zone formed various nuclei of the white matter.

#### **2.2.4.4 Histology**

The morphometric characteristics of Purkinje cell perikarya and dendritic trees were evaluated in man, cat and rat by Ruela *et al.* (1980). Size of Purkinje cell

perikaryon, number of synapses and the synaptic surface per Purkinje cell were significantly greater in man than in cat and rat.

Steinbach *et al.* (1980) conducted light and electron microscopical studies on the cerebellar cortex in cattle, sheep and goat. Differences among the three species were seen only in the thickness of the molecular, ganglion and granular layers and in the size and topography of the seven different cells and fibres of the cerebellar cortex. In contrast to other species, soma and fibres of Purkinje cells often contained numerous lamellar bodies.

Monteiro (1983) described two types of oligodendrocytes as constant features in cerebellar cortex of the rat. Type I cells exhibited rounded or elliptical nuclei, whereas the type II cells presented more irregular nuclear and cellular contours and wider perinuclear cisternae. The latter type occurred as satellites of Purkinje cells.

Axonal descending branches of stellate cells in the molecular layer of the cerebellar cortex of rat were studied by Paula *et al.* (1983). The number of axons from stellate cells formed pericellular baskets and the “pineaux” increased as their cell bodies came to lie in the deeper aspect.

Vyas and Nanda (1984) reported that intraneuronal pigment in Purkinje cells first appeared after the age of two and a half years in goats and there was no trace of extraneuronal pigment around them. Gilbert (1997) opined that a typical Purkinje cell in vertebrates might form as many as 1,00,000 synapses with other neurons, more than any other neuron studied. Each Purkinje neuron also gave rise to a slender axon, which was connected to other cells in the deep cerebellar nuclei.

Geurts *et al.* (2001) studied the granular layer of cerebellar cortex in rat. It consisted of densely packed neuronal cells, classified into granule cells and large interneurons. Granule cells, the most common cerebellar interneurons were responsible for the transduction of mossy fibre afferent input into Purkinje cells. Large interneurons modulated this signal transduction directly by inhibiting granule cells, or indirectly by acting on Golgi cells (Lugaro cells) or mossy fibre input.

### **2.2.5 Brainstem**

According to Arey (1957), brainstem consists of diencephalon, mesencephalon, pons and medulla oblongata. Jenkins (1978) reported that although

the brain became highly differentiated and much more complex than the spinal cord, evidence of the basic neural tube was present in the adult brain as brainstem.

### **2.2.5.1 Diencephalon**

Diencephalon, the rostral most division of the brainstem represented that part of original prosencephalon remaining in the midline as the telencephalon expanded dorsally and laterally over it (Keith, 1947). He identified the diencephalon and telencephalon with their cavities in human embryos of four weeks of gestational age. Arey (1957) reported that in mammals, the wall of diencephalon differentiated a dorsal roof plate and paired alar plates, the latter constituting both the sides and floor of the neural tube. Neither the basal plate nor the floor plate of lower levels extended this far rostrad. The roof plate became the thin ependymal lining of the tela choroidia of this region. Rest of the diencephalon was reported to be of alar plate origin and showed three main regions namely, the epithalamus, thalamus and hypothalamus. Cavity of the diencephalon became the third ventricle. Far caudad, the pineal body evaginated during the seventh week in man. Similar observations were made in pigs by Mc Ewen (1957), in bovine by Junge (1976) and in canine by Salazar *et al.* (1989).

#### **2.2.5.1.1 Epithalamus**

Epithalamus consisted of the pineal gland, habenular striae, habenulae and habenular commissure (Keith, 1947).

Prenatal development of the pineal body was reported in man by Keith (1947) and in fowl by Spiroff (1958). Pineal body first appeared as a hemispherical evagination from the roof of the diencephalon in the sixth week of development in human foetus and at 48 hours of incubation in fowl. The evaginated cells formed a zone of cellular proliferation comprising of glandular cells, neuroglial cells and neuroblastic elements. From the anterior wall of the pocket, a mass of cells separated early to form an anterior lobe, where as others from the fundus produced a posterior lobe. Later vascular and mesenchymal tissue invaded the glandular mass. The most rapid growth rate occurred between five and twelve days of incubation in fowl. Reiter (1981) distinguished three phases during the development of pineal gland in rats. The morphogenetic phase began at about 12<sup>th</sup> day of embryonic life and extended until parturition. The cellular proliferation phase commenced on the 16<sup>th</sup> day of conception

and terminated by several days after birth. The cellular hypertrophy and differentiation phase began roughly at birth and ended 9 to 12 weeks postpartum.

Ito and Matsushima (1969) reported that postnatal development of the pineal gland in mouse showed no sex difference.

Jain and Koranne (1976) compared the pineal glands of zebu and wild pig. The parenchymatous tissue was located in the central part of the gland in zebu, whereas it was uniformly distributed in wild pig. The pineal organ of wild pig had a lumen suggestive of a more primitive evolutionary origin of the organ than that of the zebu.

Jenkins (1978) found that the pineal body was extremely small and about 1mm long in dog. In Chinese buffalo, Yeh *et al.* (1982) reported that the organ weighed  $430.919 \pm 89.803$  mg and was blunt, thick and nearly rounded with a flat anterior surface and convex posterior surface separated into two lobes by a median groove.

Calvo *et al.* (1988) detected the presence of pigmented cells in the pineal gland of adult dogs. The localisation was constant on the basal surface of the proximal region of the gland. Frequently clusters of pigmented cells were seen in the posterior commissure and the neighbouring meningeal spaces. Ultrastructural studies revealed that these cells were a special type of pinealocytes and the pigment was melanin.

Kumar *et al.* (1995a) described the topography and histology of pineal gland in the goat. It was oval without a pineal stalk. The parenchyma was formed of pinealocytes, glial cells, fine blood capillaries and nerve fibres. Number of pinealocytes was more than that of the glial cells and was categorised into light and dark types, of which the light cells were predominant. Kumar *et al.* (1995b) reviewed the anatomy of pineal gland in domestic animals. The gland was conical in cattle, round to oval in the sheep, goats and buffaloes, fusiform or ovoid in horses, elongated cone shaped in pigs, lancet shaped in dogs and conical in cats. They also reported the occurrence of an accessory pineal gland in buffaloes on the posterior margin of the main gland.

Histomorphological studies on the pineal gland of Indian donkey (*Equus asinus*) were conducted by Pawar and Ramakrishna (2000). The pineal gland was covered by a thin capsule, which mainly consisted of collagen fibres. Trabeculae extended from the capsule into the parenchyma. Presence of melanocytes at the

centre of the parenchyma was characteristic to the pineal gland of donkey. Saggar *et al.* (2001) reported that the pineal gland in sheep showed pinealocytes, four types of glial cells, blood capillaries and nerve fibres. Round to oval pinealocytes arranged in different patterns presented fine chromatin material towards the periphery of their nuclei. Type I glial cells had round to oval nuclei with irregular distribution of chromatin material, whereas type II had smaller and strongly basophilic nuclei. Elongated type III cells were associated with blood capillaries. The nuclei of type IV glial cells had largest dimensions.

Dyce *et al.* (1996) reported that the habenular stria connected the septal area with the habenular nuclei. Habenulae developed within the most dorsal parts of the ventricular wall and received fibres from hippocampus and other parts of the telencephalon and sent fibres to mesencephalic nuclei. Left and right habenular nuclei were interconnected via the habenular commissure.

#### 2.2.5.1.2 Thalamus

Thalamus is the largest component of diencephalon related to the hypothalamus ventrally and to the internal capsule and caudate nucleus laterally and dorsally. In human beings, the main fibre paths entering and leaving the thalamus could be recognized by the end of second month of foetal life (Arey, 1957). Towards the end of third month, the thalamus enlarged to such an extent that it bulged into the third ventricle. Nuclei of thalamus were named according to their topographical relationship.

Smuts and Bezuidenhout (1987) reported the shape of thalamus as triangular in dromedary. Salazar *et al.* (1989) distinguished 18 nuclei in the thalamus of the dog. Chrisman (1991) cited that the thalamus processed more of the sensory information in animals than in man, as animals did not seem to depend on the parietal lobe of cerebral cortex for processing many sensations.

According to Dyce *et al.* (1996), in domestic animals the thalamus developed within the lateral walls of the third ventricle and bulged into the ventricle to form a bridge with its fellow, the interthalamic adhesion.

### 2.2.5.1.3 Hypothalamus

Hypothalamus is the part of diencephalon that forms the ventral and lateral walls of the ventral portion of the third ventricle. According to Buchanan (1957), in mammals the hypothalamus extended from the lamina terminalis rostral to the optic chiasma through the mamillary bodies caudally up to the cerebral peduncles and consisted of optic chiasma, infundibulum, tuber cinerium and mamillary bodies in the rostrocaudal sequence.

Magras and Karamanlidis (1971) investigated the extent of decussation in the optic chiasma in domestic animals. Non-crossing fibres in the optic chiasma constituted 12 percent in horse, 15 percent in cattle and 11 percent in sheep. But in pigs there were 28 percent of non-crossing fibres suggesting a broad field of vision in this species.

Dellmann and Mc Clure (1975) reported that in domestic animals the infundibulum revealed a hollow centre through which the third ventricle extended ventrally to form infundibular recess. Infundibulum in turn was connected to the tuber cinerium. In small ruminants the tuber cinerium was not as uniform as in large ruminants but characterized by four spherical elevations, which located rostromedial to the mamillary bodies. Mamillary bodies were two rounded eminences between the cerebral peduncles fused at the midline immediately rostral to the posterior perforated substance in the interpeduncular space.

Gruetze (1978) described the topography and cytoarchitecture of the nuclei of mamillary body in cattle. The medial mamillary nucleus was the largest unpaired nucleus. The lateral mamillary nuclei were situated in the rostral third of mamillary body and accounted for 5.3 percent of the whole volume of the nucleus. The fornix represented a rich myelinated fibre connection between the hippocampus and the mamillary body.

Mariappa (1985) reported that in elephants the optic nerves, optic chiasma and the optic tracts were slender suggesting a poorly developed "visual system".

Mori *et al.* (1990) opined that arrangements of hypothalamic nuclei were virtually identical between the Saanen goat and the Shiba goat despite differences in their body sizes.



Paramasivan and Sharma (2001) studied hypothalamus of Gaddi sheep. The preoptic nucleus composed of spindle shaped medium-sized neurons located rostrocaudal to the optic chiasma. Paraventricular nucleus was triangular with densely grouped neurons placed as a vertical plate along the wall of the third ventricle. Posterior hypothalamic nucleus was an extensive zone with loose heterogenous collection of medium to large sized neurons.

#### 2.2.5.1.4 Subcommissural Organ (SCO)

Subcommissural organ is located on the ventral aspect of posterior commissure extending from the caudal wall of pineal stalk along the roof of the third ventricle caudally to recessus mesocelicus occupying diencephalic and mesencephalic regions of brain. Talanti (1959) investigated various stages of development of SCO in bovine foetus from three months of gestation to term. The secretory material was already present in the SCO at the age of three months; it seemed to increase in amount up to the seventh month by which time it had reached the postnatal level. The results suggested that the SCO of the bovine foetus was functionally active at least by third month of intrauterine life. Perdomo *et al.* (1985) reported that SCO appeared in the second month of intrauterine life in human beings. Maximum development was seen in 45mm embryo, and exhibited the characteristic high columnar epithelium.

Subcommissural organ was 4.69-5.70mm long in buffalo calves (Ramakrishna and Saigal, 1986). Kumar *et al.* (1997) found that in male goats, SCO was 2.76 - 3.00mm long and divided into four parts. It comprised three layers of highly modified neuroglial tissue; the ependymal layer towards the free surface of ventricle, the subependymal glial zone and a hypendymal layer adjacent to posterior commissure. Reissner's fibre constituted of cilia, microvilli and glycocalyx along with heterogeneous material was present on the ependyma of SCO and cerebral aqueduct in goat but could not be detected in camel (Kumar *et al.*, 1999).

#### 2.2.5.2 Mesencephalon

Mesencephalon or midbrain represented the smallest segment of the brainstem between the diencephalon rostrally and the metencephalon caudally. A section across the midbrain in the fourth week of development in human foetus revealed the same divisions as in the spinal cord. During the third month the quadrigeminal plate developed on the dorsal part of its alar laminae. Roof of the midbrain first thickened

on each side of the midline to form two longitudinal elevations. Later a transverse constriction appeared so that four bodies of corpora quadrigemina were formed. At the same time there was a congregation of neuroblasts in the basal lamina to form two nuclei, the red nucleus and substantia nigra (Keith, 1947).

According to Wenisch *et al.* (1997), the mesencephalon was recognized for the first time at 0.8cm CRL in bovine embryos. In human foetus, even during the seventh week of development, the midbrain lay exposed under the crown of head. It remained separated from the hindbrain by a constriction, the isthmus. By the end of third month, it became overshadowed by the preponderating growth of the forebrain and hindbrain, and by the sixth month, was reduced to the peduncular body. Symmetrical proliferation of the wall of the neural tube in the mesencephalon reduced size of the neural canal to a narrow tube, the mesencephalic aqueduct. Ghosh (2002) reported that in domestic animals the mantle zone of the thick walled mesencephalon was subdivided by the sulcus limitans into a dorsal alar lamina and a ventral basal lamina.

The four areas in the midbrain of vertebrates were the tectum, tegmentum, substantia nigra and crura cerebri in a dorsoventral sequence.

#### 2.2.5.2.1 Tectum

Wenisch *et al.* (1997) reported that in bovine embryos up to 3.4cm CRL, the primordium of tectum exhibited a trilaminar pattern, the ventricular, intermediate and marginal zones. At 4.5cm CRL, formation of the specific tectal layers was marked by the origin of stratum profundum and intermedium. Macroscopically the rostral colliculus was clearly differentiated in embryos of 4.5cm CRL and reached adult structure at 80.0cm CRL.

According to Dellmann and Mc Clure (1975), the caudal colliculi of small ruminants were comparatively smaller than that of large ruminants. They were ovoid in large ruminants but rounded in small ruminants and were whiter than rostral colliculi.

Szalak and Stefan (1977) described the structure of tectum mesencephali in the wild boar. Khatra and Roy (1980) reported that the volume proportion between the rostral and caudal colliculi in buffalo was 3.51:1. Norita (1980) identified three types of neurons in the deep layers of rostral colliculus in cat. Large neurons of

35-60 $\mu$ m diameter occurred mainly in the lateral two third, medium sized neurons of 20-30 $\mu$ m formed 25-30 percent and small neurons with a very few dendritic spines forming less than 10 percent of the total neurons.

#### 2.2.5.2.2 Tegmentum

Tegmentum comprised the core of midbrain and was formed mainly by the reticular formation. The principal nuclei were the mesencephalic nuclei of trigeminal nerve, the trochlear nuclei, oculomotor nuclei, red nuclei, periaqueductal gray and the substantia nigra (Buchanan, 1957).

A gray area surrounding the aqueduct of Sylvius in dog formed the periaqueductal gray matter (Jenkins, 1978). Herrera *et al.* (1988) explained the cell types in this nucleus as fusiform and stellate neurons in young cats.

Paily and Salam (1983) described the morphology and cytoarchitecture of red nucleus in buffaloes. It measured about 5.88mm long, 2.86mm wide and 2.99mm high. Population of neurons in the left and right red nuclei of the same animal was not significantly different and the mean population was 20845 $\pm$ 1686. Percentage distribution of neurons in the middle third of the red nucleus was twice than that found in the caudal and rostral thirds (Paily and Salam, 1984).

#### 2.2.5.2.3 Substantia Nigra

Substantia nigra consisted of an outstanding lamina of gray matter on the dorsal side of the fibrous crura cerebri in the basal portion of the mesencephalon. The name attributed to the intracellular melanin pigmentation, which was absent at birth but increased with age (Jenkins, 1978).

#### 2.2.5.2.4 Crura Cerebri

Yeh *et al.* (1982) reported that the crura were longer in the Chinese buffalo when compared to cattle. De Lahunta (1983) opined that the crura cerebri developed as a result of the caudal growth of descending telencephalic projection neurons located in the internal capsule.

#### 2.2.5.3 Pons

Buchanan (1957) stated that pons was composed of a band of transverse fibres interposed between the trapezoid body caudally and the crura cerebri rostrally. The pons consisted of the dorsal and ventral portions. The dorsal part or tegmentum was

continuous with the medullary tegmentum. The basis pontis or ventral part composed of transversely crossing pontine fibres. Intermingled with pontine fibres were bundles of longitudinally coursing fibres and numerous nuclear masses namely the pontine nuclei.

Rao and Sharma (1974) reported that the pons of Indian buffaloes had a prominent central depression. Dellmann and Mc Clure (1975) found that the pons was divided into bilaterally symmetrical halves by a slight midline depression in large ruminants and in small ruminants by a pronounced groove, the basilar sulcus. It was enlarged considerably toward the trapezoid body, forming a triangle with the apex directed rostrally and the base, caudally. The transition between the ventral surface and caudal edge of the pons was more abrupt in large ruminants than in small ruminants. The rostral border of pons was convex, slightly indented at the midline in large ruminants and straight in small ruminants. Mariappa (1985) noticed that in foetal elephant the pons was very large and quadrilateral on the ventral aspect and measured 3cm long, 8cm wide and 1cm high.

King (1987) noticed that the pons showed considerable variation in size in different species. In man it was particularly large and extended much farther caudally overlapping other structures including the trapezoid body.

Ghosh (2002) reported that in domestic animals migration of alar plate neurons formed the pontine nucleus on the ventral aspect of metencephalon. Axons of these neurons coursed dorsally into the cerebellum producing the transverse fibres of pons that formed the middle cerebellar peduncle.

#### ***2.2.5.4 Medulla Oblongata***

Buchanan (1957) stated that the medulla oblongata was the caudal portion of the brain, located between the pons rostrally and spinal cord caudally, resting on the basal portion of the occipital bone. Mc Ewen (1957) opined that the histomorphogenesis of the medulla oblongata in porcine fetuses involved only a slight modification of the development of spinal cord. The potential roof plate region in the neural tube was expanded extensively instead of being replaced by proliferating alar plate and marginal layer tissue as it was in the spinal cord. This relegated the entire alar and basal plates of the neural tube to a lateral and ventral position. Myelencephalic neuroepithelial cells proliferated ventrally in the region of the basal

plate and laterally in the alar plate region. These regions were demarcated by a ventrolateral groove in the wall of the neural tube that marked the rostral continuation of the sulcus limitans. Throughout the brainstem, the mantle layer of the neural tube was broken up into nuclei that were collection of cell bodies with a common purpose. Barone and Dowcet (1964) found that the junction of medulla and pons was more rostral in cattle than in several other mammals and that caused an extension of the medulla in the same direction.

A median fissure marked ventral surface of the medulla oblongata in domestic animals. The fissure continued caudally with that of the spinal cord and flanked by longitudinal ridges, the pyramids. Rao and Sharma (1974) reported that the medullary pyramids of the Indian buffalo were narrower and poorly developed. In cattle Dellmann and Mc Clure (1975) observed that the pyramids were small but prominent rounded bundles widely separated at the point of emergence from caudal aspect of pons. However, in small ruminants the pyramids were not so prominent; they were flattened and not widely separated in the rostral portion. Many of the constituent fibres of the pyramids decussated at the transition of the spinal cord and medulla oblongata forming an interlacing bundle within the fissure. A lesser transverse ridge, the trapezoid body crossed the ventral surface of the medulla oblongata directly caudal to the larger pontine bar. The trapezoid body was more clearly demarcated in small ruminants than in cattle. The rostral half of the dorsal surface of medulla represented the caudal half of the rhomboid fossa and two prominent ridges; the caudal cerebellar peduncles bounded the fossa laterally. Yeh *et al.* (1982) noticed that the ventral surface of medulla oblongata in the Chinese buffalo was not convex, but rather flat.

Stormer *et al.* (1985) observed that the parasympathetic nucleus of the vagus and glossopharyngeal nerves occupied a central position in the caudodorsal part of the medulla, in the sheep and goats. It was longer than those in monogastric animals.

Kotter *et al.* (1992) and Ruhrig *et al.* (1994) studied the early development, differentiation and cell migration of parasympathetic nucleus of vagus nerve and glossopharyngeal nerve and nucleus of cranial nerve VII in bovine embryos with CRL ranging from 1.0cm to 53.0cm. At 3.6cm CRL, synapses were observed for the first time. Identification of the definitive nuclei was possible at 3.8cm CRL. At 53.0cm

CRL, the nuclei were topographically and cytologically corresponded to the characteristics of adult animals.

### 2.3 VENTRICLES OF BRAIN

Stromston (1947) described the ventricles of brain, in cats. The fourth ventricle was about 3mm long and 1mm wide. The third ventricle was not more than a millimeter in width. The lateral ventricles were the largest.

Larsell (1951) described the development of ventricular system in the brain of human beings. The lumen of the cerebral part of the neural tube was divided into three regions by the constrictions that formed the primary brain vesicles. As the cerebral hemispheres developed from the prosencephalon, the cavity of the latter extended into them as the lateral ventricles. The median portion of the endbrain cavity, together with the lumen of mesencephalon became the third ventricle, its rostral limit being formed by the lamina terminalis. The third ventricle retained a connection with the lateral ventricles on either side through the interventricular foramina. The space enclosed by the mesencephalon, relatively large in early stages, became constricted into the cerebral aqueduct. The lumen of the metencephalon and myelencephalon, continuous caudally with the central canal of the spinal cord, became the fourth ventricle. Similar observations were made in domestic animals by Arey (1957). The lateral ventricles followed the development of cerebral hemispheres and extended into their four pairs of lobes. The body of each lateral ventricle occupied the corresponding parietal lobe, while the anterior, posterior and inferior horns extended, respectively, into the frontal, occipital and temporal lobes.

Malik *et al.* (1978) made biometrical analysis of the cerebral ventricles in adult goats. The ventricular system measured  $7.26 \pm 0.80$ cm in length and  $4.18 \pm 0.78$ cm in width. Lignereux *et al.* (1991) observed that the conformation of the fourth ventricle, the bending of mesencephalic aqueduct and the inclination of the general axes of the cerebrum and mesencephalon in ewes were similar to those of the cow. The third ventricle presented a wide roof that lengthened caudally by large pineal and subpineal recesses, and also a large ventrally situated infundibular recess. According to Malik *et al.* (2000), the plan of ventricular system of elephant resembled that of horses, goats, pigs and buffaloes. However, the height of lateral ventricles was more than its width.

### **2.3.1 Lateral Ventricle**

Dellmann and Mc Clure (1975) reported that in domestic animals, the lateral ventricles possessed a central part at the level of interventricular foramina, the telencephalic septum, a rostral horn and temporal horn. Floor was formed by caudate nucleus rostrally and hippocampus caudally separated by a deep groove overlaid by the choroid plexus. Medial wall in its rostral part was represented by the telencephalic septum and in the caudal part by fusion of the fornix with the corpus callosum. Rostrally it became narrow and continued as a diverticulum of the rostral horn into the olfactory bulb. Caudally it continued into the temporal horn. Kii *et al.* (1997) observed that sex and body weight had no correlation with the symmetry of lateral ventricles in dogs.

### **2.3.2 Third Ventricle**

Cavity of the diencephalon formed the third ventricle (Arey, 1957). He noted that in the initial stages of development, this cavity was relatively broad, but the strongly thickening lateral walls later compressed it into a narrow median cleft. Dellmann and Mc Clure (1975) reported that in domestic animals the third ventricle was a sagittal ring shaped structure situated within the diencephalon around the interthalamic adhesion. Roof was formed by lamina epithelialis on which choroid plexus of this ventricle was located. Third ventricle showed recesses to pineal stalk, rostral to optic chiasma and to the infundibulum. Card and Rafols (1978) described the morphology and vascular relations of tanycytes in the walls and floor of third ventricle of neonatal rats. Two distinct populations of tanycytes, namely dorsal and ventral tanycytes were identified based on their location and structural characteristics.

### **2.3.3 Aqueduct of Sylvius**

The mesencephalic aqueduct was a simple tubular portion that connected the pontine portion of the fourth ventricle caudally and the third ventricle rostrally. In human foetus, Larsell (1951) observed that the cerebral aqueduct became narrow by the enlargement of the quadrigeminal plate and by thickening and differentiation of the basal plate. In domestic animals, Dellmann and Mc Clure (1975) noticed that the aqueduct was slightly dilated at the level of the caudal colliculi. Wall of the aqueduct was lined by ependymal cells, which were heavily modified under the caudal

commissure to form the subcommissural organ (SCO). The aqueduct was surrounded by periaqueductal gray matter containing small neurons and a few myelinated fibres.

#### **2.3.4 Fourth Ventricle**

Dellmann and Mc Clure (1975) described the fourth ventricle as a cavity between the rhomboid fossa ventrally, cerebellar peduncles laterally and rostral and caudal medullary vela and cerebellum dorsally. During embryonic development the originally flat surface of the caudal medullary velum became wrinkled by its association with the choroid plexus and invaginated into the ventricle. At the caudal end of the lateral edges of the fourth ventricle and above the entrance into the central canal, there was a small ridge like area, the area prostroma, one of the circumventricular organs. Absence of foramen Magendie was reported by Malik *et al.* (1978) in goats and Malik *et al.* (2000) in elephants.

#### **2.3.5 Choroid Plexus**

Developmental studies on the choroid plexus were made by Rugh (1964) in the pig. He reported that the anterior choroid plexus appeared in the roof of the third ventricle in 24mm embryo and the posterior choroid plexus developed earlier in the roof of the fourth ventricle. Shuangshoti and Netsky (1966) recognized four stages of development in the histogenesis of the choroid plexus in human beings. First indication of the myelencephalic plexus, consisting of an invagination of mesenchyme into the thin roof area was found in six weeks old embryos. In the telencephalic area, it developed during the seventh week and in the diencephalic area, at eighth week of embryonic age. The invaginations were covered by pseudostratified columnar epithelium, which later changed to low columnar or cuboidal.

Evans *et al.* (1972) studied choroid plexus and blood-brain barrier in foetal sheep from 50 days of gestation to term. They found that the rapid penetration of sucrose in foetuses of 50 to 60 days of age was due to an absence or partly developed blood-brain barrier mechanism. Davis *et al.* (1973) made a comparative ultrastructural study of the choroid plexuses in foetal pigs, from the lateral, third and fourth ventricles. There were no significant differences in the structure of choroid plexus between these regions. The fine structure was found to be similar in most respects to that reported for other domestic animals. There was a single layer of cuboidal to low columnar epithelial cells that were arranged in densely packed villous



folds around a core of vascular connective tissue. Beneath the epithelium, a sub epithelial region containing fibrillar elements and apical cell surface with microvilli was also reported.

In mouse, the plexus was first observed as a bilateral ridge at 11 days post conception (Sturrock, 1979). The major morphological development appeared to occur between 11 and 14 days after conception. By 14 days both dark and light choroid plexus epithelial cells were apparent.

In foetal goats, the primordium of the telencephalic choroid plexus developed from medial ventricular wall, rostradorsal to the interventricular foramen at 5cm CRL followed by diencephalic and mesencephalic plexuses, respectively (Malik *et al.*, 1992). Primary and secondary convolutions differentiated with the advancement of age. Rostral part of the lateral ventricle was practically free of choroid plexus, whereas it was profuse in its middle part especially at the level of interventricular foramina. In the third ventricle, choroid plexus mostly confined to the dorsal part. In the fourth ventricle a high concentration of the plexus was observed at the level of foramina of Luschka, through which it was distributed throughout the cavity. Maximum amount of secretory tissue in the lateral ventricles and a minimum in the fourth ventricle were indicative of rostro-caudal decrease in secretory activity of the ventricular system. Histologically choroid plexus consisted of dilated blood vessels, connective tissue remnants of pia mater and a layer of cuboidal or columnar cells. At a few places pseudostratified ciliated columnar epithelium was also detected.

Vascular pattern of the choroid plexus of the lateral ventricle in the goat was studied by Scala *et al.* (1994). The whole plexus was semilunar in shape and directed in an antero-posterior and latero-median fashion. The capillary network showed a variable organization in different zones of the plexus.

Dyce *et al.* (1996) cited that in domestic animals the choroid plexus of lateral and third ventricle, which merged within the interventricular foramen, developed within an invagination of pia that became entrapped between the expanding telencephalic vesicles and the roof of the diencephalon. The plexus of the fourth ventricle developed separately within the pia over the caudal medullary velum. In the course of development, these plexuses thrust themselves into the lumen of the fourth ventricle. Parts later re-emerged into the subarachnoid space by herniating

through the paired lateral openings in the roof. Rajtova (1997) reported that there were no changes in the structure of choroid plexus surface in sheep and goat foetuses in relation to the age or sex.

## 2.4 NEURONS AND NEUROGLIA

According to Arey (1957), nervous system is composed of two main categories of cells, viz., neurons and neuroglia.

### 2.4.1 Neuron

In 1891, Waldeyer formulated the neuron doctrine, which states that the individual nerve cell is the genetic, anatomic, trophic and functional unit of nervous system. Arey (1957) reported that the neuroblasts or primitive nerve cells initially had a central process extending to the lumen but when they migrated into the mantle zone, this process disappeared and the neuroblasts were temporarily became round and apolar. This migration occurred towards the end of first month of gestation in human foetuses. With further differentiation two new cytoplasmic processes appeared on opposite sides of the cell body, thus formed bipolar neuroblasts. The process at one end of the cell elongated rapidly and formed the primitive axon while the process at the other end transformed into primitive dendrites. These multipolar neuroblasts with further development formed the neuron. Later the power of cell division was lost.

He also observed that mitosis among neuroblasts ceased during the first year of postnatal life in man. Thereafter the nervous system matured and enlarged, but the ability to produce new neurons was lost. Thus the total number of neurons developed in the nervous system was remarkably constant regardless of the size of the individual. As a child grew, the number of synapses increased and the synapses became more complex.

Shape of the perikaryon varied from spherical, ovoid, pyriform, fusiform to polyhedral. Motor neurons in general and pyramidal cells of the cerebral cortex were angular neurons. Neurons of dorsal root ganglia showed rounded cell bodies. Ammon's horn of hippocampal cortex showed double pyramidal cells (Truex and Carpenter, 1969). They described the histological details of neurons in vertebrates. Cytoplasm of a neuron appeared basophilic and had a large pale nucleus with a prominent nucleolus.

The spherical nucleus varied in size from 3-18 $\mu$ m and was centrally placed. Usually a deep staining nucleolus occupied a prominent position in the nucleus. The nucleus played an important role in cytoplasmic protein formation. Masses of granular endoplasmic reticulum in the cytoplasm of neurons were named as Nissl bodies. Nissl bodies were coarser and more abundant in large neurons, especially in motor neurons, and small and scarce in small neurons. They were usually absent from the most peripheral region of the perikaryon, axon hillock as well as the axis cylinder. Nissl bodies were reported to be concerned with the synthesis of cytoplasmic proteins. All nerve cells showed neurofibrils and the axon practically constituted a cable of densely packed neurofibrils. The lipofuscin pigment was absent in the neurons of newborn human foetus. It appeared about the sixth year in the spinal ganglia, a few years later in the spinal cord and after 20 years in the cerebral cortex (Truex and Carpenter, 1969).

The total number of nerve cells in the entire nervous system in man was estimated as about 14 billion. Neurons showed wide variation in size and shape. The absolute size of the cell body varied from dwarf neurons of 4 $\mu$ m diameter (eg. granule cells of cerebellum) to giants approaching 150 $\mu$ m (eg. pyramidal cells of Betz in cerebral cortex). He also found that true unipolar neurons were rare except in early embryonic stages. In bipolar neurons a process projected from each end of the fusiform cell body as found in retina, vestibular and cochlear ganglia and in olfactory epithelium. In vertebrate embryos, all neurons of craniospinal ganglia were first bipolar but during development the opposing processes shifted around the perikaryon and combined into a single process thus forming pseudounipolar neurons. Multipolar neurons were characteristic of the brain, spinal cord and autonomic nervous system (Angevine, 1975).

Further he described two types of neurons depending on the length of axons. Cells with long axons were termed Golgi Type I neurons and those with relatively short axon that did not leave the gray matter as Golgi Type II neurons. He also reported that the Purkinje cells of the cerebellum and the hippocampal pyramidal cells showed tetraploid nature.

Melanin was not present in the foetal or in the neonatal nervous system in the dog (Jenkins, 1978), which increased in amount until puberty in the substantia nigra

and locus ceruleus. The T-shaped pseudounipolar neurons were characteristic of cerebrospinal ganglia and mesencephalic nucleus of the trigeminal nerve (Chrisman, 1991). Bhaskaran (2001) estimated that a volume of 1cc of brain contained nearly  $10^7$  neurons, in human beings.

#### **2.4.2 Neuroglia**

Langman (1981) found that the neuroepithelial cells formed majority of the primitive supporting cells, the glioblasts or spongioblasts, after the production of neuroblasts had ceased. From the inner layer, they migrated to the mantle and marginal layer and developed to form astrocytes and oligodendroglia. In the second half of development, a third type of cell that was believed to originate from mesoderm appeared and was named as mesoglia or microglia. They entered the embryonic brain when the developing brain was penetrated by the blood vessels.

Neuroglia comprised more than 90 percent of the cells that make up the nervous system. Unlike mature neurons, gliocytes remained capable of mitosis and they could give rise to tumours of the nervous system (Dellmann and Eurell, 1998).

##### **2.4.2.1 Astrocytes**

Arey (1957) reported that astrocytes appeared first in the third month in the human foetus. They were the largest and most numerous among the glial cells. Those occupying the gray matter were named protoplasmic astrocytes and those developed in the white matter became fibrous astrocytes.

Chrisman (1991) noticed that the astrocytes formed a complete membrane on the external surface of the brain and referred to as the external glial limiting membrane. They also fused with ependymal glial cell processes, and formed an internal glial limiting membrane. Astrocyte feet surrounded all blood vessels and regulated the ion and water environment of the neurons. During disease processes, these cells proliferated and produced glial scars.

##### **2.4.2.2 Oligodendrocytes**

Arey (1957) noticed that the oligodendroglia arose at a later period than astrocytes. Cammermeyer (1966) described the morphologic distinctions between oligodendrocytes and microglia cells in the cerebral cortex of rabbit. The oligodendrocytes were seen in close proximity to blood vessels. Microglia were

usually situated in juxtaposition to neurons and were rarely found along the blood vessels. It was further stated that the oligodendrocytes were rare and had a more restricted function, while the microglial cells were abundant and had a wider function. In human foetuses, Angevine (1975) found that the oligodendrocytes were intimately related to the nerve fibres, along which they formed rows or columns. This cell formed the myelin sheath in the CNS. In the gray matter, oligodendrocytes adjoining the nerve cells were the principal type of satellite cells.

#### **2.4.2.3 Microglia**

Angevine (1975) reported that the nucleus of the microglia was small but deeply stained and surrounded by scant protoplasm. The few extensions were short, and unlike the straight extensions of astrocytes, were twisted in various ways. Boya *et al.* (1979) studied the origin and evolution of amoeboid microglia in the postnatal rat and confirmed the mesodermal origin of microglia. Invasion of nervous parenchyma by globular acid phosphatase positive cells began before birth. After invasion they adapted their shape to their surroundings, sending out irregular processes. The processes were detectable with histochemical techniques because of their content of acid phosphatase granules. None of these cells gave a positive reaction for peroxidase.

The topographical distribution of amoeboid and ramified microglial cells in the telencephalon was reported by Trautwein and Schulthesis (1994) in sheep foetuses and Trautwein *et al.* (1996), in bovine foetuses. Numerous cells were found in subependymal regions of the lateral ventricles, in the septum pellucidum, within the cavum pellucidum, in the corpus callosum and in the internal and external capsule between 60 and 96 days in sheep foetuses and between three and five months of gestation in bovine. From 84 days of gestational age onwards, the occurrence of ramified microglial cells were noted in sheep foetuses. This was noted from three to four months of gestational age in bovine foetuses. Thereafter the cells gradually disappeared and not detectable at term. Distribution of microglial cells was similar to that described in the brain of rodents, but their earlier disappearance of this cell type from the telencephalon of ovine and bovine brain was interpreted as a reflection of the more rapidly proceeding brain development in these animals than in other vertebrates.

#### 2.4.2.4 Ependyma

Arey (1957) reported that when the neuroepithelial cells ceased to produce neuroblasts and glioblasts, they finally differentiated into ependymal cells. Kozlowski *et al.* (1972) and Rajtova (1999) studied the ependyma of third ventricle in foetal sheep and goat. Between 40 and 50 days of development, three to four layers of cells were noticed. Gradually the cell layers transformed into a pseudolayered type by 130 days and became the typical one layered ependyma shortly after birth. In the region of the third ventricle, between days 50 and 130, a coarctation was formed, where many foetal ependymal cells were mitotically active. The surfaces of the apical membrane of proximal processes as well as the bodies of foetal ependymal cells, except for cilia, were covered with microvilli and spherical secretory protrusions. They suggested that in small ruminants, the ependymal surface was already regionally differentiated by the end of first half of prenatal development and characterized by a high secretory activity independent of sex or age of foetuses.

Ependymal lining of the adult ventricular system was examined by Worthington and Cathcart (1963) in man, Allen and Low (1973) in dogs, Lindberg *et al.* (1991) in ox and Kumar *et al.* (1997) in goats. Ependyma was reported to be ciliated throughout in man. But in the dog, non-ciliated areas also occurred along the medial wall of the lateral ventricles. In goats, roof of the third ventricle in its mid-portion presented synchronous wave-like dense arrangement of cilia.

## 2.5 MENINGES

Meninges are fibrous membranes, which enclose, protect and nourish the brain and the spinal cord. Studies on the meninges of mammals were made by several authors (Arey, 1957; Truex and Carpenter, 1969; Dellmann and Mc Clure, 1975; Jenkins, 1978; King, 1987; Dyce *et al.*, 1996). All of them reported that there were three membranes namely, the dura mater, arachnoid and pia mater. The dura mater was referred to as the pachymeninx because of its tough fibrous nature. The arachnoid and pia mater were connected, and together they were referred to as the leptomeninx because of their thin delicate nature. All three coats arose as condensations of the neighbouring mesenchyme, although migrant cells from the neural crest might contribute slightly to the delicate pia-arachnoid that lay next the

neural tube. The tough dura mater was a distinct membrane at eight weeks of gestation, in human fetuses.

Singh and Dhingra (1978) studied on the morphogenesis of the hypophyseal meninges in goat. The hypophyseal dura mater started differentiating in embryos of 24.8mm CRL at caudodorsal surface of the primordium of neurohypophysis. The formation of arachnoid was evident in embryos of 55.5mm CRL. It assumed a typical fibrous structure at 135.0mm CRL. Pia mater encapsulated the whole primordium in 12.0mm CRL embryos.

### **2.5.1 Dura Mater**

Dellmann and Mc Clure (1975) reported that the dura mater of the cranial cavity was closely united with the endosteum of the cranial wall but in the vertebral canal it was separated from the vertebral endosteum by the epidural space. Cranial dura consisted of two layers: (1) a thin inner layer of dense fibrous tissue lined on its internal surface with a single layer of flat cells; and (2) an outer layer much richer in blood vessels and nerves, which formed the periosteum. Between these two layers were the large venous sinuses of the brain.

Histologically the dura mater was made mostly of white collagen fibres and was the thickest of the three meninges (Jenkins, 1978). Elastic fibres, fibrocytes, nerves, and lymph and blood vessels were also present. The surface facing the arachnoid was covered by simple squamous epithelium (Dellmann and Eurell, 1998).

Cranial dura had three internal folds, which helped to support the brain within the cranial vault. The first projection, falx cerebri, extended ventrally within the median longitudinal fissure toward the corpus callosum. The falx cerebri was derived from the mesodermal tissue, which occupied the cleft between the growing telencephalic vesicles. Caudally this septum fused with the second septum, tentorium cerebelli named because of its tent-like shape. The diaphragma sellae was a rostral continuation of the tentorium cerebelli on the base of the skull, which passed over the hypophysis where it had a central foramen through which passed the infundibulum. In the sheep and goat, the rostral portion of falx cerebri was narrower, being about 1cm wide; the caudal portion was perforated or incomplete (Ghosh, 2002).

### 2.5.2 Arachnoid

Arachnoid was a very thin membrane in domestic animals, which pressed against the dura mater by the pressure of cerebrospinal fluid (CSF). Reflected from it were numerous fine filaments, which blended with the pia mater. These filaments resembled a spider's web, hence the term 'arachnoid' (Buchanan, 1957). He also observed that histologically, the arachnoid in animals consisted of a lamina of delicate collagenous connective tissue coated on both sides by simple squamous epithelial cells. Many elastic fibres were seen interspersed in the arachnoid as reported by Pease and Schultz (1958) in rat.

The arachnoid in animals was not extended into the sulci of brain but merely bridged the indentation. In certain locations the cerebral arachnoid was separated from the pia by a considerable distance to form the subarachnoid cisterns. Cisterna magna was located in the angle formed by the caudal surface of the cerebellum and the dorsal surface of medulla. Cisterna fossa lateralis cerebri was seen over the lateral cerebral fissure and cisterna chiasmatis, rostral to the optic chiasma (Dellmann and Mc Clure, 1975).

Prasad and Sinha (1983) conducted histological and histochemical studies on the saccular modification of pia-arachnoid present over the pineal gland in buffaloes. Arachnoid formed primary, secondary and tertiary invaginations accompanied by vessels, nerves and connective tissue.

Studies on the arachnoid granulations were made by King (1987) in domestic animals. These were tufted prolongations of pia-arachnoid through the inner layer of dura into the dural sinuses. Histologically each granulation demonstrated numerous villi, which showed thin outer limiting membrane deep to which were bundles of collagen and elastic fibres. Arachnoid granulations more frequently occurred with advancing age.

Morse and Low (1972) described the fine structure of subarachnoid macrophages in the rat. These had fine structural characteristics, which distinguished them from macrophages. They possessed a highly vacuolated cytoplasm. Sturrock (1988) studied the development of leptomeningeal macrophages in mice and rabbits. Macrophages could be identified in the leptomeninges of spinal cord in 11<sup>th</sup> and 12<sup>th</sup> day old embryos, respectively. The structural changes found in the macrophages were



similar to those observed during the development of intraventricular macrophages and microglia.

### **2.5.3 Pia Mater**

Jenkins (1978) opined that the pia mater was the most delicate of the three, and had a high concentration of very fine elastic fibres, in canines. It was highly vascularised and extended deeply into the sulci of cerebrum and cerebellum.

According to King (1987) the pia mater was thicker than the arachnoid but thinner than the dura mater, in domestic animals. Its inner surface was fused to the brain.

Shrivastava *et al.* (1989) found that in foetal goats, the pia was composed of extracellular elements in the form of interlacing loose collagen and elastic network, indifferent mesenchymal cells, variably differentiated cells and also some macrophages, mast cells and lymphocytes. They compared the thickness of pia mater over the surface of different regions of brain in the foetal goat. The thickness was maximum over the midbrain and minimum over the medulla oblongata with peak growth in early stages of gestation. Over the cerebral hemisphere, the growth increased in mid and later stages of gestation. They suggested that the variation in the regional thickness of pia mater might be based on the regional vascularity since pia mater served as a pathway for blood vessels supplying to the different parts of brain.

## **2.6 HISTOCHEMISTRY**

### **2.6.1 Lipids and Myelin**

Kappers *et al.* (1967) indicated that certain regions of brain became medullated much earlier than others and that the series of medullations occurred in a regular way. In the cerebrum, the first fields that became medullated were those in which sensory impulses were located. Of these, the olfactory fields, paleocortex and the archicortex showed myelination at an earlier stage indicating their early phylogenetic origin. Then followed the regions of the neocortex.

Patterson *et al.* (1971) studied changes occurring in chemical composition of CNS during foetal and postnatal development of the sheep. Chemical growth proceeded linearly in the spinal cord, logarithmically in cerebrum and cerebellum and by a sigmoid fashion in the brainstem. Fat-free dry matter, protein, total lipid,

cholesterol and phospholipid content increased progressively in all parts of the CNS. Cholesterol esters were detected from 70 to 120 days of gestation. Cerebroside, the characteristic lipid of myelin, increased soon after 85 days. Rate of increase in total regional cerebroside content suggested that there were two periods of peak activity, one about 20 days before birth and the other at 10 to 20 days after birth.

Development of myelin sheath of the cranial nerves in the bovine medulla oblongata was studied by Jastrzebski (1973). Myelination in the bovine foetus began during the 20<sup>th</sup> week. In the 22<sup>nd</sup> week, half the fibres and in 25<sup>th</sup> week all the fibres had myelin sheaths, which were only half as thick as their axis cylinders. Most axis cylinders and myelin sheaths attained the same thickness in the 36<sup>th</sup> week. He opined that at this stage, the sheaths could be considered as mature.

A variable concentration of lipids in the pineal gland of goats was described by Saigal *et al.* (1976) and Kumar *et al.* (1998).

Langman (1981) indicated that myelination in human foetuses began at fourth month. He suggested that tracts in the nervous system became myelinated at about the time they started to function.

Presence of lipids in ependymal cells of subcommissural organ was reported by Ramakrishna and Saigal (1987) in buffaloes and Kumar *et al.* (1996) in goats.

Urban *et al.* (1997) studied the development of myelination in bovine foetal brain. Immunohistochemical studies revealed thin and spiral myelin sheaths during foetal and elongated myelin fibres during postnatal periods. A caudo-rostral progression of brain myelination was observed with the advancement of gestational age. Myelinated fibres were not detected in foetuses below three months of age. Myelination was similar in the brain of nine month-old foetuses and day-old calves. Density of stained myelin fibres in the brain of three-month-old calves and adult cattle was similar.

### **2.6.2 Carbohydrates**

Shuangshoti and Netsky (1966) found that glycogen was prominent in the developing choroid epithelial cells in the brain of human beings, which disappeared in the mature plexus. Truex and Carpenter (1969) reported that between 29 weeks and full term, these cells lost its glycogen in human foetuses. Once removed, the glycogen never reappeared as a normal constituent of the adult choroid epithelium.

They suggested that such disappearance of glycogen after birth, or at the beginning of aerobic oxidation, might be due to the fact that the developing nervous tissue used energy, which was released by the anaerobic metabolism of glycogen. Jenkins (1978) noticed the glycogen in the ependyma, choroid plexus and neurons of embryonic brain in canines. Epithelial and mesenchymal mucin and mucopolysaccharide were identified in the choroid plexuses of foetal mice and goats by Sturrock (1979) and Malik *et al.* (1992), respectively.

Manocha and Shantha (1969) reported that different layers of cerebral cortex in human foetuses showed a diffuse reaction with  $\beta$ -glucuronidase and were considerably weaker than other parts like hypothalamus, SCO, choroid plexus, pineal gland etc.

Kumar *et al.* (1998) demonstrated carbohydrates throughout the parenchyma of pineal gland, in the goat. Cytoplasm of pinealocytes and all types of glial cells had PAS- positive fine granules of lesser intensity whereas, the processes of cells along trabecular glial fibres showed moderate activity. Vacuolated scattered areas among the cell population were negative for PAS reaction.

Prasad and Sinha (1983) observed an intense reaction for mucin in the lining cells of arachnoid folds in the buffaloes. Glycogen granules were located in the apical portion of the cells.

Ramakrishna and Saigal (1987) reported the presence of a glycoprotein containing sulphated mucosubstances in the hypendymal cells of the subcommissural organ (SCO) in goats. Neutral mucopolysaccharides at the intercellular junctions of the ependymal cells of the SCO in goat have been located by Kumar *et al.* (1996).

### **2.6.3 Phosphatases**

Talanti (1959) reported that in the bovine foetus, the activities of alkaline and acid phosphatases were demonstrable in SCO at as early as three months of gestation. Intensity of reaction increased up to the age of four months till the postnatal levels were attained. Enzymatic activities were localized principally in the ependyma and in the parietal cells of the hypendymal ducts. In the SCO of male goats, Kumar *et al.* (1997) localized homogenous activity of acid phosphatase (ACP) throughout the ependyma and blood capillaries whereas, alkaline phosphatase (ALP) was mainly

distributed at the base of the ependyma. Weak and moderate reactions were observed towards the free surface and hypendyma, respectively.

Niespodziewanski (1964) studied the histochemical activity of phosphatases in the developing cerebellum of pigs. Greatest changes in the enzyme activity occurred up to the 10<sup>th</sup> week of foetal life. Localisation of phosphatases was not stable; initially they predominated in the nucleus, and later in the nuclear and cellular membranes or in the cytoplasm. Both these enzymes were reported to take part in the structural formation of cerebellum. In the brain of adult human beings, positive ACP activity was described in Purkinje cells, Bergmann glial cells, granule cells, Golgi type II cells, astrocytes, basket fibres and molecular layers (Manocha and Shantha, 1969).

Further they found that the ALP activity was intense in the blood vessels, pia-arachnoid and choroid plexus of brain, but ACP activity was most prominent in the neurons, particularly at the site of lipofuscin pigments. While the neurons and the axonal and dendritic processes were negative in ALP preparations, the synaptic regions were positive both on the cell surface and on the cell processes in the form of granular deposits in the cerebral cortex. The plexiform layer showed a more prominent reaction than the other layers of the cortex. The blood vessels were strongly positive. Enzyme activity was consistent in the intima, while the adventitia showed variable enzyme activity in various species. Neurons of the cerebral cortex especially the pyramidal cells gave a strong reaction for ACP. In Ammon's horn, the ACP activity was extremely strong.

Tam and Kwong (1987) reported that a high ALP activity was seen in the brain of foetal mouse and the activity diminished progressively during development. Maximum enzymatic activity was observed in the developing hypothalamus.

## *Materials and Methods*

---

### 3. MATERIALS AND METHODS

Prenatal development of the brain was studied in foetal goats of different age groups. The investigation was carried out using 52 goat foetuses comprising of 10 sexually indifferent, 22 male and 20 female foetuses. The material available in the department of Anatomy and those collected from the farms and clinics were used for the study. Body weight, body parameters and skull parameters of the subjects were recorded. The age of the foetuses was calculated from the formula derived by Singh *et al.* (1979) for the goat foetuses,

$$W^{1/2} = 0.096 (t-30), \text{ where}$$

W= Body weight of the foetus in g

t = Age of the foetus in days

The sex, body weight (ranging from 0.279g to 2800.000g), age (from 24 days of gestation to full term) and crown rump length (from 1.4cm to 41.5cm) of the foetuses are shown in table 1. Based on the age, the foetuses were divided into five groups, viz., Group 1, 2, 3, 4 and 5 representing five months of gestation as shown in table 2. Embryos of the Group 1 were fixed in toto for histological and histochemical investigations. From Group 2 onwards, the head was separated at the occipito-atlantal junction and the following measurements were recorded.

1. Length of head - From the mid-point between the bases of ears to the middle of the maxillary lip (straight and curved distances).
2. Length of cranium (Neurocranial length) - From the mid-point between the bases of ears to the mid-point between medial canthi (straight and curved distances)
3. Length of face (Splanchnocranial length) - From the mid-point between medial canthi to the middle of maxillary lip.
4. Interauricular distance - Transverse distance between the bases of ears.
5. Interorbital distance (measured at two levels)
  - (a) Transverse distance between the medial canthi (minimum interorbital distance)
  - (b) Transverse distance between the lateral canthi (maximum interorbital distance)
6. Transverse distance between dorsal commissures of nostrils.

7. Maximum cranial width (Head width) - Transverse distance between the supraorbital processes of frontal bones (straight distance).
8. Intercornual distance - Transverse distance between the horn buds.
9. Intersupraorbital foramina distance
10. Cranial height – Vertical distance between the basioccipital and the parietal bones
11. Posterior cranial height - Distance from the upper limit of foramen magnum to the frontal eminence (curved distance).
12. Skull base length - Distance from the mid-point of the ventral margin of foramen magnum to the middle of lower lip (straight distance).

The cephalic and neurocranial indices were calculated from the formulae following Archana *et al.* (1998) for the yak,

$$\text{Cephalic index} = \frac{\text{Head width}}{\text{Head length}} \times 100$$

$$\text{Neurocranial index} = \frac{\text{Neurocranial width}}{\text{Neurocranial length}} \times 100$$

After recording these, the skin of the head was removed along with the external ears and the following craniometric details were recorded on the exposed skull using Vernier Callipers.

1. Anterior width, posterior width, medial length and lateral length of parietal bone.
2. Medial length of frontal bone.
3. Mid-sagittal length and width of interparietal bone.
4. Length of nasal bone.
5. Mid-sagittal length, maximum width and minimum width of basioccipital bone.
6. Mid-sagittal length of basisphenoid.
7. Mid-sagittal length of presphenoid.
8. Maximum height and width of foramen magnum.
9. Mandibular length - It is measured as the distance from the caudal border of the vertical ramus of mandible to the rostral margin of the body of the mandible.
10. Maximum intermandibular distance: At the level of angles of the mandible.

The brain was then carefully dissected out and fixed in 10 percent neutral buffered formalin. After measuring the volume by water displacement method, these were blotted and weighed. The following details were recorded.

### 3.1 WHOLE BRAIN

1. Length - The distance between the frontal pole of cerebral hemispheres and the rostral limit of origin of the first pair of cervical spinal nerves.
2. Width - Recorded at the point where it recorded the maximum.
3. Height - Maximum height at the level of parietal lobe of cerebral hemisphere.

After recording these, the cerebral hemispheres were dissected from the brain stem just rostral to optic chiasma at the level of lamina terminalis. The cerebellum was also dissected from the brainstem. The following measurements were taken.

### 3.2 CEREBRUM

1. Weight of the right and left cerebral hemispheres separately.
2. Length, width (maximum and minimum) and height of the right and left cerebral hemispheres.
3. Average width of cerebral gyrus (width of coronal gyrus was recorded).
4. Length, width and thickness of olfactory bulb.
5. Length and width of lateral and medial olfactory tracts.
6. Width of trigonum olfactorium.
7. Length and width of the caudal part of the piriform lobe.
8. Length and thickness of corpus callosum.
9. Length of major sulci.

### 3.3 CEREBELLUM

1. Weight
2. Length - Rostro- caudal distance of the vermis of cerebellum.
3. Width - Transverse distance at the level of brachium pontis.
4. Height (maximum)
5. Length and width of vermis
6. Mean length and width of lateral cerebellar hemispheres.



### 3.4 BRAINSTEM

1. Weight
2. Length - From lamina terminalis (rostral to optic chiasma) to the rostral limit of origin of first pair of cervical spinal nerves.
3. Width - Maximum width at the level of the thalami and minimum width at the caudal end of medulla oblongata.
4. Height - Maximum at the level of rostral colliculus and minimum at the caudal end of medulla oblongata.

### 3.5 DIENCEPHALON

1. Weight
2. Length - Rostro-caudal distance from lamina terminalis to the caudal border of mamillary body.
3. Width and thickness of diencephalon.
4. Length and width of optic chiasma.
5. Width of mamillary body.

### 3.6 MESENCEPHALON

1. Weight
2. Length - Rostro-caudal distance from cranial border of rostral colliculus to the cranial border of pons.
3. Width and thickness of mesencephalon.
4. Length and width of the rostral colliculus.
5. Length and width of caudal colliculus.
6. Length of crura cerebri.
7. Width of interpeduncular fossa
8. Length, transverse diameter and vertical diameter of aqueduct of Sylvius.

### 3.7 PONS

1. Weight
2. Length and width of pons

### 3.8 MEDULLA OBLONGATA

1. Weight

2. Length - Rostro-caudal distance from the caudal border of pons to the rostral limit of origin of first pair of cervical spinal nerves.
3. Width (maximum and minimum) and thickness.
4. Width of trapezoid body.
5. Width of medullary pyramids.
6. Length, width and height of fourth ventricle.

After recording the biometry and gross features, the tissue pieces were processed and paraffin sections of 4 to 5 $\mu$ m thickness were taken for histological studies. For histochemical demonstration of lipids and phosphatases, frozen sections of 10 $\mu$ m thickness were used. Embryos of Group 1 were fixed in toto and serial sections were taken to trace the developmental pattern of the neural tube.

The following staining techniques were employed.

1. Haematoxylin and eosin staining technique for routine histological studies (Luna, 1968).
2. Van Gieson's method for collagen (Luna, 1968).
3. Holzer's method for glial fibres (Luna, 1968).
4. Sevier-Munger silver impregnation method for neural tissues (Luna, 1968).
5. Holme's silver nitrate luxol fast blue method for axis cylinder and myelin sheath (Humason, 1972).
6. Aldehyde-thionine-PAS method for central nervous system (Luna, 1968).
7. Phosphotungstic acid haematoxylin (PTAH) method for CNS tissue (Luna, 1968).
8. Periodic acid Schiff's reaction for carbohydrates (Bancroft and Stevens, 1977).
9. Best's carmine method for glycogen (Bancroft and Stevens, 1977).
10. Gomori's alkaline phosphatase cobalt method (Singh and Sulochana, 1996).
11. Gomori's method for acid phosphatase (Singh and Sulochana, 1996).
12. Oil Red O in propylene glycol method for fat (Luna, 1968).

The data on the following physical parameters were analysed statistically (Snedocor and Cochran, 1985) to find out the relationship between the following, if any:

1. The foetal age and the whole brain parameters (weight, volume, length, width and thickness of brain).
2. The foetal body weight and the whole brain parameters.

3. Body parameters (straight CRL, curved CRL, total body length, total bent length, vertebral column length, vertebral column tail length, tail length, forelimb length, hindlimb length, tibial length, chest depth and chest circumference) and the brain parameters.
4. The head parameters (head length, head width, cranial length, facial length, interauricular distance, transverse distance between medial canthi, lateral canthi and corneal buds, intersupraorbital foramina distance, posterior height from foramen magnum) and the brain parameters.
5. The skull parameters (skull length, skull width, cephalic index, neurocranial length, neurocranial index, cranial height, minimum interorbital distance and height and width of foramen magnum) and the brain parameters.
6. The parameters of skull bones forming the roof and the base of the cranial cavity.
7. The skull bone parameters (medial length of frontal, parietal, nasal, interparietal, supraoccipital, basisphenoid, presphenoid, and mandible) and the brain parameters.
8. The encephalometric parameters (weight, length, width and thickness of cerebrum, cerebellum and brainstem) and the body parameters like body weight, age and straight CRL.
9. The craniometric parameters (skull length, skull width, neurocranial length, neurocranial width, cranial height, facial length, length of frontal, parietal, basioccipital, basisphenoid and presphenoid bones, anterior width of parietal bone and height of supraoccipital bone) and the encephalometric parameters like weight, length, width and thickness of cerebrum, cerebellum and brainstem.
10. The whole brain parameters and the parameters of components of brain (cerebral, cerebellar and brainstem parameters).

### 3.9 MICROMETRY

To study the changes in the thickness of various layers of neural tube, the width of its entire wall and the component layers were measured using an ocular micrometer. The width of different layers of cerebrum, cerebellum and brainstem were also measured in order to trace their growth pattern. The data were analysed statistically (Snedocor and Cochran, 1985) to find out the significance, if any.

## *Results*

---

## 4. RESULTS

### 4.1 DEVELOPMENT OF THE NEURAL TUBE IN THE FIRST MONTH

#### 4.1.1 Brain Vesicles

In goat embryos of 24 days of age with a crown rump length (CRL) of 1.4cm, the neural tube was completely fused and the brain vesicles started developing. Five expansions were evident at the cranial end of the neural tube, the rostral-most being the telencephalon. The single lumen was yet to develop into the two lateral ventricles. Optic vesicles were seen on either side of the next region, the diencephalon. The three enlarged regions of the brain caudal to these were the mesencephalon, metencephalon and myelencephalon. In 26 days-old embryos (1.5cm CRL), demarcation between the five vesicles was more distinct.

##### 4.1.1.1 Morphogenesis

Micrometrical parameters of telencephalon during the first month of gestation are given in table 3. Width of telencephalon was more than its height. Dorsal wall was thinner than the ventral wall (Fig. 1). Lateral walls were the thickest. In 24 days-old embryos, the cavities within the two telencephalic vesicles were broadly continuous with the primary lumen of the neural tube. By 27 days of gestational age (1.6cm CRL), the lateral ventricles communicated with the third ventricle through the paired interventricular foramina of Monro (Fig. 2). Lateral ventricles were long and narrow (Fig. 3). A large cavernous sinus was located near the ventral wall of telencephalon.

Near the telencephalon, olfactory pits were seen on either side (Fig. 4). Measurements of olfactory pits are given in table 3. The wall was lined by multilayered ectodermal epithelium consisting of columnar cells with basally located elongated nuclei. Medial wall was thicker than the lateral wall. In the case of open olfactory pits, each pit was bordered by lateral and medial nasal processes (Fig. 5). By 26 days of gestation, the olfactory pits were further enlarged.

The wall of diencephalon showed a very thin dorsal roof plate and paired alar plates; the latter constituted both the sides and floor of the tube. Micrometrical parameters of diencephalon in the first month of gestation are given in table 4. Cavity of the diencephalon, the third ventricle, was relatively broad in 24 days-old subjects.

By 26 days of age, the lateral walls started thickening and compressed the lumen (Fig.6). On the ventrolateral aspect, the internal carotid arteries were seen. At the age of 27 days, basal margins of the diencephalon were united by a trough-like floor forming the hypothalamus (Fig. 7).

By 24 days of age, the epithelial lobe of hypophysis (Rathke's pouch) appeared close to the ventral wall of the diencephalon. At the age of 27 days, the Rathke's pouch developed a lumen (Fig. 8). Lateral to the diencephalon were the optic cups attached to it by the optic stalks (Fig. 9). The optic cup was formed of two layers of cells (Fig. 10). The inner layer developed into the nervous elements of the retina. The thin outer layer formed the pigmented layer. By 27 days, the lens was a closed vesicle distinct from the overlying corneal ectoderm.

The midbrain was proportionately large and elongated and was least modified from the primitive neural tube in the first month of gestation. Micrometrical parameters of mesencephalon during the first month of gestation are given in table 5. Total width of mid-brain exceeded the total height in this group. Accordingly the width of lumen was also more than the height. As in the case of telencephalon, the lateral walls were the thickest, followed by the ventral and dorsal walls (Fig. 11). Section across the midbrain revealed the same divisions as in the spinal cord; lateral neural plates made up of alar and basal laminae united by the roof and floor plates, respectively. A prominent sulcus limitans divided the alar and basal laminae (Fig. 12).

There was no clear demarcation between the metencephalon and myelencephalon in the 24 days-old embryos. Their walls bore the prominent scalloping of neuromeres (Fig. 13). The common cavity was the fourth ventricle. By 27 days of age, the basal plate became much thicker. Next to the metencephalon was the unpaired basilar artery (Fig. 14). Junction between metencephalon and myelencephalon was demarcated by the sharply defined otocyst (Fig. 13). At 27 days of age, ventral wall of metencephalon showed a bundle of nerve fibres of the trigeminal nerve (Fig. 15).

Near the beginning of the hindbrain were the large semilunar ganglia (Fig. 16). These ganglia were situated at the pontine flexure of the metencephalon. From its medial side, nerve fibres of the trigeminal nerve joined the brain wall by 27 days of age. Near these ganglia, transverse sections of mandibular and maxillary branches of

trigeminal nerve were seen (Fig. 17). Just rostral to the ganglion, portion of cavernous sinus was seen (Fig. 16). Slightly caudal to that lay the facial nerves, which appeared as emerging from the hindbrain (Fig. 18). Midway along each side of the hindbrain was the otocyst with an elongated lumen, and medial to it was the endolymph duct (Fig. 13). On the rostral side of the otocyst occurred the geniculate ganglion of the facial nerve and the acoustic ganglion of the acoustic nerve (Fig. 19). Lumen of the otocyst appeared semilunar in shape. Caudal to the otocyst, transverse section of the glossopharyngeal nerve and the jugular ganglion of the vagus nerve were seen while the trunk of the accessory nerve was sectioned lengthwise as it curved forward from the level of the spinal cord (Fig. 20).

Between the myelencephalon and the pharynx several rootlets of the hypoglossal nerve were seen on either side (Fig. 21). In 24 days-old embryos, wall of the metencephalon and myelencephalon showed the typical arrangement of longitudinal alar plates and basal plates and the sulcus limitans (Fig. 22). Micrometrical parameters of metencephalon and myelencephalon in the first month of gestation are shown in tables 6 and 7, respectively. Basal plate was thicker than the alar plate. In the myelencephalon, the lumen was diamond-shaped towards the caudal end (Fig. 22). Froriep's ganglion of spinal accessory nerve was seen on both sides. Thickness of the basal plate increased in embryos of 26 days of age and the lumen became narrower and coffin-shaped (Fig. 23). By 27 days of age, the alar plates also projected into the lumen. The lumen at this stage was slit-like except at the region of sulcus limitans (Fig. 24). Height of the myelencephalon considerably increased by that time.

Correlation and regression coefficients of brain vesicle parameters were calculated (Table 8).

#### ***4.1.1.2 Histogenesis***

At the age of 24 days, external and internal limiting membranes bounded the wall of neural tube and each measured  $4.0\mu\text{m}$  in thickness. Cellular elements of the wall (neuroepithelial cells) were arranged radially in a pseudostratified manner. At this stage, wall of the neural tube was organized so that three concentric zones were distinguished. Inner ependymal layer was the thickest of all and composed of more or less elongated cells that were radially arranged about the lumen of the neural tube

(Fig. 25). This represented the germinal layer of proliferating neuroepithelial cells. The nucleus was elongated or oval and the cell boundaries were indistinct. Mitotic figures or germinal cells with large spherical nuclei could be seen towards the luminal surface (Fig. 26). Middle nucleated mantle layer derived from proliferation of innermost cells was a narrow zone. This formed almost one-fourth of the total width of the wall. Here the nuclei were spherical and the cells were loosely arranged than those of the ependymal layer. Two types of cells were distinguished: the neuroblasts and the spongioblasts. Neuroblasts possessed larger pale staining vesicular nuclei with small dark nucleoli (Fig. 27). Nucleus of the neuroblast measured  $6.0\mu\text{m}$  in diameter with a nucleolus of about  $1.0\mu\text{m}$  size. By 27 days of age, the neuroblasts started developing small processes to become primitive neurons or multipolar neuroblasts (Fig. 27). Condensation of chromatin was evident at the periphery of the nucleus. The spongioblasts were more in number and possessed smaller ( $4.0\mu\text{m}$ ) and darker nuclei.

By 24 days of gestation, scattered nucleated erythrocytes were noticed in both ependymal and mantle layers. Blood channels lined by endothelial cells started penetrating into the neural tube wall from the pia mater by this stage (Fig. 26). As the development proceeded, the vascularity also increased. The outer non-cellular marginal layer was the thinnest, composed of growing processes of neuroblasts in the mantle layer. This layer was limited by the external limiting membrane. By 26 days, width of the marginal layer increased and showed some spongioblast nuclei (Fig. 28). In 24 days-old subjects, the ventral wall of the neural tube was more organised with all the three layers whereas, the dorsal wall showed only two layers (Fig. 11). The mantle layer was not clearly distinguishable. Later, width of the mantle layer markedly increased with a corresponding reduction in the width of ependymal layer. This was the general appearance of the neural tube wall in the first month of gestation.

In the region of the hindbrain, by 24 days, the basal plate showed a clear differentiation of mantle layer but this was not so evident in the alar plate region (Fig. 22). In 26 days-old embryos, both the basal and alar plates showed all the three layers (Fig. 23). In the basal plate, the mantle layer was the widest, followed by the ependymal and the marginal layers. In the alar plate, the ependymal layer was thicker than the mantle layer. In the ventral commissure region, only two layers were seen; the ependymal and marginal layers (Fig. 29). Roof plate was very thin and formed of



a single layer of ependymal cells. The ventral commissure and roof plate did not contain neuroblasts: they served primarily as pathways for nerve fibres crossing from one side to the other.

Surrounding the external limiting membrane of the neural tube, mesenchymal cells started condensing by 24 days of age (Fig. 25). Many nucleated red blood cells were also present in this region. This represented the future pia mater. Condensation of mesenchymal cells was more distinct towards the ventral wall. Peripherally the membranous cranial capsule surrounded this. By 27 days, the primitive pia mater fully encircled the neural tube (Fig. 30).

#### **4.1.2 Brain Flexures**

Differential growth of the rostral end of the neural tube gave rise to flexures in the developing brain. As head folding occurred, the brain bent ventrally at the level of the mesencephalon forming the cephalic flexure. The less pronounced cervical flexure indicated the boundary between the myelencephalon and the spinal cord. This was less pronounced. Unequal growth in the rhombencephalon produced a slight dorsal folding, the pontine flexure (Fig. 31). Another constricted region, the isthmus, lay at the junction between mesencephalon and metencephalon. All these flexures were developed in the 24 days-old embryos.

## **4.2 DEVELOPMENT OF THE BRAIN FROM SECOND MONTH TO TERM**

### **4.2.1 Encephalometry**

#### ***4.2.1.1 Relationship between Age and Brain Parameters***

##### **4.2.1.1.1 Weight of the Brain**

Body parameters of goat foetuses at different stages of gestation are presented in table 9. Relatively low body weight gains were recorded up to mid gestation (Fig. 32). A spurt in growth was noticed between fourth and fifth month. Straight and curved crown rump length (CRL) increased progressively with age (Fig. 33). Encephalometry of goat foetuses during prenatal period is given in table 13. Brain weight showed an increasing trend with advancement of age. From the 10<sup>th</sup> week, very rapid increase was observed in the body weight and brain weight. A spurt in brain growth was noticed between fourth and fifth month (Fig. 34). Correlation coefficients of whole brain parameters on body parameters are presented in table 29.

Brain weight was highly correlated with age of the embryo ( $r = 0.952$ ). Brain weighed  $1.108 \pm 0.163$ g,  $5.914 \pm 0.835$ g,  $14.462 \pm 0.136$ g and  $40.728 \pm 2.986$ g during second, third, fourth and fifth month of gestation, respectively (Table. 13). As a whole, brain weight increased 76-fold from 0.700g (40 days) to 53.540g (full term). About 50 percent of foetal body weight and brain weight were attained by 18 to 19 weeks of gestation.

#### 4.2.1.1.2 Volume of the Brain

Volume of the brain at different stages of gestation is given in table 13. Brain volume also increased from second month to full term. Mean values were slightly more than the corresponding values of brain weight in all the age groups studied. Brain volume was positively correlated with age ( $r = 0.954$ ) vide table 29.

#### 4.2.1.1.3 Size of the Brain

Length, width and thickness of the brain at different stages of gestation are presented in table 13. All these parameters showed an increasing trend with the advancement of age (Fig. 35). Brain length increased from 1.300cm at 40 days to 7.700cm in full term foetus. Similarly the width and thickness increased from 0.700cm and 0.600cm to 5.190cm and 3.300cm respectively. In all age groups, length of the brain was more than its width followed by the thickness (Fig. 52). Length of the brain and its various components showed more significant correlation with the age than the body weight (Tables 29 & 34).

#### 4.2.1.1.4 Cerebrum

The cerebral hemispheres were much wider caudally than rostrally and showed definite pattern of gyri and sulci identical to those of an adult in the terminal stages of pregnancy. Mean cerebral weight increased from  $0.316 \pm 0.025$ g to  $15.383 \pm 1.196$ g from the second month to the fifth month of gestation (Table. 13). Percentage contributions of cerebral hemispheres to the total brain weight were 59.04, 66.97, 70.14 and 74.16 percent, respectively during second, third, fourth and fifth month of gestation (Fig. 51). These values showed a sharp and steady increase throughout gestation and in full term foetus, the mean weight of the two cerebral hemispheres was 19.290g.

Mean length, width and thickness of the cerebral hemispheres are given in table 13. All these parameters consistently increased during prenatal period. Cerebral length increased from 0.600cm at 40 days to 5.500cm in full term foetus. Corresponding values for cerebral width and thickness were 0.350cm and 0.500cm at 40 days and 2.595cm and 3.100cm at full term, respectively. Thickness of cerebrum exceeded its width throughout the period of study. Percentage contributions of cerebral length to total brain length were 90.98, 64.35, 70.39 and 72.87 percent during second, third, fourth and fifth month, respectively. Higher percentage increase of cerebral length (240.38 percent) was recorded than the cerebral width (144.12 percent) from second month to fifth month. Percentage lengths of cerebrum to cerebellar lengths were 315.00, 322.09, 260.71 and 217.08 during second, third, fourth and fifth month, respectively.

The right cerebral hemisphere was slightly heavier (0.88 percent) than the left (Fig.54). Similarly the values for length, width and thickness also exceeded the corresponding values for the left hemisphere. Relationship between age and length, width and thickness of right and left hemispheres are shown in figures 37 and 38, respectively.

#### 4.2.1.1.5 Cerebellum

Mean weight, length, width and thickness of cerebellum at different stages are shown in table 13. There was a positive correlation between the age and cerebellar weight ( $r = 0.879$ ) vide table 37. Weight of cerebellum increased about five times from  $0.059 \pm 0.007g$  to  $0.310 \pm 0.050g$  from second month to third month of gestation. The increase was about two times from third to fourth month. During fifth month, the weight again increased by six folds. Percentage contributions of cerebellum to the total brain weight were 6.21, 6.73, 7.67 and 9.43 percent, respectively during second, third, fourth and fifth month (Fig. 51). Up to the fourth month, the cerebellar weight increased gradually and thereafter, a spurt in growth was noticed (Fig. 36). In full term foetus, the cerebellum weighed 5.980g. Relationship between age and length, width and thickness of cerebellum are shown in figure 39. A sharp increase was evident in all these parameters towards the terminal stage of pregnancy. Cerebellar length, width and thickness were highly correlated with foetal age ( $r = 0.989, 0.983$  and  $0.987$ , respectively) vide table 37. Regression coefficients of cerebellar weight on age and brain weight are presented in tables 41 and 42, respectively.

#### 4.2.1.1.6 Brainstem

Growth curves for brainstem (consisting of diencephalon, mesencephalon, pons and medulla oblongata) and its components are shown in figures 36 and 40, respectively. Unlike in the case of cerebrum and cerebellum, percentage contribution of brainstem to total brain weight decreased from second month to fifth month (Fig.51). The values were 34.76, 26.30, 22.20 and 16.41 percent during second, third, fourth and fifth month, respectively. Percentage contribution of each segment of brainstem to total brainstem weight is shown in figure 53. Diencephalon was the heaviest component in most of the age groups. Mesencephalon was proportionately large and elongated in early age groups. But later its growth rate declined due to faster growth of other brain components. Regression coefficients, using values for individual foetuses, calculated for brainstem weight on age is given in table 41. Similarly regression coefficients were also calculated for weight and length of each component on the total brainstem weight and length (Table. 42). When compared to other divisions of brain, brainstem was noted to be a slow growing region.

#### 4.2.1.2 Relationship between Body Weight and Brain Parameters

Increase in the mean weight of the brain in relation to the body weight is shown in figure 41. Weight of the brain was positively correlated with the body weight. The growth curve plotted using individual values of brain weight on body weight was curvilinear, but can be expressed as linear by considering each curve as two straight segments with a sharp change in the rate of growth becoming apparent at 19 weeks. About 50 percent of the foetal body weight and brain weight were attained by this age. Regression coefficients for brain weight on body weight were 0.033 up to 19 weeks and 0.004 during the last two weeks of gestation ( $P < 0.01$ ). Correlation coefficients of brain weight on body weight were 0.976 up to 19 weeks and 0.987 during the last two weeks. Prediction equations derived from the regression coefficients may be used to calculate normal values for brain weight from body weight (Table. 43).

The percentage contribution of brain to the body weight showed a decreasing trend during prenatal period. The mean values were 9.81, 7.89, 5.29 and 2.74 percent during second, third, fourth and fifth month of gestation, respectively. In full term foetus, brain weight was 1.86 percent of the body weight.

Relationship between body weight and length, width and thickness of the brain is shown in figure 42. Body weight was positively correlated with brain length, width and thickness ( $r = 0.851, 0.817$  and  $0.744$ , respectively) vide table 29. But more significant correlation was noticed between the body weight and the brain weight of the foetuses. Relation between body weight and weight of cerebrum, cerebellum and brainstem is shown in figure 43. All these parameters showed an increasing trend with increase in body weight. Relationship between body weight and length, width and thickness of the right and left cerebral hemispheres are shown in figures 44 and 45, respectively. Both the hemispheres showed the same trend with increase in body weight. Figure 46 shows the relation between body weight and cerebellar parameters. Thickness of cerebellum exceeded its length during the third month (mean body weight = 74.996g). In the second half of gestation, cerebellar length exceeded its thickness (Fig. 46 and Fig. 52). Except during second month, width of cerebellum exceeded its length and thickness (Fig. 52). Relation between body weight and weight of the brainstem components are shown in figure 47. Cerebrum, cerebellum and brainstem contributed 0.67, 0.21 and 0.31 percent of the body weight in the full term foetus.

#### ***4.2.1.3 Relationship between Other Body Parameters and Brain Parameters***

Weight, volume, length, width and thickness of brain showed significant positive correlation with the body parameters like CRL (straight), CRL (curved), total body length, total bent length, vertebral column length (VCL), vertebral column tail length (VCTL), tail length, forelimb length, hindlimb length, tibial length, chest depth and chest circumference at 1 percent level of significance (Table. 29). Among these parameters, maximum correlation was noticed between the brain weight and the total body length ( $r = 0.982$ ). Regression coefficients calculated for various brain parameters on the body parameters are presented in table 41. Prediction equations were also computed to facilitate the prediction of brain weight and brain size from various body parameters during prenatal period (Table. 43). Relationship between straight crown rump length and weight of the brain during prenatal period is shown in figure 48.

## 4.2.2 Craniometry

### 4.2.2.1 Head Parameters

Head parameters of goat foetuses at different ages are given in table 10. Curved head length increased from  $3.556 \pm 0.264\text{cm}$  to  $13.871 \pm 0.390\text{cm}$  from second month to fifth month. Head constituted almost one-half of the curved CRL during second month. Relation between age and the head parameters is shown in figure 49. Relationship between head length and selected body parameters at different stages of gestation is illustrated in figure 50. All the head parameters showed an increasing trend with the advancement of age. Curved length of cranium was greater than that of the face in all the age groups. Craniofacial length ratios were 3.4:1, 2.6:1, 2.3:1 and 2.1:1 during second, third, fourth and fifth month, respectively. A percentage increase of 845.70 was recorded for cranial length from second month to fifth month whereas the corresponding value for the facial length was 341.40. Transverse distance between lateral canthi was 1.2-1.4, 1.5-2.1, 1.7-2.3, 3.1-3.3 and 6.2-8.5 times of the distance between bases of ears, cornual buds, medial canthi, supraorbital foramina and nostrils, respectively during prenatal period. Correlation coefficients of head parameters on selected brain and body parameters are presented in table 30. Highly significant positive correlation was noticed between all these parameters. Curved and straight head lengths showed maximum correlation with the length of brain ( $r = 0.991$  and  $0.989$ , respectively). Regression equations derived from these are given in table 43.

Unlike brain parameters, all the head parameters showed a greater increase during early gestation than in the later stages. Percentage contributions of head length to curved crown rump length were 46.12, 42.03, 40.05 and 35.66 percent during second, third, fourth and fifth month of pregnancy, respectively. These data revealed a gradual decrease during the prenatal period. All the head parameters showed highly significant correlation with curved CRL and total bent length of the foetus (Table.30).

### 4.2.2.2 Skull Parameters

Skull parameters of goat foetuses at different stages of gestation are presented in table 11. Mean skull length, neurocranial length, facial length and skull width are

compared in figure 55. All these parameters showed a progressive increase during the prenatal period. Correlation coefficients of skull parameters on selected parameters of the brain and body are presented in table 31. All these showed significant positive relationship with each other except the cephalic index and cranial index. Skull length was highly correlated with skull width, neurocranial length, facial length and interorbital distance ( $r = 0.994, 0.993, 0.990$  and  $0.990$ , respectively). Facial region constituted almost one-third of the total skull length during gestation (Fig. 55). Cranial height and width were almost equal.

Calculated cephalic indices were  $60.78 \pm 1.91$ ,  $55.60 \pm 0.82$ ,  $50.85 \pm 0.54$  and  $53.92 \pm 0.57$  percent during second, third, fourth and fifth month of gestation, respectively (Table. 11). Skull length showed significant positive correlation with weight, volume, length, width and thickness of brain ( $r = 0.916, 0.919, 0.986, 0.991$  and  $0.979$ , respectively) vide table 31. Cranial height and brain thickness are compared in figure 56. The difference between these two parameters increased with gestational age. The related parameters were fit into regression equations (Table. 43).

#### **4.2.2.3 Skull Bones**

Measurements of skull bones at different stages of gestation are presented in table 12. The shape of cranium and face changed progressively in all the three dimensions. Cartilaginous cranial vault developed by 40 days. Boundaries of the skull bones became identifiable by 54 days of age. Mandible was the longest among the skull bones in all the age groups. Among the cranial bones, frontal bone was the largest during prenatal period. Comparison between brain length and medial length of frontal and parietal bones during gestation is shown in figure 57. A highly significant positive correlation existed among these ( $r=0.971$  and  $0.928$ , respectively). Correlation coefficients of skull bone measurements between each other; on the selected whole brain parameters and encephalometric parameters are presented in tables 32, 33 and 35, respectively. Regression coefficients were also calculated and were fitted into prediction equations (Tables 41 and 43). Cranium showed a marked expansion as a result of proportionate growth of bones that formed the roof and walls (frontal, parietal, interparietal and supraoccipital bones). Base of the cranium, formed by basioccipital, sphenoid and ethmoid bones, showed only slow growth rate when compared to the bones forming the wall and the roof.

### 4.2.3 Cerebrum

#### 4.2.3.1 *Morphogenesis*

##### 4.2.3.1.1 Development in the Second Month

The cerebral hemispheres arose as bilateral evaginations of lateral wall of telencephalon at 26 days of gestation in goat embryos. During the second month, the surface of cerebral hemispheres was almost smooth (Fig. 58). They enlarged and grew rostrally, dorsally and caudally to cover the diencephalon. The temporal lobe continued to extend on each side of the brainstem in a ventro-rostral arch to attain the adult relationship. The cavity of each vesicle became the lateral ventricle, which communicated with the third ventricle through the interventricular foramen. The cavity followed the arching growth, thus accounting for the complicated curved shape of the lateral ventricles (Fig. 59). Since the diencephalon remained stationary as a pivot point, the telencephalon including the hippocampus and fornix arched around it.

The basal portion of the telencephalon increased in thickness more rapidly than the remainder and formed the basal nuclei by 40 days of gestation (2.5cm CRL). The thin walled upper portion was the pallium. Medially, along the zone of attachment to the roof of diencephalon, the pallial wall on either side became very thin by retarded development and pushed into the corresponding lateral ventricles as the tela choroidea (Fig. 60). Tela choroidea was composed of pia mater and the ependymal cells. The line of infolding known as the choroid fissure, appeared at the level of the interventricular foramen at this stage. As the medial wall of the cerebral hemisphere expanded caudally, the line of invagination also extended with it. The tela and the associated capillaries became the choroid plexus of the lateral ventricles. The choroid plexus made its first appearance at 40 days of gestation and filled almost half of the lumen of the lateral ventricles during the seventh week (Fig. 61).

Measurements of cerebral hemispheres at different stages of gestation are given in table 14. The height of each cerebral hemisphere was more than its maximum width in the second month of gestation. Another important feature was that the weight of the right hemisphere was more than that of the left. Micrometrical parameters of the wall of cerebrum during the second month of gestation are given in



table 22. Lateral wall was found to be the thickest followed by the dorsal, ventral and medial walls, respectively.

#### 4.2.3.1.2 Development in the Third Month

In goat foetuses of 61 days of gestational age (8.3cm CRL), the cerebral surface was agyric as noticed during the second month. By 69 days (10.2cm CRL), the cerebral hemispheres grew rapidly and developed convolutions (gyri) separated by shallow furrows (sulci). The rhinal sulcus demarcated the neocortex from the paleocortex on the basal surface. A faint triangular depression at the junction between rostral and middle third of lateral surface indicated the Sylvian sulcus (Fig. 62). Another shallow crescentic impression appeared on the dorsolateral surface of cerebrum above the Sylvian sulcus, which represented the suprasylvian sulcus. The hippocampal fissure appeared on the medial aspect of the cerebral hemispheres above and parallel to the choroid fissure (Fig. 63).

By 76 days of age (12.0cm CRL), the coronal and marginal sulci appeared (Fig. 64). The coronal sulcus appeared as a linear impression parallel to the great longitudinal fissure over the frontal pole. The marginal sulcus developed on the caudodorsal aspect near the dorsal longitudinal fissure. The ventral surface of the brain showed the well-developed circle of Willis (Fig. 65). The Sylvian fissure lodged the middle cerebral artery and its branches at this stage. By 83 days (15.1cm CRL), the cruciate fissure also developed (Fig. 66). The suprasylvian fissure extended from the occipital pole of cerebral hemisphere to the rostral aspect. The cruciate fissure demarcated the frontal and parietal poles of the cerebral hemisphere.

Length, width and height of the cerebrum consistently increased during the third month (Fig. 52). Vertical distance of cerebrum was more than its maximum width. Micrometry of cerebral walls during the third month of gestation is given in table 22. As cited in the second month, the lateral wall was the thickest.

#### 4.2.3.1.3 Development in the Fourth Month

During fourth month, the cerebral surface showed more gyri and sulci. By 93 days of age (18.3cm CRL), the ansate, endomarginal and callosal sulci appeared (Fig. 67). Ansate or post cruciate sulcus appeared just caudal to the cruciate fissure and it did not reach up to the great longitudinal fissure. Rostrally the ansate sulcus was bounded by the posterior sigmoid gyrus. Endomarginal sulcus appeared medial to the

marginal sulcus on the caudodorsal aspect of the cerebral surface. On the medial surface callosal fissure demarcated the corpus callosum from the cingular gyrus.

By 101 days of age (20.0cm CRL), the marginal sulcus further elongated. Diagonal, presylvian, ectosylvian and rostral and caudal endogenual sulci started appearing towards the middle of fourth month. Mean length of major sulci of the cerebral surface during fourth and fifth month of gestation are given in table 21.

Measurements of cerebral hemispheres during the fourth month of gestation are given in tables 13 and 14. As noticed during the previous months, the right hemisphere was larger than the left.

#### 4.2.3.1.4 Development in the Fifth Month

Measurements of cerebral hemispheres during the fifth month of gestation are given in table 14. In 124 days-old fetuses (27.5cm CRL), the cerebral surface showed most of the gyri and sulci (Fig. 68). Overgrown cerebrum and cerebellum fully concealed the midbrain. The ansate fissure reached up to the great longitudinal fissure. The great longitudinal fissure became considerably wider in its most caudal part and opened into the transverse fissure between the cerebral hemispheres and the cerebellum.

The deepest and most prominent sulcus on the dorsolateral side of the hemisphere was the combined rostral, middle and caudal suprasylvian sulci. The rostral branch of Sylvian fissure was continuous with the presylvian sulcus (Fig. 69). The presylvian sulcus did not establish contact with the lateral rhinal sulcus but ran parallel to it. The coronal sulcus limited the coronal gyrus and was continuous caudally with the ansate sulcus that reached up to the great longitudinal fissure (Fig.68). The ansate sulcus in turn was continuous with the suprasylvian sulcus. This sulcus continued diagonally toward the occipital pole as the caudal suprasylvian sulcus. Oblique sulcus was located between the ectosylvian and middle suprasylvian sulci (Fig. 69).

The cingular gyrus was the only constant gyrus on the medial surface of the neopallium limited by the corpus callosum and the genual sulcus (Fig. 70). It was parallel to the corpus callosum and was subdivided by the endogenual sulcus into two

irregular dorsal and ventral parts. The callosal sulcus did not completely surround the corpus callosum on the medial side of the hippocampus.

The marginal sulcus subdivided the caudal part of the cerebral hemisphere into two unequal parts namely the ectomarginal gyrus and the medial marginal gyrus (Fig.68). The ectomarginal sulcus was absent. In fullterm foetus (41.5cm CRL), numerous secondary and tertiary sulci appeared dividing the cortical surface into a number of small gyri and the cerebral surface attained the adult pattern (Fig. 71).

#### **4.2.3.2 Histogenesis**

##### **4.2.3.2.1 Development in the Second Month**

Wall of the early telencephalic vesicle consisted of ependymal, mantle and marginal layers. This structural pattern was evident up to 40 days of gestation. However, the mantle layer in that part of the evaginating wall that was adjacent to the thalamic area of diencephalon showed a thickening. Continued proliferation of the cells in this region produced a bulge in the lumen of lateral ventricle and in the floor of interventricular foramen (Fig. 72). This prominent gray mass in the wall of cerebral hemisphere, which appeared in the sixth week of gestation, marked the embryonic appearance of the basal nuclei.

A septum pellucidum appeared as a well-developed partition between the two lateral ventricles at 58 days of gestation (7.6cm CRL). This was made up of fibre bundles with very few cells. On either side tall ciliated ependymal cells covered this (Fig. 73). Width of the septum was 455.0 $\mu$ m and that of the ependymal layer was 75.0 $\mu$ m. The cilia measured 5.5 $\mu$ m.

As described in the first month of gestation, wall of the cerebrum showed the inner ependymal, middle mantle and outer marginal layers up to 40 days of gestation. But towards the middle of the second month, migration of neuroblasts to form the outer cortical layer commenced (Fig. 74). Neuroblasts and spongioblasts of the ependymal layer left this zone and migrated outwards through the mantle layer into the marginal layer thereby giving rise to a superficial gray cortex (Fig. 75). The middle zone formed the white medullary mass of cerebral hemispheres. This white matter showed many radiating fibres and was traversed by neuroblasts and spongioblasts migrating from the inner zone to the more superficial layer. In some

areas wavy lines of neuroblasts could be seen (Fig. 76). Thus the position of gray and white substances of the spinal cord was largely reversed in the cerebrum.

During the seventh week of gestation, the outer zone or cortical plate showed two distinct layers (Fig. 74). The outer marginal layer was composed mostly of the fibres and became the molecular or plexiform layer. The inner undifferentiated cellular layer represented the future layers II to VI of the adult cortex. Total thickness of the cerebral mantle or the cortical plate measured only half of the thickness of the ependymal layer at this stage.

Towards the end of second month, cortical migration of neuroblasts was very much pronounced so that thickness of cerebral cortex greatly increased. Correspondingly thickness of the outer molecular layer also increased (Fig. 77). Organisation of the granular layer into various zones was not evident at this stage. Width of the white matter greatly increased. White matter showed large number of migrating neuroblasts and they migrated along the glial processes. On the lateral wall of cerebrum, this migration was in a wavy manner as described previously. Vasculature of the cerebral wall greatly increased at this stage.

#### 4.2.3.2.2 Development in the Third Month

During initial stages of third month, the cortical plate or cerebral mantle showed only two layers, viz., the outer molecular layer and the inner cellular layer. By the middle of third month, the inner cellular layer showed stratification (Fig. 78). It was divided into superficial and deep granular layers with a stratum between them in which the cells were relatively few. This intermediate granular layer stained more pinkish in haematoxylin and eosin preparations due to more number of fibres. Thus at 76 days of gestational age (12.0cm CRL), the cerebral cortex revealed four layers namely the outer molecular layer, superficial granular layer, intermediate granular layer and the deep granular layer. Micrometrical parameters of different layers of the cerebral wall are given in table 22. Intermediate granular layer was the thickest one. As the cerebral hemispheres enlarged and their walls increased in thickness, the surface began to show fissures. Thickness and density of the four layers were variable in different regions and also at the top, sides and floor of the sulcus. The cerebral cortex was thicker at the top of the crown of the gyrus and the thickness gradually diminished towards the floor of the sulcus. Mean thickness of the

molecular layer at the floor of the sulcus exceeded that at the top of the gyrus. Typical neurons could not be seen in the cerebral cortex even though the stratification was more distinct at 81 days (13.0cm CRL).

White matter revealed migrating neuroblasts and spongioblasts as noticed during the second month. Numerous capillaries and fibrous astrocytes were also seen in the white matter (Fig. 79). Width of inner ependymal layer gradually diminished (Fig. 80). Vascularisation of the deeper layers was especially rich. The choroid plexus completely filled the lateral ventricles (Fig. 80). In some regions, the choroid plexus epithelium was closely adherent to the ependyma. Roof of the lateral ventricle showed the corpus callosum (Fig. 81).

#### 4.2.3.2.3 Development in the Fourth Month

Histological picture of the cerebral mantle was the same as that of the third month even though width of the layers increased (Fig. 82). Differentiation of neurons was not complete and these cells had not yet attained their characteristic shape. Vascularity of the cerebral cortex greatly increased. Pyramidal cells of the cerebral cortex were not differentiated.

Unlike in the third month, white matter did not reveal waves of migrating neuroblasts and spongioblasts. This indicated that cortical migration of the cells of ependymal layer already came to an end by about 12 weeks of gestation and the cortical cells might be undergoing differentiation during the fourth month. Width of the white matter again increased. Another peculiar feature was that the inner ependymal layer became very thin by 101 days of age (20.0cm CRL) and was pseudostratified with ciliated columnar ependymal cells (Table. 22).

#### 4.2.3.2.4 Development in the Fifth Month

Mean cortical thickness was  $1274.667 \pm 79.644 \mu\text{m}$  and  $1120.000 \pm 21.466 \mu\text{m}$  at the top of the gyrus and at the bottom of the sulcus, respectively during the fifth month of gestation (Table. 23). Thickness of the cerebral cortex decreased when compared to that of the fourth month. During fifth month, the neocortex was divided into six layers. These layers were the molecular, external granular, external pyramidal, internal granular, internal pyramidal and the fusiform cell layers. This pattern was evident from 124 days of gestation (27.5 cm CRL) vide figures 83 and 84.

The molecular layer was the thickest layer formed mainly of fibre plexuses with relatively few cells (Fig. 85). The molecular layer constituted 27 and 39 percent of the total width of cerebral cortex on the top of the gyrus and at the bottom of the sulcus, respectively. Mean thickness of the molecular layer increased from  $80.000 \pm 3.578 \mu\text{m}$  to  $344.000 \pm 50.045 \mu\text{m}$  from second month to fifth month on the top of the gyrus.

The external granular layer consisted of numerous closely packed small cells (Figs. 83 and 84). Dendritic processes of pyramidal and fusiform cells passed through it to reach the molecular layer. External pyramidal layer was composed mainly of typical pyramidal neurons of two categories (Fig. 86). The larger cells measured  $15.000 \mu\text{m}$  and  $18.750 \mu\text{m}$  at 124 and 144 days, respectively and the corresponding values for smaller cells were  $11.250 \mu\text{m}$  and  $15.000 \mu\text{m}$ . Their dendrites projected to the first layer and axons entered the white matter. The internal granular layer was composed of closely packed stellate cells (Fig. 84). Internal pyramidal layer consisted principally of large pyramidal neurons that measured  $37.500 \mu\text{m}$  at 144 days with a nucleus measuring  $15.000 \mu\text{m}$  (Fig. 87). The fusiform cell layer contained spindle-shaped cells whose long axes were perpendicular to the cortical surface (Fig. 87).

The white matter filled in the space between cortex, ventricle and basal nuclei, and formed the medullary core of the various convolutions (Fig. 88). Large numbers of blood channels were seen in the white matter (Fig. 89). Afferent and efferent projection fibres arose from the whole extent of the cortex and entered the white substance, where they formed the radiating mass of fibres, the corona radiata, converging toward the brainstem. The short association fibres curved around the floor of each sulcus transversely to the long axis of the sulcus, thus connecting adjacent convolutions. The cingulum seen on the medial surface of the cerebral hemisphere was made up of long association fibres. Measurements of the corpus callosum during third, fourth and fifth month of gestation are given in table 14. Mean thickness of the corpus callosum increased from  $0.176 \pm 0.009 \text{cm}$  to  $0.249 \pm 0.088 \text{cm}$  from fourth month to the fifth month. No sex difference was detected in the shape of splenium of corpus callosum at any stage of gestation in the goat foetuses. Histologically the corpus callosum was made up of long nerve fibres running transversely (Fig. 90).

### **4.2.3.3 Olfactory Bulb and Olfactory Pathways**

#### 4.2.3.3.1 Morphogenesis

##### *4.2.3.3.1.1 Development in the Second Month*

The olfactory bulb was well developed by 48 days of gestation. It projected cranioventrally from the frontal pole of cerebral hemisphere (Fig. 91). Measurements of the olfactory bulb at different stages of gestation are shown in table 14. Cavity of the cerebral hemisphere extended into the olfactory bulb (Fig. 92). Towards the end of the second month, there was a decline in the size of the cavity due to the growth and differentiation of the neural tube wall.

##### *4.2.3.3.1.2 Development in the Third Month*

In the third month, size of the olfactory bulb gradually increased but it did not project beyond the frontal pole of cerebral hemisphere (Fig. 65). Average width was slightly more than its height. At 81 days of age (13.0cm CRL), the olfactory peduncle was well developed (Fig. 93). It was divided into the medial and lateral olfactory striae. Area between the diverging striae formed the rostral perforated substance or olfactory trigone. The lateral stria passed lateral to this to enter the rostral portions of the piriform area (Fig. 94). It was more distinct than the medial stria and was demarcated laterally by prominent rhinal fissure. The medial olfactory stria disappeared into the fissure between the cerebral hemispheres and merged into the subcallosal area.

##### *4.2.3.3.1.3 Development in the Fourth Month*

Average length, width and thickness of the olfactory bulb increased from  $0.419 \pm 0.030$ cm,  $0.239 \pm 0.029$ cm and  $0.173 \pm 0.027$ cm to  $0.681 \pm 0.034$ cm,  $0.483 \pm 0.017$ cm and  $0.466 \pm 0.012$ cm from third month to the fourth month. Medial and lateral olfactory striae were grossly visible (Fig. 95). Mean height and width were almost the same during the fourth month. Other features were similar to that of the third month.

##### *4.2.3.3.1.4 Development in the Fifth Month*

During fifth month, the mean length of olfactory bulb doubled and reached almost upto the rostral end of the frontal pole of cerebral hemisphere but did not project beyond it (Fig. 69). It rested in the cribriform fossa of the ethmoid bone.

Measurements of lateral and medial olfactory striae and trigonum olfactorium are given in table 14 (Fig. 96). Lumen of olfactory bulb greatly reduced due to thickening of its wall.

#### 4.2.3.3.2 Histogenesis

##### 4.2.3.3.2.1 *Development in the Second Month*

Histologically the olfactory bulb showed the three layers of the neural tube wall, viz., ependymal, mantle and marginal layers. But the cortical layer resulting from the migration of cells of the ependymal layer, in the neocortex region of 48 days-old subjects could not be seen in the olfactory bulb (Fig. 92). Towards the basal aspect of the olfactory bulb where it united with the frontal pole of cerebral hemisphere, a bundle of nerve fibres developed that represented the olfactory peduncle (Fig. 91). Cranial to the olfactory bulb, olfactory nerve fibres were seen running towards the bulb from the olfactory mucosa (Fig. 92). At 58 days of gestation, the cortical migration of neuroblasts was evident and the olfactory peduncle was well developed. A thin cortical layer of two to three cell- thickness was formed beneath the molecular layer.

##### 4.2.3.3.2.2 *Development in the Third Month*

During the third month, cortical migration of neuroblasts continued but stratification of the cortex was not evident. The medial and lateral olfactory striae could be seen as bundles of nerve fibres in the anterior part of cerebral hemisphere. The lateral one followed a curved path (Fig. 94).

##### 4.2.3.3.2.3 *Development in the Fourth Month*

Unlike in the third month, the cortical tissue showed stratification. It was made up of the outer molecular layer, superficial granular layer, intermediate granular layer and deep granular layer as seen in the cerebral cortex.

##### 4.2.3.3.2.4 *Development in the Fifth Month*

Microscopically the wall of the olfactory bulb showed the following layers from anterior to posterior direction, viz., the layer of olfactory nerve fibres, the glomerular layer formed by the synapses of olfactory nerve fibres with dendrites of



mitral cells, the mitral cell layer, internal granular layer consisting of small granule cells and the white substance formed by axons of mitral cells (Fig. 97). The white substance constituted the olfactory striae. In the olfactory trigone area, olfactory tubercle showed aggregation of cells.

#### ***4.2.3.4 Piriform Lobe and Hippocampus***

##### ***4.2.3.4.1 Morphogenesis***

###### ***4.2.3.4.1.1 Development in the Second Month***

Immediately above and parallel to the choroid fissure, the medial wall of cerebral hemisphere thickened forming the hippocampus, which was 128.000 $\mu$ m thick at 48 days (Fig. 98). Thus the choroid fissure demarcated the caudate nucleus and the hippocampus. Towards the end of second month, thickness of hippocampus greatly increased with some structural differentiation.

The hippocampus was separated from the thalamus by a cleft lined by a double layer of pia mater with many blood vessels and was filled with loose mesenchyme, the velum interpositum (Fig. 98). This cleft constituted the most rostral extension of the transverse cerebral fissure. Pia projected into the lateral ventricle as the choroid plexus. The lower pial layer of this fissure formed the roof of diencephalon and invaginated as the choroid plexus of the third ventricle (Fig. 73).

###### ***4.2.3.4.1.2 Development in the Third Month***

Piriform lobe appeared as a distinct convexity at the base of the brain, towards the beginning of third month (Fig. 62). Laterally this was marked by the caudal part of the rhinal sulcus; medially, by the hippocampal fissure which separated the paleocortex from the archicortex (Fig. 63). Measurements of different parts of rhinencephalon are given in table 14.

The hippocampus invaginated into the lateral ventricle through the hippocampal fissure at 61 days of age. This fissure separated the caudomedial parahippocampal gyrus (or subiculum) from the rostrolateral dentate gyrus and the fimbria (Fig. 63). At the age of 81 days, the hippocampal fissure deepened; and the invaginated portion bulged deeply into the inferior horn of the lateral ventricle. The hippocampus bulged dorsally and medially and, on reaching the medial surface,

curved inward again to form a semilunar convolution, the dentate gyrus. The dentate gyrus was narrow without any indentations at this stage. The rostromedial fimbria was characterized by a rather thin, cutting edge to which attached the choroid plexus of the lateral ventricle (Fig. 99). More medially it became a rather flat, almost concave structure separated from the dentate gyrus by a small groove. Parahippocampal gyrus was a rather smooth uniform structure, which was continuous with the medial portion of the caudal part of the piriform lobe and neopallial cortex.

#### *4.2.3.4.1.3 Development in the Fourth Month*

Measurements of the piriform lobe are given in table 14. A gradual increase in all the parameters was noticed during the prenatal period.

#### *4.2.3.4.1.4 Development in the Fifth Month*

The piriform lobe was longer than wide. The hippocampus formed a rounded eminence in the floor of the temporal horn of the lateral ventricle and arched caudodorsally and rostrally on the ventricular floor (Fig. 70). The fimbria continued rostral to the corpus callosum to become the fornix.

#### *4.2.3.4.2 Histogenesis*

##### *4.2.3.4.2.1 Development in the Second Month*

At 48 days, the hippocampus revealed an inner ependymal layer, a mantle layer showing relatively less number of cells and an outer marginal layer (Fig. 100). The neuroblasts in the mantle layer started developing into the pyramidal neurons. Many cells migrated through the marginal layer to outer aspect forming the cortex. Towards the end of second month, two neuronal aggregations were seen near the future dentate gyrus area. In a longitudinal section, wall of the hippocampus showed an internal ependymal layer, a layer of fibres containing migrating neuroblasts, a cellular layer that was continuous with the cerebral cortex and an outer molecular layer. The cellular layer showed developing pyramidal neurons. A band of fibres converged from the hippocampus ventrally as the fimbria (Fig. 101). The ependymal cells lined luminal surface of fimbria. The free border of the fimbria was directly continuous with the epithelium of the choroid plexus above.

#### 4.2.3.4.2.2 *Development in the Third Month*

By the middle of gestation, ventricular surface of the hippocampus was covered by a white layer, the alveus. These fibres converged on the medial face of the hippocampus to form the already described fimbria, lying medial to the hippocampus and dentate gyrus. Fibres from the alveus entering the fimbria constituted the beginning of the fornix system. Ventricular surface of the alveus and fimbria was lined by the inner ependymal layer, the thickness of which reduced as age advanced. At 81 days, hippocampus showed four layers, viz., inner ependymal layer, the alveus, a cellular layer containing some developing pyramidal neurons and undifferentiated neurons with condensed nuclei, and the outer molecular layer.

#### 4.2.3.4.2.3 *Development in the Fourth Month*

Unlike in the cerebral cortex, more pyramidal neurons appeared in the cellular layer of the hippocampus at 101 days of age.

#### 4.2.3.4.2.4 *Development in the Fifth Month*

In 144 days-old subjects, the hippocampus in cross section showed the following layers from the lateral ventricular surface to the interior namely the ependymal layer, stratum alveus, stratum oriens, stratum pyramidale and stratum lacunosum-moleculare (Fig. 102). Stratum alveus was located beneath the ependymal layer and was made of white matter. This layer was of variable thickness. The stratum oriens revealed a layer of polymorphous cells varying in their shape. Round, oval and stellate neurons were found.

Stratum pyramidale consisted chiefly of large pyramids (37.5 $\mu$ m) with small pyramids (18.5 $\mu$ m) scattered among them. The bodies of the pyramids were elongated and ovoid instead of being triangular (Fig. 103). Double pyramidal cells also could be located in the hippocampus. Pyramidal cells of the inferior fold of hippocampus were larger than those of the superior fold (Fig. 104). The pyramids of the inferior fold deviated more and more from the typical pattern as they approached the hilus of the dentate gyrus; their processes became shorter and more widely spread out with an uneven appearance (Fig. 105). It was difficult to recognize the layers of stratum lacunosum-moleculare separately.

The dentate gyrus histologically revealed three laminae at 144 days, viz. an outer molecular layer, a granular layer in the form of a 'U', the hilus of which was

directed toward the fimbria, and a polymorph layer (Fig. 106). The fimbria was attached to the free extremity of hippocampus as illustrated in figure 107.

#### **4.2.3.5 Basal Nuclei**

##### 4.2.3.5.1 Morphogenesis

###### *4.2.3.5.1.1 Development in the Second Month*

Basal nuclei appeared as a gray mass on the floor of the cerebrum near the thalamus at 40 days of gestation. In transverse sections, this region had a striated appearance due to the alternate arrangement of gray and white matter (corpus striatum). The medial gray mass was the caudate nucleus (Fig. 108). Large number of nerve fibres ventrolateral to this formed the internal capsule, which separated the caudate nucleus from the rest of the gray substance in the sixth week. During the seventh week, the lenticular nucleus also appeared as a narrow elongated mass of cells that was separated from the outer gray matter by a thin external capsule (Fig. 109). Lateral wall of diencephalon and medial wall of cerebrum were fused and the caudate nucleus and thalamus came into close contact. In transverse section, this junction between cerebrum and thalamus was seen just below the choroid fissure where the choroid plexus projected into the lateral ventricle (Fig. 72). Micrometrical parameters of basal nuclei at different stages of gestation are shown in table 24.

###### *4.2.3.5.1.2 Development in the Third Month*

During the third month, vascularity of the basal nuclei further increased. Largest among these vessels were seen in the corpus striatum (Fig. 110) and measured 97.5 $\mu$ m in diameter at 62 days of age. By 81 days, the diameter enhanced to 161.3 $\mu$ m. They represented the branches of the middle cerebral artery (Fig. 65). Thickness of the caudate nucleus and internal capsule gradually increased (Table. 24). At the age of 62 days, two divisions of the lenticular nucleus, viz., the globus pallidus and putamen started differentiating (Fig.111).

###### *4.2.3.5.1.3 Development in the Fourth Month*

The claustrum appeared at 101 days of gestation. This was separated from putamen by the external capsule and from the insular cortex by the extreme capsule.

#### 4.2.3.5.1.4 *Development in the Fifth Month*

Width of various components of basal nuclei greatly increased during the fifth month. Width of caudate nucleus increased from  $113.333 \pm 4.667 \mu\text{m}$  to  $259.442 \pm 4.084 \mu\text{m}$  from fourth month to fifth month (Table. 24). The internal capsule separating the caudate nucleus from the lenticular nucleus was convex internally and concave externally. This formed a laterally opening angle, which was occupied by the putamen and globus pallidus.

The external capsule was thin ( $33.667 \pm 0.601 \mu\text{m}$ ), slightly convex laterally and concave medially and blended dorsally into the internal capsule (Fig. 112). Mean width of claustrum was  $23.876 \pm 1.003 \mu\text{m}$  during the fifth month with a thin dorsal part and a slightly thicker ventral part. Claustrum was separated from the amygdaloid body by the extreme capsule (Fig. 113). The amygdaloid body was an almond shaped structure situated ventrolateral to the corpus striatum within the caudal part of the piriform lobe.

#### 4.2.3.5.2 Histogenesis

##### 4.2.3.5.2.1 *Development in the Second Month*

In the caudate nucleus, neuroblasts outnumbered the glial cells. These neuroblasts fell into two categories at 58 days of gestation (Fig. 114). Larger cells with a nuclear diameter of  $7.5 \mu\text{m}$  were lesser in number and showed peripheral condensation of chromatin. Second category comprised smaller cells that measured  $3.8 \mu\text{m}$  nuclear diameter. Both these types were not differentiated into typical multipolar neurons. Presence of a large number of blood channels was another feature. The lenticular nucleus showed lesser number of cells than the caudate nucleus (Fig. 108). Dorsally the caudate and the lenticular nuclei were continuous with each other beyond the internal capsule. Thickness of internal capsule gradually increased. Internal capsule was formed of nerve fibres passing in both directions between the thalamus and cerebral cortex and these were arranged in a radiating fashion. Apart from that, the internal capsule showed radiating columns of migrating neuroblasts.

#### *4.2.3.5.2.2 Development in the Third Month*

In the caudate nucleus, dense aggregation of neuroblasts and spongioblasts could be noticed, but the neuronal differentiation was incomplete. The lenticular nucleus was composed of islands of cells separated by fibre bundles. The medially located globus pallidus showed relatively lesser number of cells than in the putamen region. The external capsule was well developed (Fig. 111). In some regions, caudate and lenticular nuclei were interconnected by transverse cellular bands crossing the internal capsule (Fig. 110).

#### *4.2.3.5.2.3 Development in the Fourth Month*

Clastrum was made of a thin layer of gray matter similar to that of the putamen.

#### *4.2.3.5.2.4 Development in the Fifth Month*

Caudate nucleus showed large multipolar neurons scattered among small stellate cells (Fig. 115). Nissl granules appeared in the large cells in the last week of gestation. Internal capsule showed nerve fibres running in different directions. The globus pallidus contained large multipolar neurons and spindle-shaped neurons (Fig. 116). Large number of nerve fibres was also seen. Putamen contained small triangular and large multipolar neurons similar to that of the caudate nucleus (Fig. 117). The external capsule limited the putamen externally.

### **4.2.4 Cerebellum**

#### ***4.2.4.1 Morphogenesis***

##### ***4.2.4.1.1 Development in the Second Month***

Roof of the metencephalon formed the cerebellum. By 48 days of age, the metencephalic alar plates were greatly enlarged and presented a striking contrast to the thin roof of the myelencephalon. Bilateral dorsal growths or rhombic lips expanded medially and fused in the midline to completely cover the roof of the fourth ventricle in the rostral part. This transverse plate demonstrated a small midline portion (vermis) and two lateral portions (cerebellar hemispheres) at this stage (Fig. 118). The cranial and caudal portions of the thin metencephalic roof plate formed the

rostral and caudal medullary vela, respectively (Figs. 119 and 120). Measurements of cerebellum of goat fetuses at different stages of gestation are shown in table 15. Height of the vermis (141.0 $\mu$ m) was half of that of the cerebellar hemispheres at 48 days. But towards the end of second month, height of vermis greatly increased (1105.0 $\mu$ m) and reached almost the same level as that of the lateral hemispheres (Fig.121). The roof plate portion was visible at this stage as a slightly constricted portion in the middle of the vermis.

#### 4.2.4.1.2 Development in the Third Month

Average length and width of cerebellum increased from 0.320 $\pm$ 0.019cm and 0.247 $\pm$ 0.026cm in the second month to 0.602 $\pm$ 0.058cm and 0.912 $\pm$ 0.128cm, respectively in the third month (Table. 15). Fissures of various depths subdivided the entire cerebellar surface into a considerable number of leaf-like lamellae or folia. Cerebellar folia started developing at the age of 62 days (Fig.122). Width of the folia ranged from 520.0 $\mu$ m to 624.0 $\mu$ m (Table. 25). By 76 days number of lobulations again increased. Height of the vermis was more than that of the lateral hemispheres at this age (Fig. 64).

#### 4.2.4.1.3 Development in the Fourth Month

Cerebellum partially covered the mesencephalon at 93 days (18.3cm CRL) of age as illustrated in figure 67. Increase in the weight of cerebellum and whole brain with increasing age was gradual up to the fourth month of gestation. Cerebellar surface showed more gyri and sulci during the fourth month. The primary fissure separated the cerebellum into the rostral and caudal lobes. The rostral lobe was composed of the lingula (a small lobule between the cerebellar peduncles that was covered ventrally by the rostral medullary velum), the central lobule and the culmen (a very prominent lobule). Far caudally, the caudolateral fissure separated the caudal lobe from the flocculonodular part, phylogenetically the oldest part of the cerebellum. The declive, folium and tuber appeared as a single mass. Similarly the pyramid and uvula were also not subdivided. Thus at 101 days of age, instead of the nine classical lobules, six were well developed. Secondary and tertiary branches were also appeared. Cerebellar gyri and sulci were more numerous than in the cerebral cortex. Micrometrical parameters of cerebellar folia at different stages of gestation are given

in table 25. Mean width and height of folia were  $477.333 \pm 47.359 \mu\text{m}$  and  $1173.333 \pm 60.809 \mu\text{m}$  during the fourth month.

Cerebellum was connected to the other parts of the CNS by cerebellar peduncles. The caudal cerebellar peduncles emerged on the dorsal surface of the rostral half of medulla oblongata and penetrated the cerebellum from its ventral surface. The middle cerebellar peduncles entered the cerebellum between the rostral and caudal peduncles and connected it with pons. The rostral cerebellar peduncles formed the lateral boundary of the rostral part of the fourth ventricle and converged rostrally to the caudal colliculi.

#### 4.2.4.1.3 Development in the Fifth Month

Cerebellum was partly covered by the occipital poles of cerebral hemispheres from the beginning of fifth month onwards (Fig. 68). The membranous tentorium cerebelli, a crescentic fold of the dura mater, separated the cerebellum from cerebrum (Fig. 71). Cerebellum in turn covered the caudal part of the rostral and caudal colliculi of the mesencephalon (Fig. 123). With its lateral hemispheres, the cerebellum largely overlapped the lateral sides of the medulla oblongata. The median vermis was now very prominent and was clearly separated from the lateral hemispheres at 124 days of age (27.5cm CRL). The lateral hemispheres were smooth and flat on their rostral surface than the caudal surface.

Cerebellum contributed 9.43 percent of the total brain weight. Percentage length and width of cerebellum in comparison to the total length and width of brain were 33.57 and 63.35 percent, respectively. Length and width of cerebellum increased more in comparison to the corresponding parameters of cerebrum. At the beginning of fifth month itself, all the nine classical lobules appeared. They were the lingula, central lobule, culmen, declive, folium, tuber, pyramid, nodulus and the uvula in the vermis region (Fig. 123). As age advanced, number of secondary and tertiary folia again increased. In the full term foetus (41.5cm CRL), cerebellum acquired the characteristic adult appearance (Fig. 123). Measurements of the cerebellar folia at different stages of gestation revealed that the mean width of folia was the maximum during the fifth month ( $788.667 \pm 97.063 \mu\text{m}$ ) and minimum in the fourth month of gestation ( $477.333 \pm 47.359 \mu\text{m}$ ) vide table 25.



#### 4.2.4.2 *Histogenesis*

##### 4.2.4.2.1 Development in the Second Month

In 40 days-old foetus, the wall of metencephalon showed the original three layers of the neural tube wall, viz., ependymal, mantle and marginal layers. By the seventh week, a superficial population of proliferating neuroepithelial cells appeared (Fig. 118). This external granular layer or external germinal layer was unique to the foetal cerebellum. Thickness of external granular layer varied in different areas of cerebellum. On an average, the thickness was  $14.000 \pm 0.447 \mu\text{m}$  and was made of three to four layers of cells (Fig. 121). The closely packed cells were of uniform appearance and possessed dense oval nucleus. The cytoplasmic margins were not clear. Clustering of cells in the superficial part of this layer was more than in the deeper parts.

Neuroepithelial cells occupying the dorsal aspect of mantle zone differentiated into the primitive Purkinje cells towards the end of second month (Fig. 124). At 58 days (7.6cm CRL), the Purkinje cell body was oval and measured  $11.0 \mu\text{m}$  in height,  $5.6 \mu\text{m}$  in width and the nucleus had a diameter of  $3.8 \mu\text{m}$  with a nucleolus of  $1.9 \mu\text{m}$ . Beneath this, the wall of cerebellum exhibited a wide zone containing uniformly distributed cells by the age of 48 days. Towards its deeper portion, large neurons started appearing that later formed the basal cerebellar nuclei in the white matter. The internal granular layer and the white matter were not differentiated at this stage. But towards the end of second month, migrating cells from the external granular layer aggregated just beneath the primitive Purkinje cell layer to form the internal granular layer (Fig. 121), which measured  $86.300 \mu\text{m}$  in width. Deeply the white matter of the cerebellum started developing. Thus, towards the end of second month the cerebellum showed the following layers from outer to inner: the external granular layer, molecular layer, primitive Purkinje cell layer, internal granular layer and the white matter. Externally the cerebellum was surrounded by the meninges (Fig.121). Arachnoid was not clear. A large venous sinus could be seen between the endosteal and meningeal layers of dura (Fig. 125). Width of different layers of the cerebellum at different stages of gestation are shown in table 25.

Inner endymal layer lay above the fourth ventricle, the thickness of which was greatly reduced from  $63.333 \pm 1.054 \mu\text{m}$  in the first month of gestation to  $34.500 \pm 2.012 \mu\text{m}$  in the second month (Fig. 126). Internally the luminal surface was limited by the internal limiting membrane of  $5.630 \mu\text{m}$ .

#### 4.2.4.2.2 Development in the Third Month

Histological structure did not change much up to the middle of the third month. Average width of the external granular layer was  $24.250 \pm 0.783 \mu\text{m}$ . In 81 days-old subjects, size of the primitive Purkinje cells almost doubled but the Purkinje cell layer was not continuous. White matter started separating from the internal granular layer at this stage. Each folium showed a central core of white matter containing bundles of nerve fibres. Deep in the white matter, neurons of the basal cerebellar nuclei were well developed by the middle of gestation (Fig. 127). Each one possessed a round to oval cell body of  $18.8 \mu\text{m}$  diameter with a vesicular nucleus of  $11.3 \mu\text{m}$  and a nucleolus of  $2.8 \mu\text{m}$ .

#### 4.2.4.2.3 Development in the Fourth Month

During the fourth month, all layers of the cerebellum could be clearly distinguished. Mean thickness of the external granular layer ( $42.667 \pm 3.373 \mu\text{m}$ ) was maximum at this stage (Fig. 128). Outer molecular layer was more fibrous in nature and showed two types of neurons (Fig. 129). The outer stellate cells, located in the outer two-thirds of the molecular layer had small cell bodies. The basket cells were situated in the vicinity of the Purkinje cell bodies but the cell body was not clear. Purkinje cells were arranged as a definite layer by 101 days. This consisted of a single layer of flask-shaped cells arranged uniformly along the upper margin of the inner granular layer (Fig. 129). Micrometry of these cells is given in table 25. They possessed a clear vesicular nucleus with a deeply staining nucleolus, but the Nissl granules were yet to develop.

Mean thickness of the inner granular layer was  $105.333 \pm 17.333 \mu\text{m}$  during the fourth month of gestation. This layer showed closely packed chromatic nuclei (Fig. 128). The cell body of these was not clear. Irregular light spaces here and there constituted the cerebellar islands or glomeruli, which were not fully developed. The inner granular layer also showed Golgi cells that were twice larger than the granule

cells with a diameter of  $15.0\mu\text{m}$  for the cell body,  $11.3\mu\text{m}$  for the vesicular nucleus and  $1.9\mu\text{m}$  for the nucleolus at 101 days. They were more in the upper part of the granular layer (Fig. 129). Within the folium, the white matter measured  $80.008\pm 7.155\mu\text{m}$  in thickness (Fig. 128). Thickness of the white matter increased towards the basal portion of the cerebellum. Deep in the white matter, neurons of the nucleus fastigii lying near the roof of the fourth ventricle measured  $22.5\mu\text{m}$  with a nucleus of  $11.3\mu\text{m}$  in diameter and the nucleolus measured  $3.8\mu\text{m}$ . Ependyma lining the roof of fourth ventricle was pseudostratified and ciliated.

#### 4.2.4.2.4 Development in the Fifth Month

At the beginning of the fifth month, thickness of the outer granular layer was  $32.0\mu\text{m}$  (Fig. 130). In the last week of gestation, this layer became very thin and was made up of one or two layers of cells (Fig. 131). By term, this was almost single layered. The molecular and internal granular layers increased in thickness greatly during the fifth month. The Purkinje cells measured  $38.0\mu\text{m}$  in height,  $18.8\mu\text{m}$  in width and  $9.4\mu\text{m}$  in nuclear diameter with a nucleolus of  $5.8\mu\text{m}$  at 144 days. A remarkable feature was that the Nissl granules started appearing in the cytoplasm of Purkinje cells during the initial stages of fifth month of gestation (at 124 days) vide figures. 132 and 133. By 144 days these were concentrically arranged (Fig. 134). Each cell gave rise to an elaborate dendritic tree that spread in a fanlike manner in a plane at right angles to the long axis of the folium (Fig. 135). The dendritic tree arose from the neck of the cell as two or three large primary dendrites, which divided repeatedly. Each Purkinje neuron also gave rise to a slender axon, which was connected to other cells in the deep cerebellar nuclei (Fig. 136). No intraneuronal pigment could be identified during foetal stage.

The granule cell layer also showed all the features of adult cerebellum during the fifth month (Fig. 137). The granule cells measured  $3.8\mu\text{m}$  to  $4.1\mu\text{m}$  in diameter. Cerebellar glomeruli appeared as clusters of fibres among the cells of the granular layer (Fig. 137). White matter was highly vascular and thicker towards the base. Deep cerebellar nuclei were well developed. The ependymal layer showed a single layer of ciliated columnar cells.

## 4.2.5 Brainstem

### 4.2.5.1 Diencephalon

#### 4.2.5.1.1 Morphogenesis

##### 4.2.5.1.1.1 *Development in the Second Month*

Diencephalon is that part of the forebrain remaining in the midline after the telencephalic vesicles grew out from the forebrain and this is the rostral most division of brainstem. Caudally it blended with the mesencephalon. Cavity of the diencephalon was in communication with each lateral ventricle by interventricular foramen. In the sixth week of gestation, the walls of diencephalon thickened much and the lumen became narrow. At 48 days, the two thalami grew into approximation so that the third ventricle became a slit-like cavity (Fig. 138). The two thalami united across the midline by a bridge-like massa intermedia or interthalamic adhesion, which obliterated the central region of third ventricle into a small dorsal component and a larger ventral component. There was only roof plate along the median plane over the small dorsal portion of the third ventricle (Fig. 139). Measurements of diencephalon at different stages of gestation are given in tables 16 and 26. The total width of diencephalon was more than its height. In the same plane of section, in addition to diencephalon, three areas of the telencephalon could also be identified: the cortical or pallial area of the cerebral evagination, the striate area forming a junctional zone between the thalamic and hypothalamic regions of the third ventricle and the pallial area of the lateral ventricle.

A hypothalamic sulcus on the lateral wall of diencephalon divided the lateral plate into upper thalamic and lower hypothalamic regions. The roof plate became the thin ependymal lining of the tela choroidea of this region (Fig. 139). Blood vessels growing into this folded area formed the choroid plexus, which invaginated into the third ventricle during the sixth week of gestation. Towards the end of second month, the choroid plexus almost entirely filled the triangular dorsal portion of the third ventricle. A large venous sinus could be seen on the roof of the third ventricle (Fig.139). Far caudad, the epiphysis or pineal body developed during the seventh week as a conical evagination from the roof of diencephalon (Fig. 140) with a thickness of 131.0 $\mu$ m. Lumen of the third ventricle extended towards the pineal body as the pineal recess at this stage. In front of this was another small evagination that represented the habenula

Hypothalamus was narrower than the thalamus and its floor was trough-like (Fig. 141). From the floor of the diencephalon, a small diverticulum was developed during the seventh week (the infundibulum), which formed the stalk and posterior lobe of pituitary gland (Fig. 142). The anterior lobe developed from the Rathke's pouch. In the longitudinal section of pituitary gland, the pars tuberalis could be seen as the continuation of the pars distalis surrounding the stalk of the gland. Towards the end of second month, all the components like pars distalis, pars tuberalis, residual lumen, pars intermedia and pars nervosa were greatly enlarged (Fig. 143).

Far cranially, the hypothalamus showed the optic chiasma by 48 days (Fig.144). The optic nerve emerged out of the cranial cavity through the wide optic foramen between the body and wings of presphenoid bone (Fig. 145). Lumen of the third ventricle extended towards the optic chiasma as the optic recess (Fig. 146). Thickness of optic chiasma region increased from 278.0 $\mu$ m to 910.0 $\mu$ m from the seventh to the eighth week. Decussation of the optic chiasma was evident more towards the ventral aspect. Above the level of optic nerve the supraoptic nucleus started developing on the floor of the hypothalamus towards the end of second month (Fig. 147). Paraventricular nucleus was not clearly evident but a large number of neuroblasts were seen accumulated near the third ventricle at this stage. Large number of blood vessels also could be noticed on the floor of the hypothalamus.

#### *4.2.5.1.1.2 Development in the Third Month*

Thalamus, the largest unit of diencephalon was clearly subdivided into a number of nuclei at this stage. Anterior two-thirds of the two thalami formed the lateral walls of the third ventricle (Fig.148). Line of attachment of the ependyma of third ventricle formed a ridge, the taenia thalami, which lay over the stria medullaris thalami (Fig. 99). Superior surface of the thalamus was convex and free. Anteriorly it was separated from the medial surface by the taenia. Taenia thalami formed the medial boundary of the upper surface of each thalamus. Choroid plexus of the third ventricle extended across the mid plane between the two taeniae. Laterally superior surface was separated from the caudate nucleus by the sulcus terminalis, along which lay the stria terminalis (Fig. 99).

An epithalamic sulcus separated the thalamus from the epithalamus. The pineal gland lay in the depression between the rostral colliculi (Fig. 64). The base

was attached to the taeniae thalami and habenular and posterior commissures by a shallow stalk into which extended the pineal recess of the third ventricle. The stalk was divided into a dorsal lamina continuous with the dorsal commissure, and a ventral lamina, continuous with the posterior commissure.

#### *4.2.5.1.1.3 Development in the Fourth Month*

Diencephalon contributed 42.70 percent of the brainstem weight and 7.34 percent of the total brain weight during the fourth month. Mean width and height of the thalamus were  $0.720 \pm 0.005$ cm and  $1.045 \pm 0.001$ cm, respectively. These figures exceeded the corresponding dimensions of the hypothalamus. Mean height of the massa intermedia was  $0.544 \pm 0.006$ cm. The mamillary body appeared as a distinct entity on the basal surface of hypothalamus (Fig. 95). Other features were similar to that in the third month.

#### *4.2.5.1.1.4 Development in the Fifth Month*

Mean weight of diencephalon increased about three times from  $1.062 \pm 0.025$ g to  $3.129 \pm 0.286$ g from the fourth month to the fifth month. Width of diencephalon was more than its height and length throughout the prenatal period. Diencephalon was the widest component in the brain stem (Fig. 149). Average length, width and height were  $1.423 \pm 0.052$ cm,  $2.476 \pm 0.054$ cm and  $1.467 \pm 0.033$ cm, respectively (Table. 16). On the ventral surface of diencephalon, the infundibulum appeared as a hollow stalk in the specimens where the pituitary was removed. Infundibulum in turn was connected to the tuber cinerium, which had an irregular surface.

#### *4.2.5.1.2 Histogenesis*

##### *4.2.5.1.2.1 Development in the Second Month*

By 40 days of gestation, the roof plate of diencephalon converted into the tela choroidea and along with the growing blood vessels formed the choroid plexus of the third ventricle. Alar plates of diencephalon showed three zones as in the neural tube wall. Width of the ependymal layer gradually reduced (Fig. 138) and these cells carried cilia on their luminal surface. Towards the middle portion of thalamus, thickness of this layer was more. Middle or mantle zone was the thickest layer, which contributed most of the thickness of the wall. The outer marginal layer was thin.

Bundles of nerve fibres divided the mantle layer especially towards the lumen. Proliferation of neuroblasts in localised regions of the mantle layer led to aggregation of cell bodies. These masses or aggregations of gray substance, the nuclei, were subdivided by nerve fibres into several parts. These nuclei first appeared in the goat foetuses in the seventh week of gestation. Primitive neurons in such aggregations were small in size with dark compact nucleus and inconspicuous cytoplasm. Small scattered neurons with light staining nucleus and numerous blood channels lined with endothelial cells were also seen in this area. In general, cellular density was more towards the dorsal aspect of thalamus than in its ventral regions and in the hypothalamus.

The region of interthalamic adhesion did not contain any nerve fibre. Its average height was  $0.130 \pm 0.013$  cm during second month. On either side of massa intermedia, bundles of nerve fibres in the mantle layer represented the internal capsule (Fig. 150). In the hypothalamus also bundles of nerve fibres and aggregation of primitive neurons were noticed. Mamillary body formed the caudal limit of the hypothalamus.

The developing eyeball demarcated the area of diencephalon (Fig. 151). The tunics started developing at 48 days of gestation. Different layers of cornea also started differentiating at this stage (Fig. 151). The anterior epithelium, corneal substance proper and the caudal endothelium could be distinguished. The sclera was formed of bundles of collagen fibres and cells (Fig. 152). Thickness of vascular tunic increased towards the rostral aspect. Retina was thickest at its caudal part. Towards the middle of second month, outer pigmented and inner neural layers developed. Layer of rods and cones, the ganglion cell layer and the optic nerve fibre layer began development towards the end of second month. The lens was very large and strongly eosinophilic, and the anterior epithelium that was multilayered in the first month became monolayered at this stage (Fig. 151). The primary lens fibres reached the anterior wall of the lens vesicle occluding its lumen at 40 days. The eyelids were also developed. Anterior and posterior chambers were yet to develop.

At the junction between diencephalon and mesencephalon, immediately beneath the posterior commissure, on the dorsal surface of aqueduct of Sylvius, the ependymal cells were highly modified to form the subcommissural organ. It was in the form of a sharply curved plate of cells (Fig. 153). The cells, the tanyctes, were

columnar in shape and possessed elongated or oval nuclei. Unlike the ependymal cells, they showed no cilia.

#### *4.2.5.1.2.2 Development in the Third Month*

Thin layers of white matter covered the dorsal and lateral surfaces of the thalamus in the third month. That on the dorsal surface formed the stratum zonale and the white matter on the lateral surface was the external medullary lamina (Fig. 99). At 81 days, a vertical plate of white substance, the internal medullary lamina, extended into the thalamus from the stratum zonale dividing it into medial and lateral portions. The medial nuclei occupied the dorso-medial portion of the central half of the thalamus. Wedged between this and the ventral nuclei caudally was the centromedian nucleus, the largest of the intralaminar nuclei. The internal medullary lamina partially surrounded this nucleus. Typical neurons were not differentiated in these nuclei (Fig. 154). Thickness of the inner ependymal layer greatly reduced and the cilia on their luminal surface measured about 7.5 $\mu$ m in height (Fig. 155).

In the middle of gestation, a thin connective tissue capsule covered the pineal gland (Fig. 156). The parenchymal cells were arranged in a cord-like manner. There was a small central lumen, the pineal recess of the third ventricle. The lining epithelium was stratified columnar with basally located spherical nucleus and eosinophilic cytoplasm. The glial cells were scattered among the pinealocytes from which they could be distinguished by their smaller and darker nuclei (Fig. 157). Number of pinealocytes was more than that of the glial cells. The pinealocytes were not categorised into light and dark types in the third month of gestation.

Column of the fornix divided the hypothalamic nuclei into medial and lateral nuclear groups. Trough-like floor of the hypothalamus is shown in figure 158. Width of the optic tract and diameter of the supraoptic nucleus greatly increased at 81 days of age (Fig. 159).

By 76 days of age, the posterior commissure appeared as a rounded bundle of fibres that crossed the mid plane beneath the stalk of the pineal body at the junction between the diencephalon and mesencephalon (Fig. 160). This was just dorsal to the level where the cerebral aqueduct opened into the third ventricle. Just beneath the posterior commissure was the subcommissural organ lined by the tanyocytes



(Fig. 160). Thickness of the subcommissural organ greatly increased. Other features of the diencephalon were similar to that found during the second month of gestation.

#### *4.2.5.1.2.3 Development in the Fourth Month*

The ependymal lining of the third ventricle was pseudostratified during fourth month. Another feature noticed during this period was that neurons appeared in most of the thalamic and hypothalamic nuclei (Fig. 161). During the third month, they were mostly neuroblasts with the exception of a few neurons.

Supraoptic nucleus of the hypothalamus showed long spindle shaped cells. Most of these were bipolar cells (Fig. 162). Each one measured  $18.8\mu\text{m}$  with a nucleus of  $11.3\mu\text{m}$  and nucleolus of  $3.8\mu\text{m}$  at 101 days. Paraventricular nucleus also started developing during the fourth month.

Measurements of pineal gland increased progressively during the fourth month. Histological structure was same as that of the third month. Pinealocytes were not differentiated into light and dark cells.

#### *4.2.5.1.2.4 Development in the Fifth Month*

Anterior nucleus of the thalamus was partially flanked medially and laterally by the internal medullary lamina (Fig. 163). Dorsomedial nucleus showed a rostral magnocellular portion consisting of large polygonal deeply staining cells and a caudal parvocellular portion made up of small pale staining cells at 144 days (Fig. 164). Interthalamic adhesion showed midline nuclei consisting of small fusiform dark staining cells. Reticular nucleus could be located lateral to the external medullary lamina (Fig. 165). Mamillothalamic tract became very wide (Fig. 166).

Supraoptic and paraventricular nuclei of hypothalamus were composed mostly of bipolar cells (Fig. 167) and peripherally distributed Nissl substance. Paraventricular nucleus was triangular with densely grouped neurons placed as a vertical plate along the wall of the third ventricle. The supraoptic and paraventricular nuclei were interconnected by scattered cells that formed an incomplete bridge between the two.

The pineal gland was elongated-oval in shape, located in the central depression at the caudal end of the thalamus in between the rostral colliculi of corpora

quadrigemina (Fig. 123). The accessory pineal gland could not be located in the present study. Pineal gland was attached to the caudal part of the third ventricle by habenular and posterior commissures between which the recess of third ventricle extended.

Histologically the pineal gland acquired the adult characteristics towards the terminal stages of pregnancy. A fibrous capsule covered the gland and simple ciliated columnar ependymal cells covered the surface facing the third ventricle. From the capsule, connective tissue septae penetrated the gland dividing the parenchyma into small lobules (Fig. 168). The parenchyma was divided into an outer cortex and inner medulla. Parenchyma consisted of pinealocytes and glial cells scattered throughout in the fibrous network of interstitial tissue, fine blood vessels and nerve fibres. The nerve fibre bundles of the pineal gland formed fibre tract towards the posterior commissure, the epithalamo-epiphyseal tract. In the medulla, the cells were loosely arranged when compared to the periphery. The small central lumen appeared during third month of gestation was no longer seen.

The pinealocytes were of two types: the light and dark cells of which the light cells predominated (Fig. 169). The round to oval irregular nuclei of light pinealocytes had fine chromatin localised more towards the periphery. The dark cells showed uniform distribution of chromatin. The parenchyma showed a greater population of pinealocytes than glial cells. Four types of glial cells could be identified based on nuclear morphology, viz. glial cells with round, oval or cone-shaped nucle (type I), smaller glial cells with round or oval strongly basophilic nuclei (type. II), glial cells with elongated nuclei closely associated with the blood capillaries (type III) and a few cells with large nuclei (type IV). The nerve fibres were distributed irregularly adjacent to the pinealocytes. Pigmented cells and corpora arenacea were not observed in the foetal pineal gland.

#### ***4.2.5.2 Mesencephalon***

##### ***4.2.5.2.1 Morphogenesis***

###### ***4.2.5.2.1.1 Development in the Second Month***

The mesencephalon lying in front of hindbrain lay exposed under the crown of head upto the middle of second month of gestation. The mamillary bodies formed the

rostral limit of mesencephalon; its caudal limit was the isthmus. The cephalic flexure lay in the ventral aspect of midbrain as a sharp bend even during the second month of gestation. Thickness of the wall of mesencephalon gradually increased and the lumen was typically diamond-shaped at 48 days. In cross section the wall showed three regions, the tectum, tegmentum and crura cerebri. The alar plates now developed into the primordium of corpora quadrigemina or the tectum. A conspicuous roof plate that was present in early stages lost its separate identity. Microscopically the rostral colliculus could be distinguished from the caudal colliculus at 48 days of gestational age. The junction was limited by a groove.

The alar plates developed slowly than the basal plates as noticed in the other regions of brainstem. The basal plates gave rise to two regions, the upper tegmentum and lower crura cerebri that were evident during the seventh week (Fig. 170). Towards the end of second month, the cerebral peduncles bulged conspicuously on the ventral surface of brain as two rounded masses. These crura were separated by the intercrural fossa. This region was pierced by numerous blood vessels, which constituted the caudal perforated substance. The alar and basal plates were separated by the sulcus limitans. The primitive neural cavity gradually became narrow to form the aqueduct (Fig. 170). Measurements of mesencephalon at different stages of pregnancy are given in tables 17 and 27. The alar plate was thinner than the basal plate.

#### *4.2.5.2.1.2 Development in the Third Month*

Growth rate of mesencephalon was less when compared to that of the brain. The cephalic flexure was no longer visible. Wall of mesencephalon further thickened and the corpora quadrigemina appeared as a distinct entity. As in the case of diencephalon, width of mesencephalon was more than its height during the prenatal period. Mean transverse and dorsoventral distances were  $1.044 \pm 0.037$ cm and  $0.826 \pm 0.028$ cm, respectively (Table. 17). Transverse distance of mesencephalon at the level of tectum was more than that at the level of the crura cerebri. The cerebral aqueduct passing through the mesencephalon became narrow in 76 days-old subjects (Fig. 171). It was lined by pseudostratified ciliated ependymal cells (Fig. 172). At 81 days, the ependymal layer consisted of a single layer of ciliated columnar cells. Distance from the ventral median groove to the cerebral aqueduct exceeded that from

the dorsal groove to the aqueduct during the prenatal period. Mean distance of the aqueduct from dorsal longitudinal groove increased from  $116.000 \pm 3.425 \mu\text{m}$  in the second month to  $589.333 \pm 73.253 \mu\text{m}$  in the third month (Table. 27). Similarly the mean distance from ventral median groove to aqueduct increased from  $1061.333 \pm 38.013 \mu\text{m}$  to  $1944.333 \pm 260.037 \mu\text{m}$ .

#### *4.2.5.2.1.3 Development in the Fourth Month*

Average length, width and height of mesencephalon were  $0.947 \pm 0.009 \text{cm}$ ,  $1.283 \pm 0.015 \text{cm}$  and  $1.194 \pm 0.010 \text{cm}$ , respectively during the fourth month. Mean weight increased from  $0.604 \pm 0.067 \text{g}$  in the third month to  $0.922 \pm 0.008 \text{g}$  during the fourth month. Mesencephalon contributed 37.07 percent of the brainstem weight and 6.37 percent of the total brain weight. Mean width and height of aqueduct of Sylvius were  $0.209 \pm 0.002 \text{cm}$  and  $0.193 \pm 0.002 \text{cm}$ , respectively. Average distance from dorsal longitudinal groove and ventral longitudinal groove to the aqueduct was  $0.093 \pm 0.001 \text{cm}$  and  $0.359 \pm 0.009 \text{cm}$ , respectively.

#### *4.2.5.2.1.4 Development in the Fifth Month*

The mesencephalon acquired the adult characteristics during the fifth month of pregnancy (Fig. 149). Weight of mesencephalon almost doubled from  $0.922 \pm 0.008 \text{g}$  to  $1.844 \pm 0.105 \text{g}$  from fourth month to fifth month. Mesencephalon contributed 25.51 percent of the total length of brainstem at this stage.

#### *4.2.5.2.2 Histogenesis*

##### *4.2.5.2.2.1 Development in the Second Month*

A section across the mesencephalon in goat foetus at the beginning of second month of gestation revealed the same three zones of the neural tube wall. However, the lumen became narrow and thickness of wall increased in the sixth week. During the seventh week, the primordial quadrigeminal plate appeared. The neuroblasts invaded the dorsal marginal zone of tectum to form the rostral and caudal colliculi.

##### *4.2.5.2.2.1.1 Tectum*

The cellular density was comparatively more in the tectal area than in the tegmentum or the crura cerebri. The ependymal layer was thicker when compared to

the basal plate region (Fig. 170). Mantle layer showed scattered small neuroblasts with nuclear diameter of  $6.0\mu\text{m}$  and a nucleolar width of  $2.0\mu\text{m}$ . Cell boundaries were not clear. Average width of mantle layer in this stage was  $143.0\mu\text{m}$ . The marginal layer was composed of fibres and nuclei of spongioblasts. Surrounding this the migrated collicular cells were seen. Towards the basal plate, the ependymal layer was very thin with two to three layers of cells. Ependymal cells had developed cilia.

#### 4.2.5.2.2.1.2 Tegmentum

In the basal plate, neuroblasts aggregated to form nuclei during the seventh week. Tegmentum contained network of fibres and cells representing the reticular formation (Fig. 170). Multipolar neurons of the red nucleus started appearing by 48 days of age. The cell body of such neurons measured  $11.0\mu\text{m}$ ; the nucleus,  $8.0\mu\text{m}$  and nucleolus,  $3.0\mu\text{m}$ .

Basal plates of both sides were united by a septum-like raphe. This was formed by the processes of the ependymal cells of the floor plate that elongated to keep pace with the thickening of the ventral wall. The ependymal layer was thicker in the ventral commissure of the aqueduct than in the other regions.

#### 4.2.5.2.2.1.3 Crura Cerebri

During the seventh week, marginal layer of the two basal plates gradually enlarged to form the crura cerebri. At 58 days, they bulged ventrally as two spherical masses.

#### 4.2.5.2.2.2 *Development in the Third Month*

Histological pattern was similar to that found in the second month until the middle of third month. At 76 days, the mesencephalon revealed numerous nuclear masses. Mesencephalic nuclei of trigeminal nerve, nuclei of oculomotor and trochlear nerves, tegmental nuclei, red nuclei and the substantia nigra were the main nuclei (Figs. 173 and 174). The undifferentiated neurons of these nuclei showed vesicular nuclei with prominent nucleoli and eosinophilic cytoplasm.

#### 4.2.5.2.2.2.1 Tectum

The colliculi of both sides were separated by a median longitudinal groove, in the rostral portion of which lay the pineal body (Fig. 64). Each colliculus was connected to the thalamus by fibre bundles. The caudal colliculi were ovoid in shape and were whiter than rostral colliculi.

Mesencephalic nucleus of trigeminal nerve appeared in the lateral margin of the central gray of the aqueductal region at 81 days of gestation. This was primarily composed of large unipolar neurons. They appeared as small islands of cells arranged in a flower-like manner (Fig. 173). Each neuron measured  $26.3\mu\text{m}$  in length and  $18.8\mu\text{m}$  in width. They possessed eccentric vesicular nucleus ( $15.0\mu\text{m}$ ) with a nucleolus of  $3.8\mu\text{m}$ . However, unlike the ganglion cells, those lying within this nucleus were not encapsulated.

#### 4.2.5.2.2.2.2 Tegmentum

Tegmentum lay between the substantia nigra and the cerebral aqueduct. In this, the red nucleus formed the largest nuclear mass. At 76 days of age, the multipolar neurons of this nucleus possessed relatively less number of processes (Fig. 174). By the age of 81 days, the magnocellular and parvocellular parts could be distinguished. The magnocellular part revealed large neurons of  $37.5\mu\text{m}$  diameter with a vesicular nucleus of  $15.0\mu\text{m}$  and a nucleolus of  $3.8\mu\text{m}$  (Fig. 175). They possessed many processes. Axons of these cells formed the rubrospinal tract. Parvocellular part showed smaller neurons of  $18.8\mu\text{m}$  and the nucleus measured  $7.5\mu\text{m}$  with a nucleolus of  $2.8\mu\text{m}$  (Fig. 176). Numerous fibre bundles including the oculomotor nerve fibres traversed the red nucleus (Fig. 177).

In addition to the red nucleus, the tegmentum showed a number of smaller aggregations of cells collectively called the tegmental nuclei. A number of fibre tracts also ascended or descended through it, and there were several decussations. The nuclei of the oculomotor and trochlear nerves appeared as masses of nerve cells ventral to the aqueduct close to the mid plane at 81 days of age. The cells of oculomotor nuclei were arranged as two lateral large celled nuclei and an unpaired median nucleus composed of smaller cells that connected the lateral nuclei of the two sides.

#### 4.2.5.2.2.3 Crura Cerebri

The white substance of the crura was made up of fibre bundles predominantly. The deeper layer of the cerebral peduncles was composed of gray substance, the substantia nigra that appeared at 81 days of age but the neurons were of primitive type (Fig. 178).

#### 4.2.5.2.2.3 *Development in the Fourth Month*

Histological picture did not change much during the fourth month. Size and number of the neurons and glial cells increased.

#### 4.2.5.2.2.3.1 Tectum

Length of rostral colliculus exceeded that of the width, but the situation was reverse in the caudal colliculus (Table. 17).

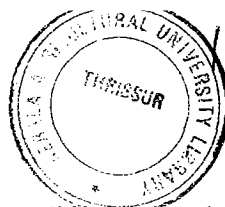
#### 4.2.5.2.2.3.2 Tegmentum

Mesencephalic nucleus of trigeminal nerve showed the same flower-like arrangement of neurons as noticed during the third month. These neurons measured 30.0 $\mu\text{m}$  in length and 21.8 $\mu\text{m}$  in width at 101 days. The nucleus was eccentric in position (Fig. 179).

Neurons of the magnocellular part of the red nucleus measured 52.5 $\mu\text{m}$ ; nuclear size was 22.5 $\mu\text{m}$  and the nucleolus measured 5.6 $\mu\text{m}$  at 101 days (Fig. 180). In the parvocellular part, these figures were 22.5 $\mu\text{m}$ , 11.3 $\mu\text{m}$  and 3.8 $\mu\text{m}$ , respectively. Cells of the red nucleus were one among the largest neurons that could be seen in the entire brain during the fourth month. Cells of the lateral paired portion of the oculomotor nucleus measured 37.5 $\mu\text{m}$  with the nucleus of 20.6 $\mu\text{m}$  and the nucleolus of 5.6 $\mu\text{m}$ . Cells of the unpaired median part measured 26.3 $\mu\text{m}$ , 13.1 $\mu\text{m}$  and 3.8 $\mu\text{m}$  respectively. In some neurons of the midbrain tegmentum, Nissl granules started appearing in the middle of fourth month (Fig. 205).

#### 4.2.5.2.2.3.3 Crura Cerebri

The cerebral peduncle increased in thickness during this period. Substantia nigra became more prominent but the neurons were still of primitive type.



172458

#### 4.2.5.2.2.4 *Development in the Fifth Month*

Most of the neurons of the mesencephalon were differentiated during the last week of gestation. The nerve cell distribution was diffused rather than focal. Cytoplasm of these showed basophilia. Myelination also began. Large blood vessels were seen throughout. The principal vessels supplying the midbrain were the caudal cerebral, rostral cerebellar, caudal communicating branch and rostral choroidal arteries. Aqueduct was lined by simple ciliated columnar epithelium measuring  $7.500 \pm 0.224 \mu\text{m}$  in height (Fig. 181).

##### 4.2.5.2.2.4.1 Tectum

The rostral colliculi were almost hemispherical separated by a deep furrow, which opened into a wide subpineal fossa (Fig. 149). The caudal colliculi extended laterally beyond the rostral ones, they were round in shape, whitish, with a prominent point, which was directed dorsocaudolaterally. The transverse sulcus between the rostral and caudal colliculi was rather deep in its lateral and laterocaudal parts but became shallower towards the midline.

Each colliculus showed a laminated structure consisting of several alternating gray and white matter (Fig. 182). The outermost layer, stratum zonale was made up of fine nerve fibres. Stratum cinerium or superficial gray layer consisted of small cells. The corticotectal fibres and most of the optic fibres terminated here. Stratum opticum was composed mainly of nerve fibres from retina and lateral geniculate body. The remaining layers or stratum lemnisci was made up of gray and white matter.

##### 4.2.5.2.2.4.2 Tegmentum

Various nuclei of the midbrain tegmentum increased progressively in size. Periaqueductal gray appeared as distinct entity and showed fusiform and stellate neurons (Fig. 181). The oculomotor, trochlear, tegmental and red nuclei all were well developed by the last week of gestation (Fig. 183). The median raphe between the two halves of mesencephalon was also well developed. In the rapheal region of the ventral tegmentum was the interpeduncular nucleus, a collection of medium-sized, multipolar cells (Fig. 184). This nucleus was situated immediately dorsal to the interpeduncular fossa.



#### 4.2.5.2.2.4.3 Crura Cerebri

The corticospinal tract appeared as a compact bundle of myelinated nerve fibres at caudal levels of mesencephalon (Fig. 185). The fibres converged in the corona radiata and passed downward through the internal capsule, crura cerebri, pons and medulla oblongata. It passed close to the emerging root fibres of the cranial nerves III, IV and XII. In the medulla oblongata region, this corticospinal tract emerged as the medullary pyramid.

### 4.2.5.3 Pons

#### 4.2.5.3.1 Morphogenesis

##### 4.2.5.3.1.1 *Development in the Second Month*

Basal plate of metencephalon greatly enlarged to form the pons at the floor of the fourth ventricle. Motor nuclei of origin for cranial nerves V, VI and VII started developing in the seventh week. The trigeminal nerve emerged from the pons as illustrated in figure 186. The semilunar ganglion measured 800.0 $\mu$ m in length and 560.0 $\mu$ m in width at 48 days of age. Measurements of the pons during different stages of gestation are given in table 18. The fourth ventricle was filled with the CSF at 48 days. Immediately beneath the fourth ventricle was the tegmental portion of the pons, which formed a thick floor to the cavity of the metencephalon. Below this was the more conspicuous basilar portion of the pons. The floor plate formed a raphe as mentioned in the case of mesencephalon. Cross section of the basilar artery could be seen on the floor.

##### 4.2.5.3.1.2 *Development in the Third Month*

Pons occupied approximately the central portion of the brainstem. It contributed 21.88 percent of the total length of the brainstem. Transverse distance of the pons was more than the dorsoventral distance during first, second and third months of gestation. A fibrous protuberance developed on the ventral aspect by 76 days of age (Fig. 65). Laterally they continued into the middle cerebellar peduncles. Dorsal surface of the pons that formed the floor of the fourth ventricle was marked by a deep median sulcus. On either side of the median sulcus was the sulcus limitans (Fig. 187). The ventral midline enclosed a shallow indentation in direct continuation of the ventral median fissure of the medulla oblongata by 76 days and this groove

lodged the basilar artery (Fig. 65). The semilunar ganglion grew rapidly and was seen on the cerebral surface of the petrous temporal bone. The trigeminal nerve emerged from the junction of pons and medulla oblongata (Fig. 188).

#### *4.2.5.3.1.3 Development in the Fourth Month*

Gross features resembled to that in the third month. Length, width and thickness of pons were  $0.770\pm 0.014\text{cm}$ ,  $0.722\pm 0.010\text{cm}$  and  $0.754\pm 0.011\text{cm}$ , respectively (Table. 18). Unlike in the earlier age groups, the dorsoventral distance exceeded the transverse distance.

#### *4.2.5.3.1.4 Development in the Fifth Month*

Mean weight of pons increased three and a half times during the fifth month. As noticed during the fourth month, the height of pons exceeded its width. The rostral border of pons was straight. So also, the transition between the ventral surface and caudal edge of the pons was gradual. Other gross features resembled the earlier age groups.

#### *4.2.5.3.2 Histogenesis*

##### *4.2.5.3.2.1 Development in the Second Month*

Up to the sixth week of gestation, the pons showed the three original layers of the neural tube wall. In the seventh week of gestation, nuclei started appearing in the mantle layer. These were the motor nuclei of origin for cranial nerves V, VI and VII and the pontine nuclei (Fig. 189). Cell boundaries of these primitive neurons were not so clear. Some alar plate neurons migrated ventrally from the lateral wall to the basal plate to form the pontine nuclei (Fig. 190). Nerve fibres passing in all directions broke up the gray substance into a mixture of gray and white known as the reticular formation. The semilunar ganglion showed a large number of unipolar neurons at 4.0cm stage. Their cell body measured  $7.5\mu\text{m}$  and the nuclear diameter was  $3.7\mu\text{m}$  with a nucleolus of about  $1.9\mu\text{m}$  size. In 7.6cm foetus, these values were  $22.5\mu\text{m}$ ,  $11.2\mu\text{m}$  and  $3.7\mu\text{m}$ , respectively.

#### 4.2.5.3.2.2 *Development in the Third Month*

Sensory nucleus of the trigeminal nerve could be seen in the alar plate region near the lateral margin of the central gray surrounding the fourth ventricle. Large motor neurons of the trigeminal nerve were seen towards the middle portion (Fig.191). Each one measured  $41.3\mu\text{m}$  with a central vesicular nucleus of  $15.0\mu\text{m}$  and a nucleolus of  $3.8\mu\text{m}$ . These were larger than the sensory neurons. Ventral portion of pons was made of longitudinal and transverse fibres interspersed with irregular masses of gray substance, the pontine nuclei (Fig. 192). Semilunar ganglion showed typical unipolar neurons surrounded by capsule cells by 76 days of gestational age (Fig. 217).

#### 4.2.5.3.2.3 *Development in the Fourth Month*

Histological structure of pons did not change much during the fourth month. The median raphe of the medulla oblongata continued into the pons dividing it into similar halves. The dorsal longitudinal fasciculus became a sharply defined round bundle, which lay close to the raphe below the gray matter on the floor of the fourth ventricle. Size of the neurons and glial cells increased progressively.

#### 4.2.5.3.2.4 *Development in the Fifth Month*

The pons was divided into a dorsal or tegmental part and a basilar part. Longitudinal fibres entering the pons were gathered together into a compact bundle at 144 days constituting the corticospinal tract. Transverse fibres of the pons were divided into superficial and deep fibres according to their position with reference to the longitudinal fibres. The superficial fibres lay ventral and lateral to them, while deep fibres lay dorsally. The pontine nuclei appeared as closely packed cellular aggregations placed between these fibres (Fig. 193). At the dorsolateral aspect of the pons was the large rounded section of the rostral cerebellar peduncle. Fibres of the middle cerebellar peduncle passed dorsal and ventral to the corticospinal tract. The medial lemnisci were located on each side of the median raphe. These bundles were separated from the ventral portion of the pons by transversely oriented fibres composing the trapezoid body (Fig. 194).

#### **4.2.5.4 Medulla Oblongata**

##### 4.2.5.4.1 Morphogenesis

##### 4.2.5.4.1.1 *Development in the Second Month*

Medulla oblongata, the caudal most segment of the brainstem, extended from the level of first pair of cervical spinal nerves to the caudal edge of pons. It lay on the unossified basioccipital and this cartilaginous skeleton developed in the sixth week of gestation. Measurements of medulla oblongata at different stages of gestation are given in table 19. The trapezoid body started developing at 48 days (Fig. 195). By 40 days, the roof plate region of the embryonic rhombencephalon expanded enormously. As a result, the entire alar and basal plates of the neural tube were displaced laterally and ventrally. The lumen became the fourth ventricle covered dorsally by the thin, single layer of ependyma, the roof plate. This constituted the anterior and posterior medullary vela (Figs. 119 and 120). These vela were continuous with the cerebellum cranially and the roof of the central canal of spinal cord caudally. The sulcus limitans present on the ventrolateral wall of the fourth ventricle provided the plane of division of the medulla into a ventromedial basal plate and a dorsolateral alar plate. The lumen was filled with CSF. The point of emergence of the facial nerve from the medulla is illustrated in figure 196. The endolymph duct also could be seen within the petrous temporal.

Vascular mesenchyme occupied the ependymal roof; rostrally the combined membrane, the tela choroidea, infolded as vascular tufts into the cavity of the myelencephalon constituting the choroid plexus of the fourth ventricle. This developed in the goat foetus in the sixth week of gestation (Fig. 197). Later during the seventh week, the ependymal roof plate became broad and thin. The cavity of the rhombencephalon thus expanded to the sides flattened dorsoventrally and was filled with CSF. The rhombic lip, ridge where the tela joined the alar plate was made up of 3 to 4 layers of cells.

Caudally the medulla oblongata was continuous with the spinal cord. The fourth ventricle narrowed posteriorly to be continued as the central canal of spinal cord (Fig. 198). Dorsal wall of this region showed thickened epithelium constituting the circumventricular organ.

#### 4.2.5.4.1.2 *Development in the Third Month*

During the third month medullary pyramids and the trapezoid body appeared on the ventral surface of the medulla. The medullary pyramids could be distinguished from 81 days and were in the form of longitudinal ridges on either side of the ventral median fissure but they were not widely separated in the rostral portion (Fig. 199).

The dorsal surface of the medulla formed the floor of fourth ventricle as noted in the second month. The caudal medullary velum projected from the dorso-medial angle of medulla oblongata (Fig. 200). Floor of the ventricle was marked by a deep median sulcus, which became shallower rostrally. On each side of the median sulcus was a continuous ridge, the medial eminence, bounded laterally by the sulcus limitans (Fig. 200). The medial eminence, or trigonum hypoglossi was formed by the nucleus of hypoglossal nerve. The lateral eminence was occupied by the caudal poles of the medial and inferior vestibular nuclei. In between the medial and lateral eminences was the intermediate eminence, the trigonum vagi.

Mean weight of medulla oblongata was  $0.220 \pm 0.032$ g during third month. Width of medulla oblongata was more than its height throughout gestation. Average length and width of medullary pyramids were  $0.805 \pm 0.031$ cm and  $0.230 \pm 0.013$ cm, respectively. The trapezoid body was clearly demarcated and the mean rostrocaudal distance was  $0.117 \pm 0.005$ cm.

#### 4.2.5.4.1.3 *Development in the Fourth Month*

Medulla oblongata contributed 17.57 percent of the brainstem weight and 3.02 percent of the total brain weight. Percentage contribution of medulla oblongata to the total brainstem weight increased progressively during gestation (Fig. 53). During the fourth month, mean length, width and thickness of the medulla oblongata were  $1.183 \pm 0.027$ cm,  $0.855 \pm 0.019$ cm and  $0.682 \pm 0.011$ cm, respectively. Unlike in the pons region, maximum width of medulla oblongata exceeded the maximum height. Morphological features did not change much during the fourth month. Length and width of medullary pyramids increased 15.03 and 93.04 percent, respectively from third to fourth month.

#### 4.2.5.4.1.4 *Development in the Fifth Month*

Grossly, medulla oblongata was adult-like in the full term foetus (Fig. 96). Trapezoid body was clearly demarcated from the pons. Cranio-caudal length of trapezoid body was  $0.298 \pm 0.003$  cm. Mean weight of medulla oblongata increased three-fold during fifth month. Corresponding changes were also noticed in the length, height and width of medulla oblongata (Table. 19). Ventral median fissure was flanked by the pyramids. Mean length and width of medullary pyramids were  $1.585 \pm 0.088$  cm and  $0.656 \pm 0.008$  cm, respectively.

#### 4.2.5.4.2 Histogenesis

##### 4.2.5.4.2.1 *Development in the Second Month*

Up to the sixth week of gestation the myelencephalon showed the same basic structural pattern of the neural tube wall. Thickness of the ependymal layer reduced as gestational age advanced. Proliferation of neuroblasts in localised regions of mantle layer led to aggregation of cell bodies that were functionally alike. These masses of gray substance, the nuclei, were evident at 48 days (Fig. 120). Nerve fibres crossing in different directions broke up the gray substance into a mixture of gray and white known as the reticular formation (Fig. 195). The midline raphe replaced the floor plate region.

An important observation noticed in the brain as a whole during the second month of gestation was that the differentiation of neurons and formation of their aggregations occurred earlier in the brainstem than in the cerebrum and cerebellum. But the hippocampus was an exception where the pyramidal neurons started developing towards the middle of the second month.

##### 4.2.5.4.2.2 *Development in the Third Month*

Arrangement of gray and white substances in the medulla oblongata showed a much more complex pattern during the third month than the simple relations in the spinal cord. The main difference from spinal cord was that a sharp demarcation between gray and white substances disappeared in the medulla oblongata. In the caudal part, the central canal was still present (Fig. 201). The median raphe extended in the median plane from the subventricular gray to the pyramids, dividing the

medulla into bilaterally symmetrical halves. Periaqueductal gray could be seen ventral to the median fissure at dorsal aspect of the raphe. Remainder of the gray substance was broken up into cell groups widely distributed throughout with numerous oblique and transverse bundles of nerve fibres passing among them constituting the extensive reticular formation. The medullary pyramids were formed of large bundles of nerve fibres. Lateral to the medullary pyramid was the inferior olivary nucleus, which appeared as a folded bag with the hilus directed medially and composed of small rounded or pear-shaped cells at 81 days.

Medullary reticular formation showed large number of cells of various sizes and types, arranged in diverse aggregations and enmeshed in a complicated fibre network. The reticular area located medial and dorsal to the rostral half of inferior olivary nucleus was occupied by the nucleus reticularis gigantocellularis composed of characteristic large cells as well as medium and small cells (Fig. 202).

#### *4.2.5.4.2.3 Development in the Fourth Month*

Ependymal cells lining the fourth ventricle became single layered in most regions (Fig. 203). Each cell measured 15.0 $\mu$ m in length, 7.5 $\mu$ m in width with a nucleus of 6.6 $\mu$ m and the cilia measured 15.0 $\mu$ m. The cilia were very thick and long. Neurons of the olivary nucleus were very large with oval cell body (diameter-45.0 $\mu$ m, nuclear size-16.9 $\mu$ m and nucleolar size-4.7 $\mu$ m). Externally a capsule surrounded the olivary nucleus (Fig. 204). The median lemniscus was seen on either side of the median raphe towards the ventral aspect.

#### *4.2.5.4.2.4 Development in the Fifth Month*

The arrangement of gray and white substances in the medulla oblongata showed a much more complex pattern than the simple relations found in the spinal cord. The caudal portion beyond the fourth ventricle showed a gradual transition. The reticular formation was well developed. The median raphe was formed of fibres that crossed at all angles from both sides. Medullary pyramids were well developed.

Nuclei and fibre tracts associated with cranial nerves V to XII were located at different levels (Fig. 206). The hypoglossal nucleus was located on the medial aspect of medulla oblongata at the dorsomedial angle on either side of median raphe beneath the floor of the fourth ventricle. Multipolar neurons were intermingled with

numerous myelinated fibres. Hypoglossal nerve rootlets left the ventral surface of the nucleus, passed ventrally lateral to the median lemniscus and emerged on the surface along the ventrolateral sulcus between the pyramid and the olivary nucleus (Fig. 207).

### 4.3 VENTRICLES OF BRAIN

The dilated cavities of the brain vesicles were the forerunners of the ventricular system and these were continuous with the central canal of the spinal cord. They underwent extensive alterations as a result of future cellular proliferation, growth and brain flexures. By 24 days of gestation (1.4cm CRL), the embryonic lumen of the neural tube at the rostral end was divided into five regions, viz., telocoele, diacoele, mesocoele, metacoele and myelocoele. As the cerebral hemispheres developed, the cavity (telocoele) also extended into them. The growth pattern of ventricles of brain at different stages of gestation is shown in figure 208.

#### 4.3.1 Lateral Ventricles

Lateral ventricles appeared as a distinct entity by 27 days of gestation. They communicated with each other and with the third ventricle through the interventricular foramina or Foramina of Monro (Fig. 2). Measurements of lateral ventricles at different stages of pregnancy are given in table 20. Percentage increase in length and width were 562.40 and 752.51 percent, respectively from the first month of pregnancy to the fifth month. Mean height of lateral ventricle increased from  $0.097 \pm 0.013$ cm to  $0.417 \pm 0.012$ cm from first month to third month. Thereafter the height gradually decreased due to the thickening of the cerebral walls reaching  $0.163 \pm 0.009$ cm during fifth month. At full term, the lateral ventricles measured 2.743cm in length and 0.576cm in width.

The lateral ventricles followed the development of cerebral hemispheres and extended into their four pairs of lobes by 48 days of gestation. The rostral horn extended forward and downward into the frontal lobe of cerebral hemisphere and also into the olfactory bulb (Fig. 92). The posterior horn extended into the central white matter of the occipital lobe. The choroid plexus did not extend into these horns. Inferior horn began at the junction of the body and posterior horn and curved ventrally and rostrally into the temporal lobe (Fig. 59). The interventricular foramen was located between the column of fornix and the anterior limit of the thalamus. The roof



of the ventricle was formed by the corpus callosum and the medial wall by the septum pellucidum. Septum pellucidum appeared as a well-developed partition between the two lateral ventricles by 58 days of age (7.6cm CRL) vide figure 73. The floor was formed by the caudate nucleus in front and hippocampus caudally separated by the choroid fissure (Figs. 60 and 98).

#### 4.3.2 Third Ventricle

Third ventricle or the cavity of diencephalon was an unpaired, cleft-like space lying between the two thalami and extending downward into the hypothalamus. Measurements of third ventricle at different stages of pregnancy are given in table 20. Percentage increase in length, width and height were 935.08, 280.44 and 1289.61, respectively from first month of gestation to the fifth month.

During the initial stages of pregnancy, the third ventricle was relatively broad (Fig. 6). By 26 days of gestation (1.5cm CRL), lateral walls of the diencephalon started thickening, which compressed the lumen. By 27 days (1.6cm CRL), the floor of the third ventricle appeared trough-like (Fig. 7). By 48 days of age (4.0cm CRL), the two thalami grew into approximation so that the third ventricle became a slit-like cavity (Fig. 138). It was wider in the region of the hypothalamic sulcus,. At the roof portion, the third ventricle widened to form a triangular space. This was almost completely filled with choroid plexus. There was only roof plate along the median plane over the small dorsal portion of the third ventricle (Fig. 139). This was covered by a layer of pia mater, the tela choroidia, which was continuous with the pia mater lining the cerebral fissure.

The third ventricle showed three recesses. The funnel-like infundibular recess extended into the infundibulum (Figs. 141 and 158) while the optic recess projected ventrally in front of the optic chiasma (Fig. 146). Posteriorly, the pineal recess extended between the habenular and posterior commissures into the stalk of the pineal body (Figs. 140 and 156). Cilia appeared on the surface of the ependymal cells facing the third ventricle in the middle of gestation. The ependymal lining acquired its adult characteristic during fourth month. The third ventricle appeared adult-like towards the terminal stage of pregnancy (Fig. 123).

### 4.3.3 Aqueduct of Sylvius

The space enclosed by the mesencephalon, the mesocoele was relatively large during the initial stages of pregnancy (Fig. 11). It became gradually narrow by the enlargement of the corpora quadrigemina and the basal plate (Fig. 170). The aqueduct began at the caudal limit of the third ventricle and opened into the rostral end of the fourth ventricle (Fig. 123). The aqueduct became a narrow canal in 76 days-old subjects (Fig. 171). Transverse diameter of the aqueduct during second month ( $0.210 \pm 0.024$ cm) reduced to  $0.152 \pm 0.015$ cm in the third month. The average width was  $0.346 \pm 0.044$ cm during the fifth month. Mean vertical diameter increased from  $0.084 \pm 0.001$ cm to  $0.214 \pm 0.017$ cm from the first to the fifth month (Table. 20). As in the case of mesencephalon, the transverse diameter exceeded the vertical diameter throughout gestation. The aqueduct was narrow at its beginning portion; the diameter increased at the level of rostral colliculi and the greatest width was recorded at the level of the caudal colliculi (Fig. 123). The cranial part was at a higher level than the caudal portion.

Ciliated ependymal cells lined the wall of the aqueduct and these were multilayered up to 62 days of age. At the age of 76 days, this was pseudostratified (Fig. 172). By 81 days, a single layer of ciliated columnar cells appeared. Typical adult-like ependyma could be noticed at 144 days (Fig. 181). Ependymal cells under the caudal commissure were heavily modified to form the subcommissural organ, which appeared during the second month of gestation.

### 4.3.4 Fourth Ventricle

Lumen of the hindbrain (metacoele and myelocoele) was diamond-shaped in cross section by 24 days of gestation (Fig. 22). Due to the thickening of the basal plates, the lumen became coffin-shaped at 26 days of age (Fig. 23). By 27 days, it was slit-like except at the region of the sulcus limitans (Fig. 24).

Stretching of the roof plate to form thin roof of the fourth ventricle commenced at 40 days of gestation. This thin layer formed of ependymal cells constituted the anterior and posterior medullary vela (Figs. 119 and 120). Cavity of the rhombencephalon expanded to the sides to form the fourth ventricle. Ventrolateral wall of this cavity was demarcated by the sulcus limitans into a

ventromedial basal plate and dorsolateral alar plate. During the third month of gestation, dorsal surface of the brainstem that formed floor of the fourth ventricle was marked by a deep median sulcus that became shallower rostrally.

Measurements of the fourth ventricle at different stages of gestation are given in table 20. During fifth month, the fourth ventricle was adult-like and was bounded by the rhomboid fossa ventrally, cerebellar peduncles laterally and rostral and caudal medullary vela and cerebellum dorsally (Fig. 149). Ventricular system communicated with the subarachnoid space by the foramina of Luschka (Fig. 200). The median foramen of Magendie could not be located. Caudally, the fourth ventricle was continuous with the central canal of spinal cord (Fig. 198). Area prostroma, the circumventricular organ associated with the fourth ventricle could be located at this region.

#### **4.3.5 Choroid Plexus**

In the present study, the choroid plexus could be located for the first time in 40 days-old subjects (Fig. 197). Plexus of the fourth ventricle showed more number of primary convolutions than that in the anterior regions which indicated that the choroid plexus of the fourth ventricle appeared a little earlier than in the other two ventricles. The originally flat surface of the caudal medullary velum became wrinkled and invaginated into the fourth ventricle by the blood vessels of pia mater (Fig. 120). As a result of disproportionate growth of various parts of the ventral wall of the cerebral hemisphere, the choroid plexus protruded into the lateral ventricle along the choroid fissure (Fig. 209). The horizontal cleft persisted between the cerebral vesicle above and the diencephalon below was lined by a double layer of pia mater with many blood vessels and was filled with loose mesenchyme to form the velum interpositum (Figs. 60 and 98). Upper layer of this protruded into the lateral ventricle and the lower layer formed the roof of the diencephalon and became invaginated as the choroid plexus of the third ventricle. Thus choroid plexus of the third ventricle was continuous with that of the lateral ventricle through the interventricular foramen and along the line of vesicle evagination. Each primordium enlarged, became lobulated and each lobule later demonstrated secondary and tertiary branches (Fig. 60). Extensive alterations in the shape and structure accompanied the different stages of development.

Histologically choroid plexus consisted of dilated blood vessels, connective tissue remnants of pia mater and a layer of ependymal cells (Fig. 197).

In the lateral ventricle, stalk of the choroid plexus was double layered, each layer having inner pial membrane and outer layer of ependymal cells (Fig. 210). The ependymal layer was tall and pseudostratified in the initial stages. Cytoplasm of these cells appeared eosinophilic. The nucleus was large, round to ovoid and centrally located. The thin intervening space showed erythrocytes and loose mesenchyme. Both nucleated and non-nucleated erythrocytes could be seen at 40 days of age (2.5cm CRL). That portion of the ependymal lining of the ventricle which was originally reflected from the fornix to the dorsal surface of the thalamus across the choroid fissure, was carried into the third ventricle with the choroid plexus and thus formed its ependymal covering. By 48 days the choroid plexus of the lateral ventricle branched several times, but not fully filled the cavity. Towards the stalk portion, the cells were pseudostratified with eosinophilic cytoplasm. Single layer of low columnar cells lined the portions of choroid plexus away from the stalk region. The spherical nucleus was seen towards the apical portion of the cell. Basal part of the cell was clear and vacuolated (Fig. 211). The capillary wall showed fenestrations.

Measurements of choroid plexus epithelium in the brain ventricles at different stages of gestation are given in table 28. There was a gradual decrease in the height of these cells as age advanced. Among the three ventricles, epithelium of lateral ventricle showed maximum height followed by third and fourth ventricles. Lumen of the plexus showed dilated blood channels filled with non-nucleated erythrocytes by 48 days (Fig. 211). Some other connective tissue elements including fibroblasts and connective tissue fibres were also noticed. Numerous tubules were formed by folding of the surface epithelium into the stroma during the differentiation of the plexus (Fig. 211). As the number of lobulations of the choroid plexus increased, there was a proportionate increase in the number of the tubules. Ventricles showed accumulation of secretion from the middle of second month. By 58 days (7.6cm CRL), almost two-third portion of the lateral ventricle was filled with the choroid plexus. In the third ventricle, the plexus filled the triangular roof portion. In the fourth ventricle, the primordium showed numerous secondary folds at 48 days (Fig. 212). By the end of second month, the plexus greatly enlarged and filled almost half of the ventricle.

Towards the middle of gestation, the branching pattern of the choroid plexus was more complex in the fourth ventricle (Fig. 213). The epithelium was pseudostratified towards the stalk portion but simple low columnar in the remaining regions. In the lateral ventricle, the choroid plexus reached its maximum size at the beginning of the third month (Fig. 80). The plexus filled about three-fourth of the ventricle reaching up to the anterior levels. In some regions, the plexus epithelium lay close to the internal limiting membrane or seen fused to it (Fig. 80). By 76 days, the plexus epithelium was mostly simple low columnar and vacuolation of the cytoplasm was more evident (Fig. 214). In addition to the modified ependyma, many other cell types were evident. By 80 days of age (13.0cm CRL), entire choroid epithelium of lateral ventricle showed vacuolated cytoplasm (Fig. 215). In the third ventricle also, the choroid epithelium showed glycogen granules during third month (Fig. 148). During the fourth month also the same pattern was seen. In every specimen examined, the epithelium was simple low columnar type, but areas of stratification and pseudostratification could always be identified. The epithelium was always pseudostratified at the stalk of the plexus. These findings indicated that the choroid epithelium was of multiple type, although largely simple low columnar. Towards term, the cells were typically cuboidal in shape with centrally placed nucleus and eosinophilic cytoplasm and no glycogen granules could be located at this stage. Mesenchymal elements were replaced by large amounts of connective tissue fibres, predominantly collagen fibres. The blood channels were greatly enlarged. Maximum amount of secretory tissue was seen in the lateral ventricles followed by the third and fourth ventricles.

#### 4.4 NEURONS AND NEUROGLIA

##### 4.4.1 Neurons

In goat embryos of 24 days of gestation, neuroepithelial cells were arranged radially in a pseudostratified manner in the inner ependymal layer of the neural tube wall (Fig. 25). Germinal cells with mitotic figures could be distinguished towards the luminal surface (Fig. 26). The middle mantle layer showed larger cells, the neuroblasts and smaller cells, the spongioblasts. Neuroblasts possessed large pale staining vesicular nucleus with small dark nucleolus. At the age of 27 days, these cells started developing small processes to become multipolar neuroblasts (Fig. 27).

Primitive neurons could be clearly distinguished from spongioblasts at 40 days (Fig. 216). Cortical migration of the neuroblasts in the cerebrum and cerebellum commenced towards the middle of the second month (Fig. 75).

Aggregation of neuroblasts, the nuclei, first appeared in the seventh week in the thalamus, mesencephalic tegmentum, pons and medulla oblongata (Figs. 189 and 190). Neurons of the deep cerebellar nuclei started appearing by 48 days and well distinguished by the middle of gestation (Fig. 127). The cell body was round to oval in shape ( $18.8\mu\text{m}$ ) with a large vesicular nucleus of  $11.3\mu\text{m}$  and a nucleolus of  $2.8\mu\text{m}$ . The cytoplasm showed neurofibrils, but the Nissl granules were not developed (Figs. 127 and 180). In the cell body region, these neurofibrils interlaced, but in the processes they ran straight. In the red nucleus also, similar kinds of neurons appeared during the seventh week. By 81 days these neurons ( $37.5\mu\text{m}$ ) were typically multipolar with an axon and several dendrites (Fig. 175). Primitive Purkinje cells ( $11.3\mu\text{m}$ ) were differentiated by 58 days of gestation (Fig. 124). Multipolar motor neurons of the trigeminal nucleus ( $41.3\mu\text{m}$ ) appeared in the pons by 76 days (Fig. 191) and measured  $75.4\mu\text{m}$  at 144 days of age. A large multipolar neuron of the nucleus reticularis gigantocellularis with numerous processes is illustrated in figure 202. Unipolar neurons of the mesencephalic nucleus of the trigeminal nerve were arranged in a flower-like manner with eccentric nucleus by 81 days of age (Figs. 173 and 179). Unipolar neurons also could be seen in the semilunar ganglion (Fig. 217) surrounded by satellite cells.

Even though the internal granular layer started appearing towards the terminal stages of second month, the granule cells of the cerebellum could be distinguished during the fourth month. Cell body of these was not clear (Fig. 128). During fifth month, these cells measured 3.8 to  $4.1\mu\text{m}$  (Fig. 137). Golgi cells of the inner granular layer of the cerebellum appeared during the fourth month and were twice larger than that of the granule cells (Fig. 137).

Most of the neurons of the thalamus and hypothalamus developed during the fourth month. Bipolar neurons appeared in the supraoptic nucleus of the hypothalamus during the same period (Figs. 162 and 167). Multipolar neurons of the magnocellular part of the red nucleus measured  $52.5\mu\text{m}$  during the fourth month, which were one among the largest neurons of the entire brain noticed during that period (Fig. 180).

Pyramidal neurons of the cerebral cortex appeared during the fifth month (Figs. 86 and 87). Double pyramidal cells were noticed in the hippocampus (Fig. 103). Large multipolar neurons appeared at different levels of brainstem during the fifth month (Figs. 193 and 206).

Nissl granules started appearing in the cytoplasm of some of the neurons in the middle of fourth month (Fig. 205). In the Purkinje cells they appeared during the initial stages of fifth month (Fig. 132). At 144 days, these were concentrically arranged (Fig. 134). Towards term, the Nissl granules appeared in most of the neurons of the brain. These granules extended into the dendrites also. Nissl granules were absent in the granule cells of cerebellum. An elaborate dendritic tree of the Purkinje cell that spreads in a fan-like manner is illustrated in figure 135. The long slender axon extended through the internal granular layer into the white matter (Fig. 136). The axons were surrounded by vacant areas, myelin sheath and oligodendroglial nucleus indicating the process of myelination (Fig. 218). Nucleus of most of the neurons appeared vesicular and centrally placed with a deeply staining nucleolus. In the granule cells of the cerebellum, the nucleus was chromatic and non-vesicular.

#### **4.4.2 Neuroglia**

Neuroglia developed from the precursors, the spongioblasts. By the age of 24 days, neuroepithelial cells of the inner ependymal layer were already started differentiating into neuroblasts and spongioblasts and migrated into the middle mantle layer. The nuclei of the spongioblasts were smaller and darker without a nucleolus unlike that of neuroblasts that possessed larger vesicular nucleus with a prominent nucleolus (Fig. 27). Towards the middle of second month, migration of spongioblasts along with the neuroblasts to form the outer cortical layer of the cerebrum commenced. By 58 days of age, the spongioblasts started differentiating into astrocytes and oligodendrocytes.

##### **4.4.2.1 Astrocytes**

Astrocytes were the largest among the glial cells (Fig. 154) and the nucleus measured 7.5µm at 58 days of age. The astrocytes with their processes formed a delicate frame work in which the neural elements were suspended. The protoplasmic astrocytes were most numerous in the gray matter and possessed numerous freely

branching thick processes. The nucleus was finely granular, ovoid and pale. In the white matter, fibrous astrocytes with long thin processes were numerous (Fig. 79). These were also present in the gray matter. Presence of glycogen granules also helped to distinguish them from the oligodendroglia and microglia (Fig. 219). Numerous processes of astrocytes formed a supportive framework throughout brain (Fig. 220). They also formed the glial limiting membrane (Fig. 119).

#### ***4.4.2.2 Oligodendrocytes***

Oligodendrocytes were characterized by round nucleus of 3.8 $\mu$ m diameter at 58 days and were smaller than that of the astrocytes. Their cell bodies were not distinct. They were numerous both in the gray and white matter (Figs. 176, 179 and 180). Some of them were closely apposed to neuronal cell bodies. Interfascicular cells appeared in rows between the nerve fibres in the white matter (Figs. 88 and 90). During the fifth month, the spiral myelin sheath and the nuclei and cytoplasm of oligodendrocytes encircling the axon could be identified (Fig. 218). The size of the cells increased at this stage. Oligodendrocytes also appeared throughout both the gray and white matter in the form of perivascular satellites (Fig. 222). Their cell bodies were closely applied to capillaries and their processes were directed away from them.

#### ***4.4.2.3 Microglia***

Microglia appeared at a later stage (76 days of age) when compared to other types of glial cells and their number was comparatively less. They were distinguished from oligodendrocytes by smaller, denser and ovoid or elongated nuclei (Figs. 221 and 222). They were located in the gray matter as juxtaneuronal cells and less frequently along the vessel wall. In the telencephalon they could be located in the subependymal regions of the lateral ventricles (Fig. 222).

#### ***4.4.2.4 Ependyma***

Ependymal cells also developed from the spongioblasts. The processes of primitive spongioblasts, at first, were attached to both the internal and external limiting membranes of the neural tube. Those which lost their attachments to the internal limiting membrane and, in most instances, to the external membrane as well, assumed the characteristics of astrocytes and oligodendrocytes while those which



retained their attachment to the internal limiting membrane, developed into adult ependymal cells and lined the ventricles of brain. During the first month, the inner ependymal layer was very thick and stratified (Fig. 25). As age advanced, the thickness gradually reduced and by the middle of second month, this layer was very thin (Fig. 126) and they developed cilia on their luminal surface at the age of 58 days (Fig. 73). By the middle of third month, they acquired the shape of adult ependyma but were pseudostratified (Figs. 155 and 172). Ependymal cells became single layered in 101 days-old subjects and co-arctation of cilia was noticed on the surface (Fig. 203). Ependymal cells also showed glycogen granules during third and fourth months and in the first half of fifth month of gestation (Figs. 148 and 219).

Choroid plexus of the lateral ventricle was lying closely adherent to the inner ependymal layer during third month (Fig. 80). Glial fibres, as a whole, formed a supportive framework throughout the brain.

#### 4.5 MENINGES

The meninges arose as condensation of the neighbouring mesenchyme. The pia mater started differentiating by 24 days (1.4cm CRL) of age (Fig. 30). Externally, the dura mater started developing at the age of 40 days (2.5cm CRL). The cartilagenous cranial vault also appeared during this stage. The arachnoid developed in between these two by 48 days of age (4.0cm CRL).

##### 4.5.1 Dura Mater

Dura mater started differentiating by 40 days and was a distinct entity at 48 days. It was made up of two layers that were closely adherent (Fig. 223) except in regions of cranial venous sinuses (Fig. 224). The outer layer constituted internal periosteum of the cranial bones while the inner layer formed the dura mater proper. At the age of 48 days, the outer layer measured 15.0 $\mu$ m and the inner, 3.8 $\mu$ m. It was the thickest among the three meninges. Thickness of dura varied greatly at different locations. It was generally thicker in the ventral aspect of brain, especially in the hypothalamic region (52.5 $\mu$ m at 48 days) vide figure 141. On the sides and top of the brain it was thin. Dura was made up of collagen fibres predominantly. Elastic fibres were also present. The outer layer was rich in blood vessels (Fig. 225). The inner layer folded itself to form several partitions that projected into the cranial cavity, viz.,

falx cerebri, tentorium cerebelli and diaphragma selle (Fig. 71). The surface facing the arachnoid was covered by simple squamous epithelium. A thin subdural space separated the dura and arachnoid (Fig. 223).

#### **4.5.2 Arachnoid**

Arachnoid was very thin ( $3.8\mu\text{m}$ ) and appeared by 48 days of gestational age. Connective tissue fibres of the arachnoid formed an outer surface parallel to the inner surface of the dura mater and was covered on either sides by simple squamous epithelium (Fig. 226). From the arachnoid, strands of fibres formed a loose reticulum across the subarachnoid space, which lay between the arachnoid and pia mater (Figs. 224 and 225). These arachnoid trabeculae were attached to the pia mater. The subarachnoid space contained a loose sponge-like tissue with spaces filled with cerebrospinal fluid. This space was also traversed by numerous blood vessels to and from the pia mater and the nerves (Figs. 223 and 226). Arachnoid followed the infoldings of the dura mater but it did not follow the sulci of cerebrum and cerebellum and bridged over them (Fig. 227). The network of trabeculae and spongy reticulum occupied the sulci. In some regions, the subarachnoid spaces were of considerable depth constituting subarachnoid cisterns, viz., cisterna magna, cisterna fossa lateralis and cisterna pontis.

#### **4.5.3 Pia Mater**

The pia mater started differentiating by 24 days of age. Fine connective tissue fibres, mesenchymal cells and erythrocytes constituted the pia. In 27 days-old subjects, the pia mater appeared as a continuous layer (Fig. 30). In most regions it was double-layered. Pia mater was highly vascularized and extended deep into the sulci of cerebrum and cerebellum and measured  $5.5\mu\text{m}$  at 40 days. It was thicker than the arachnoid but thinner than the dura mater. Its inner surface was fused to the brain. Depending on the vascularity, thickness of the pia varied over the surface of different regions of brain and in different age groups. In the diencephalon region, it was comparatively thicker and formed roof of the third ventricle (Fig. 139). In the regions of brainstem and cerebellum, thickness was maximum towards the end of second month. But in the cerebral surface, it showed maximum development during fifth month (Fig. 228). Choroid plexus of lateral and third ventricles, which merged

within the interventricular foramen, developed within an invagination of pia that became entrapped between the expanding telencephalic vesicles and the roof of the diencephalon. The plexus of the fourth ventricle developed separately within the pia over the caudal medullary velum.

## 4.6 HISTOCHEMISTRY

### 4.6.1 Lipids and Myelin

When neural paths were first developed in the early embryo, all the nerve fibres were unmyelinated. Myelination in the goat foetal brain began during the third month. In the initial stages only a mild reaction was noticed. During the fifth month, most of the fibres were myelinated and the spiral myelin sheath and the nuclei and cytoplasm of oligodendrocytes encircling the axon could be identified (Fig. 218). In the telencephalon, myelinated fibres could be demonstrated in the white matter, olfactory pathways, hippocampal fibres and in the internal capsule. Myelination was initially observed in the olfactory pathways and hippocampus. The optic chiasma and optic nerve fibres were also myelinated during third month. In the cerebellum, the white matter showed a strong positive reaction (Fig. 229). A moderate reaction was noticed in the molecular layer. No lipids could be demonstrated in the external granular layer, Purkinje cell layer and the internal granular layer. In the brainstem region, myelinated fibres could be demonstrated throughout the extent from the third month. But the medullary pyramids gave a positive reaction at a later stage (fifth month).

Lipid granules were also demonstrated in the pineal gland and in the tanycytes of the subcommissural organ. The cortical region of the pineal showed a more intense reaction than the medulla (Fig. 230). The epithalamo-epiphyseal tract fibres of the pineal gland showed intense reaction. The capsule and trabeculae showed negative reaction. The habenular commissure to which the pineal stalk was attached showed a strong positive reaction indicating heavy myelination of the commissural fibres (Fig. 231). The blood vessels, meninges, choroid plexus and the ependymal lining of the brain ventricles did not show any lipid granules. Towards term, degree of myelination was much more advanced. This is associated with the functional maturity of the kid at birth.

### 4.6.2 Carbohydrates

Glycogen granules could be located in the ependymal cells lining the ventricles of brain and in astrocytes, which helped to distinguish them from oligodendrocytes and microglia (Fig. 219). Neurons of the brain and modified ependymal cells of the choroid plexus of brain ventricles also showed a positive reaction from the middle of second month of gestation (Fig. 148). But towards term the glycogen granules disappeared from the choroid epithelium. Blood vessels of pia-arachnoid, choroid plexus and the brain tissue showed a positive reaction for periodic acid Schiff's (PAS) staining method (Fig. 232). The simple squamous epithelial covering on either side of the arachnoid was also positive. The cerebral and cerebellar cortices showed a mild positive reaction. PAS-positive granules were also observed in the parenchyma of pineal gland and subcommissural organ. Neurons of supraoptic and paraventricular nuclei of hypothalamus gave a strong positive reaction.

### 4.6.3 Phosphatases

In the cerebral cortex, the outer plexiform layer gave a more prominent reaction for alkaline phosphatase (ALP) than other layers (Fig. 233). White matter of the cerebrum also showed a positive reaction. The neurons and glial cells were negative. But the nucleoli of neurons gave a positive reaction. The tunica intima of blood vessels both in the gray and white matter showed a strong positive reaction. In the cerebellum, the white matter (*arbor vitae*) was strongly positive (Fig. 234). Granule cells of cerebellum also showed a positive reaction. Purkinje cells, molecular layer, cerebellar glomeruli and deep cerebellar neurons showed negligible activity. In the brainstem, ALP activity was noticed in the blood vessels and neuropil. Activity was particularly strong in the hypothalamus especially in the highly vascularized supraoptic and paraventricular nuclei. Choroid plexus of the ventricles and pia-arachnoid gave a strong positive reaction (Fig. 235). The dura mater showed no activity. Ependymal cells lining the ventricles and tanocytes of the subcommissural organ showed a positive reaction. A mild reaction for ALP was noticed in the pineal gland.

Acid phosphatase (ACP) activity was less pronounced in the foetal brain when compared to that of ALP. In general, ACP activity was noticed in the cytoplasm of all neurons and glial cells. In the glial cells the activity was weak and granules were

difficult to distinguish. In the telencephalon, pyramidal neurons of the cortex and neurons of the hippocampus showed more activity. In the hypothalamus, neurons of the supraoptic and paraventricular nuclei also showed positive reaction. In the brainstem, moderate activity was observed in the nuclei of cranial nerves. The choroid plexus, meninges and blood vessels did not show any ACP activity. In the cerebellum, positive activity was noticed in Purkinje cells, granule cells, Golgi cells and glial cells (Fig. 236). In some Purkinje cells, the activity also extended into the dendrites. Among the various neurons of the brain, the Purkinje cells, pyramidal neurons and cranial nerve nuclei showed more activity indicating a higher rate of metabolism in these cells. The granule cells of cerebrum and cerebellum showed only mild activity. White matter of the cerebellum showed a moderate activity (Fig. 237). The ependymal cells reacted positively for ACP and ALP. More enzyme activity was noticed at the luminal borders of these cells. Histoenzymic studies on the pineal gland revealed a moderate ACP reaction in pinealocytes and glial cells as uniformly distributed granules (Fig. 238). The reaction was more intense in the pineal cortex.

## *Tables*

---

**Table 1. Body weight, age and straight CRL of goat fetuses at different stages**

| Sl. No. | Sex | Body weight (g) | Foetal age in days | Straight CRL (cm) |
|---------|-----|-----------------|--------------------|-------------------|
| 1       | I   | 0.279           | 24                 | 1.400             |
| 2       | I   | 0.365           | 26                 | 1.500             |
| 3       | I   | 0.401           | 26                 | 1.500             |
| 4       | I   | 0.428           | 26                 | 1.500             |
| 5       | I   | 0.429           | 26                 | 1.500             |
| 6       | I   | 0.480           | 27                 | 1.600             |
| 7       | I   | 1.304           | 40                 | 2.500             |
| 8       | I   | 1.305           | 40                 | 2.500             |
| 9       | I   | 4.351           | 47                 | 3.900             |
| 10      | I   | 4.789           | 48                 | 4.000             |
| 11      | M   | 11.504          | 54                 | 6.000             |
| 12      | M   | 13.612          | 55                 | 7.100             |
| 13      | F   | 17.669          | 57                 | 7.500             |
| 14      | M   | 18.103          | 57                 | 7.500             |
| 15      | M   | 20.030          | 58                 | 7.600             |
| 16      | F   | 20.315          | 58                 | 7.600             |
| 17      | M   | 25.907          | 61                 | 8.300             |
| 18      | F   | 27.000          | 61                 | 8.300             |
| 19      | M   | 27.686          | 62                 | 8.600             |
| 20      | F   | 28.628          | 62                 | 8.700             |
| 21      | F   | 46.263          | 67                 | 9.500             |
| 22      | F   | 50.468          | 69                 | 10.200            |
| 23      | M   | 88.000          | 76                 | 12.000            |
| 24      | F   | 94.000          | 77                 | 13.000            |
| 25      | F   | 110.000         | 80                 | 13.000            |
| 26      | M   | 115.000         | 81                 | 13.000            |
| 27      | M   | 130.000         | 83                 | 15.100            |
| 28      | F   | 157.000         | 86                 | 15.500            |

**Table 1. Continued.....**

| Sl. No. | Sex | Body weight (g) | Foetal age in days | Straight CRL (cm) |
|---------|-----|-----------------|--------------------|-------------------|
| 29      | F   | 220.000         | 93                 | 18.300            |
| 30      | F   | 240.000         | 95                 | 18.800            |
| 31      | F   | 240.000         | 95                 | 19.200            |
| 32      | M   | 250.000         | 96                 | 19.000            |
| 33      | F   | 250.000         | 96                 | 18.300            |
| 34      | M   | 250.000         | 96                 | 20.300            |
| 35      | F   | 280.000         | 98                 | 20.300            |
| 36      | M   | 320.000         | 101                | 20.000            |
| 37      | M   | 325.000         | 102                | 19.800            |
| 38      | F   | 360.000         | 104                | 20.500            |
| 39      | F   | 700.000         | 123                | 26.500            |
| 40      | M   | 740.000         | 124                | 27.500            |
| 41      | M   | 750.000         | 125                | 26.400            |
| 42      | M   | 760.000         | 125                | 29.500            |
| 43      | M   | 810.000         | 127                | 28.100            |
| 44      | F   | 1040.000        | 128                | 29.500            |
| 45      | F   | 1400.000        | 130                | 34.000            |
| 46      | M   | 1630.000        | 140                | 39.500            |
| 47      | M   | 1680.000        | 142                | 39.000            |
| 48      | F   | 1800.000        | 144                | 40.500            |
| 49      | F   | 2080.000        | 145                | 38.500            |
| 50      | M   | 2260.000        | 146                | 36.500            |
| 51      | M   | 2300.000        | 147                | 37.000            |
| 52      | M   | 2880.000        | Full term          | 41.500            |

I- Indifferent

M- Male

F- Female



**Table 2. Age, body weight, straight CRL and number of goat foetuses used for the study**

| Groups | Age in days   | Body weight (g)  | Straight CRL (cm) | Number of foetuses |
|--------|---------------|------------------|-------------------|--------------------|
| 1      | 1-30          | 0.279-0.480      | 1.4-1.6           | 6                  |
| 2      | 31-60         | 1.304-20.315     | 2.5-7.6           | 10                 |
| 3      | 61-90         | 25.907-157.000   | 8.3-15.5          | 12                 |
| 4      | 91-120        | 220.000-360.000  | 18.3-20.5         | 10                 |
| 5      | 121-Full term | 700.000-2880.000 | 26.5-41.5         | 14                 |

**Table 3. Micrometrical parameters of telencephalon in the first month of gestation in goat foetuses,  $\mu\text{m}$**

| Parameters                  | Range<br>(n=6) | Mean $\pm$ S.E.        |
|-----------------------------|----------------|------------------------|
| <b>TELENCEPHALON</b>        |                |                        |
| a. Total length             | 3000-5000      | 4000.000 $\pm$ 356.148 |
| b. Total width              | 1280-2032      | 1621.333 $\pm$ 133.461 |
| c. Total height             | 816-1696       | 1245.333 $\pm$ 156.681 |
| d. Width of lumen           | 1088-1536      | 1304.000 $\pm$ 77.700  |
| e. Height of lumen          | 608-1360       | 965.333 $\pm$ 132.176  |
| <b>LATERAL WALL</b>         |                |                        |
| f. Total width              | 96-120         | 130.667 $\pm$ 10.667   |
| g. Width of ependymal layer | 56-96          | 78.000 $\pm$ 6.673     |
| h. Width of mantle layer    | 24-40          | 34.000 $\pm$ 2.875     |
| i. Width of marginal layer  | 16-24          | 18.667 $\pm$ 1.687     |
| <b>DORSAL WALL</b>          |                |                        |
| j. Total width              | 72-96          | 83.333 $\pm$ 4.185     |
| k. Width of ependymal layer | 40-48          | 46.000 $\pm$ 1.366     |
| l. Width of mantle layer    | 16-28          | 20.000 $\pm$ 2.530     |
| m. Width of marginal layer  | 16-20          | 17.333 $\pm$ 0.843     |
| <b>VENTRAL WALL</b>         |                |                        |
| n. Total width              | 76-96          | 85.333 $\pm$ 3.676     |
| o. Width of ependymal layer | 44-48          | 46.667 $\pm$ 0.843     |
| p. Width of mantle layer    | 16-28          | 21.333 $\pm$ 2.231     |
| q. Width of marginal layer  | 16-20          | 17.333 $\pm$ 0.843     |
| <b>OLFACTORY PIT</b>        |                |                        |
| r. Total width              | 128-448        | 261.333 $\pm$ 60.809   |
| s. Total height             | 224-688        | 453.333 $\pm$ 84.731   |
| t. Width of wall            | 32-48          | 40.000 $\pm$ 2.921     |
| u. Width of lumen           | 64-352         | 181.333 $\pm$ 55.220   |
| v. Height of lumen          | 160-592        | 373.333 $\pm$ 78.890   |
| <b>ROOF PLATE</b>           |                |                        |
| w. Thickness                | 24-64          | 40.667 $\pm$ 6.566     |

**Table 4. Micrometrical parameters of diencephalon in the first month of gestation in goat foetuses,  $\mu\text{m}$**

| Parameters                  | Range<br>(n=6) | Mean $\pm$ S.E         |
|-----------------------------|----------------|------------------------|
| <b>DIENCEPHALON</b>         |                |                        |
| a. Total length             | 1251-1475      | 1336.667 $\pm$ 35.882  |
| b. Total width              | 912-2080       | 1376.000 $\pm$ 220.970 |
| c. Total height             | 1024-1184      | 1104.000 $\pm$ 25.466  |
| d. Width of lumen           | 288-640        | 458.667 $\pm$ 61.646   |
| e. Height of lumen          | 752-800        | 773.333 $\pm$ 8.176    |
| <b>LATERAL WALL</b>         |                |                        |
| f. Total width              | 208-480        | 333.333 $\pm$ 47.359   |
| g. Width of ependymal layer | 96-112         | 104.000 $\pm$ 2.921    |
| h. Width of mantle layer    | 80-320         | 192.000 $\pm$ 41.876   |
| i. Width of marginal layer  | 32-48          | 37.333 $\pm$ 3.373     |
| <b>DORSAL WALL</b>          |                |                        |
| j. Total width              | 128-368        | 248.000 $\pm$ 41.053   |
| k. Width of ependymal layer | 64-96          | 81.333 $\pm$ 4.807     |
| l. Width of mantle layer    | 32-232         | 132.000 $\pm$ 35.100   |
| m. Width of marginal layer  | 32-40          | 34.667 $\pm$ 1.687     |
| <b>VENTRAL WALL</b>         |                |                        |
| n. Total width              | 96-128         | 114.667 $\pm$ 5.333    |
| o. Width of ependymal layer | 56-80          | 67.333 $\pm$ 4.185     |
| p. Width of mantle layer    | 24-40          | 31.333 $\pm$ 2.171     |
| q. Width of marginal layer  | 16-16          | 16.000 $\pm$ 0.000     |
| <b>OTOCYST</b>              |                |                        |
| r. Total width              | 224-256        | 240.000 $\pm$ 4.169    |
| s. Total height             | 368-560        | 450.667 $\pm$ 33.413   |
| t. Width of wall            | 24-32          | 28.667 $\pm$ 1.229     |
| u. Width of lumen           | 168-192        | 182.667 $\pm$ 4.341    |
| v. Height of lumen          | 304-512        | 393.333 $\pm$ 35.262   |
| <b>OPTIC CUP</b>            |                |                        |
| w. Diameter                 | 192-448        | 344.000 $\pm$ 46.510   |
| <b>SEMILUNAR GANGLION</b>   |                |                        |
| x. Width                    | 240-320        | 292.000 $\pm$ 14.274   |
| y. Length                   | 464-624        | 550.667 $\pm$ 26.806   |
| <b>NODOSE GANGLION</b>      |                |                        |
| z. Width                    | 160-224        | 192.000 $\pm$ 9.906    |
| aa. Length                  | 112-176        | 144.000 $\pm$ 9.906    |
| <b>ROOF PLATE</b>           |                |                        |
| bb. Thickness               | 48-176         | 114.667 $\pm$ 22.690   |
| <b>FLOOR PLATE</b>          |                |                        |
| cc. Thickness               | 144-208        | 168.000 $\pm$ 9.238    |

**Table 5. Micrometrical parameters of mesencephalon in the first month of gestation in goat foetuses,  $\mu\text{m}$**

| Parameters                  | Range<br>(n=6) | Mean $\pm$ S.E        |
|-----------------------------|----------------|-----------------------|
| <b>MESENCEPHALON</b>        |                |                       |
| a. Total length             | 1544-1576      | 1560.000 $\pm$ 4.619  |
| b. Total width              | 960-1344       | 1184.333 $\pm$ 64.250 |
| c. Total height             | 960-1056       | 1010.000 $\pm$ 15.029 |
| d. Width of lumen           | 640-1008       | 861.333 $\pm$ 68.560  |
| e. Height of lumen          | 816-856        | 835.667 $\pm$ 6.249   |
| <b>BASAL PLATE</b>          |                |                       |
| f. Total width              | 160-260        | 212.500 $\pm$ 16.915  |
| g. Total height             | 306-400        | 350.333 $\pm$ 17.175  |
| h. Width of ependymal layer | 80-104         | 93.333 $\pm$ 4.088    |
| i. Width of mantle layer    | 64-132         | 90.167 $\pm$ 10.635   |
| j. Width of marginal layer  | 16-52          | 29.000 $\pm$ 5.459    |
| <b>ALAR PLATE</b>           |                |                       |
| k. Total width              | 144-230        | 190.333 $\pm$ 14.726  |
| l. Total height             | 480-660        | 573.333 $\pm$ 32.215  |
| m. Width of ependymal layer | 80-117         | 97.667 $\pm$ 6.535    |
| n. Width of mantle layer    | 48-108         | 70.000 $\pm$ 12.033   |
| o. Width of marginal layer  | 16-26          | 22.667 $\pm$ 2.108    |
| <b>ROOF PLATE</b>           |                |                       |
| p. Total width              | 33-45          | 39.000 $\pm$ 2.191    |
| q. Width of ependymal layer | 23-29          | 26.000 $\pm$ 1.095    |
| r. Width of marginal layer  | 10-16          | 13.000 $\pm$ 1.095    |
| <b>VENTRAL COMMISSURE</b>   |                |                       |
| s. Total width              | 130-156        | 143.000 $\pm$ 4.747   |
| t. Width of ependymal layer | 100-117        | 109.000 $\pm$ 3.148   |
| u. Width of marginal layer  | 30-39          | 34.000 $\pm$ 1.673    |

**Table 6. Micrometrical parameters of metencephalon in the first month of gestation in goat foetuses,  $\mu\text{m}$**

| Parameters                  | Range<br>(n=6) | Mean $\pm$ S.E         |
|-----------------------------|----------------|------------------------|
| <b>METENCEPHALON</b>        |                |                        |
| a. Total length             | 288-324        | 312.000 $\pm$ 6.450    |
| b. Total width              | 880-1872       | 1480.000 $\pm$ 190.472 |
| c. Total height             | 1100-1600      | 1308.333 $\pm$ 93.360  |
| d. Width of lumen           | 640-910        | 820.667 $\pm$ 56.502   |
| e. Height of lumen          | 672-1010       | 817.500 $\pm$ 50.750   |
| <b>BASAL PLATE</b>          |                |                        |
| f. Total width              | 360-455        | 419.000 $\pm$ 18.808   |
| g. Total height             | 640-820        | 725.000 $\pm$ 33.015   |
| h. Width of ependymal layer | 78-120         | 105.000 $\pm$ 8.556    |
| i. Width of mantle layer    | 214-325        | 279.333 $\pm$ 21.199   |
| j. Width of marginal layer  | 26-39          | 34.667 $\pm$ 2.741     |
| <b>ALAR PLATE</b>           |                |                        |
| k. Total width              | 328-390        | 369.333 $\pm$ 13.071   |
| l. Total height             | 481-780        | 607.000 $\pm$ 56.636   |
| m. Width of ependymal layer | 78-169         | 119.000 $\pm$ 16.856   |
| n. Width of mantle layer    | 182-351        | 242.000 $\pm$ 34.528   |
| o. Width of marginal layer  | 26-52          | 39.000 $\pm$ 4.747     |
| <b>ROOF PLATE</b>           |                |                        |
| p. Total width              | 152-195        | 172.000 $\pm$ 7.908    |
| q. Width of ependymal layer | 60-65          | 63.333 $\pm$ 1.054     |
| r. Width of marginal layer  | 92-135         | 110.333 $\pm$ 8.102    |
| <b>VENTRAL COMMISSURE</b>   |                |                        |
| s. Total width              | 180-210        | 195.000 $\pm$ 5.477    |
| t. Width of ependymal layer | 85-100         | 92.000 $\pm$ 2.757     |
| u. Width of marginal layer  | 95-110         | 103.000 $\pm$ 2.757    |

**Table 7. Micrometrical parameters of myelencephalon in the first month of gestation in goat fetuses,  $\mu\text{m}$**

| Parameters                  | Range<br>(n=6) | Mean $\pm$ S.E        |
|-----------------------------|----------------|-----------------------|
| <b>MYELENCEPHALON</b>       |                |                       |
| a. Total length             | 1296-1408      | 1345.333 $\pm$ 16.319 |
| b. Total width              | 896-1360       | 1178.667 $\pm$ 63.688 |
| c. Total height             | 784-1200       | 936.000 $\pm$ 72.355  |
| d. Width of lumen           | 640-896        | 797.333 $\pm$ 47.718  |
| e. Height of lumen          | 560-784        | 680.000 $\pm$ 38.478  |
| <b>BASAL PLATE</b>          |                |                       |
| f. Total width              | 224-432        | 321.333 $\pm$ 36.039  |
| g. Total height             | 480-720        | 585.333 $\pm$ 42.050  |
| h. Width of ependymal layer | 80-104         | 92.667 $\pm$ 4.185    |
| i. Width of mantle layer    | 112-288        | 195.333 $\pm$ 31.163  |
| j. Width of marginal layer  | 16-64          | 33.333 $\pm$ 8.620    |
| <b>ALAR PLATE</b>           |                |                       |
| k. Total width              | 112-304        | 220.667 $\pm$ 33.028  |
| l. Total height             | 304-360        | 329.333 $\pm$ 10.414  |
| m. Width of ependymal layer | 64-160         | 106.667 $\pm$ 16.707  |
| n. Width of mantle layer    | 32-80          | 62.000 $\pm$ 8.929    |
| o. Width of marginal layer  | 16-64          | 34.000 $\pm$ 8.989    |
| <b>ROOF PLATE</b>           |                |                       |
| p. Width of ependymal layer | 16-20          | 18.000 $\pm$ 0.894    |
| <b>VENTRAL COMMISSURE</b>   |                |                       |
| q. Total width              | 144-240        | 189.333 $\pm$ 15.549  |
| r. Width of ependymal layer | 76-84          | 80.667 $\pm$ 1.229    |
| s. Width of marginal layer  | 64-156         | 108.667 $\pm$ 15.779  |

**Table 8. Correlation and regression coefficients of brain vesicle parameters in the first month of gestation**

| Parameters                       |                                  | Correlation coefficient | Regression of y on x (b±S.E.) |
|----------------------------------|----------------------------------|-------------------------|-------------------------------|
| Independent variable (x)         | Dependent variable (y)           |                         |                               |
| Length of telencephalon          | Length of metencephalon          | 0.895**                 | 0.040±0.010**                 |
| Length of telencephalon          | Length of myelencephalon         | 0.849**                 | 0.015±0.005**                 |
| Width of telencephalon           | Width of diencephalon            | 0.983**                 | 1.627±0.154**                 |
| Height of telencephalon          | Height of diencephalon           | 0.986**                 | 0.160±0.014**                 |
| Height of telencephalon          | Height of mesencephalon          | 0.973**                 | 0.093±0.011**                 |
| Height of telencephalon          | Height of metencephalon          | 0.822**                 | 0.380±0.131**                 |
| Height of diencephalon           | Height of mesencephalon          | 0.981**                 | 0.579±0.057**                 |
| Height of metencephalon          | Height of myelencephalon         | 0.847**                 | 0.616±0.193**                 |
| Width of lumen of diencephalon   | Width of lumen of mesencephalon  | 0.847**                 | 0.616±0.193**                 |
| Height of lumen of telencephalon | Height of lumen of diencephalon  | 0.999**                 | 0.061±0.004**                 |
| Height of lumen of telencephalon | Height of lumen of mesencephalon | 0.972**                 | 0.046±0.006**                 |
| Height of lumen of diencephalon  | Height of lumen of mesencephalon | 0.988**                 | 0.755±0.058**                 |

\*\* P<0.01 (significant at 1% level)

Table 9. Body parameters of goat foetuses at different ages

| Sl. No. | Parameters   | 2 <sup>nd</sup> month (n=10) |                    | 3 <sup>rd</sup> month (n=12) |                     | 4 <sup>th</sup> month (n=10) |                      | 5 <sup>th</sup> month (n=14) |                        |
|---------|--|------------------------------|--------------------|------------------------------|---------------------|------------------------------|----------------------|------------------------------|------------------------|
|         |  | Range                        | Mean $\pm$ SE      | Range                        | Mean $\pm$ SE       | Range                        | Mean $\pm$ SE        | Range                        | Mean $\pm$ SE          |
| 1       | Body weight (g)  | 1.304-20.315                 | 11.298 $\pm$ 2.450 | 25.907-157.000               | 74.996 $\pm$ 13.381 | 220.000-360.000              | 273.500 $\pm$ 14.569 | 700.000-2880.00              | 1487.857 $\pm$ 190.734 |
| 2       | Age (days)   | 40.000-58.000                | 51.400 $\pm$ 2.262 | 61.000-86.000                | 72.083 $\pm$ 2.723  | 93.000-104.000               | 97.600 $\pm$ 1.127   | 123.000-150.000              | 135.429 $\pm$ 2.719    |
| 3       | CRL (straight) from forehead to base of tail (cm)          | 2.500-7.600                  | 5.620 $\pm$ 0.686  | 8.300-15.500                 | 11.267 $\pm$ 0.767  | 18.300-20.500                | 19.450 $\pm$ 0.265   | 26.400-41.500                | 33.857 $\pm$ 1.520     |
| 4       | CRL (curved) (cm)  | 4.900-9.600                  | 7.710 $\pm$ 0.670  | 10.500-18.800                | 14.310 $\pm$ 0.857  | 21.700-25.400                | 24.270 $\pm$ 0.407   | 30.900-45.200                | 38.900 $\pm$ 1.329     |
| 5       | Total body length from tuber scapulae to tuber ischii (cm) | 1.100-4.550                  | 3.167 $\pm$ 0.428  | 4.960-9.000                  | 7.057 $\pm$ 0.505   | 11.300-13.000                | 12.280 $\pm$ 0.169   | 16.000-29.000                | 22.236 $\pm$ 1.329     |
| 6       | Total bent length from premaxilla to tail tip (cm)         | 5.900-12.300                 | 9.890 $\pm$ 0.826  | 13.200-24.200                | 18.192 $\pm$ 1.161  | 28.600-32.600                | 31.210 $\pm$ 0.386   | 41.000-62.400                | 51.257 $\pm$ 2.015     |
| 7       | Head length (straight) (cm)                                | 1.570-3.100                  | 2.617 $\pm$ 0.188  | 3.380-5.790                  | 4.438 $\pm$ 0.280   | 6.930-7.700                  | 7.237 $\pm$ 0.063    | 8.800-11.900                 | 10.089 $\pm$ 0.280     |
| 8       | Head length (curved) (cm)                                  | 2.500-4.500                  | 3.556 $\pm$ 0.264  | 4.700-8.200                  | 6.018 $\pm$ 0.372   | 9.000-10.200                 | 9.720 $\pm$ 0.136    | 11.800-16.200                | 13.871 $\pm$ 0.390     |



Table 9. Continued .....

| Sl. No. | Parameters                        | 2 <sup>nd</sup> month (n=10) |                   | 3 <sup>rd</sup> month (n=12) |                    | 4 <sup>th</sup> month (n=10) |                    | 5 <sup>th</sup> month (n=14) |                    |
|---------|-----------------------------------|------------------------------|-------------------|------------------------------|--------------------|------------------------------|--------------------|------------------------------|--------------------|
|         |                                   | Range                        | Mean $\pm$ SE     | Range                        | Mean $\pm$ SE      | Range                        | Mean $\pm$ SE      | Range                        | Mean $\pm$ SE      |
| 9       | Head width (cm)                   | 0.800-1.880                  | 1.383 $\pm$ 0.138 | 1.950-3.000                  | 2.589 $\pm$ 0.129  | 3.200-4.400                  | 3.902 $\pm$ 0.166  | 4.500-6.500                  | 5.491 $\pm$ 0.167  |
| 10      | Vertebral column length (cm)      | 3.400-5.900                  | 5.020 $\pm$ 0.321 | 6.800-12.900                 | 9.433 $\pm$ 0.642  | 15.700-17.800                | 16.770 $\pm$ 0.239 | 23.700-40.300                | 30.900 $\pm$ 1.520 |
| 11      | Vertebral column tail length (cm) | 4.000-7.700                  | 6.250 $\pm$ 0.478 | 8.300-15.500                 | 11.417 $\pm$ 0.793 | 19.600-22.100                | 21.140 $\pm$ 0.225 | 29.000-51.700                | 38.043 $\pm$ 2.003 |
| 12      | Tail length (cm)                  | 0.600-1.800                  | 1.230 $\pm$ 0.173 | 1.100-2.600                  | 1.983 $\pm$ 0.170  | 3.800-5.000                  | 4.370 $\pm$ 0.133  | 3.200-11.400                 | 7.164 $\pm$ 0.600  |
| 13      | Forelimb length (cm)              | 0.740-4.680                  | 2.790 $\pm$ 0.452 | 4.700-10.000                 | 6.717 $\pm$ 0.570  | 12.600-15.000                | 13.520 $\pm$ 0.213 | 20.600-35.700                | 26.936 $\pm$ 1.279 |
| 14      | Hind limb length (cm)             | 0.700-4.200                  | 2.675 $\pm$ 0.412 | 4.400-11.400                 | 6.742 $\pm$ 0.675  | 12.500-15.000                | 13.680 $\pm$ 0.221 | 20.200-32.000                | 26.421 $\pm$ 1.194 |
| 15      | Tibial length (cm)                | 0.600-1.680*                 | 1.11 $\pm$ 0.138  | 1.400-3.000                  | 2.275 $\pm$ 0.156  | 3.700-4.600                  | 4.080 $\pm$ 0.102  | 6.500-12.00                  | 8.243 $\pm$ 0.432  |
| 16      | Chest depth (cm)                  | 1.000-2.100                  | 1.535 $\pm$ 0.125 | 2.300-4.300                  | 3.165 $\pm$ 0.217  | 4.900-5.700                  | 5.420 $\pm$ 0.083  | 7.300-13.800                 | 9.807 $\pm$ 0.503  |
| 17      | Chest circumference (cm)          | 2.500-6.400                  | 4.750 $\pm$ 0.434 | 6.500-12.000                 | 9.000 $\pm$ 0.550  | 13.400-15.500                | 14.340 $\pm$ 0.240 | 17.500-31.300                | 24.207 $\pm$ 1.057 |

\*Number of foetuses = 8

Table 10. Head parameters of goat foetuses at different ages, cm

| Parameters   | 2 <sup>nd</sup> month (n=8) |                 | 3 <sup>rd</sup> month (n=12) |                 | 4 <sup>th</sup> month (n=10) |                 | 5 <sup>th</sup> month (n=14) |                  |
|--|-----------------------------|-----------------|------------------------------|-----------------|------------------------------|-----------------|------------------------------|------------------|
|  | Range                       | Mean± SE        | Range                        | Mean± SE        | Range                        | Mean± SE        | Range                        | Mean± SE         |
| Head length (curved)                               | 2.500-<br>4.500             | 3.556<br>±0.264 | 4.700-<br>8.200              | 6.018<br>±0.372 | 9.000-<br>10.200             | 9.720<br>±0.136 | 11.800-<br>16.200            | 13.871<br>±0.390 |
| Cranial length (curved)                            | 2.200-<br>3.200             | 2.750<br>±0.134 | 3.300-<br>5.900              | 4.343<br>±0.258 | 6.500-<br>7.100              | 6.790<br>±0.074 | 2.200-<br>10.800             | 9.457<br>±0.223  |
| Facial length (curved)                             | 0.300-<br>1.400             | 0.810<br>±0.140 | 1.300-<br>2.400              | 1.692<br>±0.118 | 2.500-<br>3.100              | 2.930<br>±0.073 | 3.600-<br>5.600              | 4.414<br>±0.176  |
| Interauricular distance                            | 1.500-<br>2.700             | 2.125<br>±0.156 | 2.700-<br>4.200              | 3.333<br>±0.142 | 4.600-<br>5.000              | 4.870<br>±0.056 | 5.800-<br>10.300             | 7.907<br>±0.503  |
| Transverse distance<br>between lateral canthi      | 1.06.-<br>3.400             | 2.595<br>±0.340 | 3.100-<br>5.900              | 4.575<br>±0.300 | 6.200-<br>6.700              | 6.440<br>±0.058 | 7.020-<br>11.300             | 9.223<br>±0.380  |
| Transverse distance<br>between medial canthi       | 0.700-<br>1.500             | 1.150<br>±0.112 | 1.500-<br>2.700              | 2.003<br>±0.121 | 3.600-<br>3.920              | 3.853<br>±0.031 | 3.940-<br>5.800              | 4.963<br>±0.163  |
| Transverse distance<br>between cornual buds        | 1.700-<br>1.830             | 1.773<br>±0.024 | 2.100-<br>3.000              | 2.472<br>±0.093 | 2.800-<br>4.000              | 3.110<br>±0.125 | 4.100-<br>5.700              | 4.988<br>±0.127  |
| Intersupraorbital<br>foramina distance             | 0.500-<br>1.100             | 0.829<br>±0.088 | 1.000-<br>1.800              | 1.383<br>±0.085 | 1.900-<br>2.200              | 2.007<br>±0.038 | 2.300-<br>3.400              | 2.879<br>±0.098  |
| Trans. dist. bet. dorsal<br>commissure of nostrils | 0.200-<br>0.400             | 0.305<br>±0.028 | 0.380-<br>0.900              | 0.555<br>±0.046 | 0.960-<br>1.000              | 0.982<br>±0.005 | 1.080-<br>1.820              | 1.488<br>±0.066  |
| Posterior cranial height                           | 2.000-<br>3.000             | 2.525<br>±0.141 | 3.000-<br>4.300              | 3.583<br>±0.143 | 5.400-<br>6.100              | 5.770<br>±0.079 | 6.600-<br>8.000              | 7.393<br>±0.145  |

Table 11. Skull parameters of goat foetuses at different ages

| Parameters                         | 2 <sup>nd</sup> month (n=8) |                  | 3 <sup>rd</sup> month (n=12) |                  | 4 <sup>th</sup> month (n=10) |                  | 5 <sup>th</sup> month (n=14) |                  |
|------------------------------------|-----------------------------|------------------|------------------------------|------------------|------------------------------|------------------|------------------------------|------------------|
|                                    | Range                       | Mean±SE          | Range                        | Mean±SE          | Range                        | Mean±SE          | Range                        | Mean±SE          |
| Skull length (cm)                  | 1.470-<br>2.960             | 2.429 ±<br>0.223 | 3.280-<br>5.600              | 4.333<br>±0.277  | 6.820-<br>7.600              | 7.136<br>±0.064  | 8.000-<br>11.200             | 9.939<br>±0.247  |
| Skull width (cm)                   | 0.940-<br>1.650             | 1.455<br>±0.110  | 1.800-<br>3.200              | 2.430<br>±0.176  | 3.300-<br>3.820              | 3.629<br>±0.052  | 4.480-<br>5.900              | 5.356<br>±0.135  |
| Cephalic index (%)                 | 55.740-<br>69.570           | 60.780<br>±1.912 | 51.490-<br>62.650            | 55.598<br>±0.818 | 48.387-<br>53.670            | 50.850<br>±0.536 | 51.110-<br>57.580            | 53.920<br>±0.567 |
| Neurocranial length (cm)           | 1.180-<br>2.000             | 1.772<br>±0.128  | 2.300-<br>3.980              | 3.036<br>±0.190  | 4.320-<br>4.700              | 4.578<br>±0.041  | 5.500-<br>7.800              | 6.743<br>±0.216  |
| Cranial index (%)                  | 79.000-<br>84.210           | 81.926<br>±0.686 | 70.630-<br>87.710            | 79.557<br>±1.442 | 76.390-<br>84.070            | 78.839<br>±0.902 | 75.640-<br>85.960            | 79.609<br>±0.897 |
| Cranial height (cm)                | 0.900-<br>1.430             | 1.281<br>±0.082  | 1.620-<br>3.400              | 2.615<br>±0.209  | 3.700-<br>3.940              | 3.801<br>±0.024  | 4.100-<br>6.900              | 4.943<br>±0.195  |
| Facial length (cm)                 | 0.290-<br>0.960             | 0.701<br>±0.111  | 0.960-<br>1.620              | 1.300<br>±0.089  | 2.440-<br>2.900              | 2.588<br>±0.053  | 3.000-<br>4.300              | 3.557<br>±0.100  |
| Interorbital length (minimum) (cm) | 0.480-<br>0.980             | 0.758<br>±0.066  | 1.000-<br>2.100              | 1.443<br>±0.117  | 2.400-<br>2.620              | 2.531<br>±0.021  | 3.000-<br>4.650              | 3.867<br>±0.154  |
| Height of foramen magnum (cm)      | 0.180-<br>0.300             | 0.273<br>±0.018  | 0.300-<br>0.600              | 0.413<br>±0.034  | 0.600-<br>0.720              | 0.656<br>±0.016  | 0.790-<br>1.440              | 1.165<br>±0.067  |
| Width of foramen magnum (cm)       | 0.200-<br>0.400             | 0.339<br>±0.028  | 0.340-<br>0.620              | 0.459<br>±0.031  | 0.700-<br>0.800              | 0.722<br>±0.010  | 0.800-<br>2.000              | 1.283<br>±0.095  |

Table 12. Craniometry of goat foetuses at different ages, cm

| Parameters                          | 2 <sup>nd</sup> month<br>(n=6) |                 | 3 <sup>rd</sup> month<br>(n=12) |                 | 4 <sup>th</sup> month<br>(n=10) |                  | 5 <sup>th</sup> month<br>(n=14) |                 |
|-------------------------------------|--------------------------------|-----------------|---------------------------------|-----------------|---------------------------------|------------------|---------------------------------|-----------------|
|                                     | Range                          | Mean ±SE        | Range                           | Mean ±SE        | Range                           | Mean ±SE         | Range                           | Mean ±SE        |
| Length of nasal bone                | 0.700-<br>0.960                | 0.860<br>±0.047 | 0.960-<br>1.620                 | 1.300<br>±0.089 | 2.440-<br>2.780                 | 2.518<br>±0.030  | 3.000-<br>4.300                 | 3.500<br>±0.102 |
| Medial length of frontal bone       | 1.100-<br>1.500                | 1.400<br>±0.063 | 1.600-<br>2.400                 | 1.964<br>±0.085 | 2.940-<br>3.320                 | .086<br>±0.041   | 3.500-<br>5.200                 | 4.386<br>±0.157 |
| Medial length of parietal bone      | 0.420-<br>0.480                | 0.457<br>±0.011 | 0.490-<br>1.080                 | 0.738<br>±0.064 | 1.100-<br>1.250                 | 1.182<br>±0.020  | 1.300-<br>1.450                 | 1.362<br>±0.012 |
| Lateral length of parietal          | 0.600-<br>0.700                | 0.660<br>±0.019 | 0.700-<br>1.500                 | 1.094<br>±0.104 | 1.550-<br>1.710                 | 1.624<br>±0.019  | 1.850-<br>3.200                 | 2.654<br>±0.135 |
| Anterior width of parietal          | 0.800-<br>1.100                | 0.967<br>±0.042 | 1.190-<br>2.100                 | 1.626<br>±0.100 | 2.280-<br>2.720                 | 2.424<br>±0.053  | 3.000-<br>4.000                 | 3.491<br>±0.109 |
| Posterior width of parietal         | 0.900-<br>1.000                | 0.967<br>±0.021 | 0.960-<br>1.610                 | .252<br>±0.076  | 1.800-<br>2.330                 | 2.038<br>±0.070  | 2.400-<br>3.400                 | 2.920<br>±0.082 |
| Midsagittal length of interparietal | 0.460-<br>0.500                | 0.490<br>±0.007 | 0.480-<br>0.790                 | 0.628<br>±0.035 | 0.800-<br>1.100                 | 0.946<br>±0.028  | 1.120-<br>1.800                 | 1.441<br>±0.075 |
| Width of interparietal              | 0.940-<br>1.000                | 0.987<br>±0.010 | 1.100-<br>1.500                 | 1.294<br>±0.046 | 1.620-<br>1.960                 | 1.776<br>±0.042  | 2.200-<br>3.300                 | 2.600<br>±0.065 |
| Height of supraoccipital            | 0.740-<br>0.800                | 0.780<br>±0.010 | 1.000-<br>1.400                 | 1.211<br>±0.047 | 1.600-<br>1.840                 | 1.701<br>±0.027  | 2.400-<br>2.900                 | 2.659<br>±0.038 |
| Width of supraoccipital             | 1.200-<br>1.300                | 1.267<br>±0.017 | 1.280-<br>1.760                 | 1.518<br>±0.056 | 2.130-<br>2.820                 | 2.239<br>±0.068  | 3.100-<br>3.900                 | 3.433<br>±0.085 |
| Length of basioccipital             | 0.290-<br>0.310                | 0.302<br>±0.003 | 0.290-<br>0.440                 | 0.365<br>±0.016 | 0.500-<br>0.600                 | 0.555<br>±0.015  | 0.690-<br>0.910                 | 0.809<br>±0.024 |
| Maximum width of basioccipital      | 0.350-<br>0.420                | 0.405<br>±0.011 | 0.400-<br>0.620                 | 0.505<br>±0.023 | 0.800-<br>0.900                 | 0.868<br>±0.006  | 0.960-<br>1.340                 | 1.191<br>±0.040 |
| Minimum width of basioccipital      | 0.210-<br>0.240                | 0.228<br>±0.005 | 0.200-<br>0.400                 | 0.287<br>±0.019 | 0.400-<br>0.580                 | 0.471<br>±0.022  | 0.600-<br>1.000                 | 0.779<br>±0.035 |
| Length of basisphenoid              | 0.270-<br>0.300                | 0.293<br>±0.005 | 0.310-<br>0.440                 | 0.373<br>±0.015 | 0.500-<br>0.620                 | 0.558 ±<br>0.016 | 0.649-<br>0.930                 | 0.833<br>±0.025 |
| Length of presphenoid               | 0.370-<br>0.410                | 0.397<br>±0.006 | 0.420-<br>0.520                 | 0.462<br>±0.011 | 0.580-<br>0.740                 | 0.678<br>±0.017  | 0.750-<br>0.910                 | 0.846<br>±0.017 |
| Length of mandible                  | 1.300-<br>1.900                | 1.733<br>±0.092 | 1.970-<br>3.400                 | 2.546<br>±0.156 | 4.250-<br>4.640                 | 4.484<br>±0.050  | 5.100-<br>8.200                 | 6.471<br>±0.294 |
| Maximum intermandibular distance    | 0.460-<br>0.800                | 0.677<br>±0.064 | 0.810-<br>1.600                 | 1.277<br>±0.083 | 1.660-<br>1.900                 | 1.750<br>±0.024  | 2.460-<br>2.810                 | 2.608<br>±0.022 |

Table 13. Encephalometry of goat foetuses at different ages

| Sl. No. | Parameters                      | 2 <sup>nd</sup> month (n=10) |                 | 3 <sup>rd</sup> month (n=12) |                 | 4 <sup>th</sup> month (n=10) |                  | 5 <sup>th</sup> month (n=14) |                  |
|---------|---------------------------------|------------------------------|-----------------|------------------------------|-----------------|------------------------------|------------------|------------------------------|------------------|
|         |                                 | Range                        | Mean<br>±SE     | Range                        | Mean<br>±SE     | Range                        | Mean<br>±SE      | Range                        | Mean<br>±SE      |
| 1       | Brain weight (g)                | 0.700-<br>2.300              | 1.108<br>±0.163 | 2.480-<br>11.100             | 5.914<br>±0.835 | 14.090-<br>15.000            | 14.462<br>±0.136 | 19.700-<br>53.540            | 40.728<br>±2.986 |
| 2       | Brain volume (ml)               | 0.700-<br>2.400              | 1.170<br>±0.171 | 2.500-<br>11.500             | 6.075<br>±0.883 | 14.800-<br>15.000            | 14.970<br>±0.021 | 20.000-<br>54.000            | 41.143<br>±2.974 |
| 3       | Brain length (cm)               | 1.300-<br>2.200              | 1.821<br>±0.109 | 2.280-<br>4.300              | 3.013<br>±0.194 | 4.300-<br>5.200              | 4.874<br>±0.112  | 5.700-<br>7.700              | 6.959<br>±0.182  |
| 4       | Brain width (cm)                | 0.700-<br>1.460              | 1.120<br>±0.096 | 1.530-<br>2.900              | 2.114<br>±0.148 | 3.510-<br>3.780              | 3.597<br>±0.027  | 4.100-<br>5.190              | 4.761<br>±0.120  |
| 5       | Brain thickness (cm)            | 0.600-<br>1.300              | 0.990<br>±0.086 | 1.320-<br>2.300              | 1.818<br>±0.115 | 2.400-<br>2.600              | 2.443<br>±0.022  | 2.790-<br>3.300              | 3.001<br>±0.043  |
| 6       | Average weight of cerebrum (g)  | 0.200-<br>0.420              | 0.316<br>±0.025 | 0.430-<br>4.500              | 1.862<br>±0.359 | 5.150-<br>5.560              | 5.288<br>±0.048  | 7.000-<br>19.290             | 15.383<br>±1.196 |
| 7       | Average length of cerebrum (cm) | 0.600-<br>1.310              | 1.008<br>±0.081 | 1.310-<br>2.850              | 1.939<br>±0.139 | 3.300-<br>3.630              | 3.431<br>±0.036  | 4.450-<br>5.500              | 5.071<br>±0.078  |
| 8       | Average width of cerebrum (cm)  | 0.350-<br>0.730              | 0.560<br>±0.048 | 0.765-<br>1.450              | 1.057<br>±0.074 | 1.755-<br>1.890              | 1.800<br>±0.015  | 2.050-<br>2.595              | 2.380<br>±0.060  |
| 9       | Average height of cerebrum (cm) | 0.500-<br>1.100              | 0.823<br>±0.068 | 0.950-<br>2.100              | 1.367<br>±0.091 | 2.400-<br>2.490              | 2.431<br>±0.010  | 2.700-<br>3.100              | 2.969<br>±0.026  |
| 10      | Weight of cerebellum (g)        | 0.040-<br>0.100              | 0.059<br>±0.007 | 0.118-<br>0.510              | 0.310<br>±0.050 | 0.540-<br>0.720              | 0.614<br>±0.025  | 1.460-<br>5.980              | 3.841<br>±0.421  |

Table 13. Continued.....

| Sl. No. | Parameters                       | 2 <sup>nd</sup> month (n=10) |                 | 3 <sup>rd</sup> month (n=12) |                 | 4 <sup>th</sup> month (n=10) |                 | 5 <sup>th</sup> month (n=14) |                 |
|---------|----------------------------------|------------------------------|-----------------|------------------------------|-----------------|------------------------------|-----------------|------------------------------|-----------------|
|         |                                  | Range                        | Mean<br>±SE     | Range                        | Mean<br>±SE     | Range                        | Mean<br>±SE     | Range                        | Mean<br>±SE     |
| 11      | Length of cerebellum (cm)        | 0.270-<br>0.420              | 0.320<br>±0.019 | 0.400-<br>0.960              | 0.602<br>±0.058 | 1.100-<br>1.600              | 1.316<br>±0.058 | 2.000-<br>2.700              | 2.336<br>±0.070 |
| 12      | Width of cerebellum (cm)         | 0.160-<br>0.360              | 0.247<br>±0.026 | 0.390-<br>1.470              | 0.912<br>±0.128 | 1.490-<br>1.730              | 1.588<br>±0.030 | 2.100-<br>3.640              | 3.016<br>±0.167 |
| 13      | Thickness of cerebellum (cm)     | 0.028-<br>0.181              | 0.072<br>±0.019 | 0.270-<br>1.000              | 0.726<br>±0.082 | 1.010-<br>1.500              | 1.145<br>±0.055 | 1.600-<br>2.700              | 2.082<br>±0.080 |
| 14      | Weight of brain stem (g)         | 0.330-<br>0.440              | 0.374<br>±0.014 | 0.460-<br>2.270              | 1.437<br>±0.237 | 2.310-<br>2.820              | 2.487<br>±0.060 | 3.440-<br>8.880              | 6.685<br>±0.531 |
| 15      | Length of brain stem (cm)        | 1.200-<br>1.490              | 1.359<br>±0.033 | 1.500-<br>2.670              | 2.021<br>±0.151 | 2.700-<br>2.960              | 2.851<br>±0.025 | 3.400-<br>5.700              | 4.630<br>±0.236 |
| 16      | Maximum width of brain stem (cm) | 0.600-<br>0.960              | 0.755<br>±0.050 | 1.000-<br>1.860              | 1.429<br>±0.100 | 1.900-<br>1.990              | 1.947<br>±0.011 | 2.100-<br>3.300              | 2.670<br>±0.104 |
| 17      | Thickness of brain stem (cm)     | 0.200-<br>0.420              | 0.330<br>±0.026 | 0.440-<br>1.100              | 0.724<br>±0.069 | 1.200-<br>1.440              | 1.304<br>±0.028 | 1.480-<br>1.840              | 1.686<br>±0.038 |
| 18      | Cerebrum: brain ratio            | 0.183-<br>0.389              | 0.306<br>±0.019 | 0.173-<br>0.517              | 0.298<br>±0.031 | 0.353-<br>0.395              | 0.366<br>±0.003 | 0.256-<br>0.509              | 0.377<br>±0.014 |
| 19      | Cerebellum: brain ratio          | 0.043-<br>0.060              | 0.055<br>±0.001 | 0.041-<br>0.063              | 0.050<br>±0.002 | 0.038-<br>0.048              | 0.042<br>±0.001 | 0.055-<br>0.165              | 0.093<br>±0.007 |
| 20      | Brainstem: brain ratio           | 0.191-<br>0.472              | 0.377<br>±0.099 | 0.160-<br>0.330              | 0.230<br>±0.017 | 0.164-<br>0.188              | 0.172<br>±0.003 | 0.131-<br>0.229              | 0.023<br>±0.006 |

Table 14. Measurements of cerebral hemispheres of goat foetuses at different ages, cm

| Sl. No. | Parameters                                 | 2 <sup>nd</sup> month (n=10) |               | 3 <sup>rd</sup> month (n=12) |               | 4 <sup>th</sup> month (n=10) |               | 5 <sup>th</sup> month (n=14) |                |
|---------|--|------------------------------|---------------|------------------------------|---------------|------------------------------|---------------|------------------------------|----------------|
|         |  | Range                        | Mean±SE       | Range                        | Mean±SE       | Range                        | Mean±SE       | Range                        | Mean±SE        |
| 1       | Length of left cerebral hemisphere         | 0.600-1.300                  | 0.993 ± 0.078 | 1.300-2.900                  | 1.927 ± 0.142 | 3.300-3.620                  | 3.418 ± 0.033 | 4.400-5.500                  | 5.059 ± 0.077  |
| 2       | Length of right cerebral hemisphere        | 0.600-1.310                  | 1.022 ± 0.084 | 1.320-2.800                  | 1.951 ± 0.136 | 3.300-3.640                  | 3.432 ± 0.036 | 4.500-5.500                  | 5.083 ± 0.078  |
| 3       | Maximum width of left cerebral hemisphere  | 0.350-0.730                  | 0.560 ± 0.048 | 0.760-1.400                  | 1.046 ± 0.072 | 1.750-1.880                  | 1.787 ± 0.013 | 2.040-2.590                  | 3.372 ± 0.060  |
| 4       | Maximum width of right cerebral hemisphere | 0.350-0.730                  | 0.560 ± 0.048 | 0.770-1.500                  | 1.068 ± 0.076 | 1.760-1.900                  | 1.800 ± 0.013 | 2.060-2.600                  | 2.389 ± 0.060  |
| 5       | Minimum width of left cerebral hemisphere  | 0.300-0.520                  | 0.442 ± 0.027 | 0.480-1.100                  | 0.766 ± 0.069 | 1.420-1.530                  | 1.471 ± 0.012 | 1.500-1.700                  | 1.604 ± 0.016  |
| 6       | Minimum width of right cerebral hemisphere | 0.240-0.500                  | 0.403 ± 0.033 | 0.480-1.100                  | 0.768 ± 0.057 | 1.410-1.540                  | 1.478 ± 0.012 | 1.500-1.700                  | 1.619 ± 0.017  |
| 7       | Height of left cerebral hemisphere         | 0.500-1.100                  | 0.814 ± 0.066 | 1.000-2.100                  | 1.355 ± 0.088 | 2.400-2.520                  | 2.429 ± 0.014 | 2.700-3.300                  | 2.957 ± 0.051  |
| 8       | Height of right cerebral hemisphere        | 0.500-1.100                  | 0.822 ± 0.067 | 0.900-2.100                  | 1.377 ± 0.094 | 2.400-2.530                  | 2.434 ± 0.014 | 2.700-3.300                  | 2.959 ± 0.051  |
| 9       | Weight of left cerebral hemisphere         | 0.200-0.410                  | 0.310 ± 0.023 | 0.420-4.200                  | 1.727 ± 0.357 | 5.100-5.420                  | 5.208 ± 0.039 | 6.620-19.700                 | 15.516 ± 1.230 |
| 10      | Weight of right cerebral hemisphere        | 0.200-0.420                  | 0.041 ± 0.002 | 0.430-4.700                  | 1.814 ± 0.389 | 5.200-5.480                  | 5.296 ± 0.036 | 7.370-19.880                 | 15.733 ± 1.213 |
| 11      | Length of olfactory bulb                   | 0.070-0.280*                 | 0.202 ± 0.030 | 0.280-0.560                  | 0.419 ± 0.030 | 0.600-0.840                  | 0.681 ± 0.034 | 0.910-1.340                  | 1.230 ± 0.041  |

Table 14. Continued.....

| Sl. No. | Parameters                        | 2 <sup>nd</sup> month (n=10) |               | 3 <sup>rd</sup> month (n=12) |               | 4 <sup>th</sup> month (n=10) |               | 5 <sup>th</sup> month (n=14) |                |
|---------|-----------------------------------|------------------------------|---------------|------------------------------|---------------|------------------------------|---------------|------------------------------|----------------|
|         |                                   | Range                        | Mean±SE       | Range                        | Mean±SE       | Range                        | Mean±SE       | Range                        | Mean±SE        |
| 12      | Width of olfactory lobe           | 0.040-0.070*                 | 0.050 ± 0.004 | 0.100-0.360                  | 0.239 ± 0.029 | 0.400-0.580                  | 0.483 ± 0.017 | 0.560-0.840                  | 0.700 ± 0.018  |
| 13      | Thickness of olfactory lobe       | 0.040-0.060*                 | 0.049 ± 0.004 | 0.080-0.340                  | 0.173 ± 0.027 | 0.400-0.500                  | 0.466 ± 0.012 | 3.418 ± 0.033                | 0.510 ± 0.005  |
| 14      | Length of lateral olfactory stria | Not developed                |               | 0.200-0.600                  | 0.321 ± 0.036 | 0.900-1.000                  | 0.966 ± 0.013 | 1.000-1.700                  | 1.333 ± 0.055  |
| 15      | Width of lateral olfactory stria  | Not developed                |               | 0.100-0.400                  | 0.244 ± 0.032 | 0.350-0.410                  | 0.398 ± 0.006 | 0.420-0.510                  | 0.459 ± 0.010  |
| 16      | Length of medial olfactory stria  | Not developed                |               | 0.200-0.260                  | 0.229 ± 0.006 | 0.300-0.410                  | 0.350 ± 0.013 | 0.410-0.5910                 | 0.422 ± 0.003  |
| 17      | Width of medial olfactory stria   | Not developed                |               | 0.030-0.160                  | 0.089 ± 0.012 | 0.200-0.420                  | 0.284 ± 0.030 | 0.430-0.500                  | 0.459 ± 0.006  |
| 18      | Width of trigonum olfactorium     | Not developed                |               | 0.200-0.540                  | 0.318 ± 0.032 | 0.700-0.780                  | 0.726 ± 0.008 | 0.820-0.940                  | 0.888 ± 0.010  |
| 19      | Length of piriform lobe           | Not developed                |               | 0.500-1.600                  | 0.965 ± 0.104 | 1.610-1.700                  | 1.633 ± 0.009 | 1.910-2.700                  | 2.397 ± 0.070  |
| 20      | Width of piriform lobe            | Not developed                |               | 0.440-0.940                  | 0.692 ± 0.055 | 1.000-1.210                  | 1.104 ± 0.020 | 1.280-1.500                  | 1.408 ± 0.018  |
| 21      | Length of corpus callosum         | Not developed                |               | 0.690-1.500                  | 0.993 ± 0.088 | 1.600-1.920                  | 1.767 ± 0.030 | 1.980-2.900                  | 2.551 ± 0.085  |
| 22      | Thickness of corpus callosum      | Not developed                |               | 0.080-0.130                  | 0.109 ± 0.005 | 0.140-0.210                  | 0.176 ± 0.009 | 0.210-0.300                  | 0.249 ± 0.088. |

\* Number of foetuses = 8



Table 15. Measurements of cerebellum of goat foetuses at different ages

| Parameters                           | 2 <sup>nd</sup> month (n=10) |               | 3 <sup>rd</sup> month (n=12) |               | 4 <sup>th</sup> month (n=10) |               | 5 <sup>th</sup> month (n=14) |               |
|--------------------------------------|------------------------------|---------------|------------------------------|---------------|------------------------------|---------------|------------------------------|---------------|
|                                      | Range                        | Mean± SE      | Range                        | Mean± SE      | Range                        | Mean± SE      | Range                        | Mean± SE      |
| Weight of cerebellum (g)             | 0.040-0.100                  | 0.059 ± 0.007 | 0.118-0.510                  | 0.310 ± 0.050 | 0.540-0.720                  | 0.614 ± 0.025 | 1.460-5.980                  | 3.841 ± 0.421 |
| Length of cerebellum (cm)            | 0.270-0.420                  | 0.320 ± 0.019 | 0.400-0.960                  | 0.602 ± 0.058 | 1.100-1.600                  | 1.316 ± 0.058 | 2.000-2.700                  | 2.336 ± 0.070 |
| Width of cerebellum (cm)             | 0.160-0.360                  | 0.247 ± 0.026 | 0.390-1.470                  | 0.912 ± 0.128 | 1.490-1.730                  | 1.588 ± 0.030 | 2.100-3.640                  | 3.016 ± 0.167 |
| Thickness of cerebellum (cm)         | 0.028-0.181                  | 0.072 ± 0.019 | 0.270-1.000                  | 0.726 ± 0.082 | 1.010-1.500                  | 1.145 ± 0.055 | .600-2.700                   | 2.082 ± 0.080 |
| Length of vermis (cm)                | 0.270-0.420                  | 0.320 ± 0.019 | 0.400-0.880                  | 0.598 ± 0.056 | 1.100-1.580                  | 1.267 ± 0.062 | 1.900-2.700                  | 2.329 ± 0.073 |
| Width of vermis (cm)                 | 0.025-0.243                  | 0.110 ± 0.026 | 0.195-0.460                  | 0.302 ± 0.024 | 0.500-0.710                  | 0.595 ± 0.028 | 0.900-1.120                  | 1.014 ± 0.023 |
| Thickness of vermis (cm)             | 0.013-0.111                  | 0.049 ± 0.013 | 0.260-1.000                  | 0.722 ± 0.082 | 1.000-1.400                  | 1.125 ± 0.050 | 1.500-2.700                  | 2.076 ± 0.087 |
| Length of left lateral lobe (cm)     | 0.230-0.300                  | 0.258 ± 0.008 | 0.290-0.700                  | 0.390 ± 0.042 | 0.890-1.020                  | 0.936 ± 0.016 | 1.100-2.080                  | 1.633 ± 0.091 |
| Length of right lateral lobe (cm)    | 0.240-0.300                  | 0.261 ± 0.008 | 0.300-0.700                  | 0.396 ± 0.041 | 0.900-1.020                  | 0.939 ± 0.016 | 1.100-2.100                  | 1.636 ± 0.092 |
| Width of left lateral lobe (cm)      | 0.065-0.080                  | 0.070 ± 0.002 | 0.096-0.430                  | 0.283 ± 0.04  | 0.420-0.510                  | 0.463 ± 0.012 | 0.600-1.200                  | 0.931 ± 0.054 |
| Width of right lateral lobe (cm)     | 0.068-0.095                  | 0.075 ± 0.003 | 0.097-0.440                  | 0.286 ± 0.044 | 0.420-0.510                  | 0.471 ± 0.010 | 0.600-1.210                  | 0.932 ± 0.054 |
| Thickness of left lateral lobe (cm)  | 0.028-0.170                  | 0.070 ± 0.017 | 0.270-0.800                  | 0.603 ± 0.054 | 0.890-0.940                  | 0.913 ± 0.007 | 1.100-1.810                  | 1.453 ± 0.064 |
| Thickness of right lateral lobe (cm) | 0.030-0.180                  | 0.072 ± 0.019 | 0.270-0.820                  | 0.608 ± 0.055 | 0.890-0.950                  | 0.916 ± 0.008 | 1.100-1.810                  | 1.454 ± 0.065 |

Table 16. Measurements of diencephalon of goat foetuses at different ages

| Parameters                   | 2 <sup>nd</sup> month (n=8) |                 | 3 <sup>rd</sup> month (n=12) |                 | 4 <sup>th</sup> month (n=10) |                 | 5 <sup>th</sup> month (n=14) |                 |
|------------------------------|-----------------------------|-----------------|------------------------------|-----------------|------------------------------|-----------------|------------------------------|-----------------|
|                              | Range                       | Mean<br>±S.E.   | Range                        | Mean<br>±S.E.   | Range                        | Mean<br>±S.E.   | Range                        | Mean<br>±S.E.   |
| Weight of diencephalon(g)    | 0.110-<br>0.200             | 0.147<br>±0.040 | 0.210-<br>0.700              | 0.485<br>±0.058 | 1.000-<br>1.200              | 1.062<br>±0.025 | 1.270-<br>4.240              | 3.129<br>±0.286 |
| Length of diencephalon(cm)   | 0.300-<br>0.520             | 0.435<br>±0.033 | 0.520-<br>1.100              | 0.788<br>±0.061 | 1.100-<br>1.200              | 1.175<br>±0.013 | 1.240-<br>1.800              | 1.423<br>±0.052 |
| Width of diencephalon(cm)    | 0.370-<br>1.100             | 0.818<br>±0.111 | 1.100-<br>1.900              | 1.564<br>±0.089 | 1.920-<br>2.100              | 1.967<br>±0.017 | 2.200-<br>2.800              | 2.476<br>±0.054 |
| Height of diencephalon(cm)   | 0.400-<br>0.480             | 0.439<br>±0.013 | 0.500-<br>0.960              | 0.728<br>±0.056 | 0.980-<br>1.100              | 1.018<br>±0.014 | 1.260-<br>1.600              | 1.467<br>±0.033 |
| Length of thalamus (cm)      | 0.300-<br>0.410             | 0.371<br>±0.016 | 0.410-<br>0.920              | 0.614<br>±0.052 | 1.100-<br>1.140              | 1.075<br>±0.016 | 1.200-<br>1.740              | 1.346<br>±0.044 |
| Width of mamillary body (cm) | Not developed               |                 | 0.200-<br>0.410              | 0.278<br>±0.020 | 0.410-<br>0.500              | 0.452<br>±0.010 | 0.520-<br>0.680              | 0.590<br>±0.010 |

Table 17. Measurements of mesencephalon of goat foetuses at different ages

| Parameters                          | 2 <sup>nd</sup> month (n=8) |              | 3 <sup>rd</sup> month (n=12) |              | 4 <sup>th</sup> month (n=10) |              | 5 <sup>th</sup> month (n=14) |              |
|-------------------------------------|-----------------------------|--------------|------------------------------|--------------|------------------------------|--------------|------------------------------|--------------|
|                                     | Range                       | Mean±S.E.    | Range                        | Mean±S.E     | Range                        | Mean±S.E     | Range                        | Mean±S.E     |
| Weight of mesencephalon (g)         | 0.080-1.120                 | 0.140 ±0.022 | 0.240-0.920                  | 0.604 ±0.067 | 0.900-0.960                  | 0.922 ±0.008 | 1.150-2.200                  | 1.844 ±0.105 |
|                                     | 0.720-0.810                 | 0.775 ±0.014 | 0.800-0.910                  | 0.876 ±0.012 | 0.920-1.000                  | 0.947 ±0.009 | 1.060-1.300                  | 1.181 ±0.020 |
| Length of mesencephalon (cm)        | 0.700-0.880                 | 0.785 ±0.026 | 0.900-1.220                  | 1.044 ±0.037 | 1.200-1.320                  | 1.283 ±0.015 | 1.360-2.060                  | 1.781 ±0.069 |
|                                     | 0.610-0.710                 | 0.657 ±0.012 | 0.710-1.010                  | 0.826 ±0.028 | 1.140-1.240                  | 1.194 ±0.010 | 1.360-1.650                  | 1.515 ±0.031 |
| Length of rostral colliculus (cm)   | 0.500-0.630*                | 0.575 ±0.024 | 0.620-0.800                  | 0.692 ±0.022 | 0.800-0.820                  | 0.808 ±0.003 | 0.880-1.100                  | 0.966 ±0.015 |
|                                     | 0.300-0.340*                | 0.320 ±0.007 | 0.340-0.620                  | 0.528 ±0.031 | 0.640-0.810                  | 0.745 ±0.024 | 0.840-1.000                  | 0.903 ±0.018 |
| Length of caudal colliculus (cm)    | 0.170-0.190*                | 0.180 ±0.004 | 0.190-0.250                  | 0.219 ±0.007 | 0.240-0.300                  | 0.272 ±0.006 | 0.300-0.600                  | 0.421 ±0.022 |
|                                     | 0.260-0.320*                | 0.288 ±0.010 | 0.320-0.400                  | 0.365 ±0.009 | 0.440-0.580                  | 0.500 ±0.014 | 0.580-0.800                  | 0.696 ±0.016 |
| Width of interpeduncular fossa (cm) | Not developed               |              | 0.100-0.240                  | 0.148 ±0.014 | 0.300-0.360                  | 0.318 ±0.008 | 0.390-0.460                  | 0.423 ±0.007 |

\* Number of foetuses = 6

Table 18. Measurements of pons of goat foetuses at different ages

| Parameters                | 2 <sup>nd</sup> month (n=8) |                 | 3 <sup>rd</sup> month (n=12) |                 | 4 <sup>th</sup> month (n=10) |                 | 5 <sup>th</sup> month (n=14) |                 |
|---------------------------|-----------------------------|-----------------|------------------------------|-----------------|------------------------------|-----------------|------------------------------|-----------------|
|                           | Range                       | Mean<br>±S.E.   | Range                        | Mean<br>±S.E.   | Range                        | Mean<br>±S.E.   | Range                        | Mean<br>±S.E.   |
| Weight of pons (g)        | 0.020-<br>0.050             | 0.035<br>±0.006 | 0.050-<br>0.150              | 0.107<br>±0.011 | 0.160-<br>0.200              | 0.176<br>±0.005 | 0.250-<br>0.980              | 0.618<br>±0.075 |
| Length of pons (cm)       | 0.260-<br>0.310             | 0.285<br>±0.009 | 0.300-<br>0.600              | 0.442<br>±0.033 | 0.700-<br>0.840              | 0.770<br>±0.014 | 1.100-<br>1.700              | 1.416<br>±0.047 |
| Width of pons (cm)        | 0.360-<br>0.500             | 0.432<br>±0.027 | 0.500-<br>0.640              | 0.580<br>±0.013 | 0.640-<br>0.750              | 0.722<br>±0.010 | 0.750-<br>0.890              | 0.810<br>±0.011 |
| Thickness of pons<br>(cm) | 0.160-<br>0.200             | 0.178<br>±0.007 | 0.200-<br>0.710              | 0.452<br>±0.057 | 0.700-<br>0.800              | 0.754<br>±0.011 | 0.820-<br>1.000              | 0.896<br>±0.016 |

Table 19. Measurements of medulla oblongata (MO) of goat foetuses at different ages

| Parameters                                  | 2 <sup>nd</sup> month (n=8) |                 | 3 <sup>rd</sup> month (n=12) |                 | 4 <sup>th</sup> month (n=10) |                 | 5 <sup>th</sup> month (n=14) |                 |
|---|-----------------------------|-----------------|------------------------------|-----------------|------------------------------|-----------------|------------------------------|-----------------|
|   | Range                       | Mean<br>±S.E.   | Range                        | Mean<br>±S.E.   | Range                        | Mean<br>±S.E.   | Range                        | Mean<br>±S.E.   |
| Weight of MO (g)                            | 0.030-<br>0.070             | 0.052<br>±0.006 | 0.080-<br>0.350              | 0.220<br>±0.032 | 0.390-<br>0.520              | 0.437<br>±0.016 | 0.540-<br>2.000              | 1.411<br>±0.134 |
| Length of MO (cm)                           | 0.500-<br>0.630             | 0.564<br>±0.019 | 0.620-<br>1.030              | 0.805<br>±0.053 | 1.100-<br>1.300              | 1.183<br>±0.027 | 1.440-<br>2.300              | 1.869<br>±0.072 |
| Maximum width of MO (cm)                    | 0.440-<br>0.510             | 0.475<br>±0.011 | 0.520-<br>0.800              | 0.702<br>±0.030 | 0.810-<br>1.000              | 0.855<br>±0.019 | 1.100-<br>1.600              | 1.447<br>±0.038 |
| Minimum width of MO (cm)                    | 0.240-<br>0.310             | 0.284<br>±0.010 | 0.320-<br>0.410              | 0.384<br>±0.009 | 0.420-<br>0.500              | 0.467<br>±0.010 | 0.510-<br>0.900              | 0.740<br>±0.035 |
| Thickness of MO (cm)                        | 0.240-<br>0.400             | 0.308<br>±0.022 | 0.400-<br>0.530              | 0.468<br>±0.014 | 0.600-<br>0.710              | 0.682<br>±0.011 | 0.710-<br>1.000              | 0.839<br>±0.023 |
| Length of medullary pyramids (cm)           | Not fully developed         |                 | 0.680-<br>0.890              | 0.805<br>±0.031 | 0.890-<br>1.000              | 0.926<br>±0.011 | 1.080-<br>1.980              | 1.585<br>±0.088 |
| Width of medullary pyramids (cm)            | Not fully developed         |                 | 0.200-<br>0.270              | 0.230<br>±0.013 | 0.340-<br>0.600              | 0.444<br>±0.033 | 0.620-<br>0.720              | 0.656<br>±0.008 |
| Cranio-caudal length of trapezoid body (cm) | Not fully developed         |                 | 0.100-<br>0.150              | 0.117<br>±0.005 | 0.200-<br>0.260              | 0.230<br>±0.007 | 0.270-<br>0.320              | 0.298<br>±0.003 |

Table 20. Measurements of ventricles of brain of goat foetuses at different ages, cm

| Parameters               | 1 <sup>st</sup> month |                 | 2 <sup>nd</sup> month |                 | 3 <sup>rd</sup> month |                 | 4 <sup>th</sup> month |                 | 5 <sup>th</sup> month |                 |
|--------------------------|-----------------------|-----------------|-----------------------|-----------------|-----------------------|-----------------|-----------------------|-----------------|-----------------------|-----------------|
|                          | Range                 | Mean<br>±SE     | Range                 | Mean<br>±SE     | Range                 | Mean<br>±SE     | Range                 | Mean<br>±SE     | Range                 | Mean<br>±SE     |
| Lateral ventricle        |                       |                 |                       |                 |                       |                 |                       |                 |                       |                 |
| a. Length                | 0.285-<br>0.481       | 0.383<br>±0.036 | 0.518-<br>0.819       | 0.749<br>±0.049 | 1.244-<br>1.674       | 1.434<br>±0.070 | 2.010-<br>2.367       | 2.153<br>±0.054 | 2.316-<br>2.743       | 2.537<br>±0.059 |
| b. Width                 | 0.054-<br>0.077       | 0.065<br>±0.039 | 0.213-<br>0.269       | 0.241<br>±0.011 | 0.272-<br>0.350       | 0.306<br>±0.014 | 0.392-<br>0.424       | 0.417<br>±0.012 | 0.530-<br>0.576       | 0.554<br>±0.008 |
| c. Height                | 0.061-<br>0.136       | 0.097<br>±0.013 | 0.235-<br>0.458       | 0.345<br>±0.048 | 0.384-<br>0.450       | 0.417<br>±0.012 | 0.280-<br>0.293       | 0.288<br>±0.002 | 0.136-<br>0.189       | 0.163<br>±0.009 |
| Interventricular foramen |                       |                 |                       |                 |                       |                 |                       |                 |                       |                 |
| d. Width                 | 0.011-<br>0.014       | 0.013<br>±0.001 | 0.045-<br>0.050       | 0.047<br>±0.001 | 0.040-<br>0.066       | 0.051<br>±0.004 | 0.029-<br>0.034       | 0.032<br>±0.001 | 0.021-<br>0.026       | 0.023<br>±0.009 |
| Third ventricle          |                       |                 |                       |                 |                       |                 |                       |                 |                       |                 |
| e. Length                | 0.125-<br>0.148       | 0.134<br>±0.003 | 0.500-<br>0.590       | 0.537<br>±0.014 | 0.541-<br>0.835       | 0.703<br>±0.047 | 0.917-<br>1.241       | 1.087<br>±0.053 | 1.042-<br>1.877       | 1.387<br>±0.152 |
| f. Width                 | 0.029-<br>0.064       | 0.046<br>±0.006 | 0.064-<br>0.074       | 0.069<br>±0.002 | 0.076-<br>0.093       | 0.089<br>±0.004 | 0.136-<br>0.157       | 0.145<br>±0.003 | 0.171-<br>0.178       | 0.175<br>±0.001 |
| g. Height                | 0.075-<br>0.080       | 0.077<br>±0.001 | 0.224-<br>0.584       | 0.403<br>±0.078 | 0.642-<br>0.707       | 0.677<br>±0.013 | 0.707-<br>0.914       | 0.865<br>±0.032 | 1.058-<br>1.080       | 1.070<br>±0.003 |

Table 20. Continued.....

| Parameters          | 1 <sup>st</sup> month |                 | 2 <sup>nd</sup> month |                 | 3 <sup>rd</sup> month |                 | 4 <sup>th</sup> month |                 | 5 <sup>th</sup> month |                 |
|---------------------|-----------------------|-----------------|-----------------------|-----------------|-----------------------|-----------------|-----------------------|-----------------|-----------------------|-----------------|
|                     | Range                 | Mean<br>±SE     | Range                 | Mean<br>±SE     | Range                 | Mean<br>±SE     | Range                 | Mean<br>±SE     | Range                 | Mean<br>±SE     |
| Aqueduct of Sylvius |                       |                 |                       |                 |                       |                 |                       |                 |                       |                 |
| h. Length           | 0.154-<br>0.158       | 0.156<br>±0.001 | 0.614-<br>0.819       | 0.728<br>±0.032 | 0.807-<br>0.981       | 0.888<br>±0.028 | 0.899-<br>0.934       | 0.913<br>±0.005 | 0.907-<br>1.300       | 1.146<br>±0.064 |
| i. Width            | 0.064-<br>0.101       | 0.085<br>±0.001 | 0.152-<br>0.272       | 0.210<br>±0.024 | 0.125-<br>0.202       | 0.152<br>±0.015 | 0.200-<br>0.216       | 0.209<br>±0.021 | 0.336-<br>0.365       | 0.346<br>±0.044 |
| j. Height           | 0.082-<br>0.086       | 0.084<br>±0.001 | 0.088-<br>0.134       | 0.112<br>±0.008 | 0.093-<br>0.184       | 0.130<br>±0.017 | 0.186-<br>0.200       | 0.193<br>±0.021 | 0.208-<br>0.219       | 0.214<br>±0.017 |
| Fourth ventricle    |                       |                 |                       |                 |                       |                 |                       |                 |                       |                 |
| k. Length           | 0.150-<br>0.162       | 0.155<br>±0.002 | 0.040-<br>0.400       | 0.311<br>±0.029 | 0.402-<br>0.610       | 0.566<br>±0.033 | 0.688-<br>0.818       | 0.735<br>±0.019 | 1.280-<br>2.102       | 1.463<br>±0.013 |
| l. Width            | 0.064-<br>0.090       | 0.080<br>±0.005 | 0.157-<br>0.261       | 0.210<br>±0.021 | 0.328-<br>0.560       | 0.434<br>±0.042 | 0.564-<br>0.600       | 0.586<br>±0.005 | 0.602-<br>0.802       | 0.702<br>±0.043 |
| m. Height           | 0.056-<br>0.078       | 0.068<br>±0.004 | 0.144-<br>0.157       | 0.150<br>±0.002 | 0.192-<br>0.248       | 0.229<br>±0.097 | 0.243-<br>0.304       | 0.269<br>±0.009 | 0.392-<br>0.408       | 0.402<br>±0.012 |

(Number of samples = 6)

**Table 21. Length of some of the cerebral fissures in goat foetuses during fourth and fifth month of gestation\***

| Length of fissures (cm)    | 4 <sup>th</sup> month (n=10) |                   | 5 <sup>th</sup> month (n=14) |                   |
|----------------------------|------------------------------|-------------------|------------------------------|-------------------|
|                            | Range                        | Mean $\pm$ SE     | Range                        | Mean $\pm$ SE     |
| Great longitudinal fissure | 3.800-4.100                  | 4.017 $\pm$ 0.048 | 4.500-8.400                  | 6.250 $\pm$ 0.541 |
| Transverse fissure         | 1.700-2.200                  | 2.117 $\pm$ 0.083 | 1.900-3.400                  | 2.700 $\pm$ 0.241 |
| Rhinal sulcus              | 3.000-3.300                  | 3.100 $\pm$ 0.045 | 3.900-5.100                  | 4.700 $\pm$ 0.238 |
| Sylvian fissure            | 1.500-1.800                  | 1.683 $\pm$ 0.054 | 1.500-2.400                  | 1.917 $\pm$ 0.145 |
| Presylvian sulcus          | 1.100-1.200                  | 1.120 $\pm$ 0.016 | 0.900-2.000                  | 1.383 $\pm$ 0.178 |
| Ectosylvian sulcus         | 1.900-2.000                  | 1.923 $\pm$ 0.017 | 1.700-4.500                  | 3.067 $\pm$ 0.466 |
| Suprasylvian sulcus        | 1.400-2.200                  | 1.967 $\pm$ 0.174 | 2.400-4.000                  | 2.650 $\pm$ 0.296 |
| Marginal sulcus            | 1.100-2.200                  | 2.083 $\pm$ 0.232 | 1.500-3.500                  | 2.500 $\pm$ 0.425 |
| Endomarginal sulcus        | 1.500-2.600                  | 1.800 $\pm$ 0.179 | 1.500-4.400                  | 3.367 $\pm$ 0.238 |
| Coronal sulcus             | 1.100-1.600                  | 1.417 $\pm$ 0.087 | 1.900-2.600                  | 2.283 $\pm$ 0.114 |
| Cruciate sulcus            | 0.300-0.600                  | 0.500 $\pm$ 0.063 | 0.500-0.700                  | 0.633 $\pm$ 0.033 |
| Ansate sulcus              | 0.400-0.500                  | 0.417 $\pm$ 0.017 | 0.700-1.100                  | 0.867 $\pm$ 0.076 |
| Diagonal sulcus            | 0.400-0.500                  | 0.433 $\pm$ 0.021 | 0.500-1.300                  | 0.817 $\pm$ 0.142 |
| Oblique sulcus             | 0.400-0.600                  | 0.500 $\pm$ 0.026 | 0.600-0.700                  | 0.658 $\pm$ 0.019 |

\* Most of the gyri and sulci could be measured from the fourth month



Table 22. Micrometrical of cerebral wall of goat foetuses during second, third and fourth month of gestation,  $\mu\text{m}$ 

| Parameters                    | Dorsal wall        |                    | Ventral wall       |                    | Medial wall        |                    | Lateral wall       |                    |                   |                    |                   |
|-------------------------------|--------------------|--------------------|--------------------|--------------------|--------------------|--------------------|--------------------|--------------------|-------------------|--------------------|-------------------|
|                               | 2 <sup>nd</sup> m. | 3 <sup>rd</sup> m. | 2 <sup>nd</sup> m. | 3 <sup>rd</sup> m. | 2 <sup>nd</sup> m. | 3 <sup>rd</sup> m. | 2 <sup>nd</sup> m. | 3 <sup>rd</sup> m. |                   |                    |                   |
| Total thickness               | 962.67<br>±44.32   | 2082.67<br>±321.77 | 3245.33<br>±75.09  | 1442.67<br>±228.32 | 2344.00<br>±51.23  | 680.00<br>±12.22   | 864.00<br>±26.77   | 1733.33<br>±114.76 | 1394.67<br>±39.93 | 2376.00<br>±288.91 | 3448.00<br>±37.12 |
| Thickness of cerebral mantle  | 317.33<br>±20.41   | 669.33<br>±80.68   | 1757.33<br>±37.05  | 474.67<br>±63.29   | 1248.00<br>±20.24  | 184.00<br>±3.58    | 280.00<br>±13.55   | 578.67<br>±50.67   | 338.67<br>±9.62   | 674.67<br>±76.56   | 1824.00<br>±38.53 |
| Width of molecular layer      | 80.00<br>±3.58     | 82.67<br>±9.62     | 321.33<br>±10.21   | 109.33<br>±22.78   | 224.00<br>±4.13    | 34.67<br>±1.69     | 52.00<br>±4.84     | 122.67<br>±15.27   | 73.33<br>±3.21    | 75.33<br>±5.51     | 341.33<br>±5.33   |
| Width of outer granular layer | 36.00<br>±3.43     | 146.67<br>±23.88   | 401.33<br>±8.86    | 57.33<br>±3.21     | 296.00<br>±6.85    | 34.67<br>±1.69     | 48.00<br>±2.92     | 89.33<br>±27.28    | 57.33<br>±3.21    | 134.67<br>±20.07   | 420.00<br>±10.07  |
| Width of intermediate layer   | 124.00<br>±7.08    | 256.00<br>±24.44   | 560.00<br>±9.24    | 197.33<br>±25.02   | 392.00<br>±3.58    | 66.67<br>±2.67     | 118.67<br>±7.28    | 229.33<br>±12.84   | 129.33<br>±3.21   | 274.67<br>±42.01   | 577.33<br>±8.86   |
| Width of inner granular layer | 77.33<br>±7.64     | 184.00<br>±30.85   | 474.67<br>±9.83    | 116.00<br>±16.23   | 336.00<br>±8.26    | 48.00<br>±0.00     | 62.67<br>±3.82     | 142.67<br>±16.83   | 78.67<br>±1.33    | 184.00<br>±29.14   | 485.33<br>±15.27  |
| Thickness of white matter     | 288.00<br>±7.16    | 1018.67<br>±240.98 | 1450.67<br>±370.50 | 487.33<br>±73.06   | 1057.33<br>±30.11  | 237.33<br>±7.64    | 296.00<br>±5.47    | 1104.00<br>±72.03  | 512.00<br>±21.07  | 1224.00<br>±227.02 | 1582.67<br>±41.33 |
| Width of ependymal layer      | 357.33<br>±31.10   | 394.67<br>±49.17   | 37.33<br>±2.67     | 513.33<br>±71.09   | 38.67<br>±3.21     | 258.67<br>±10.47   | 288.00<br>±15.46   | 40.00<br>±3.58     | 546.67<br>±27.53  | 472.00<br>±27.94   | 41.33<br>±3.21    |

(Number of samples = 6)

**Table 23. Micrometrical parameters of cerebral hemispheres of goat foetuses in the fifth month of gestation,  $\mu\text{m}$**

| Parameters                           | Range (n=6) | Mean $\pm$ S.E.        |
|--------------------------------------|-------------|------------------------|
| Height of gyrus                      | 3520-6240   | 4800.000 $\pm$ 374.094 |
| Width of gyrus                       | 3520-4608   | 4000.000 $\pm$ 151.902 |
| Depth of sulcus                      | 2320-5840   | 4354.667 $\pm$ 474.428 |
| Width of sulcus                      |             |                        |
| a. at origin                         | 800-1360    | 1053.333 $\pm$ 86.204  |
| b. in the middle                     | 320-608     | 405.333 $\pm$ 44.813   |
| c. at bottom                         | 144-320     | 261.333 $\pm$ 29.406   |
| At the top of gyrus                  |             |                        |
| a. Total width of cerebral cortex    | 912-1440    | 1274.667 $\pm$ 79.644  |
| b. Width of molecular layer          | 192-464     | 344.000 $\pm$ 50.045   |
| c. Width of external granular layer  | 48-96       | 74.667 $\pm$ 7.911     |
| d. Width of external pyramidal layer | 80-240      | 170.667 $\pm$ 26.345   |
| e. Width of internal granular layer  | 176-240     | 202.667 $\pm$ 12.162   |
| f. Width of internal pyramidal layer | 128-288     | 221.333 $\pm$ 26.264   |
| g. Width of fusiform layer           | 160-480     | 261.333 $\pm$ 48.295   |
| At the bottom of sulcus              |             |                        |
| a. Total width of cerebral cortex    | 1040-1184   | 1120.000 $\pm$ 21.466  |
| b. Width of molecular layer          | 400-480     | 440.000 $\pm$ 10.733   |
| c. Width of external granular layer  | 64-108      | 79.333 $\pm$ 7.757     |
| d. Width of external pyramidal layer | 96-144      | 122.667 $\pm$ 6.746    |
| e. Width of internal granular layer  | 112-224     | 173.333 $\pm$ 19.118   |
| f. Width of internal pyramidal layer | 80-160      | 112.000 $\pm$ 13.064   |
| g. Width of fusiform layer           | 128-256     | 176.000 $\pm$ 18.475   |
| Width of white matter                | 800-1312    | 1122.667 $\pm$ 70.644  |

**Table 24. Micrometrical parameters of basal nuclei at different ages in goat foetuses,  $\mu\text{m}$** 

| Parameters                   | 2 <sup>nd</sup> month |                         | 3 <sup>rd</sup> month |                         | 4 <sup>th</sup> month |                         | 5 <sup>th</sup> month |                         |
|------------------------------|-----------------------|-------------------------|-----------------------|-------------------------|-----------------------|-------------------------|-----------------------|-------------------------|
|                              | Range<br>(n=6)        | Mean<br>$\pm$ S.E.      | Range<br>(n=6)        | Mean<br>$\pm$ S.E.      | Range<br>(n=6)        | Mean<br>$\pm$ S.E.      | Range<br>(n=6)        | Mean<br>$\pm$ S.E.      |
| Total width                  | 54-<br>180            | 116.333<br>$\pm$ 11.757 | 190-<br>300           | 267.667<br>$\pm$ 16.118 | 420-<br>510           | 467.000<br>$\pm$ 23.285 | 667-<br>774           | 714.333<br>$\pm$ 15.991 |
| Width of caudate nucleus     | 22-<br>73             | 48.500<br>$\pm$ 7.636   | 70-<br>80             | 75.000<br>$\pm$ 2.236   | 102-<br>126           | 113.333<br>$\pm$ 4.667  | 250-<br>270           | 259.442<br>$\pm$ 4.084  |
| Width of internal capsule    | 8-<br>25              | 20.667<br>$\pm$ 4.234   | 30-<br>50             | 40.833<br>$\pm$ 4.167   | 58-<br>69             | 63.000<br>$\pm$ 2.453   | 86-<br>127            | 105.333<br>$\pm$ 7.046  |
| Width of lenticular nucleus* |                       |                         |                       |                         | 92-<br>102            | 97.000<br>$\pm$ 2.236   | 185-<br>280           | 236.667<br>$\pm$ 16.104 |
| Width of external capsule*   | 24-<br>49             | 37.667<br>$\pm$ 7.011   | 70-<br>120            | 94.333<br>$\pm$ 8.106   | 28-<br>32             | 30.333<br>$\pm$ 0.802   | 32-<br>35             | 33.667<br>$\pm$ 0.601   |
| Width of claustrum*          |                       |                         |                       |                         | 12-<br>15             | 13.667<br>$\pm$ 0.601   | 21-<br>26             | 23.876<br>$\pm$ 1.003   |
| Width of extreme capsule*    |                       |                         |                       |                         | 6-<br>7               | 6.500<br>$\pm$ 0.224    | 9-<br>13              | 11.333<br>$\pm$ 0.802   |

\* These layers were not clearly separated during second and third month

**Table 25. Micrometrical parameters of cerebellar folia in goat foetuses at different ages,  $\mu\text{m}$** 

| Parameters                                  | 2 <sup>nd</sup> month            |                          | 3 <sup>rd</sup> month |                         | 4 <sup>th</sup> month |                          | 5 <sup>th</sup> month |                           |
|---|----------------------------------|--------------------------|-----------------------|-------------------------|-----------------------|--------------------------|-----------------------|---------------------------|
|   | Range<br>(n=6)                   | Mean<br>$\pm$ S.E.       | Range<br>(n=6)        | Mean<br>$\pm$ S.E.      | Range<br>(n=6)        | Mean<br>$\pm$ S.E.       | Range<br>(n=6)        | Mean<br>$\pm$ S.E.        |
| Height of folium                            | Not developed                    |                          | 1010-1052             | 1031.000<br>$\pm$ 9.391 | 1040-1360             | 1173.333<br>$\pm$ 60.809 | 1168-2480             | 1674.667<br>$\pm$ 219.795 |
| Width of folium                             | Not developed                    |                          | 520-624               | 527.000<br>$\pm$ 23.255 | 336-672               | 477.333<br>$\pm$ 47.359  | 448-1020              | 788.667<br>$\pm$ 97.063   |
| Width of cerebellar cortex                  | Cortex and medulla not separated |                          |                       |                         | 144-288               | 208.000<br>$\pm$ 25.799  | 192-464               | 354.667<br>$\pm$ 47.042   |
| Width of external granular layer            | 13-15                            | 14.000<br>$\pm$ 0.447    | 22.5-26.0             | 24.250<br>$\pm$ 0.783   | 32-48                 | 42.667<br>$\pm$ 3.373    | 8-32                  | 22.667<br>$\pm$ 4.341     |
| Width of molecular layer                    | 45-49                            | 47.000<br>$\pm$ 0.894    | 46-51                 | 48.500<br>$\pm$ 1.118   | 48-64                 | 50.667<br>$\pm$ 2.667    | 48-280                | 161.333<br>$\pm$ 36.393   |
| Purkinje cells                              |                                  |                          |                       |                         |                       |                          |                       |                           |
| a. Height                                   | 7.5-11.3                         | 9.400<br>$\pm$ 0.850     | 12.8-18.4             | 15.600<br>$\pm$ 1.252   | 26.2-26.4             | 26.000<br>$\pm$ 0.026    | 18.8-38.0             | 28.150<br>$\pm$ 4.043     |
| b. Width                                    | 4.0-5.6                          | 4.800<br>$\pm$ 0.358     | 6.2-7.4               | 6.800<br>$\pm$ 0.268    | 15.4-16.92            | 16.160<br>$\pm$ 0.340    | 16.3-18.8             | 17.550<br>$\pm$ 0.559     |
| c. Nuclear diameter                         | 2.0-3.8                          | 2.900<br>$\pm$ 0.402     | 3.0-3.6               | 3.300<br>$\pm$ 0.134    | 5.6-9.4               | 7.500<br>$\pm$ 0.850     | 9.2-9.4               | 9.350<br>$\pm$ 0.034      |
| d. Nucleolar diameter                       | 1.0-1.9                          | 1.450<br>$\pm$ 0.201     | 1.5-2.0               | 1.750<br>$\pm$ 0.112    | 3.7-3.8               | 3.750<br>$\pm$ 0.022     | 3.8-5.8               | 4.733<br>$\pm$ 0.418      |
| Width of internal granular layer            | 767-949*                         | 839.800<br>$\pm$ 40.696* | 364-378*              | 371.000<br>$\pm$ 3.130* | 64-176                | 105.333<br>$\pm$ 17.333  | 112-232               | 170.667<br>$\pm$ 18.894   |
| Width of white matter of folium             |                                  |                          |                       |                         | 48-96                 | 80.008<br>$\pm$ 7.155    | 64-112                | 77.333<br>$\pm$ 7.636     |
| Width of white matter at base of cerebellum | Not developed                    |                          | 980-1040              | 1010-13.416             | 1280-1520             | 1421.333<br>$\pm$ 37.276 | 1792-2640             | 2197.333<br>$\pm$ 166.106 |
| Width of ependymal layer                    | 30-39                            | 34.500<br>$\pm$ 2.012    | 11.25-26.00           | 18.625<br>$\pm$ 3.298   | 11.0-11.4             | 11.167<br>$\pm$ 0.067    | 7.4-7.6               | 7.500<br>$\pm$ 0.037      |

\*Internal granular layer and white matter were not clearly separated. So total width is given.

**Table 26. Micrometrical parameters of diencephalon of goat foetuses at different ages,  $\mu\text{m}$**

| Parameters                 | 2 <sup>nd</sup> month (n=6) |                           | 3 <sup>rd</sup> month (n=6) |                           | 4 <sup>th</sup> month (n=6) |                           | 5 <sup>th</sup> month (n=6) |                           |
|----------------------------|-----------------------------|---------------------------|-----------------------------|---------------------------|-----------------------------|---------------------------|-----------------------------|---------------------------|
|                            | Range                       | Mean $\pm$ S.E            | Range                       | Mean $\pm$ S.E            | Range                       | Mean $\pm$ S.E            | Range                       | Mean $\pm$ S.E            |
| Height of thalamus         | 2821-2990                   | 2905.500<br>$\pm$ 37.790  | 3887-4962                   | 4279.667<br>$\pm$ 216.591 | 10400-10472                 | 10446.667<br>$\pm$ 10.426 | 11026-11080                 | 11052.000<br>$\pm$ 8.809  |
| Height of massa intermedia | 1014-1586                   | 1300.000<br>$\pm$ 127.903 | 1495-1885                   | 1681.333<br>$\pm$ 71.415  | 5216-5618                   | 5436.000<br>$\pm$ 62.315  | 6240-6410                   | 6333.333<br>$\pm$ 31.482  |
| Width of thalamus          | 1144-2210                   | 1677.000<br>$\pm$ 238.365 | 2990-4888                   | 3687.667<br>$\pm$ 381.245 | 7136-7451                   | 7196.167<br>$\pm$ 51.146  | 9650-9462                   | 9555.667<br>$\pm$ 34.325  |
| Height of hypothalamus     | 1365-2743                   | 2054.000<br>$\pm$ 308.130 | 1781-3733                   | 2726.333<br>$\pm$ 356.912 | 5003-5142                   | 5066.333<br>$\pm$ 25.676  | 6180-6817                   | 6454.167<br>$\pm$ 128.107 |
| Width of hypothalamus      | 1040-2080                   | 1560.000<br>$\pm$ 232.551 | 1898-3380                   | 2569.667<br>$\pm$ 274.105 | 646-689                     | 679.500<br>$\pm$ 6.771    | 7456-7751                   | 7618.333<br>$\pm$ 58.504  |
| Thickness of optic chiasma | 278-910                     | 594.000<br>$\pm$ 141.319  | 910-962                     | 925.167<br>$\pm$ 7.812    | 2042-2078                   | 2056.000<br>$\pm$ 5.441   | 2316-2451                   | 2379.333<br>$\pm$ 22.037  |
| Thickness of optic tract   | 650-660                     | 655.000<br>$\pm$ 2.236    | 852-856                     | 854.000<br>$\pm$ 0.516    | 1178-1198                   | 1188.833<br>$\pm$ 4.167   | 1247-1276                   | 1266.167<br>$\pm$ 5.115   |
| Width of ependymal layer   | 19-20                       | 19.500<br>$\pm$ 0.224     | 18-20                       | 19.333<br>$\pm$ 0.333     | 11-13                       | 11.833<br>$\pm$ 0.401     | 7.5                         | 7.500<br>$\pm$ 0.000      |

**Table 27. Micrometrical parameters of mesencephalon of goat foetuses at different ages,  $\mu\text{m}$** 

| Parameters   | 2 <sup>nd</sup> month (n=6) |                           | 3 <sup>rd</sup> month (n=6) |                           | 4 <sup>th</sup> month (n=6) |                            | 5 <sup>th</sup> month (n=6) |                            |
|--|-----------------------------|---------------------------|-----------------------------|---------------------------|-----------------------------|----------------------------|-----------------------------|----------------------------|
|  | Range                       | Mean $\pm$ S.E.           | Range                       | Mean $\pm$ S.E.           | Range                       | Mean $\pm$ S.E.            | Range                       | Mean $\pm$ S.E.            |
| Width of mesencephalon at the level of tectum        | 2400-5088                   | 3757.333<br>$\pm$ 578.726 | 6384-8640                   | 7333.333<br>$\pm$ 346.691 | 13056-13792                 | 13482.667<br>$\pm$ 139.403 | 14720-15968                 | 15242.667<br>$\pm$ 164.920 |
| Width of mesencephalon at the level of crura cerebri | 2240-4688                   | 3464.000<br>$\pm$ 526.215 | 5568-7680                   | 6141.333<br>$\pm$ 330.350 | 12160-12800                 | 12480.000<br>$\pm$ 116.847 | 13888-14240                 | 14042.667<br>$\pm$ 49.171  |
| Transverse diameter of aqueduct                      | 1520-2720                   | 2096.000<br>$\pm$ 244.299 | 1248-2016                   | 1522.667<br>$\pm$ 151.250 | 2000-2160                   | 2085.333<br>$\pm$ 21.730   | 3360-3648                   | 3458.667<br>$\pm$ 43.802   |
| Vertical diameter of aqueduct                        | 880-1344                    | 1117.333<br>$\pm$ 75.660  | 928-1840                    | 1296.000<br>$\pm$ 165.144 | 1856-2000                   | 1925.333<br>$\pm$ 20.518   | 2080-2192                   | 2141.000<br>$\pm$ 17.295   |
| Distance of aqueduct from dorsal median groove       | 104-128                     | 116.000<br>$\pm$ 3.425    | 400-816                     | 589.333<br>$\pm$ 73.253   | 880-960                     | 926.667<br>$\pm$ 11.392    | 1008-1440                   | 1272.000<br>$\pm$ 74.447   |
| Distance of aqueduct from ventral median groove      | 992-1248                    | 1061.333<br>$\pm$ 38.013  | 1328-2736                   | 1944.333<br>$\pm$ 260.037 | 3360-3840                   | 3594.667<br>$\pm$ 87.701   | 5920-7840                   | 6405.333<br>$\pm$ 304.187  |
| Depth of dorsal median groove                        | 864-928                     | 906.667<br>$\pm$ 9.834    | 800-968                     | 916.000<br>$\pm$ 26.753   | 2400-2752                   | 2682.667<br>$\pm$ 56.894   | 3792-4384                   | 4160.000<br>$\pm$ 104.593  |
| Width of dorsal median groove                        | 80-120                      | 106.667<br>$\pm$ 6.442    | 128-184                     | 156.000<br>$\pm$ 8.944    | 256-352                     | 309.333<br>$\pm$ 17.849    | 288-512                     | 416.000<br>$\pm$ 38.533    |
| Width of ependymal layer                             | 7.5-15                      | 11.250<br>$\pm$ 1.667     | 18-20                       | 19.333<br>$\pm$ 0.333     | 11-15                       | 13.033<br>$\pm$ 0.721      | 6.5-8.5                     | 7.500<br>$\pm$ 0.224       |

**Table 28. Micrometrical parameters of choroid plexus epithelium in the ventricles of brain at different stages of gestation,  $\mu\text{m}$**

| Parameters                  | 2 <sup>nd</sup> month | 3 <sup>rd</sup> month | 4 <sup>th</sup> month | 5 <sup>th</sup> month |
|-----------------------------|-----------------------|-----------------------|-----------------------|-----------------------|
| <b>LATERAL VENTRICLE</b>    |                       |                       |                       |                       |
| a. Height of epithelium     | 21.034                | 18.875                | 13.125                | 11.250                |
| b. Width of epithelium      | 13.125                | 13.125                | 13.021                | 11.250                |
| c. Diameter of the nucleus  | 7.500                 | 7.500                 | 5.625                 | 5.625                 |
| d. Total width at the stalk | 48.000                | 39.500                | 30.000                | 30.000                |
| <b>THIRD VENTRICLE</b>      |                       |                       |                       |                       |
| a. Height of epithelium     | 19.248                | 16.274                | 11.250                | 9.375                 |
| b. Width of epithelium      | 12.251                | 11.250                | 11.000                | 9.375                 |
| c. Diameter of the nucleus  | 7.500                 | 5.625                 | 5.625                 | 4.688                 |
| d. Total width at the stalk | 46.030                | 39.500                | 30.000                | 26.250                |
| <b>FOURTH VENTRICLE</b>     |                       |                       |                       |                       |
| a. Height of epithelium     | 17.132                | 15.125                | 9.362                 | 9.112                 |
| b. Width of epithelium      | 11.250                | 11.250                | 9.133                 | 9.112                 |
| c. Diameter of the nucleus  | 7.500                 | 5.625                 | 4.688                 | 4.688                 |
| d. Total width at the stalk | 37.500                | 32.000                | 26.250                | 26.250                |

**Table 29. Correlation coefficients (r) of whole brain parameters on body parameters**

| Body parameters                   | Brain weight (g) | Brain volume (ml) | Brain length (cm) | Brain width (cm) | Brain thickness (cm) |
|-----------------------------------|------------------|-------------------|-------------------|------------------|----------------------|
| Body weight (g)                   | 0.958            | 0.956             | 0.851             | 0.817            | 0.744                |
| Age (days)                        | 0.952            | 0.954             | 0.990             | 0.988            | 0.964                |
| CRL (straight) (cm)               | 0.977            | 0.978             | 0.980             | 0.973            | 0.931                |
| CRL (curved) (cm)                 | 0.967            | 0.969             | 0.986             | 0.981            | 0.943                |
| Total body length (cm)            | 0.982            | 0.983             | 0.971             | 0.961            | 0.917                |
| Total bent length (cm)            | 0.973            | 0.975             | 0.986             | 0.979            | 0.940                |
| Head length (straight) (cm)       | 0.939            | 0.941             | 0.991             | 0.993            | 0.967                |
| Head length (curved) (cm)         | 0.946            | 0.948             | 0.989             | 0.991            | 0.963                |
| Head width (straight) (cm)        | 0.952            | 0.953             | 0.978             | 0.977            | 0.960                |
| Vertebral Column Length (cm)      | 0.977            | 0.978             | 0.970             | 0.957            | 0.910                |
| Vertebral Column Tail Length (cm) | 0.979            | 0.981             | 0.972             | 0.960            | 0.912                |
| Tail length (cm)                  | 0.945            | 0.947             | 0.932             | 0.925            | 0.875                |
| Forelimb length (cm)              | 0.977            | 0.978             | 0.974             | 0.960            | 0.916                |
| Hindlimb length (cm)              | 0.977            | 0.978             | 0.980             | 0.968            | 0.924                |
| Tibial length (cm)                | 0.947            | 0.948             | 0.955             | 0.939            | 0.904                |
| Chest depth (cm)                  | 0.977            | 0.979             | 0.971             | 0.960            | 0.918                |
| Chest circumference (cm)          | 0.971            | 0.972             | 0.974             | 0.969            | 0.932                |

(All the 'r' values were significant at 1% level)



**Table 30. Correlation coefficients (r) of head parameters on selected brain and body parameters**

| Head parameters (cm)                                      | Brain weight (g) | Brain volume (ml) | Brain length (cm) | Brain width (cm) | Brain thickness (cm) | Body weight (g) | Age (days) | CRL (curved) (cm) | Total bent length (cm) |
|---|------------------|-------------------|-------------------|------------------|----------------------|-----------------|------------|-------------------|------------------------|
| Head length (straight)                                    | 0.939            | 0.941             | 0.991             | 0.993            | 0.967                | 0.885           | 0.995      | 0.985             | 0.988                  |
| Head length (curved)                                      | 0.946            | 0.948             | 0.989             | 0.991            | 0.963                | 0.863           | 0.996      | 0.989             | 0.991                  |
| Head width (straight)                                     | 0.952            | 0.953             | 0.978             | 0.977            | 0.960                | 0.879           | 0.994      | 0.984             | 0.987                  |
| Cranial length  | 0.940            | 0.942             | 0.989             | 0.991            | 0.963                | 0.851           | 0.994      | 0.986             | 0.987                  |
| Facial length   | 0.948            | 0.950             | 0.982             | 0.983            | 0.955                | 0.879           | 0.991      | 0.986             | 0.989                  |
| Interauricular distance                                   | 0.957            | 0.957             | 0.952             | 0.944            | 0.911                | 0.925           | 0.965      | 0.964             | 0.973                  |
| Transverse distance between lateral canthi                | 0.925            | 0.927             | 0.970             | 0.975            | 0.965                | 0.849           | 0.976      | 0.968             | 0.969                  |
| Transverse distance between medial canthi                 | 0.903            | 0.907             | 0.979             | 0.987            | 0.969                | 0.809           | 0.978      | 0.970             | 0.969                  |
| Transverse distance between cornual buds                  | 0.903            | 0.904             | 0.943             | 0.947            | 0.947                | 0.824           | 0.966      | 0.949             | 0.950                  |
| Intersupraorbital foramina distance                       | 0.928            | 0.930             | 0.974             | 0.982            | 0.973                | 0.844           | 0.985      | 0.976             | 0.976                  |
| Transverse distance between dorsal commissure of nostrils | 0.950            | 0.952             | 0.987             | 0.984            | 0.956                | 0.875           | 0.988      | 0.984             | 0.987                  |
| Posterior height from foramen magnum                      | 0.888            | 0.891             | 0.967             | 0.979            | 0.963                | 0.782           | 0.972      | 0.957             | 0.955                  |

(All the 'r' values were significant at 1% level)

Table 31. Correlation coefficients of skull parameters on selected brain and body parameters

| Skull parameters (cm)     | Brain weight (g)    | Brain volume (ml)   | Brain length (cm)   | Brain width (cm)    | Brain thickness (cm) | Body weight (g)     | Age (days)          | CRL (straight )     | Total body length (cm) |
|---------------------------|---------------------|---------------------|---------------------|---------------------|----------------------|---------------------|---------------------|---------------------|------------------------|
| Skull length              | 0.916**             | 0.919**             | 0.986**             | 0.991**             | 0.979**              | 0.817**             | 0.989**             | 0.969**             | 0.956**                |
| Skull width               | 0.930**             | 0.932**             | 0.984**             | 0.987**             | 0.974**              | 0.833**             | 0.991**             | 0.976**             | 0.965**                |
| Cephalic index            | 0.093 <sup>NS</sup> | 0.093 <sup>NS</sup> | 0.141 <sup>NS</sup> | 0.152 <sup>NS</sup> | 0.213 <sup>NS</sup>  | 0.074 <sup>NS</sup> | 0.168 <sup>NS</sup> | 0.150 <sup>NS</sup> | 0.149 <sup>NS</sup>    |
| Neurocranial length       | 0.938**             | 0.941**             | 0.986**             | 0.986**             | 0.972**              | 0.853**             | 0.991**             | 0.981**             | 0.975**                |
| Neurocranial index        | 0.168 <sup>NS</sup> | 0.170 <sup>NS</sup> | 0.279 <sup>NS</sup> | 0.307 <sup>NS</sup> | 0.383 <sup>NS</sup>  | 0.10 <sup>NS</sup>  | 0.302 <sup>NS</sup> | 0.261 <sup>NS</sup> | 0.247 <sup>NS</sup>    |
| Cranial height            | 0.874**             | 0.878**             | 0.955**             | 0.967**             | 0.981**              | 0.799**             | 0.960**             | 0.933**             | 0.930**                |
| Facial length             | 0.904**             | 0.906**             | 0.977**             | 0.987**             | 0.967**              | 0.811**             | 0.982**             | 0.961**             | 0.946**                |
| Min.interorbital distance | 0.945**             | 0.947**             | 0.986**             | 0.985**             | 0.963**              | 0.871**             | 0.992**             | 0.982**             | 0.978**                |
| Height of foramen magnum  | 0.975**             | 0.975**             | 0.964**             | 0.956**             | 0.913**              | 0.922**             | 0.974**             | 0.986**             | 0.986**                |
| Width of foramen magnum   | 0.965**             | 0.966**             | 0.941**             | 0.926**             | 0.887**              | 0.950**             | 0.950**             | 0.969**             | 0.980**                |

\*\*P&lt;0.01 (significant at 1% level)

NS – Not Significant

Table 32. Correlation coefficients (r) of parameters of bones forming the roof of the skull on those forming the base

| Parameters of bones forming roof of the skull(cm) | Length of basioccipital (cm) | Maximum width of basioccipital (cm) | Minimum width of basioccipital (cm) | Width of occipital condyle (cm) | Height of occipital condyle (cm) | Length of basisphe-noid (cm) | Length of presphenoid (cm) | Length of mandible (cm) |
|---|------------------------------|-------------------------------------|-------------------------------------|---------------------------------|----------------------------------|------------------------------|----------------------------|-------------------------|
| Length of nasal bone                              | 0.978                        | 0.913                               | 0.970                               | 0.949                           | 0.914                            | 0.979                        | 0.962                      | 0.984                   |
| Medial length of frontal                          | 0.985                        | 0.988                               | 0.976                               | 0.956                           | 0.928                            | 0.986                        | 0.975                      | 0.989                   |
| Medial length of parietal                         | 0.948                        | 0.989                               | 0.913                               | 0.982                           | 0.966                            | 0.944                        | 0.966                      | 0.939                   |
| Lateral length of parietal                        | 0.976                        | 0.955                               | 0.978                               | 0.929                           | 0.892                            | 0.979                        | 0.942                      | 0.977                   |
| Anterior width of parietal                        | 0.986                        | 0.973                               | 0.979                               | 0.960                           | 0.934                            | 0.987                        | 0.973                      | 0.989                   |
| Posterior width of parietal                       | 0.994                        | 0.987                               | 0.982                               | 0.955                           | 0.926                            | 0.993                        | 0.978                      | 0.983                   |
| Middle length of interparietal                    | 0.980                        | 0.989                               | 0.975                               | 0.934                           | 0.898                            | 0.977                        | 0.954                      | 0.983                   |
| Width of interparietal                            | 0.972                        | 0.979                               | 0.957                               | 0.945                           | 0.933                            | 0.973                        | 0.967                      | 0.957                   |
| Height of supraoccipital                          | 0.985                        | 0.964                               | 0.971                               | 0.938                           | 0.920                            | 0.989                        | 0.970                      | 0.973                   |
| Width of supraoccipital                           | 0.982                        | 0.980                               | 0.973                               | 0.940                           | 0.916                            | 0.984                        | 0.969                      | 0.974                   |

(All the 'r' values were significant at 1% level)

**Table 33. Correlation coefficients (r) of craniometric parameters on whole brain parameters**

| Craniometric Parameters (cm)        | Brain weight (g) | Brain length (cm) | Brain width (cm) |
|-------------------------------------|------------------|-------------------|------------------|
| Skull length                        | 0.916            | 0.986             | 0.991            |
| Skull width                         | 0.930            | 0.984             | 0.987            |
| Neurocranial length                 | 0.938            | 0.986             | 0.986            |
| Neurocranial width                  | 0.931            | 0.984             | 0.987            |
| Cranial height                      | 0.874            | 0.955             | 0.967            |
| Facial length                       | 0.904            | 0.977             | 0.987            |
| Minimum interorbital distance       | 0.945            | 0.986             | 0.985            |
| Height of foramen magnum            | 0.975            | 0.964             | 0.956            |
| Width of foramen magnum             | 0.965            | 0.941             | 0.926            |
| Length of nasal bone                | 0.912            | 0.983             | 0.989            |
| Medial length of frontal bone       | 0.917            | 0.971             | 0.977            |
| Medial length of parietal bone      | 0.796            | 0.928             | 0.959            |
| Middle length of interparietal bone | 0.936            | 0.959             | 0.960            |
| Height of supraoccipital bone       | 0.908            | 0.967             | 0.970            |
| Length of basioccipital bone        | 0.913            | 0.959             | 0.970            |
| Length of basisphenoid bone         | 0.920            | 0.962             | 0.971            |
| Length of presphenoid bone          | 0.839            | 0.925             | 0.946            |
| Length of mandible                  | 0.934            | 0.975             | 0.980            |

(All the 'r' values were significant at 1% level)

**Table 34. Correlation coefficients (r) of encephalometric parameters on body weight, age and CRL (straight)**

| Encephalometric parameters         | Body weight<br>(g) | Age<br>(days) | Straight CRL<br>(cm) |
|------------------------------------|--------------------|---------------|----------------------|
| Average weight of cerebrum (g)     | 0.947              | 0.943         | 0.968                |
| Average length of cerebrum (cm)    | 0.828              | 0.994         | 0.976                |
| Average width of cerebrum (cm)     | 0.816              | 0.988         | 0.973                |
| Average thickness of cerebrum (cm) | 0.745              | 0.967         | 0.939                |
| Weight of cerebellum (g)           | 0.963              | 0.879         | 0.909                |
| Length of cerebellum (cm)          | 0.890              | 0.989         | 0.984                |
| Width of cerebellum (cm)           | 0.912              | 0.983         | 0.989                |
| Thickness of cerebellum (cm)       | 0.875              | 0.987         | 0.975                |
| Weight of brainstem (g)            | 0.951              | 0.943         | 0.964                |
| Length of brainstem (cm)           | 0.937              | 0.973         | 0.985                |
| Width of brainstem (cm)            | 0.862              | 0.981         | 0.971                |
| Thickness of brainstem (cm)        | 0.788              | 0.980         | 0.957                |

(All the 'r' values were significant at 1% level)

Table. 35 Correlation coefficients (r) of craniometric parameters on encephalometric parameters

| Craniometric parameters(cm) | Mean length of Cerebrum | Mean width of Cerebrum | Mean thickness of Cerebrum | Length of Cerebellum | Width of Cerebellum | Thickness of Cerebellum | Length of brainstem |
|-----------------------------|-------------------------|------------------------|----------------------------|----------------------|---------------------|-------------------------|---------------------|
| Skull length                | 0.988                   | 0.991                  | 0.979                      | 0.966                | 0.961               | 0.973                   | 0.949               |
| Skull width                 | 0.984                   | 0.987                  | 0.964                      | 0.967                | 0.971               | 0.976                   | 0.959               |
| Neurocranial length         | 0.982                   | 0.986                  | 0.962                      | 0.966                | 0.975               | 0.975                   | 0.966               |
| Neurocranial width          | 0.983                   | 0.987                  | 0.962                      | 0.967                | 0.971               | 0.976                   | 0.959               |
| Cranial height              | 0.953                   | 0.967                  | 0.948                      | 0.923                | 0.935               | 0.962                   | 0.924               |
| Facial length               | 0.985                   | 0.987                  | 0.979                      | 0.969                | 0.948               | 0.965                   | 0.935               |
| Medial length of frontal    | 0.967                   | 0.977                  | 0.955                      | 0.951                | 0.955               | 0.962                   | 0.944               |
| Medial length of parietal   | 0.939                   | 0.959                  | 0.963                      | 0.887                | 0.885               | 0.915                   | 0.858               |
| Anterior width of parietal  | 0.972                   | 0.982                  | 0.959                      | 0.955                | 0.963               | 0.972                   | 0.948               |
| Height of supraoccipital    | 0.976                   | 0.970                  | 0.955                      | 0.955                | 0.947               | 0.966                   | 0.929               |
| Length of basioccipital     | 0.962                   | 0.970                  | 0.947                      | 0.948                | 0.949               | 0.952                   | 0.931               |
| Length of basisphenoid      | 0.966                   | 0.971                  | 0.948                      | 0.953                | 0.954               | 0.959                   | 0.871               |
| Length of presphenoid       | 0.929                   | 0.946                  | 0.939                      | 0.896                | 0.893               | 0.909                   | 0.953               |

(All the 'r' values were significant at 1% level)

**Table 36. Correlation coefficients (r) of cerebral parameters on selected whole brain parameters and body parameters**

| Cerebral parameters (cm)          | Brain weight (g) | Brain length (cm) | Brain width (cm) | Brain thickness (cm) | Body weight (g) | Age (days) | CRL (straight) |
|-----------------------------------|------------------|-------------------|------------------|----------------------|-----------------|------------|----------------|
| Length of left cerebrum           | 0.977            | 0.990             | 0.989            | 0.966                | 0.827           | 0.993      | 0.975          |
| Length of right cerebrum          | 0.933            | 0.990             | 0.990            | 0.966                | 0.830           | 0.994      | 0.977          |
| Maximum width of left cerebrum    | 0.924            | 0.991             | 1.000            | 0.976                | 0.819           | 0.989      | 0.974          |
| Maximum width of right cerebrum   | 0.922            | 0.991             | 1.000            | 0.978                | 0.816           | 0.988      | 0.973          |
| Minimum width of left cerebrum    | 0.805            | 0.941             | 0.965            | 0.964                | 0.673           | 0.932      | 0.892          |
| Minimum width of right cerebrum   | 0.814            | 0.946             | 0.970            | 0.968                | 0.683           | 0.938      | 0.901          |
| Thickness of right cerebrum       | 0.871            | 0.968             | 0.980            | 0.971                | 0.755           | 0.966      | 0.940          |
| Weight of left cerebrum           | 0.991            | 0.938             | 0.912            | 0.835                | 0.946           | 0.939      | 0.965          |
| Weight of right cerebrum          | 0.990            | 0.940             | 0.914            | 0.838                | 0.943           | 0.941      | 0.966          |
| Length of olfactory lobe          | 0.948            | 0.969             | 0.966            | 0.938                | 0.855           | 0.983      | 0.971          |
| Width of olfactory lobe           | 0.901            | 0.975             | 0.982            | 0.968                | 0.794           | 0.976      | 0.951          |
| Thickness of olfactory lobe       | 0.803            | 0.942             | 0.960            | 0.953                | 0.673           | 0.922      | 0.884          |
| Length of lateral olfactory stria | 0.916            | 0.977             | 0.984            | 0.947                | 0.824           | 0.973      | 0.959          |
| Width of lateral olfactory stria  | 0.798            | 0.923             | 0.950            | 0.968                | 0.674           | 0.916      | 0.877          |
| Length of medial olfactory stria  | 0.787            | 0.899             | 0.932            | 0.948                | 0.659           | 0.910      | 0.870          |
| Width of medial olfactory stria   | 0.901            | 0.948             | 0.963            | 0.930                | 0.799           | 0.968      | 0.945          |
| Width of trigonum olfactorium     | 0.846            | 0.957             | 0.976            | 0.967                | 0.717           | 0.951      | 0.919          |
| Length of piriform lobe           | 0.898            | 0.973             | 0.982            | 0.973                | 0.784           | 0.971      | 0.950          |
| Width of piriform lobe            | 0.829            | 0.938             | 0.961            | 0.974                | 0.701           | 0.940      | 0.903          |
| Length of corpus callosum         | 0.909            | 0.975             | 0.985            | 0.970                | 0.802           | 0.975      | 0.957          |
| Thickness of corpus callosum      | 0.885            | 0.947             | 0.967            | 0.960                | 0.790           | 0.963      | 0.938          |

(All the 'r' values were significant at 1% level)

**Table 37. Correlation coefficients (r) of cerebellar parameters on selected whole brain and body parameters**

| Cerebellar parameters                | Brain weight (g) | Brain length (cm) | Brain width (cm) | Brain thickness (cm) | Body weight (g) | Age (days) | Straight CRL (cm) |
|--------------------------------------|------------------|-------------------|------------------|----------------------|-----------------|------------|-------------------|
| Weight of cerebellum (g)             | 0.977            | 0.867             | 0.831            | 0.753                | 0.986           | 0.879      | 0.924             |
| Length of cerebellum (cm)            | 0.963            | 0.977             | 0.971            | 0.927                | 0.890           | 0.989      | 0.984             |
| Width of cerebellum (cm)             | 0.978            | 0.976             | 0.969            | 0.930                | 0.912           | 0.983      | 0.989             |
| Thickness of cerebellum (cm)         | 0.949            | 0.971             | 0.973            | 0.958                | 0.875           | 0.987      | 0.975             |
| Length of vermis (cm)                | 0.968            | 0.973             | 0.967            | 0.921                | 0.896           | 0.988      | 0.984             |
| Width of vermis (cm)                 | 0.942            | 0.975             | 0.979            | 0.949                | 0.847           | 0.990      | 0.978             |
| Thickness of vermis (cm)             | 0.948            | 0.970             | 0.970            | 0.953                | 0.874           | 0.983      | 0.972             |
| Length of left lateral lobe (cm)     | 0.981            | 0.970             | 0.957            | 0.897                | 0.930           | 0.974      | 0.985             |
| Length of right lateral lobe (cm)    | 0.981            | 0.970             | 0.957            | 0.896                | 0.931           | 0.973      | 0.985             |
| Width of left lateral lobe (cm)      | 0.974            | 0.964             | 0.955            | 0.916                | 0.917           | 0.971      | 0.975             |
| Width of right lateral lobe (cm)     | 0.974            | 0.966             | 0.956            | 0.917                | 0.918           | 0.971      | 0.976             |
| Thickness of left lateral lobe (cm)  | 0.935            | 0.974             | 0.977            | 0.962                | 0.856           | 0.978      | 0.967             |
| Thickness of right lateral lobe (cm) | 0.934            | 0.973             | 0.976            | 0.963                | 0.855           | 0.978      | 0.966             |

(All the 'r' values were significant at 1% level)



**Table 38. Correlation coefficients (r) of brainstem and diencephalic parameters on selected whole brain and body parameters**

| Brainstem and diencephalic parameters | Brain weight (g) | Brain length (cm) | Brain width (cm) | Brain thickness (cm) | Body weight (g) | Age (days) | Straight CRL (cm) |
|---------------------------------------|------------------|-------------------|------------------|----------------------|-----------------|------------|-------------------|
| Weight of brainstem (g)               | 0.987            | 0.935             | 0.914            | 0.854                | 0.951           | 0.943      | 0.964             |
| Length of brainstem (cm)              | 0.982            | 0.966             | 0.955            | 0.911                | 0.937           | 0.973      | 0.985             |
| Weight of diencephalon (g)            | 0.982            | 0.919             | 0.894            | 0.820                | 0.954           | 0.925      | 0.949             |
| Length of diencephalon (cm)           | 0.855            | 0.947             | 0.966            | 0.978                | 0.773           | 0.952      | 0.924             |
| Width of diencephalon (cm)            | 0.832            | 0.930             | 0.950            | 0.981                | 0.732           | 0.940      | 0.909             |
| Height of diencephalon (cm)           | 0.915            | 0.975             | 0.981            | 0.978                | 0.817           | 0.984      | 0.964             |
| Length of thalamus (cm)               | 0.885            | 0.966             | 0.982            | 0.977                | 0.801           | 0.972      | 0.949             |
| Width of mamillary body (cm)          | 0.846            | 0.944             | 0.965            | 0.972                | 0.726           | 0.948      | 0.915             |

(All the 'r' values were significant at 1% level)

**Table 39. Correlation coefficients (r) of mesencephalic parameters on selected whole brain, body and brainstem parameters**

| Mesencephalic parameters            | Brain weight (g) | Brain length (cm) | Brain width (cm) | Brain thickness (cm) | Body weight (g) | Age (days) | Weight of brain-stem (g) | Length of brainstem (cm) | Weight of dience-phalon (g) | Length of dience-phalon (cm) | Width of dience-phalon (cm) | Height of dience-phalon (cm) |
|-------------------------------------|------------------|-------------------|------------------|----------------------|-----------------|------------|--------------------------|--------------------------|-----------------------------|------------------------------|-----------------------------|------------------------------|
| Weight of mesencephalon(g)          | 0.978            | 0.971             | 0.960            | 0.926                | 0.911           | 0.977      | 0.974                    | 0.985                    | 0.958                       | 0.918                        | 0.913                       | 0.959                        |
| Length of mesencephalon,cm          | 0.755            | 0.816             | 0.824            | 0.851                | 0.687           | 0.839      | 0.756                    | 0.786                    | 0.749                       | 0.877                        | 0.902                       | 0.893                        |
| Width of mesencephalon,cm           | 0.910            | 0.941             | 0.944            | 0.932                | 0.841           | 0.952      | 0.911                    | 0.937                    | 0.903                       | 0.952                        | 0.954                       | 0.974                        |
| Thickness of mesencephalon,cm       | 0.882            | 0.956             | 0.966            | 0.958                | 0.787           | 0.964      | 0.869                    | 0.918                    | 0.855                       | 0.966                        | 0.957                       | 0.980                        |
| Length of rostral colliculus (cm)   | 0.726            | 0.838             | 0.861            | 0.907                | 0.629           | 0.850      | 0.728                    | 0.776                    | 0.708                       | 0.908                        | 0.954                       | 0.884                        |
| Width of rostral colliculus (cm)    | 0.656            | 0.796             | 0.835            | 0.860                | 0.472           | 0.801      | 0.656                    | 0.709                    | 0.630                       | 0.824                        | 0.868                       | 0.832                        |
| Length of caudal colliculus (cm)    | 0.904            | 0.920             | 0.921            | 0.914                | 0.865           | 0.939      | 0.907                    | 0.924                    | 0.904                       | 0.930                        | 0.941                       | 0.937                        |
| Width of caudal colliculus (cm)     | 0.878            | 0.940             | 0.953            | 0.954                | 0.788           | 0.957      | 0.874                    | 0.902                    | 0.864                       | 0.950                        | 0.969                       | 0.959                        |
| Width of interpeduncular fossa (cm) | 0.875            | 0.967             | 0.984            | 0.973                | 0.759           | 0.969      | 0.867                    | 0.918                    | 0.843                       | 0.956                        | 0.938                       | 0.962                        |

(All the 'r' values were significant at 1% level)

**Table 40. Correlation coefficients (r) of parameters of pons and medulla oblongata (MO) on selected whole brain, body and brainstem parameters**

| Parameters of pons and MO                    | Brain weight (g) | Brain length (cm) | Brain width (cm) | Brain thickness (cm) | Body weight (g) | Age (days) | Weight of brainstem (g) | Length of brainstem (cm) |
|--|------------------|-------------------|------------------|----------------------|-----------------|------------|-------------------------|--------------------------|
| Weight of pons (g)                           | 0.958            | 0.870             | 0.841            | 0.778                | 0.981           | 0.886      | 0.960                   | 0.953                    |
| Length of pons (cm)                          | 0.964            | 0.981             | 0.974            | 0.949                | 0.889           | 0.993      | 0.952                   | 0.972                    |
| Width of pons (cm)                           | 0.716            | 0.843             | 0.874            | 0.919                | 0.607           | 0.852      | 0.714                   | 0.768                    |
| Height of pons (cm)                          | 0.817            | 0.938             | 0.965            | 0.987                | 0.697           | 0.938      | 0.823                   | 0.883                    |
| Weight of pons (g)                           | 0.990            | 0.916             | 0.890            | 0.822                | 0.969           | 0.925      | 0.987                   | 0.973                    |
| Length of MO (cm)                            | 0.956            | 0.974             | 0.971            | 0.943                | 0.889           | 0.985      | 0.951                   | 0.974                    |
| Maximum width of MO (cm)                     | 0.941            | 0.957             | 0.949            | 0.934                | 0.857           | 0.973      | 0.937                   | 0.948                    |
| Minimum width of MO (cm)                     | 0.945            | 0.937             | 0.931            | 0.900                | 0.891           | 0.952      | 0.947                   | 0.948                    |
| Thickness of MO (cm)                         | 0.867            | 0.950             | 0.966            | 0.968                | 0.778           | 0.959      | 0.860                   | 0.911                    |
| Length of medullary pyramids (cm)            | 0.940            | 0.971             | 0.971            | 0.946                | 0.861           | 0.969      | 0.944                   | 0.978                    |
| Width of medullary pyramids (cm)             | 0.885            | 0.954             | 0.972            | 0.946                | 0.777           | 0.966      | 0.875                   | 0.922                    |
| Craniocaudal distance of trapezoid body (cm) | 0.850            | 0.948             | 0.969            | 0.962                | 0.723           | 0.953      | 0.838                   | 0.888                    |

(All the 'r' values were significant at 1% level)

**Table 41. Regression coefficients of brain parameters on body and skull parameters**

| Regression coefficients                                   | b ± S.E. of b  |
|---|----------------|
| Brain weight on body weight                               | **0.022±0.001  |
| Brain weight on age                                       | **0.493±0.024  |
| Brain weight on CRL (straight)                            | **1.457±0.048  |
| Brain weight on total body length                         | **2.127±0.061  |
| Brain weight on head length (straight)                    | **5.385±0.298  |
| Brain weight on head width                                | **10.165±0.493 |
| Brain length on CRL (straight)                            | **0.175±0.005  |
| Brain length on total body length                         | **0.252±0.009  |
| Brain length on skull length                              | **0.644±0.017  |
| Brain length on neurocranial length                       | **0.966±0.025  |
| Brain length on medial length of frontal                  | **1.414±0.052  |
| Brain length on medial length of parietal                 | **4.312±0.262  |
| Brain length on length of basioccipital                   | **7.792±0.347  |
| Brain length on length of basisphenoid                    | **7.542±0.322  |
| Brain length on length of presphenoid                     | **7.624±0.473  |
| Brain width on interauricular distance                    | **0.528±0.028  |
| Brain width on transverse distance between lateral canthi | **0.495±0.017  |
| Brain width on transverse distance between medial canthi  | **0.872±0.021  |
| Brain width on transverse distance between cornual buds   | **0.898±0.046  |
| Brain width on intersupraorbital foramen distance         | **1.620±0.047  |
| Brain width on skull width                                | **0.869±0.021  |
| Brain width on anterior width of parietal bone            | **1.258±0.036  |
| Brain width on posterior width of parietal bone           | **1.508±0.048  |
| Brain width on width of supraorbital bone                 | **1.304±0.058  |
| Brain thickness on posterior height of skull              | **0.349±0.015  |
| Brain thickness on height of supraoccipital bone          | **0.905±0.037  |
| Average cerebral weight on age                            | **0.189±0.010  |
| Cerebellar weight on age                                  | **0.048±0.004  |
| Brainstem weight on age                                   | **0.078±0.004  |

\*\*P<0.01 (significant at 1% level)

**Table 42. Regression coefficients of individual values among brain parameters**

| Regression coefficients                             | b ± S.E. of b  |
|---|----------------|
| Brain weight on brain volume                        | **0.993±0.003  |
| Brain weight on brain length                        | **7.896±0.402  |
| Brain weight on brain width                         | **10.881±0.687 |
| Brain weight on brain thickness                     | **18.738±1.700 |
| Brain weight on average weight of cerebrum          | **2.567±0.051  |
| Brain weight on weight of cerebellum                | **8.956±0.431  |
| Brain weight on weight of brainstem                 | **6.165±0.152  |
| Average cerebral weight on brain weight             | **0.383±0.008  |
| Average cerebral weight on cerebellar weight        | **3.359±0.208  |
| Weight of cerebellum on brain weight                | **0.101±0.005  |
| Weight of brainstem on brain weight                 | **0.158±0.004  |
| Brain length on brain width                         | **1.401±0.030  |
| Brain length on brain thickness                     | **2.519±0.111  |
| Brain length on average length of cerebrum          | **1.270±0.027  |
| Brain length on length of cerebellum                | **2.426±0.080  |
| Brain length on length of brainstem                 | **1.443±0.058  |
| Brain width on width of cerebellum                  | **1.246±0.048  |
| Brain width on width of brainstem                   | **1.876±0.055  |
| Brain weight on weight of left cerebral hemisphere  | **2.523±0.051  |
| Brain weight on weight of right cerebral hemisphere | **2.498±0.053  |
| Brainstem weight on weight of diencephalon          | **2.015±0.039  |
| Brainstem weight on weight of mesencephalon         | **3.858±0.136  |
| Brainstem weight on weight of pons                  | **9.245±0.408  |
| Brainstem weight on weight of medulla oblongata     | **4.387±0.107  |
| Length of brainstem on length of diencephalon       | **2.880±0.189  |
| Length of brainstem on length of rostral colliculus | **4.043±0.495  |
| Length of brainstem on length of caudal colliculus  | **9.771±0.609  |
| Length of brainstem on length of pons               | **2.695±0.097  |
| Length of brainstem on length of medulla oblongata  | **2.326±0.082  |

\*\*P&lt;0.01 (significant at 1% level)

**Table 43. Regression equations for prediction of unknown brain parameters in goat foetuses**

| Predicted parameters<br>(Y) | Known parameters<br>(X)                    | Regression equations<br>(Y = a + bX) |
|-----------------------------|--|--------------------------------------|
| Brain weight                | CRL (straight)                             | $Y = -9.92 + 1.457X$                 |
| Brain weight                | Total body length                          | $Y = -8.13 + 2.127X$                 |
| Brain weight                | Age  | $Y = -28.27 + 0.493X$                |
| Brain weight                | Body weight (from 6 to 19 weeks)           | $Y = 3.04 + 0.033X$                  |
| Brain weight                | Body weight (last two weeks)               | $Y = 41.93 + 0.004X$                 |
| Weight of brainstem         | Brain weight                               | $Y = 0.29 + 0.158X$                  |
| Brain length                | CRL (straight)                             | $Y = 1.08 + 0.175X$                  |
| Brain length                | Total body length                          | $Y = 1.34 + 0.252X$                  |
| Brain length                | Skull length                               | $Y = 0.41 + 0.644X$                  |
| Brain length                | Neurocranial length                        | $Y = 0.35 + 0.966X$                  |
| Brain length                | Medial length of frontal bone              | $Y = 0.54 + 1.414X$                  |
| Brain length                | Length of basisphenoid                     | $Y = 0.51 + 7.542X$                  |
| Brain width                 | Transverse distance between lateral canthi | $Y = 0.13 + 0.495X$                  |
| Brain width                 | Transverse distance between medial canthi  | $Y = 0.35 + 0.872X$                  |
| Brain width                 | Transverse distance between cornual buds   | $Y = 0.27 + 0.898X$                  |
| Brain width                 | Intersupraorbital foramina distance        | $Y = 0.08 + 1.620X$                  |
| Brain width                 | Skull width                                | $Y = 0.15 + 0.869X$                  |
| Brain width                 | Anterior width of parietal                 | $Y = 0.33 + 1.258X$                  |
| Brain width                 | Posterior width of parietal                | $Y = 0.33 + 1.508X$                  |
| Brain thickness             | Posterior height of skull                  | $Y = 0.43 + 0.349X$                  |
| Brain thickness             | Height of supraoccipital                   | $Y = 0.69 + 0.905X$                  |

# *Figures*

---



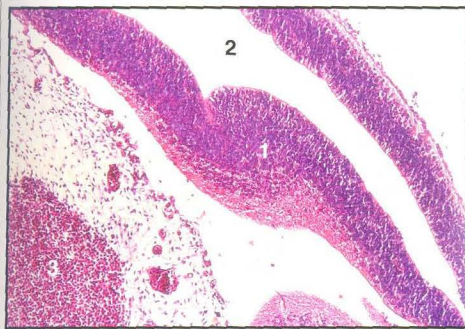
- 1. Dorsal wall
- 2. Ventral wall
- 3. Lumen
- 4. Body wall

**Fig. 1** C.S. of the telencephalon (24 days of gestation). H&E. x 100



- 1. Lateral ventricle
- 2. Foramen of Monro
- 3. Third ventricle
- 4. Diencephalon
- 5. Telencephalon

**Fig. 2** C.S. of the neural tube wall at the junction between telencephalon and diencephalon (27 days). H&E. x 100



- 1. Wall of telencephalon
- 2. Lateral ventricle
- 3. Cavernous sinus

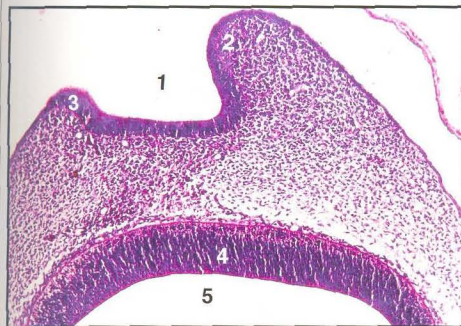
**Fig. 3** C.S. of the telencephalon (27 days). H&E. x 100





- 1. Olfactory pit
- 2. Lateral wall of telencephalon
- 3. Lumen of neural tube

**Fig. 4** C.S. of the cephalic end of goat embryo at the cephalic end of telencephalon (24 days). H&E. x 100



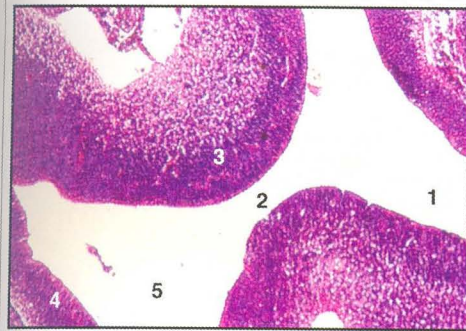
- 1. Open olfactory pit
- 2. Lateral nasal process
- 3. Medial nasal process
- 4. Lateral telencephalic wall
- 5. Lumen of neural tube

**Fig. 5** C.S. of the cephalic end of goat embryo at the level of telencephalon showing open olfactory pits (24 days). H&E. x 100



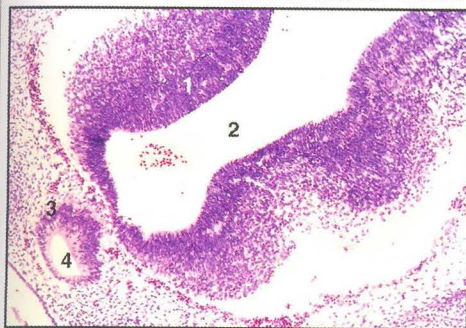
- 1. Lateral wall
- 2. Lumen
- 3. Internal carotid artery

**Fig. 6** C.S. of the diencephalon (26 days). H&E. x 100



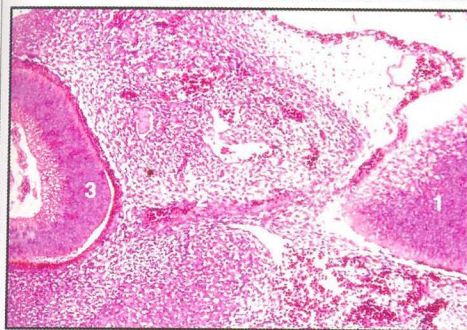
1. Lateral ventricle
2. Third ventricle
3. Thalamus
4. Hypothalamus
5. Floor of third ventricle

**Fig. 7** C.S. of the neural tube at the junction between telencephalon and diencephalon (27 days). H&E. x 100



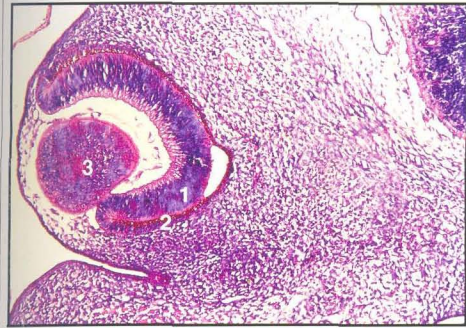
1. Diencephalic wall
2. Third ventricle
3. Rathke's pouch
4. Lumen of Rathke's pouch

**Fig. 8** Section of the diencephalon at the level of Rathke's pouch (27 days). H&E. x 100



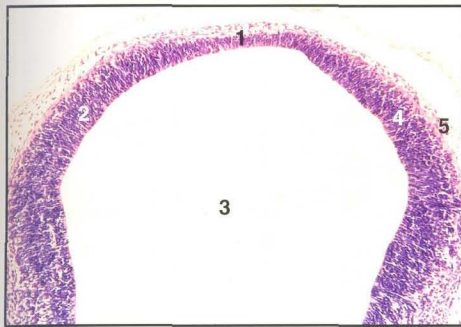
1. Diencephalic wall
2. Optic stalk
3. Optic cup

**Fig. 9** C.S. of the neural tube at the level of optic cup (27 days). H&E. x 1



- 1. Inner layer
- 2. Outer pigmented layer
- 3. Lens vesicle

**Fig. 10** C.S. of the optic cup (26 days). H&E. x 100



- 1. Roof plate
- 2. Alar plate
- 3. Lumen
- 4. Ependymal layer
- 5. Marginal layer

**Fig. 11** C.S. of the dorsal half of mesencephalon (26 days). H&E. x 100



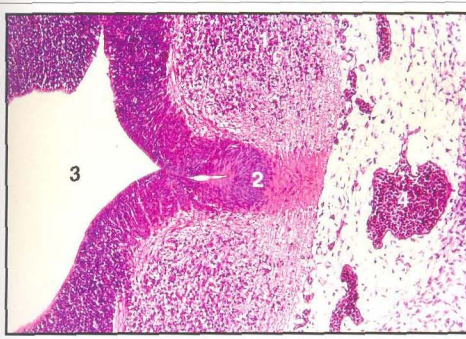
- 1. Alar plate
- 2. Basal plate
- 3. Sulcus limitans
- 4. Floor plate
- 5. Mesocoele

**Fig. 12** C.S. of the ventral half of the mesencephalon (26 days). H&E. x 100



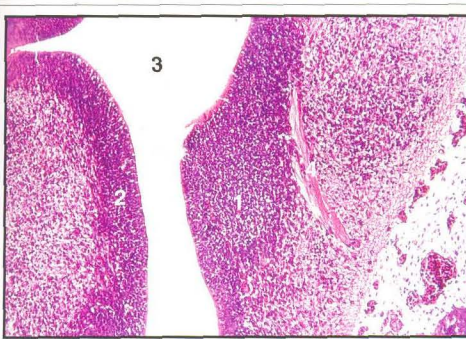
- 1. Metencephalic wall
- 2. Neuromere
- 3. Otocyst
- 4. Endolymph duct
- 5. Lumen of hind brain

**Fig. 13** Frontal section of the metencephalon (24 days). H&E. x 100



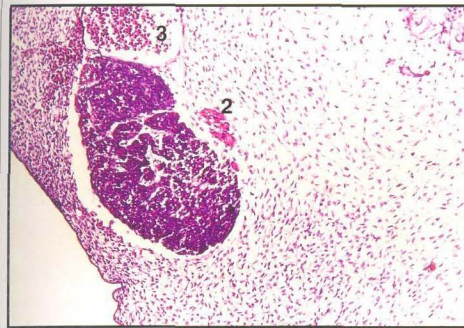
- 1. Basal plate
- 2. Floor plate
- 3. Metacoel
- 4. Basilar artery

**Fig. 14** C.S. of the metencephalon (27 days). H&E. x 100



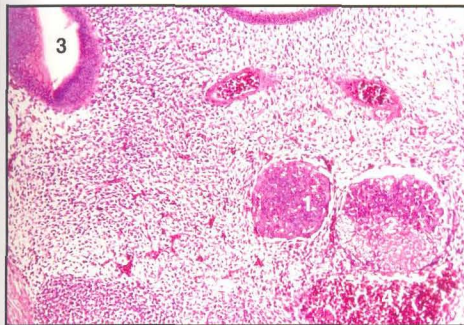
- 1. Basal plate
- 2. Alar plate
- 3. Metacoel
- 4. Bundle of nerve fibres

**Fig. 15** C.S. of the metencephalon (27 days). H&E. x 100



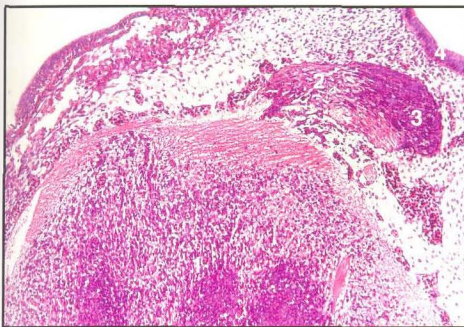
- 1. Semilunar ganglion
- 2. Trigeminal nerve fibres
- 3. Cavernous sinus

**Fig. 16** C.S. of the semilunar ganglion (24 days), H&E. x 100



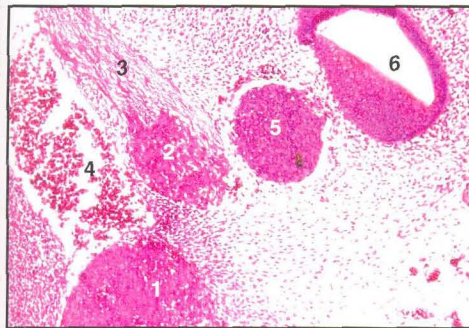
- 1. Mandibular nerve
- 2. Maxillary nerve
- 3. Otocyst
- 4. Cavernous sinus

**Fig. 17** C.S. of the cephalic end of the goat embryo at the level of otocyst (27 days), H&E. 100



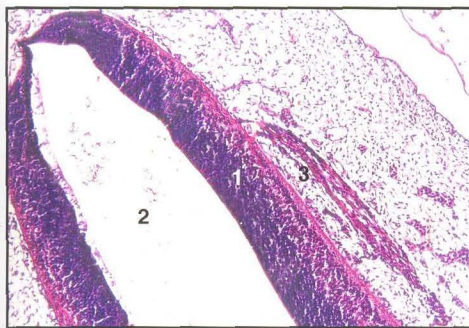
- 1. Wall of hind brain
- 2. Facial nerve
- 3. Geniculate ganglion
- 4. Wall of otocyst

**Fig. 18** C.S. of the hind brain at the level of facial nerve (27 days), H&E. x 100



1. Semilunar ganglion
2. Geniculate ganglion
3. Facial nerve
4. Anterior cardinal vein
5. Ganglion acousticum
6. Otocyst

**Fig.19** C.S. of the cephalic part of goat foetus showing ganglia and nerves in the mesenchyme (27 days). H&E. x 100



1. Myelencephalic wall
2. Myelocoele
3. Accessory nerve

**Fig. 20** L.S. of the myelencephalon (24 days). H&E. x 100



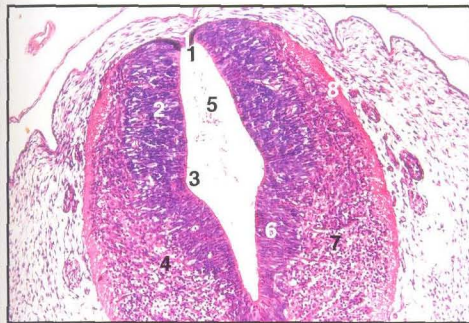
1. Myelencephalon
2. Hypoglossal nerve rootlets
3. Mesenchyme

**Fig.21** Section of goat foetus through myelencephalon and pharynx (26 days). H&E. x 100



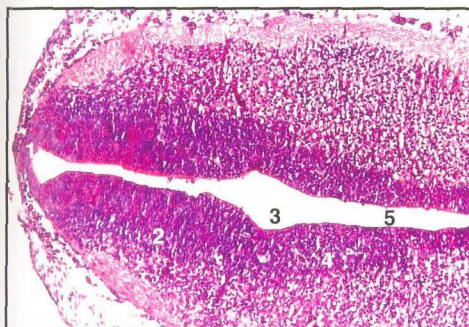
- 1. Roof plate
- 2. Alar plate
- 3. Sulcus limitans
- 4. Basal plate
- 5. Floor plate
- 6. Lumen
- 7. Froriep's Ganglion
- 8. Mantle layer

Fig. 22 C.S. of the myelencephalon (24 days). H&E. x 100



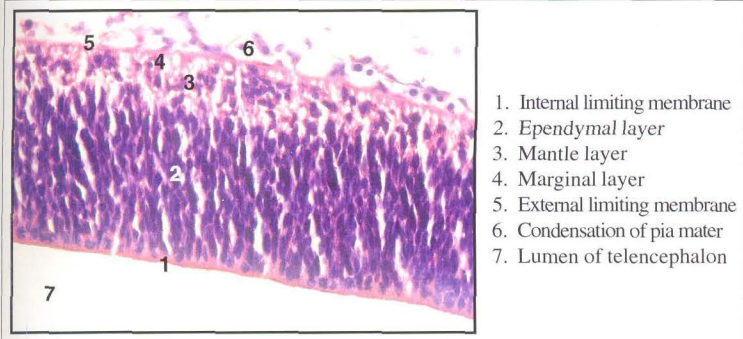
- 1. Roof plate
- 2. Alar plate
- 3. Sulcus limitans
- 4. Basal plate
- 5. Coffin-shaped lumen
- 6. Ependymal layer
- 7. Mantle layer
- 8. Marginal layer

Fig. 23 C.S. of the myelencephalon (26 days). H&E. x 100



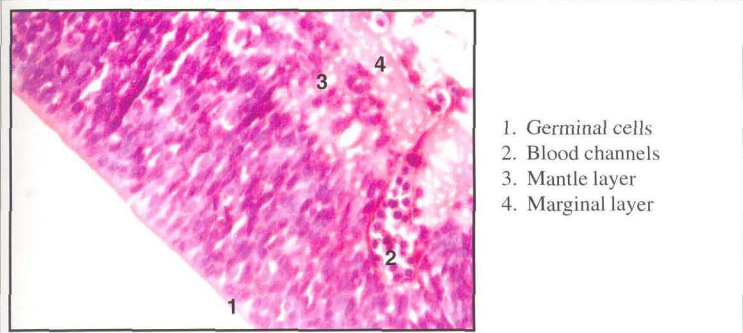
- 1. Roof plate
- 2. Alar plate
- 3. Sulcus limitans
- 4. Basal plate
- 5. Lumen

Fig. 24 C.S. of the myelencephalon (27 days). H&E. x 100



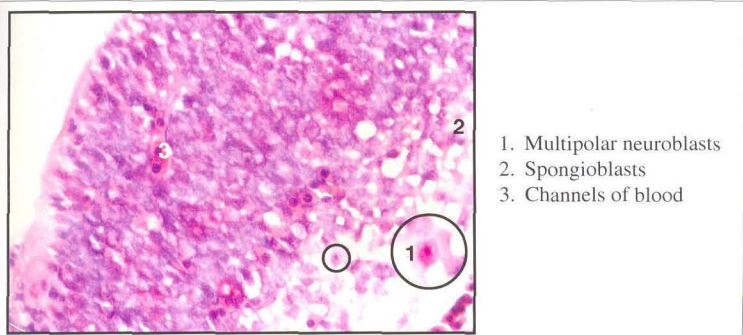
- 1. Internal limiting membrane
- 2. Ependymal layer
- 3. Mantle layer
- 4. Marginal layer
- 5. External limiting membrane
- 6. Condensation of pia mater
- 7. Lumen of telencephalon

**Fig. 25 C.S of the wall of telencephalon (24 days). H&E. x 100**



- 1. Germinal cells
- 2. Blood channels
- 3. Mantle layer
- 4. Marginal layer

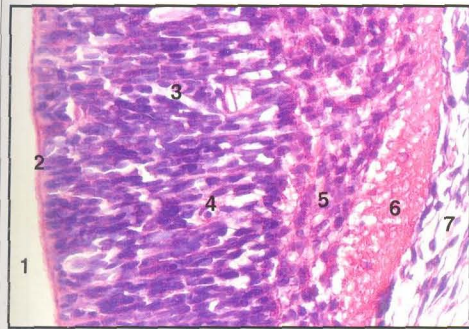
**Fig. 26 C.S. of the telencephalic wall showing a blood channel (24days). H&E. x 100**



- 1. Multipolar neuroblasts
- 2. Spongioblasts
- 3. Channels of blood

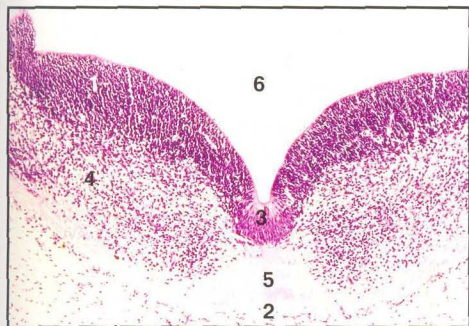
**Fig. 27 C.S. of the wall of telencephalon (27 days). H&E. x 400**





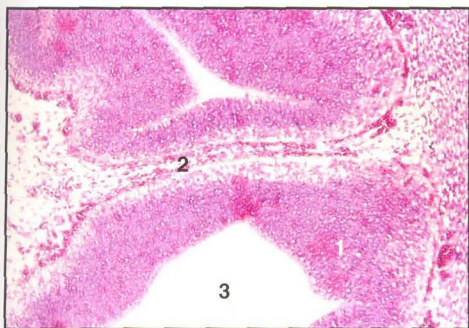
1. Lumen
2. Internal limiting membrane
3. Scattered RBCs
4. Mantle layer
5. Marginal layer
6. Spongioblast nucleus
7. Mesenchymal cells

**Fig. 28 C.S. of the wall of telencephalon (26 days). H&E. x 400**



1. Basal plate
2. Floor plate
3. Ependymal layer
4. Mantle layer
5. Marginal layer
6. Lumen

**Fig. 29 C.S. of the metencephalic floor (26 days). H&E. x 100**



1. Telencephalic wall
2. Primitive pia mater
3. Lateral ventricle

**Fig. 30 C.S. of the telencephalon showing double layer of pia mater (27 days). H&E. x 100**



1. Wall of rhombencephalon
2. Pontine flexure
3. Fourth ventricle

**Fig. 31** L.S. of the cephalic end of the embryo showing pontine flexure (40 days). H&E. x 100

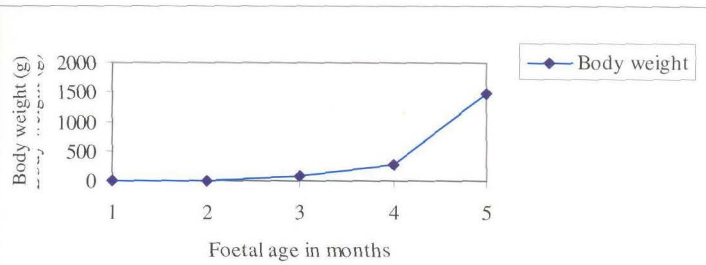


**Fig. 32** Relation between body weight and age

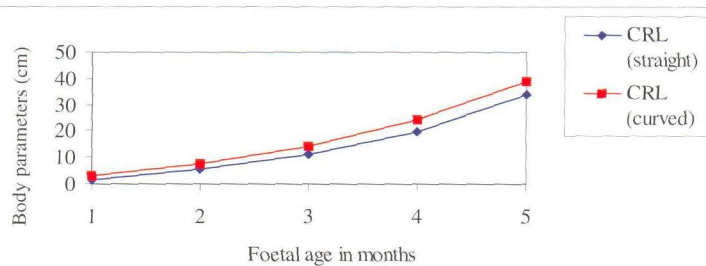


**Fig. 33** Relation between age and body parameters

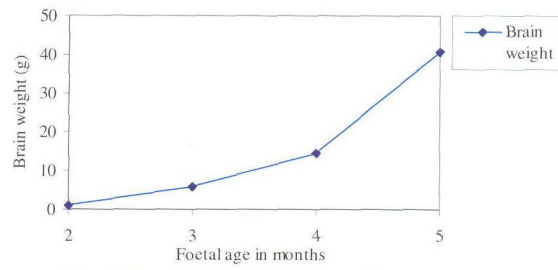


**Fig. 34 Relation between age and brain weight**

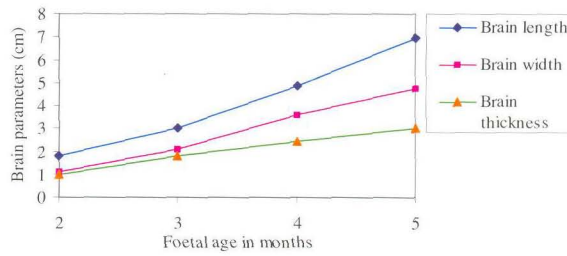


**Fig. 35 Relation between age and brain parameters**

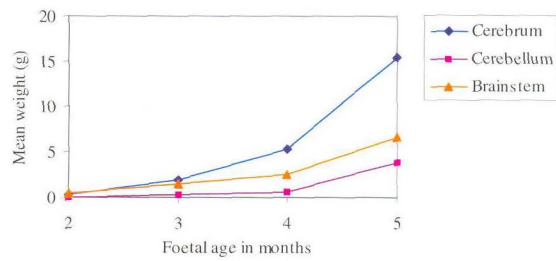


**Fig. 36 Relation between age and weight of cerebrum, cerebellum and brainstem**

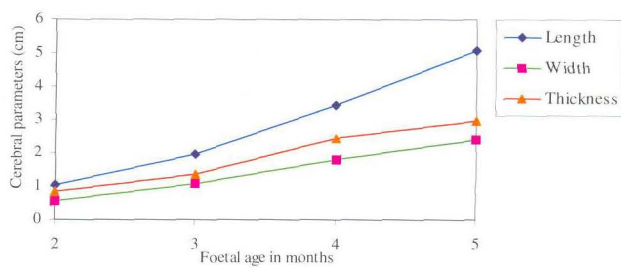


**Fig. 37** Relation between age and parameters of right cerebral hemisphere

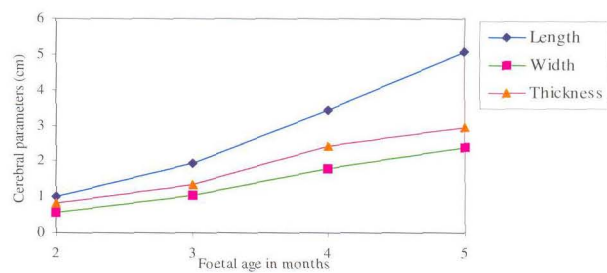


**Fig. 38** Relation between age and parameters of left cerebral hemisphere

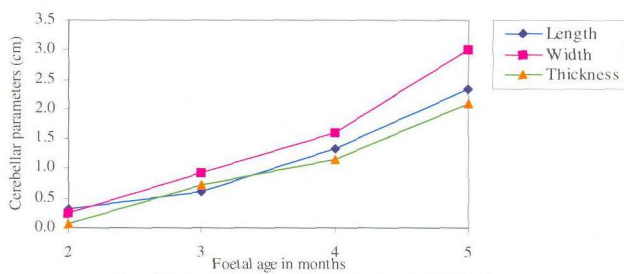


**Fig. 39** Relation between age and cerebellar parameters

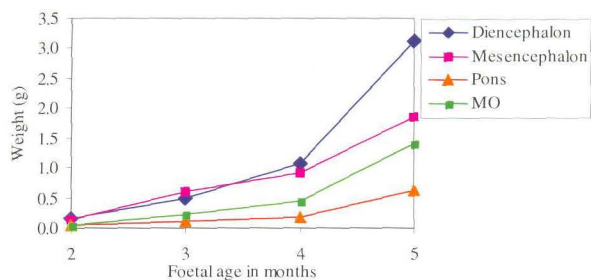


**Fig. 40** Relation between age and weight of brainstem components

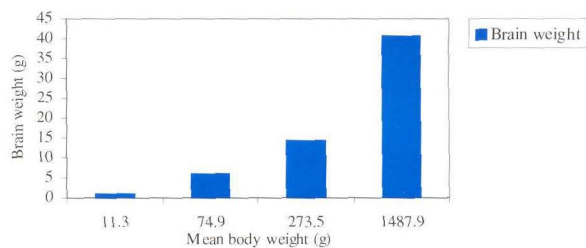


**Fig. 41** Relation between body weight and brain weight

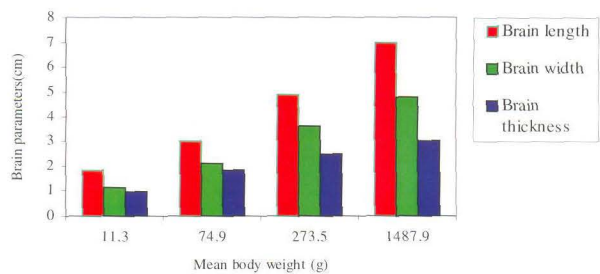


**Fig. 42** Relation between body weight and brain parameters

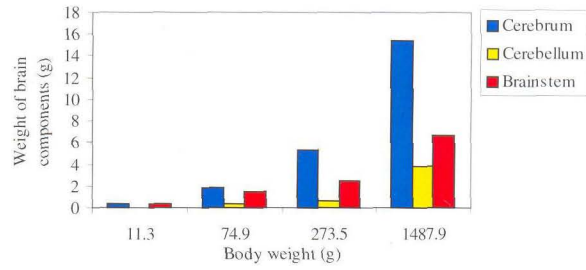


**Fig. 43** Relation between body weight and weights of cerebrum, cerebellum and brainstem

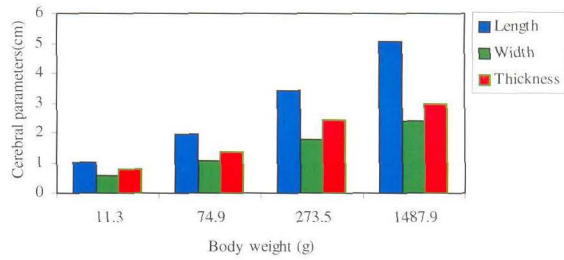


**Fig. 44** Relation between body weight and parameters right cerebral hemisphere

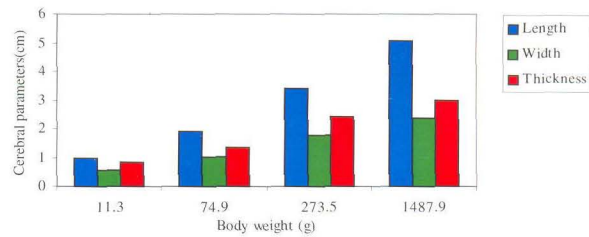


**Fig. 45** Relation between body weight and parameters of left cerebral hemisphere

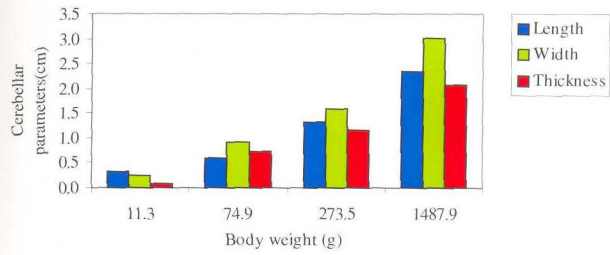


**Fig. 46** Relation between body weight and cerebellar parameters

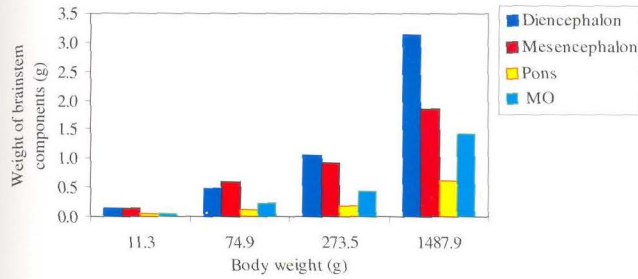


**Fig. 47** Relation between body weight and weight of brainstem components

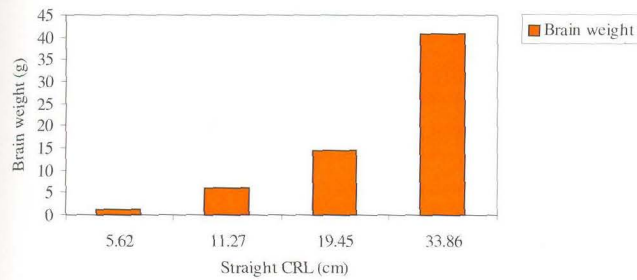


**Fig. 48** Relation between CRL(straight) and brain weight

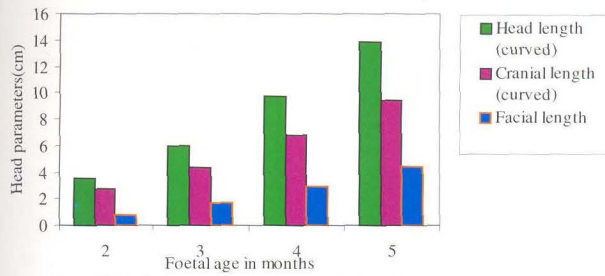


Fig. 49 Relation between age and head parameters

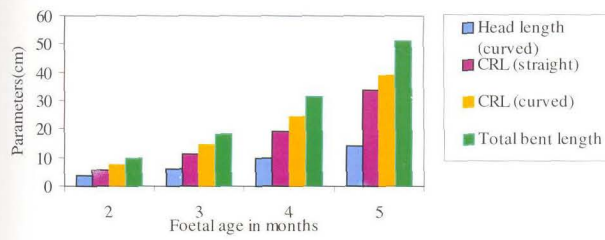


Fig. 50 Relation between age and parameters of head and body at different stages of gestation

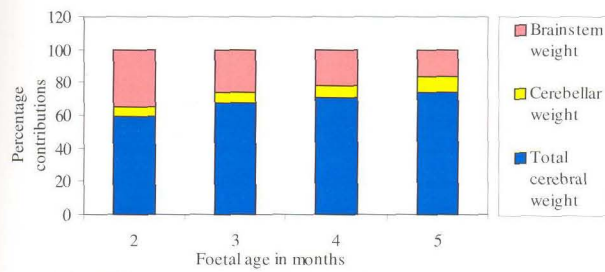


Fig. 51 Percentage contributions of brain components to the total brain weight during gestation



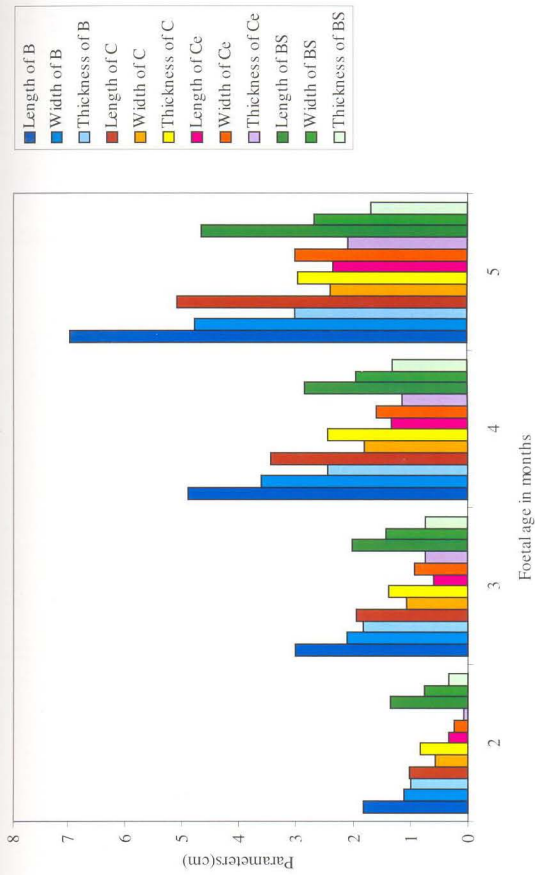
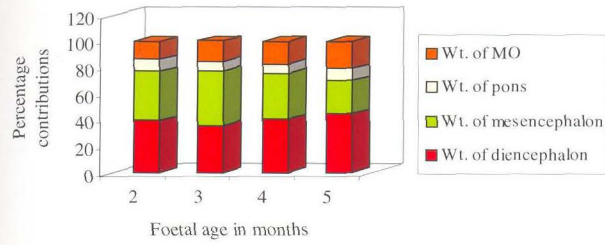
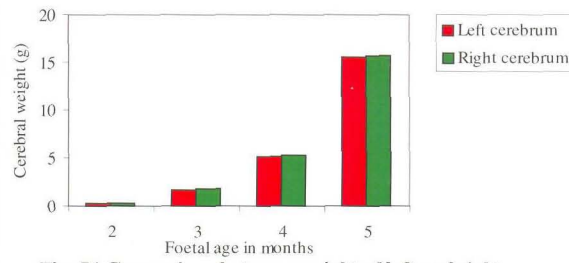


Fig. 52 Mean length, width and thickness of whole brain(B), cerebrum (C), cerebellum (Ce) and brainstem (BS) at different stages of gestation



**Fig. 53 Percentage contributions of components of brainstem to the total brainstem weight during gestation**



**Fig. 54 Comparison between weight of left and right cerebral hemispheres during gestation**

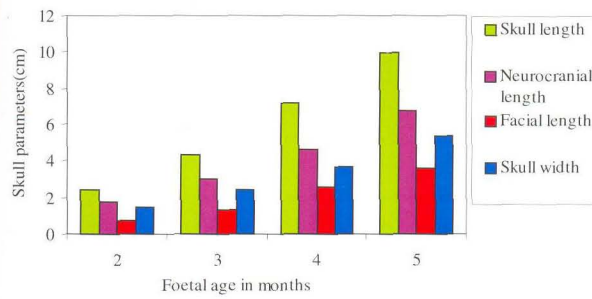


**Fig. 55 Comparison between skull parameters at different stages of gestation**

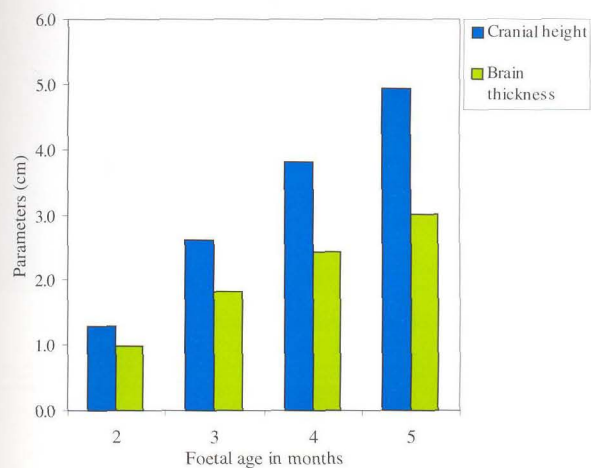


**Fig. 56 Comparison between cranial height and brain thickness during gestation**

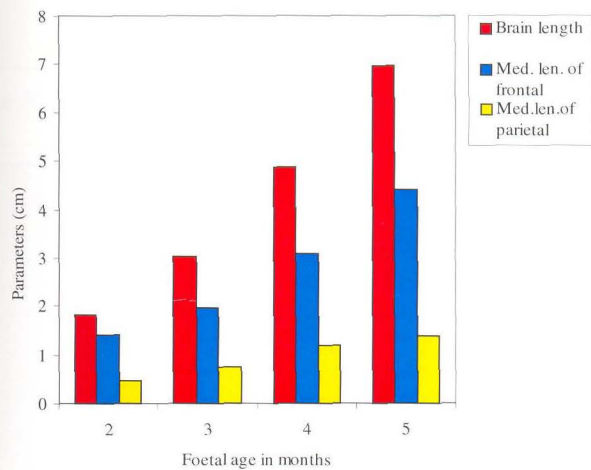
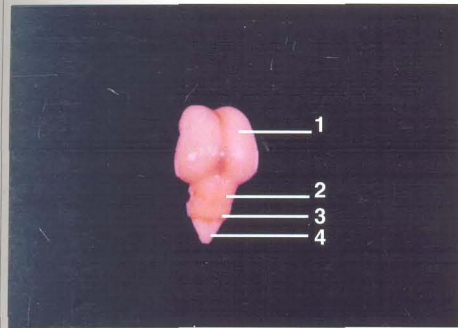


**Fig. 57 Comparison between brain length and length of skull bones during gestation**



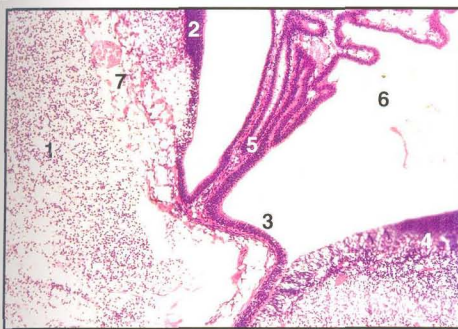
- 1. Cerebral hemisphere
- 2. Corpora quadrigemina
- 3. Cerebellum
- 4. Medulla oblongata

**Fig. 58 Dorsal surface of the brain (55 days)**



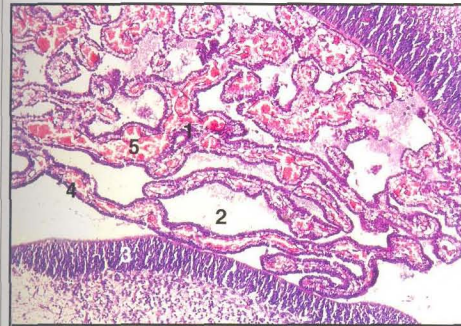
- 1. Medial wall
- 2. Lateral wall
- 3. Ventral wall
- 4. Temporal extension of lateral ventricle

**Fig. 59 C.S. of the cerebral hemisphere showing the lateral ventricle (48 days), H&E. x 100**



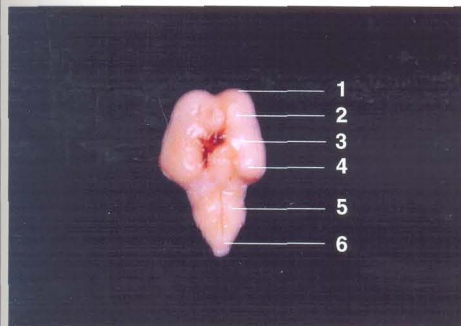
- 1. Thalamus
- 2. Caudate nucleus
- 3. Choroid fissure
- 4. Hippocampus
- 5. Choroid plexus
- 6. Lateral ventricle
- 7. Velum interpositum

**Fig. 60 C.S. of the cerebrum and diencephalon (48 days), H&E. x 100**



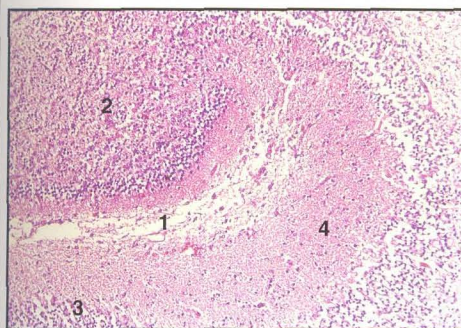
- 1. Choroid plexus
- 2. Lateral ventricle
- 3. Wall of cerebrum
- 4. Choroid epithelium
- 5. Lumen of choroid plexus

**Fig. 61 C.S. of the cerebrum (48 days). H&E. x 100**



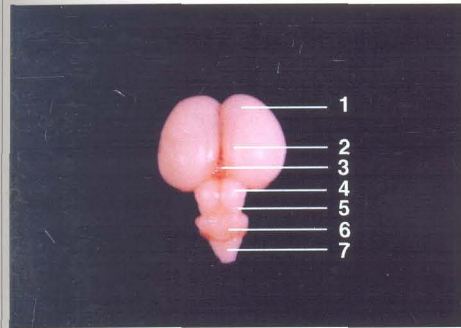
- 1. Cerebrum
- 2. Olfactory bulb
- 3. Sylvian fissure
- 4. Piriform lobe
- 5. Pons
- 6. Medulla oblongata

**Fig. 62 Ventral surface of brain showing Sylvian fissure (69 days)**



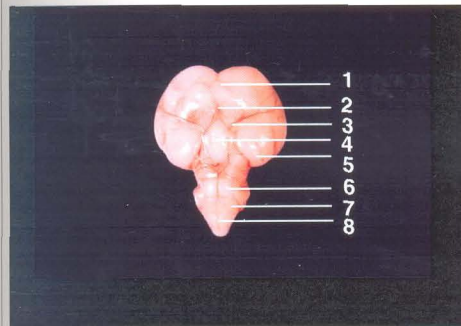
- 1. Hippocampal fissure
- 2. Dentate gyrus
- 3. Parahippocampal gyrus
- 4. Molecular layer

**Fig. 63 C.S. of cerebrum showing the hippocampal fissure (81 days). H&E. x 100**



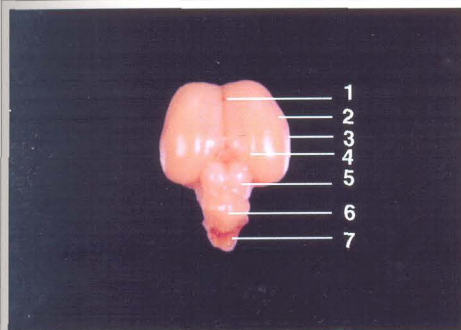
- 1. Cerebrum
- 2. Marginal sulcus
- 3. Pineal gland
- 4. Rostral colliculus
- 5. Caudal colliculus
- 6. Cerebellum
- 7. Medulla oblongata

**Fig. 64 Dorsal surface of brain showing developing sulci on the cerebral surface (76 days)**



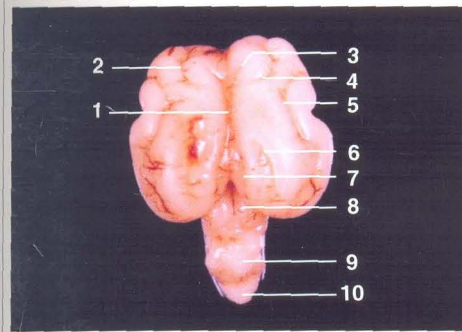
- 1. Olfactory bulb
- 2. Circle of Willis
- 3. Middle cerebral artery
- 4. Pituitary
- 5. Piriform lobe
- 6. Pons
- 7. Medulla oblongata
- 8. Basilar artery

**Fig. 65 Ventral surface of brain showing circle of Willis (76 days)**



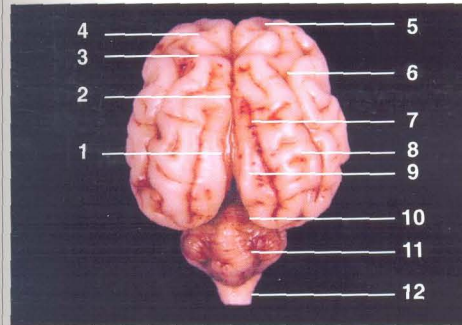
- 1. Cruciate fissure
- 2. Suprasylvian sulcus
- 3. Cerebrum
- 4. Marginal fissure
- 5. Corpora quadrigemina
- 6. Cerebellum
- 7. Medulla oblongata

**Fig. 66 Dorsal surface of brain (83 days)**



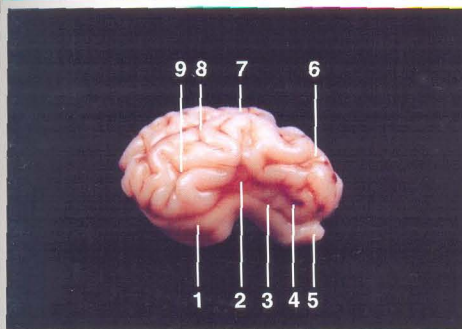
1. Great longitudinal fissure
2. Coronal fissure
3. Cruciate fissure
4. Ansate sulcus
5. Suprasylvian fissure
6. Marginal sulcus
7. Endomarginal sulcus
8. Mesencephalon
9. Cerebellum
10. Medulla Oblongata

**Fig. 67 Dorsal surface of the brain showing developing sulci on the cerebral surface (93 days)**



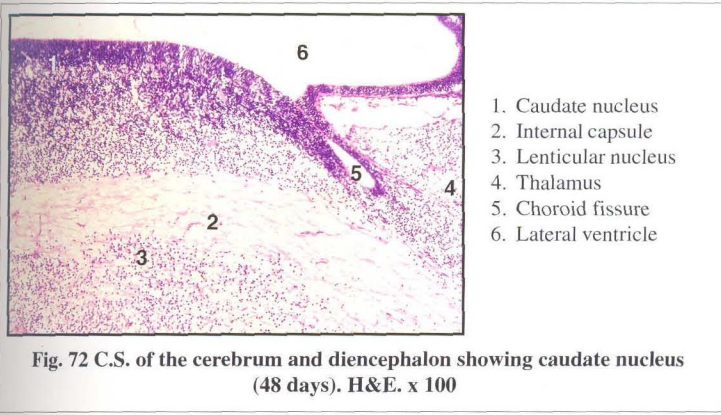
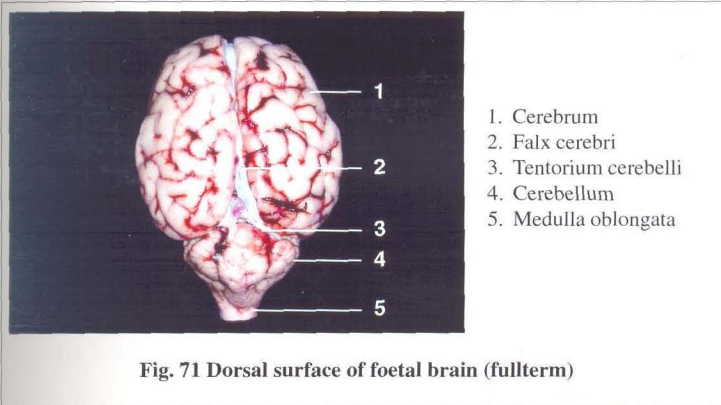
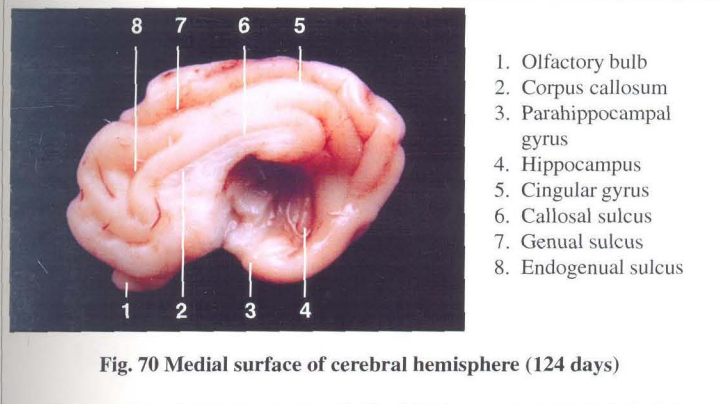
1. Endomarginal fissure
2. Great longitudinal fissure
3. Ansate fissure
4. Cruciate fissure
5. Coronal sulcus
6. Suprasylvian sulcus
7. Marginal sulcus
8. Ectomarginal gyrus
9. Marginal gyrus
10. Transverse fissure
11. Cerebellum
12. Medulla oblongata

**Fig. 68 Dorsal surface of brain (124 days)**

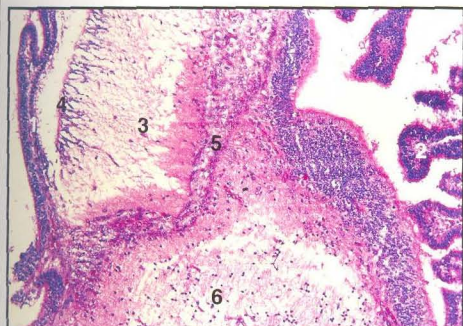


1. Piriform lobe
2. Sylvian fissure
3. Lateral rhinal sulcus
4. Presylvian sulcus
5. Olfactory bulb
6. Oblique sulcus
7. Suprasylvian sulcus
8. Ectosylvian sulcus
9. Diagonal sulcus

**Fig. 69 Lateral view of cerebral hemisphere (124 days)**

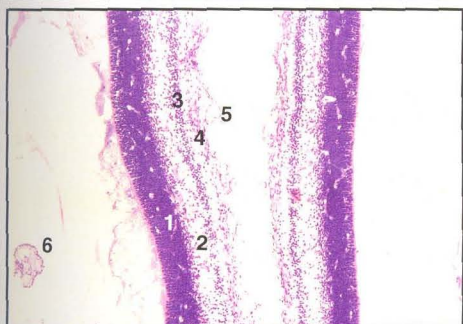






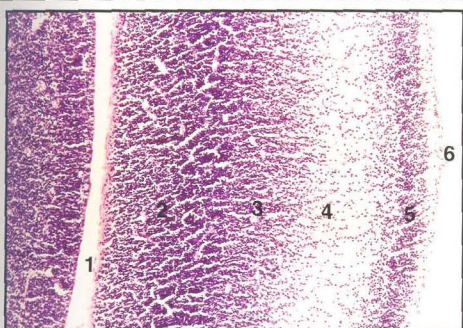
1. Choroid plexus of LV
2. Choroid plexus of third ventricle
3. Septum pellucidum
4. Ciliated ependyma
5. Velum interpositum
6. Thalamus

**Fig. 73 C.S. of the brain showing septum pellucidum and thalamus (58 days). H&E. x 100**



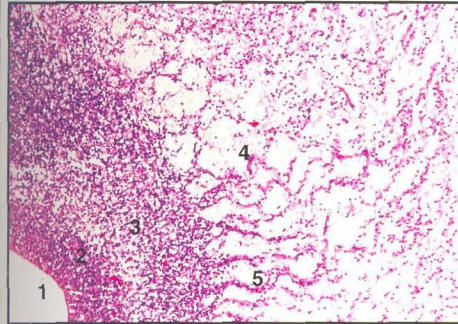
1. Ependymal layer
2. White matter
3. Cortical plate
4. Outer marginal layer
5. Pia mater
6. LV with choroid plexus

**Fig. 74 C.S. of the cerebral hemispheres showing the thin medial walls of both sides (48 days). H&E. x 100**



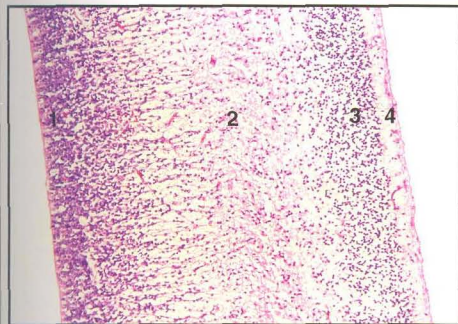
1. Lateral ventricle
2. Ependymal layer
3. Mantle layer
4. White matter
5. Superficial gray cortex
6. Pia mater

**Fig. 75 C.S. of the lateral cerebral wall showing cortical migration of cells (48 days). H&E. x 100**



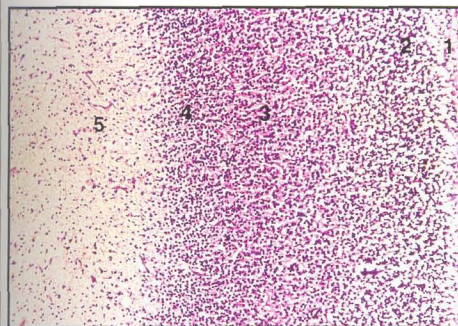
- 1. Lateral ventricle
- 2. Ependymal layer
- 3. Mantle layer
- 4. White matter
- 5. Wavy lines of migrating cells

**Fig. 76 C.S. of the cerebral wall showing wavy lines of migrating neuroblasts through the white matter (58 days). H&E. x 100**



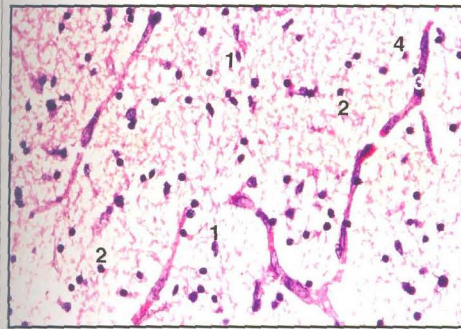
- 1. Ependymal layer
- 2. White matter
- 3. Inner cellular layer of cortical plate
- 4. Outer molecular layer

**Fig. 77 C.S. of the lateral cerebral wall showing different layers (58 days). H&E. x 100**



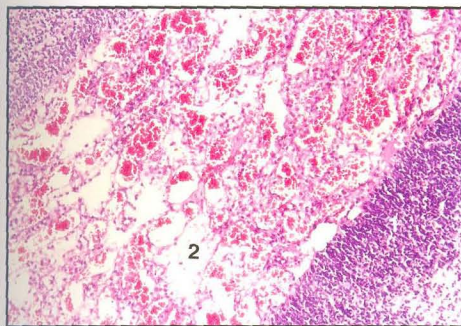
- 1. Outer molecular layer
- 2. Superficial granular layer
- 3. Intermediate granular layer
- 4. Deep granular layer
- 5. White matter

**Fig. 78 C.S. of the cerebral wall showing stratification of cerebral cortex (76 days). H&E. x 100**



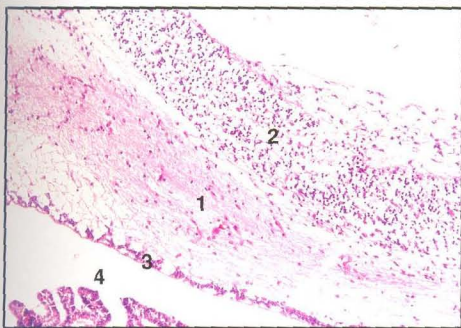
- 1. Fibrous astrocytes
- 2. Oligodendroglia
- 3. Capillaries
- 4. Microglia

**Fig. 79 White matter of the cerebrum (76 days). H&E. x 400**



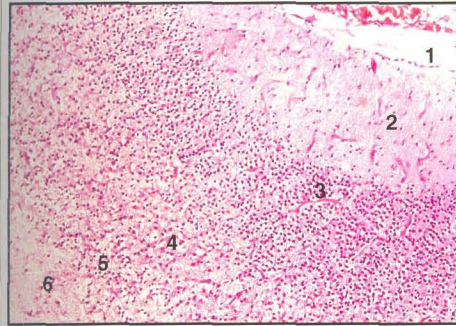
- 1. Ependymal layer of cerebral wall
- 2. Choroid plexus
- 3. Region of adhesion of choroid plexus with ependymal layer

**Fig. 80 C.S. of the cerebrum showing choroid plexus in the lateral ventricle (61 days). H&E. x 100**



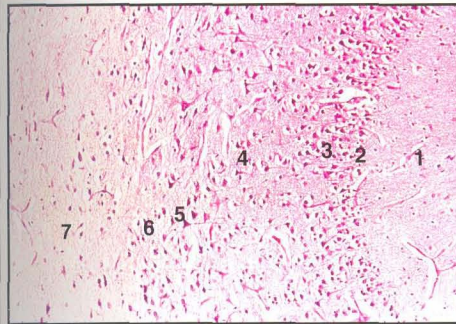
- 1. Corpus callosum
- 2. Cortical cells
- 3. Ependyma
- 4. LV with choroid plexus

**Fig. 81 C.S. of the corpus callosum forming the roof of the lateral ventricle (61 days). H&E. x 100**



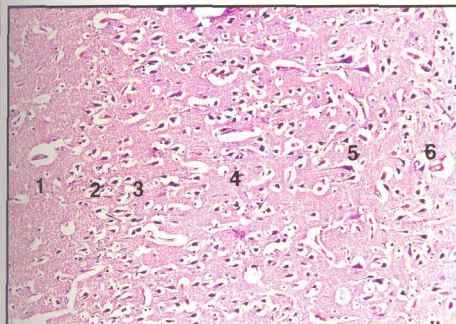
1. Sulcus
2. Outer molecular layer
3. Superficial granular layer
4. Intermediate granular layer
5. Deep granular layer
6. White matter

**Fig. 82 C.S. of the cerebral cortex (101 days). H&E. x 100**



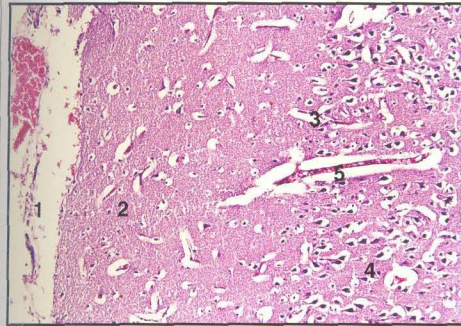
1. Outer molecular layer
2. External granular layer
3. External pyramidal layer
4. Internal granular layer
5. Internal pyramidal layer
6. Fusiform cell layer
7. White matter

**Fig. 83 T.S. of the cerebral cortex showing layers of cerebral cortex at the bottom of the sulcus (124 days). H&E. x 100**



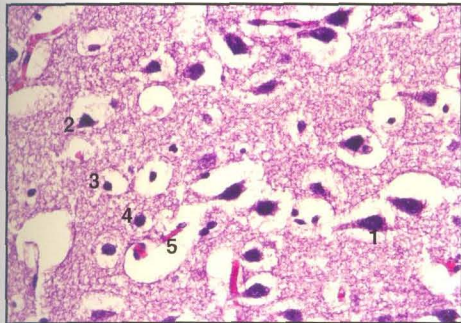
1. Outer molecular layer
2. External granular layer
3. External pyramidal layer
4. Internal granular layer
5. Internal pyramidal layer
6. Fusiform cell layer

**Fig. 84 T.S. of the cerebral cortex showing layers of cerebral cortex on the top of the gyrus (144 days). H&E. x 100**



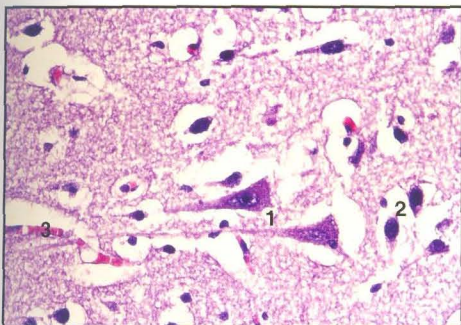
- 1. Pia mater
- 2. Outer molecular layer
- 3. Outer granular layer
- 4. Outer pyramidal layer
- 5. Blood vessel

Fig. 85 T.S. of the cerebral cortex showing the superficial layers (144 days).  
H&E. x 400



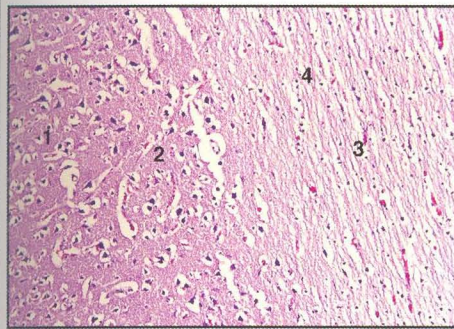
- 1. Large pyramidal cell
- 2. Small pyramidal cell
- 3. Oligodendroglia
- 4. Astrocyte
- 5. Capillary

Fig. 86 T.S. of the cerebral cortex showing external pyramidal layer  
(144 days). H&E. x 400



- 1. Large pyramidal neurons of inner pyramidal layer
- 2. Fusiform cell layer
- 3. Capillary

Fig. 87 T.S. of the cerebral cortex showing deeper layers of cerebral cortex  
(144 days). H&E. x 400



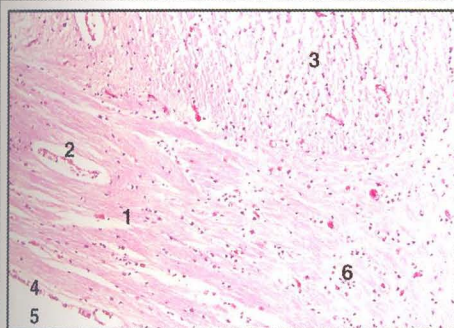
1. Inner pyramidal layer
2. Fusiform cell layer
3. White matter
4. Oligodendrocytes

Fig. 88 T.S. of the cerebral cortex showing inner layers of cerebral cortex and white matter (144 days). H&E. x 100



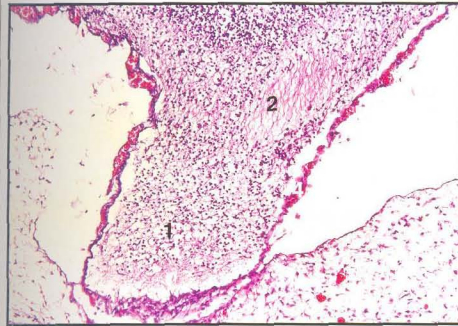
1. Capillaries lined by endothelial cells
2. Glial cells

Fig. 89 White matter of the cerebrum (144 days). H&E. x 400



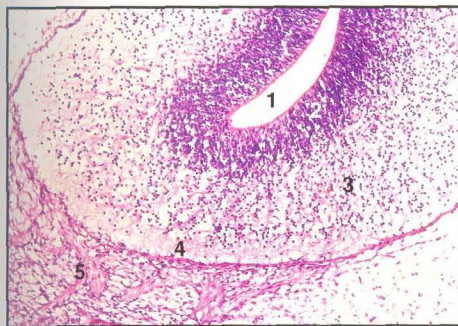
1. Corpus callosum
2. Capillary
3. Cells of the cortex
4. Ependymal lining
5. Lateral ventricle
6. Oligodendrocytes

Fig. 90 T.S. of the cerebral cortex showing corpus callosum (144 days). H&E. x 100



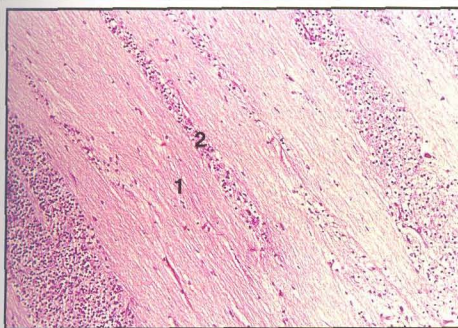
- 1. Olfactory bulb
- 2. Olfactory peduncle
- 3. Frontal pole of cerebrum
- 4. Pia mater

**Fig. 91 L.S. of the olfactory bulb and the cerebrum (48 days). H&E. x 100**



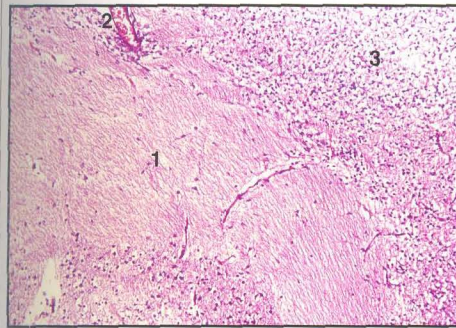
- 1. Lateral ventricle
- 2. Ependymal layer
- 3. Mantle layer
- 4. Marginal layer
- 5. Olfactory nerve fibres

**Fig. 92 L.S. of the olfactory bulb and olfactory nerve fibres (48 days). H&E. x 100**



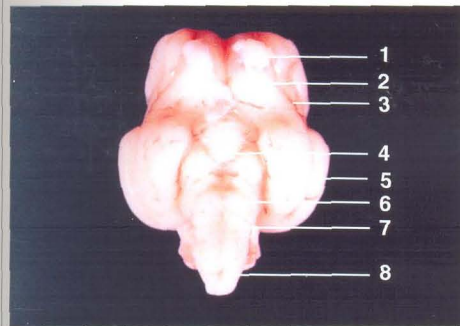
- 1. Fibres of the olfactory peduncle
- 2. Column of cells

**Fig. 93 Section of the olfactory peduncle (81 days). H&E. x 100**



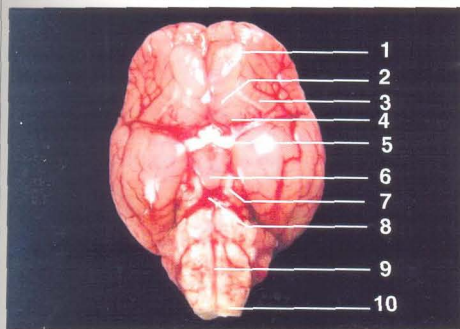
- 1. Lateral olfactory stria
- 2. Blood vessel
- 3. Cerebral cortex

**Fig. 94** Section of the lateral olfactory stria (81 days). H&E. x 100



- 1. Olfactory bulb
- 2. Lateral olfactory stria
- 3. Rhinal sulcus
- 4. Mamillary body
- 5. Piriform lobe
- 6. Pons
- 7. Trapezoid body
- 8. Medulla oblongata

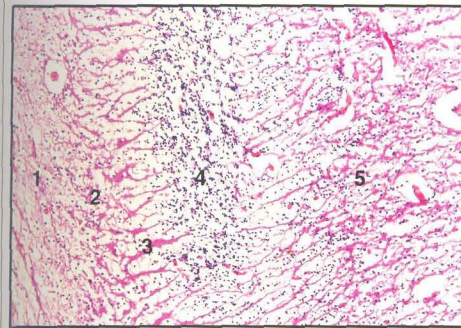
**Fig. 95** Ventral surface of the brain (101 days)



- 1. Olfactory bulb
- 2. Medial olfactory stria
- 3. Lateral olfactory stria
- 4. Trigonum olfactorium
- 5. Optic chiasma
- 6. Mamillary body
- 7. Oculomotor nerve
- 8. Circle of Willis
- 9. Basilar artery
- 10. Medulla oblongata

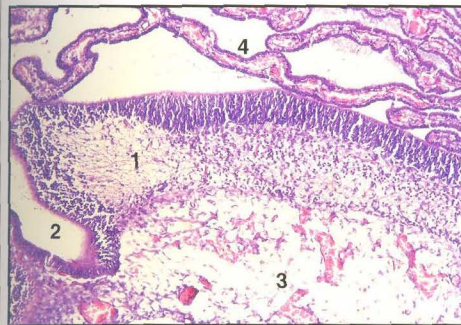
**Fig. 96** Ventral surface of the brain (Full term)





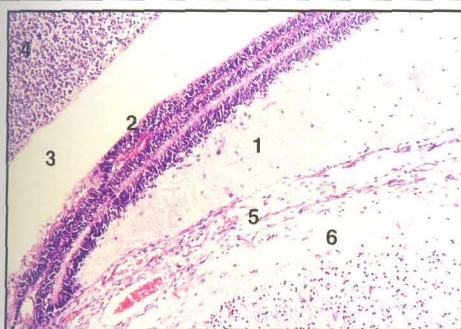
1. Layer of olfactory nerve fibres
2. Glomerular layer
3. Mitral cell layer
4. Internal granular layer
5. White substance

**Fig. 97 L.S. of the olfactory bulb (144 days). H&E. 100**



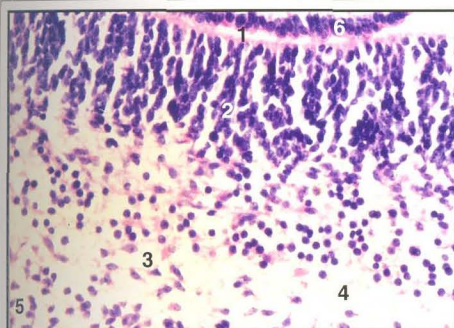
1. Hippocampus
2. Choroid fissure
3. Velum interpositum
4. Choroid plexus of LV

**Fig. 98 L.S. of the hippocampus (48 days). H&E. x 100**



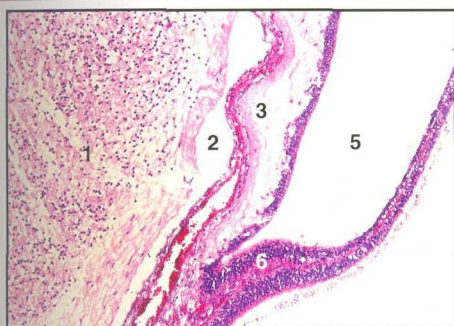
1. Fimbria
2. Choroid plexus of LV
3. Lateral ventricle
4. Lateral cerebral wall
5. Sulcus terminalis containing stria terminalis
6. External medullary lamina of the thalamus

**Fig. 99 C.S. of the fimbria and thalamus (62 days). H&E. x 100**



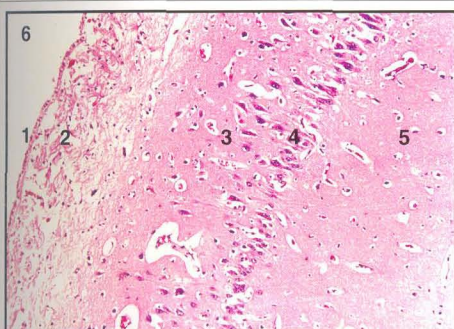
1. Internal limiting membrane
2. Ependymal layer
3. Mantle layer with pyramidal neurons
4. Marginal layer
5. Outer cellular cortex
6. Choroid epithelium of LV

**Fig. 100** Layers of the hippocampus (48 days). H&E. x 400



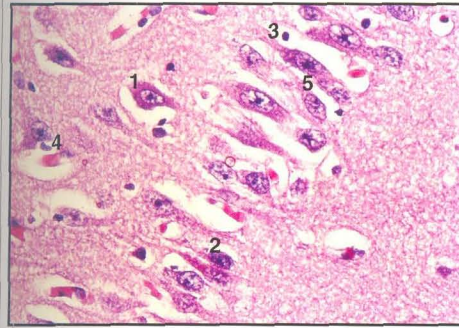
1. Thalamus
2. Velum interpositum
3. Fimbria
4. Ependymal lining of fimbria
5. Lateral ventricle
6. Stem of choroid plexus

**Fig. 101** C.S. of the fimbria and thalamus (58 days). H&E. x 100



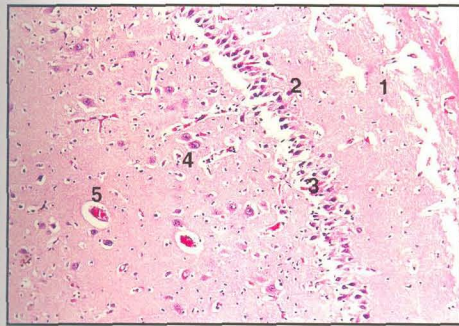
1. Ependymal layer
2. Stratum alveus
3. Stratum oriens
4. Stratum pyramidale
5. Stratum lacunosum-moleculare
6. Lateral ventricle

**Fig. 102** C.S. of the hippocampus (144 days). H&E. x 100



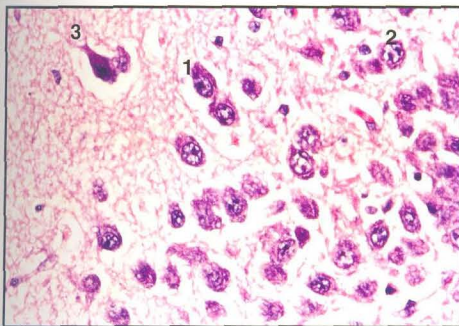
1. Large pyramidal cells
2. Small pyramidal cells
3. Oligodendroglia
4. Capillary
5. Double pyramidal cells

Fig. 103 C.S. of the hippocampus showing stratum pyramidale (144 days).  
H&E. x 400



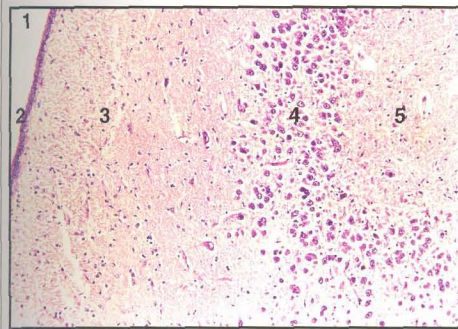
1. Stratum alveus
2. Stratum oriens
3. Stratum pyramidale
4. Stratum lacunosum-moleculare
5. Capillary

Fig. 104 C.S. of the hippocampus through the superior fold (144 days).  
H&E. x 100



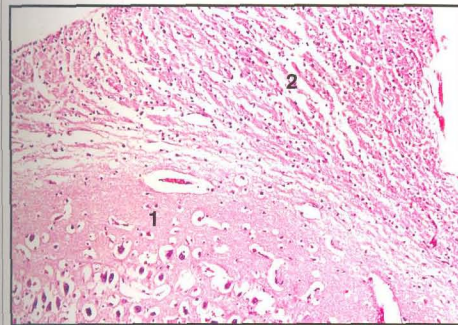
1. Ovoid cells of the granular layer
2. Nucleus showing two nucleoli
3. Dendrites

Fig. 105 C.S. of the hippocampus through the dentate gyrus (124 days).  
H&E. x 400



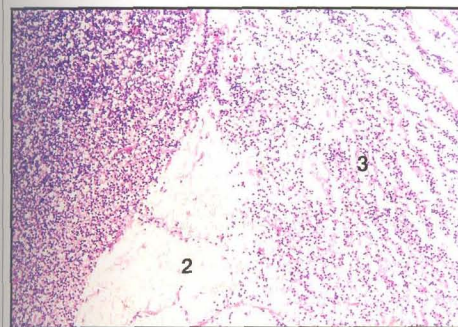
- 1. Lateral ventricle
- 2. Ependyma (pseudostratified)
- 3. Outer molecular layer
- 4. Granular layer
- 5. Polymorph layer

**Fig. 106 C.S. of the hippocampus through the dentate gyrus (124 days). H&E. x 100**



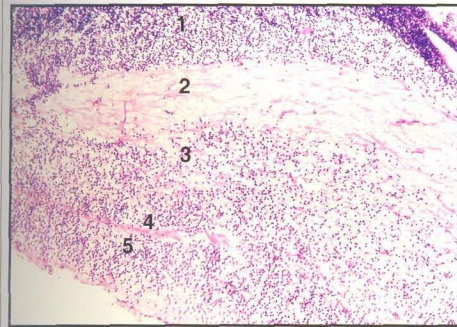
- 1. Hippocampus
- 2. Fimbria

**Fig. 107 C.S. of the hippocampus showing fimbria (144 days). H&E. x 100**



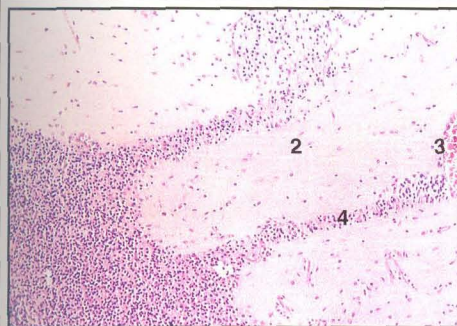
- 1. Caudate nucleus
- 2. Internal capsule
- 3. Lenticular nucleus

**Fig. 108 C.S. of the corpus striatum (58 days). H&E. x 100**



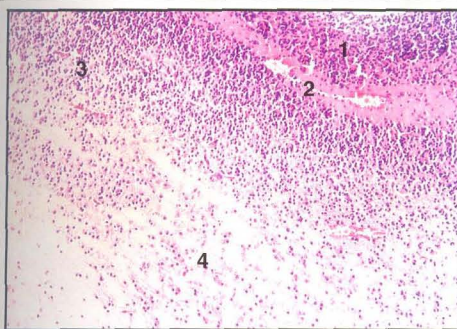
1. Caudate nucleus
2. Internal capsule
3. Lenticular nucleus
4. External capsule
5. Cerebral cortex

Fig. 109 C.S. of the basal nuclei (48 days). H&E. x 100



1. Caudate nucleus
2. Internal capsule
3. Blood vessel
4. Transverse cellular bands in internal capsule

Fig. 110 C.S. of the caudate nucleus and internal capsule (76 days). H&E. x 100



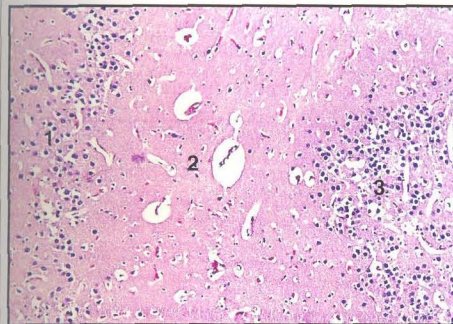
1. Insular cortex
2. External capsule
3. Putamen
4. Globus pallidus

Fig. 111 C.S. of the putamen, external capsule and insular cortex (62 days). H&E. x 100



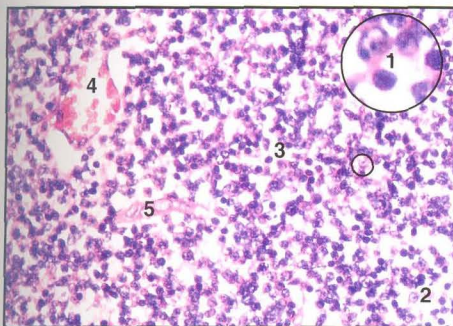
1. Internal capsule
2. Lenticular nucleus
3. External capsule
4. Blood vessel

Fig. 112 T.S. of the corpus striatum showing the junction between internal and external capsules (144 days). H&E. x 100



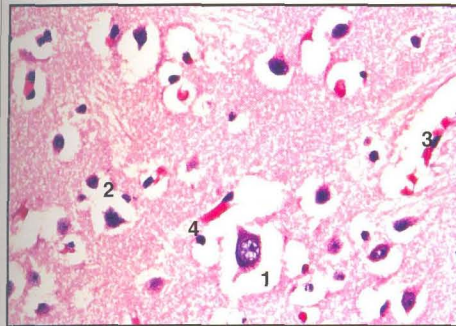
1. Claustrum
2. Extreme capsule
3. Amygdaloid body

Fig. 113 T.S. of the basal nuclei showing claustrum, extreme capsule and amygdaloid body (144 days). H&E. x 100



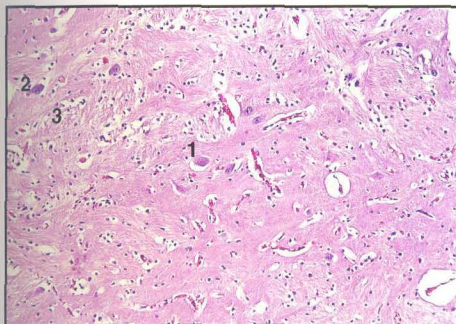
1. Large neuroblasts
2. Small neuroblasts
3. Spongioblasts
4. Blood vessel
5. Capillary endothelium

Fig. 114 C.S. of the caudate nucleus (58 days). H&E. x 400



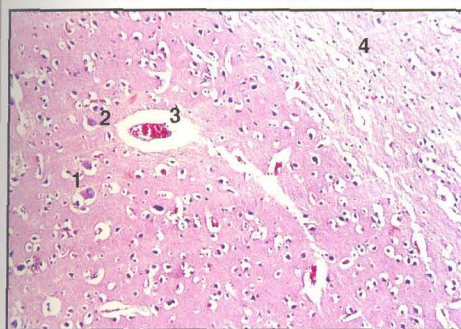
1. Large multipolar neurons
2. Small stellate neurons
3. Capillaries
4. Glial cells

**Fig. 115 C.S. of the Caudate nucleus (144 days). H&E. x 400**



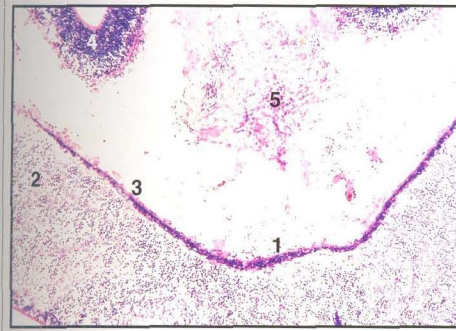
1. Large multipolar neurons
2. Spindle-shaped neurons
3. Nerve fibre bundles

**Fig. 116 C.S. of the globus pallidus (144 days) H&E. x 100**



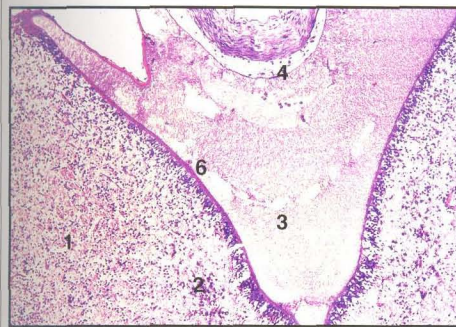
1. Mutipolar neurons
2. Small neurons
3. Blood vessel
4. External capsule

**Fig. 117 C.S. of the putamen (144 days). H&E. x 100**



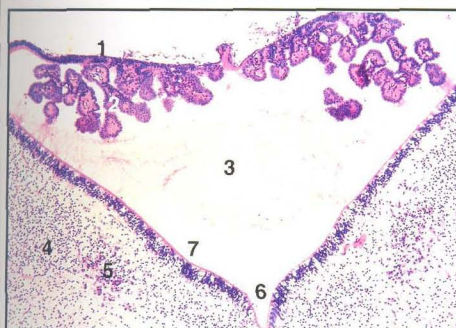
1. Vermis
2. Rhombic lip
3. External granular layer
4. Cerebral hemisphere
5. Falx cerebri

Fig. 118 C.S. of the cerebellum (48 days). H&E. x 100



1. Medulla oblongata
2. Nuclear aggregation
3. Fourth ventricle with CSF
4. Rostral medullary velum
5. Body wall
6. Internal glial limiting membrane

Fig. 119 C.S. of the medulla oblongata at the level of rostral medullary velum (48 days). H&E. x 100



1. Caudal medullary velum
2. Choroid plexus
3. Fourth ventricle
4. Medulla oblongata
5. Nuclear aggregation
6. Median sulcus
7. Sulcus limitans

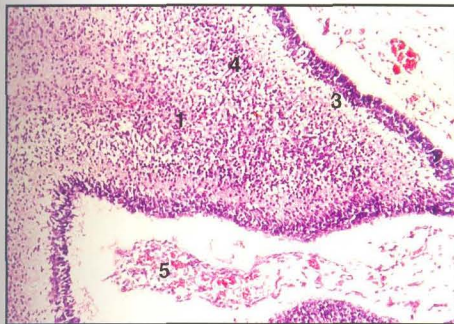
Fig. 120 C.S. of the medulla oblongata showing caudal medullary velum and the choroid plexus of the fourth ventricle (48 days). H&E. x 100





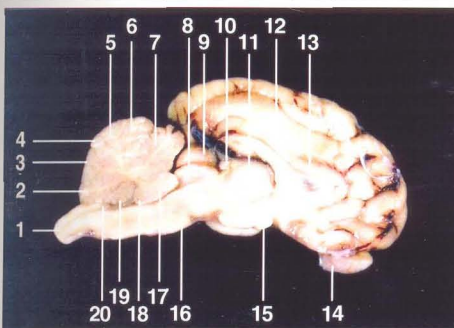
1. Vermis
2. Left cerebellar hemisphere
3. Pia mater
4. External granular layer
5. Molecular layer
6. Internal granular layer

**Fig. 121 C.S. of the cerebellum showing the vermis and lateral hemisphere (58 days). H&E. x 100**



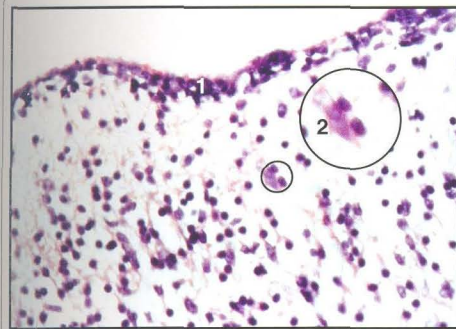
1. Folium
2. External granular layer
3. Outer molecular layer
4. Internal granular layer
5. Pia mater

**Fig. 122 T.S. of the cerebellar folium (62 days). H&E. x 100**



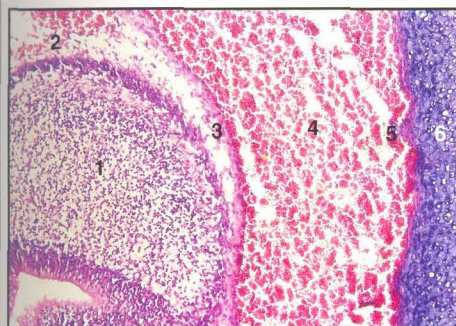
1. Medulla oblongata
2. Uvula
3. Pyramid
4. Tuber
5. Folium
6. Declive
7. Culmen
8. Aqueduct of Sylvius
9. Rostral colliculus
10. Pineal gland
11. Thalamus
12. Third ventricle
13. Septum pellucidum
14. Olfactory bulb
15. Optic chiasma
16. Pons
17. Central lobule
18. Lingula
19. Nodulus
20. Fourth ventricle

**Fig. 123 Midsagittal section of the brain (Full term foetus)**



1. External granular layer
2. Purkinje cells

Fig. 124 C.S. of the cerebellum showing external granular layer and primitive Purkinje cells (58 days). H&E. x 400



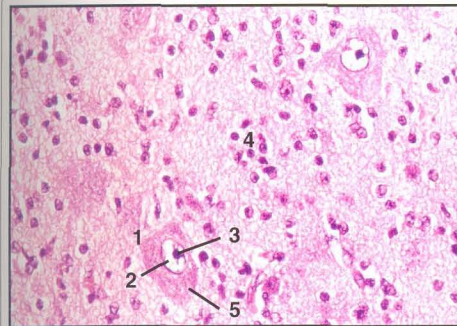
1. Cerebellum
2. Pia mater
3. Meningeal layer of dura
4. Venous sinus
5. Endosteal layer of dura
6. Bone

Fig. 125 L.S. of the metencephalon showing layers of dura mater (48 days). H&E. x 100



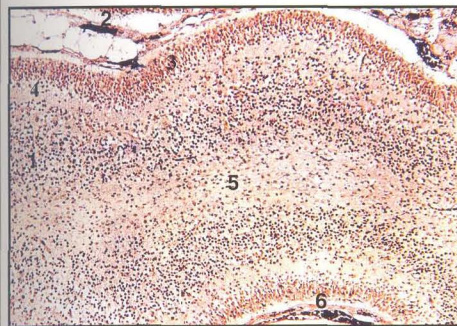
1. Cerebellum
2. Ependymal layer
3. Fourth ventricle
4. Choroid plexus

Fig. 126 C.S. of the cerebellum and fourth ventricle (48 days). H&E. x 100



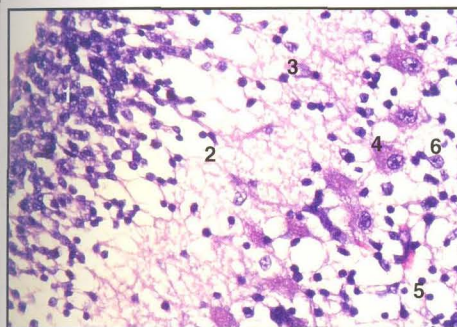
1. Neuronal cell body
2. Nucleus
3. Nucleolus
4. Glial cell nuclei
5. Neurofibrils

Fig. 127 Neurons of the deep cerebellar nucleus (76 days). H&E. x 400



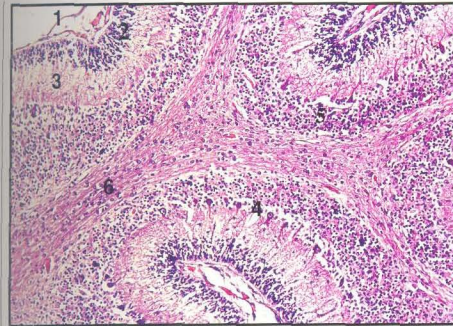
1. Inner granular layer
2. Pia mater
3. External granular layer
4. Outer molecular layer
5. White matter
6. Blood vessel

Fig. 128 L.S. of the cerebellar folium (101 days). Sevier-Munger silver impregnation method x 100



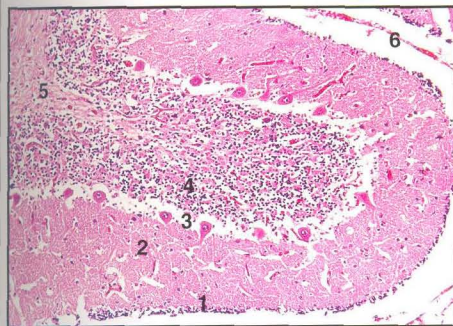
1. External granular layer
2. Outer molecular layer
3. Outer stellate cells
4. Purkinje cells
5. Inner granular layer
6. Golgi cells

Fig. 129 C.S. of the cerebellum showing layers of the cerebellar cortex (101 days). H&E. x 400



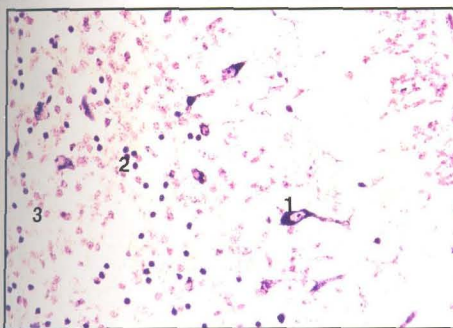
1. Pia mater
2. External granular layer
3. Outer molecular layer
4. Purkinje cell layer
5. Inner granular layer
6. Arbor vitae (white matter)

Fig. 130 Sagittal section of cerebellum (124 days). H&E. x 100



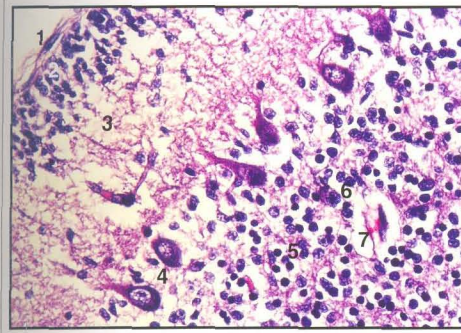
1. External granular layer
2. Outer molecular layer
3. Purkinje cell layer
4. Inner granular layer
5. White matter
6. Pia mater

Fig. 131 Section of the cerebellar folium (144 days). H&E. x 100



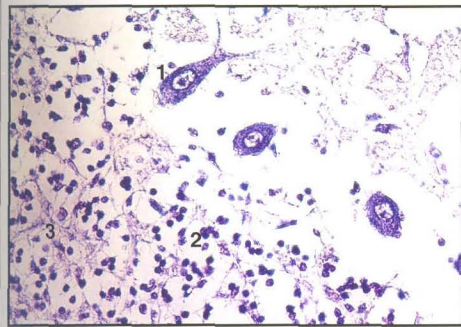
1. Purkinje cells with Nissl granules in the cytoplasm
2. Glial nuclei
3. Granule cells

Fig. 132 L.S. of the cerebellar folium (124 days). PTAH. X 400



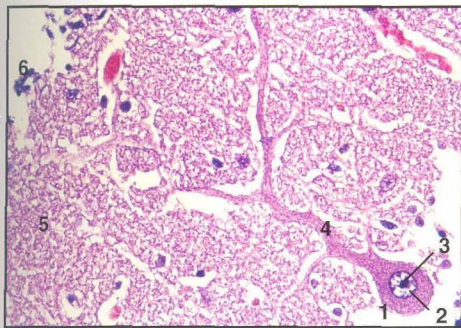
1. Pia mater
2. External granular layer
3. Outer molecular layer
4. Purkinje cell layer
5. Granule cells
6. Golgi cell
7. Blood vessel

Fig. 133 L.S. of the cerebellar folium (124 days). H&E. x 400



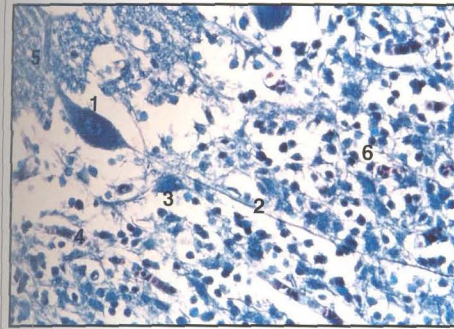
1. Purkinje cells with Nissl granules
2. Inner granular layer
3. Cerebellar glomeruli

Fig. 134 L.S. of the cerebellar folium (144 days). PTAH. X 400



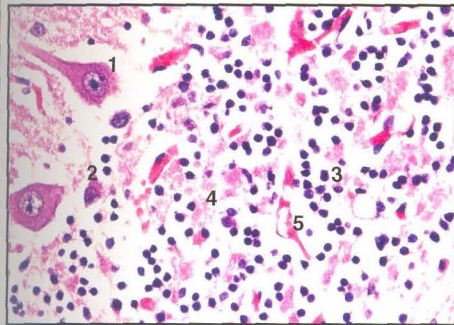
1. Purkinje cell body
2. Nucleus
3. Nucleolus
4. Dendritic tree
5. Outer molecular layer
6. External granular layer

Fig. 135 L.S. of the cerebellar folium (144 days). H&E. x 400



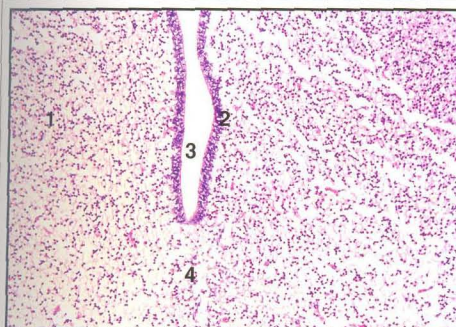
1. Purkinje cell
2. Axon of Purkinje cell
3. Golgi cell
4. Capillaries
5. Outer molecular layer
6. Inner granular layer

Fig. 136 Section of cerebellar folium (144 days). Holme's silver nitrate luxol fast blue method x 400



1. Purkinje cell
2. Golgi cell
3. Granule cell
4. Cerebellar glomeruli
5. Blood capillaries

Fig. 137 Section of cerebellar folium (144 days). H&E. x 400



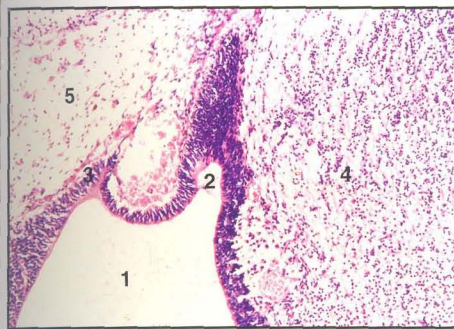
1. Thalamus
2. Ependymal layer
3. Slit-like third ventricle
4. Massa intermedia

Fig. 138 C.S. of the thalamus showing third ventricle and massa intermedia (48 days). H&E. x 100



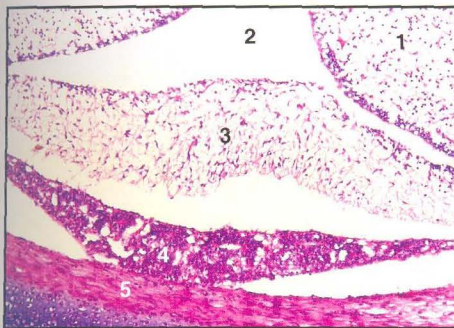
- 1. Pia mater
- 2. Venous sinus
- 3. Roof plate
- 4. Choroid plexus
- 5. Third ventricle

Fig. 139 C.S. through the dorsal portion of third ventricle showing choroid plexus (58 days). H&E. x 100



- 1. Third ventricle
- 2. Pineal evagination
- 3. Habenulae
- 4. Rostral colliculus
- 5. Pia mater

Fig. 140 L.S. of the diencephalon and mesencephalon showing pineal evagination (48 days). H&E. x 100



- 1. Hypothalamus
- 2. Third ventricle
- 3. Floor of hypothalamus
- 4. Pars distalis of pituitary
- 5. Dura mater (diaphragma selle)

Fig. 141 C.S. of the hypothalamus showing trough-like floor (58 days). H&E. x 100



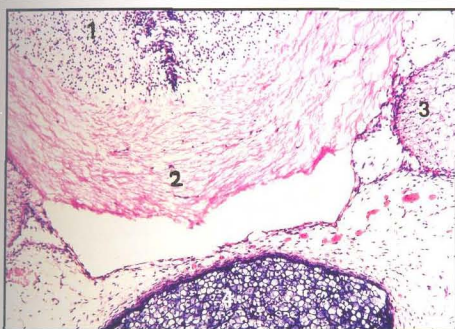
1. Hypothalamus
2. Infundibulum
3. Pars nervosa
4. Pars intermedia
5. Residual lumen
6. Pars distalis
7. Sella turcica of basisphenoid
8. Infundibular recess

Fig. 142 C.S. of the hypothalamus and pituitary (48 days). H&E. x 100



1. Infundibulum
2. Pars nervosa
3. Pars intermedia
4. Residual lumen
5. Pars distalis
6. Infundibular recess
7. Basisphenoid

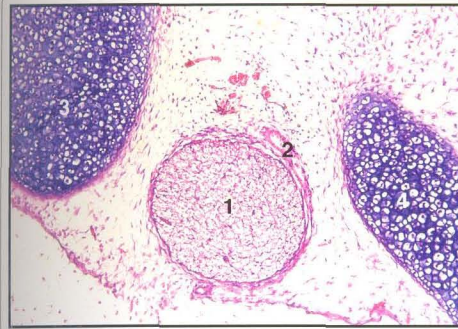
Fig. 143 L.S. of the hypothalamus and pituitary (48 days). H&E. x 100



1. Hypothalamus
2. Optic chiasma
3. Optic nerve
4. Presphenoid

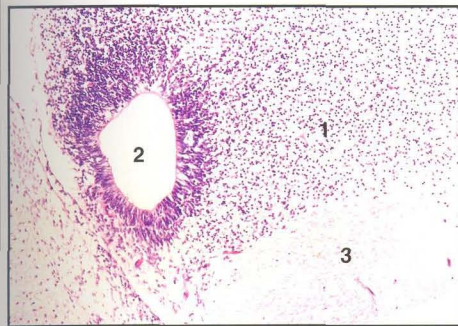
Fig. 144 C.S. of the hypothalamus showing optic chiasma and optic nerve (48 days). H&E. x 100





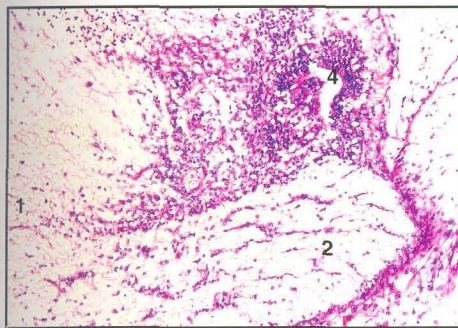
1. Optic nerve
2. Pia mater surrounding the optic nerve
3. Body of presphenoid
4. Wing of presphenoid

Fig. 145 C.S. of the optic nerve emerging through the optic foramen (48 days). H&E. x 100



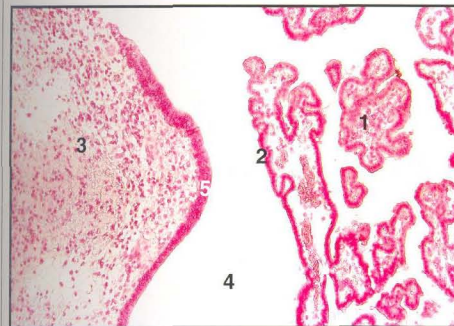
1. Hypothalamus
2. Optic recess of third ventricle
3. Optic chiasma
4. Ependymal layer

Fig.146 Section of hypothalamus showing optic recess of third ventricle (48 days). H&E. x 100



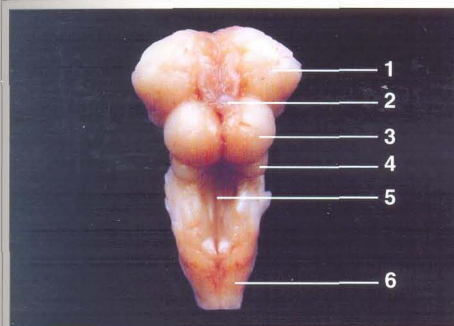
1. Optic chiasma
2. Optic nerve
3. Supraoptic nucleus
4. Optic recess of third ventricle

Fig. 147 C.S. of optic chiasma and supraoptic nucleus (58 days). H&E. x 100



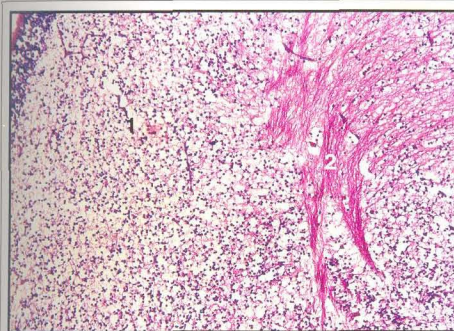
1. Choroid plexus
2. Choroid epithelium
3. Thalamus
4. Third ventricle
5. Ependymal layer

Fig. 148 Choroid plexus of the fourth ventricle (80 days). Best's carmine x 100



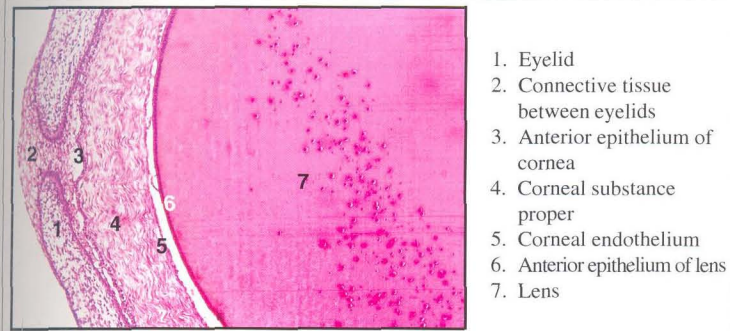
1. Thalamus
2. Pineal gland
3. Rostral colliculus
4. Caudal colliculus
5. Fourth ventricle
6. Medulla oblongata

Fig. 149 Dorsal view of the brainstem (124 days)



1. Thalamus
2. Internal capsule
3. Ependymal cells

Fig. 150 L.S. of thalamus showing internal capsule (48 days). H&E. x 100



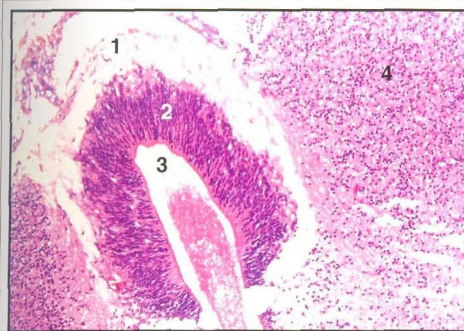
1. Eyelid
2. Connective tissue between eyelids
3. Anterior epithelium of cornea
4. Corneal substance proper
5. Corneal endothelium
6. Anterior epithelium of lens
7. Lens

**Fig. 151 Section of the eye ball (48 days). H&E. x 100**



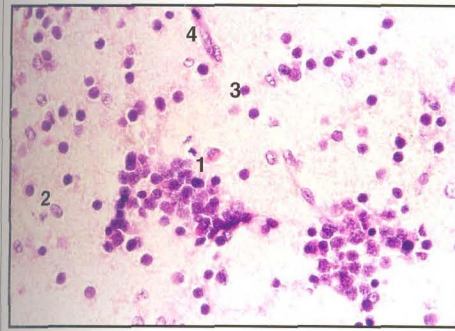
1. Cornea
2. Anterior epithelium of cornea
3. Corneal epithelium proper
4. Sclera
5. Retina
6. Lens

**Fig. 152 Section of eye ball showing cornea, sclera, lens and retina (48 days). H&E. x 100**



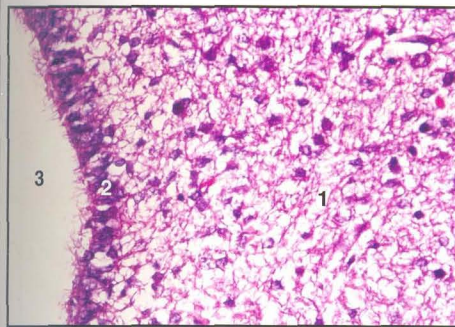
1. Posterior commissure
2. Subcommissural organ
3. Aqueduct of Sylvius
4. Mesencephalon

**Fig. 153 C.S. of the subcommissural organ lined by tanyocytes (58 days). H&E. x 100**



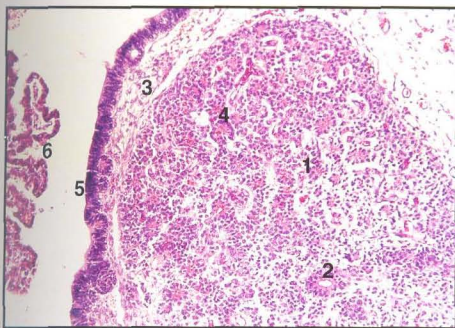
1. Nuclei of neuroblasts
2. Astrocyte nucleus
3. Oligodendrocyte
4. Capillary endothelium

Fig. 154 Neuronal aggregations in the thalamus (62 days). H&E. x 100



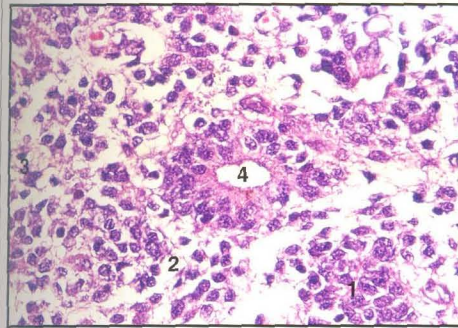
1. Thalamus
2. Ciliated ependyma
3. Third ventricle

Fig. 155 C.S. of the thalamus showing ciliated ependymal cells lining the third ventricle (76 days). H&E. x 400



1. Pineal gland
2. Central lumen
3. Capsule
4. Cell cords
5. Third ventricle and lining ependyma
6. Choroid plexus of third ventricle

Fig. 156 C.S. of the pineal gland (76 days). H&E. x 100



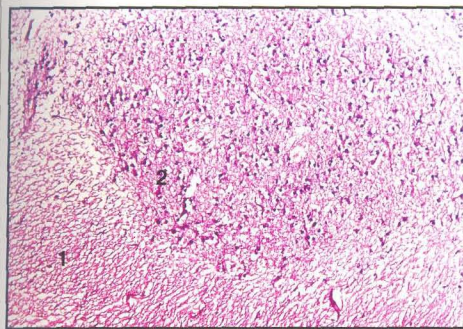
- 1. Cords of cells
- 2. Pinealocytes
- 3. Glial cells
- 4. Central lumen

**Fig. 157 C.S.of the pineal gland showing pinealocytes and glial cells (76 days).  
H&E. x 400**



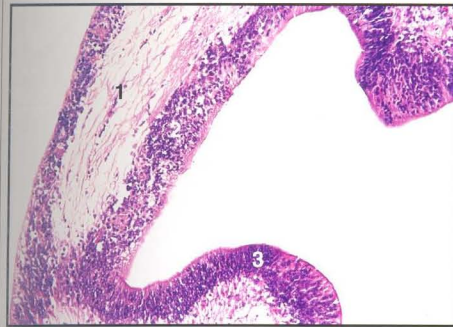
- 1. Hypothalamus
- 2. Third ventricle
- 3. Ependymal layer
- 4. Floor of hypothalamus

**Fig. 158 C.S.of the hypothalamus showing the trough-like floor (81 days).  
H&E. x 100**



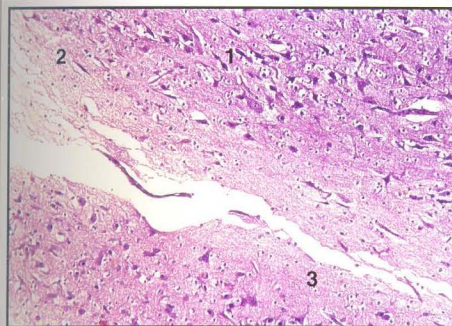
- 1. Optic tract
- 2. Supraoptic nucleus

**Fig. 159 C.S.of the hypothalamus showing optic tract and supraoptic nucleus  
(81 days). H&E. 100**



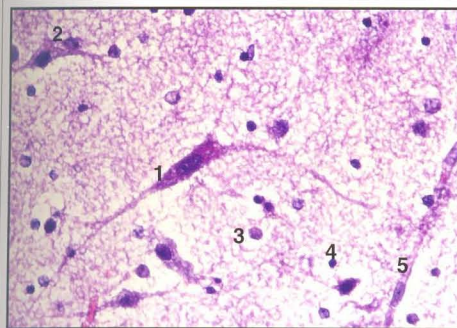
1. Posterior commissure
2. Subcommissural organ
3. Tanycytes

**Fig. 160 C.S. of the posterior commissure showing subcommissural organ (76 days). H&E. x 100**



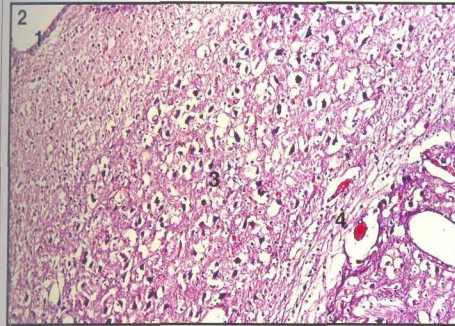
1. Neurons
2. Dorsal part
3. Ventral part

**Fig. 161 C.S. of the diencephalon showing two parts of supraoptic nucleus (101 days). H&E. x 100**



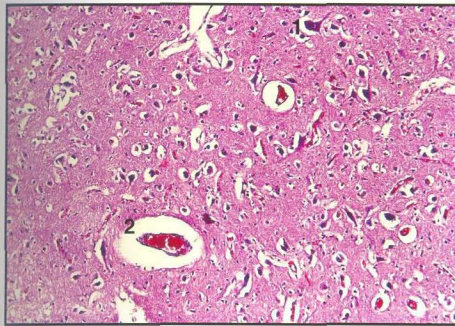
1. Spindle-shaped neuron
2. Bipolar neuron
3. Astrocyte nucleus
4. Oligodendrocyte
5. Capillary endothelium

**Fig. 162 C.S. of the supraoptic nucleus of hypothalamus (101 days). H&E. x 400**



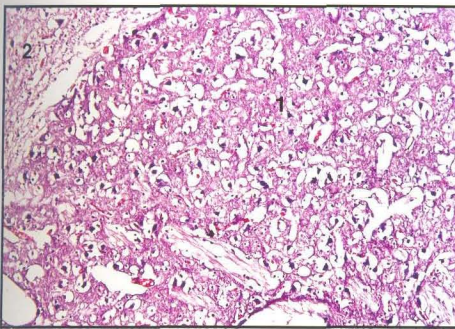
- 1. Third ventricle
- 2. Ependyma
- 3. Anterior nucleus
- 4. Internal medullary lamina

**Fig. 163 C.S.of the thalamus showing anterior nucleus (144 days). H&E. x 100**



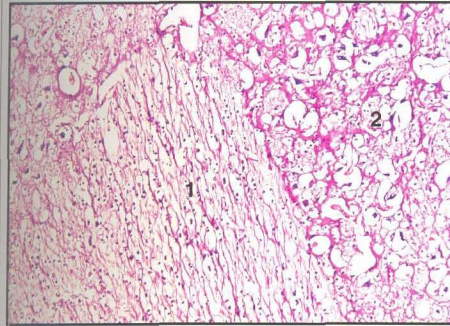
- 1. Large multipolar neurons
- 2. Blood vessel

**Fig. 164 C.S.of the thalamus showing dorsomedial nucleus (144 days). H&E. x 100**



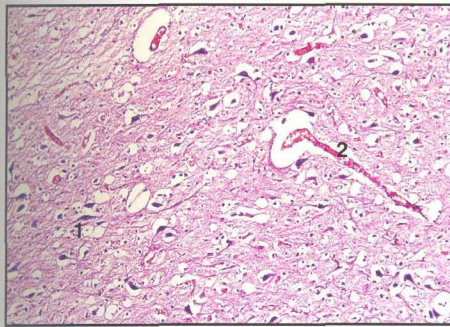
- 1. Reticular nucleus
- 2. External medullary lamina

**Fig. 165 C.S.of the thalamus showing reticular nucleus (144 days). H&E. x 100**



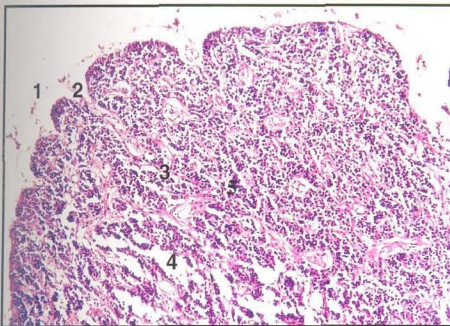
- 1. Mamillothalamic tract
- 2. Gray matter

**Fig. 166 C.S.of the hypothalamus showing mamillothalamic tract (144 days). x 100**



- 1. Bipolar neurons
- 2. Blood vessels

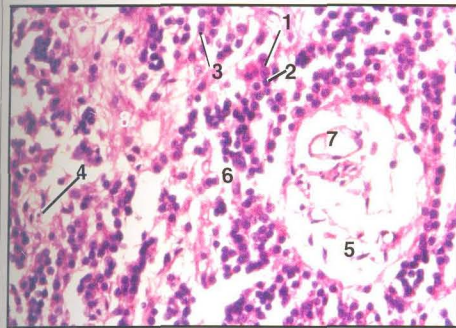
**Fig. 167 C.S.of the hypothalamic nucleus showing supraoptic nucleus (144 days). H&E. x 100**



- 1. Capsule
- 2. Connective tissue septum
- 3. Cortex
- 4. Medulla
- 5. Cell cords

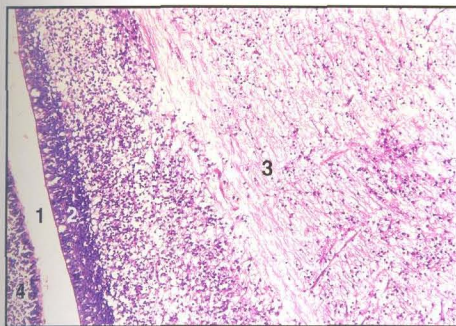
**Fig. 168 C.S.of the pineal gland (144 days). H&E. x 100**





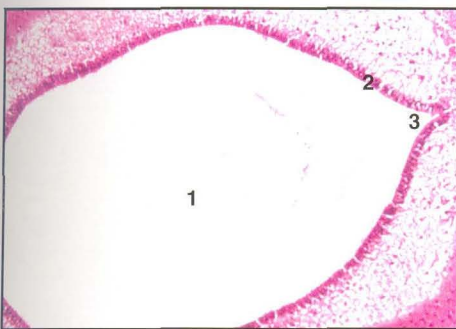
1. Light pinealocytes
2. Dark pinealocytes
3. Type I glial cell
4. Type II glial cell
5. Type III glial cell
6. Type IV glial cell
7. Blood vessel
8. Nerve fibres

**Fig. 169 C.S.of the pineal gland (144 days). x 400**



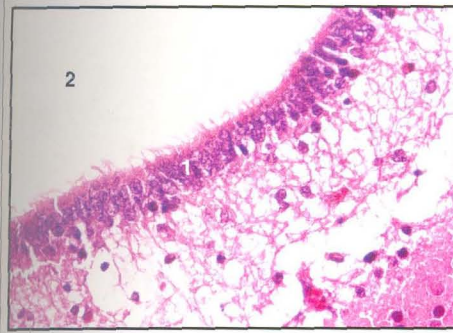
1. Aqueduct of Sylvius
2. Ependymal layer
3. Tegmentum (reticular formation)
4. Basal plate ependyma

**Fig. 170 L.S.of the mesencephalon (48 days). H&E. x 100**



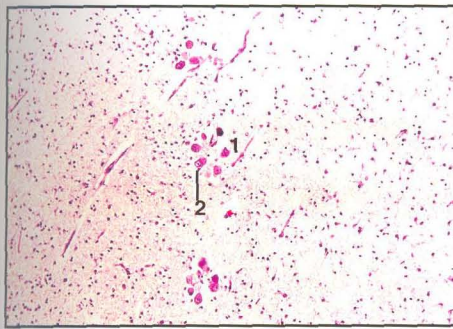
1. Aqueduct
2. Ependymal layer
3. Median fissure

**Fig. 171 C.S.of the aqueduct of Sylvius (76 days). H&E. x 100**



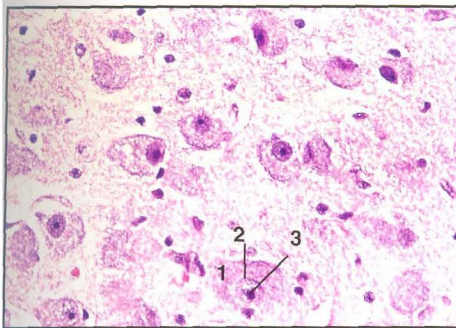
- 1. Ependymal cells with cilia
- 2. Aqueduct of Sylvius

Fig. 172 C.S.of the aqueduct showing pseudostratified ciliated ependymal cells (76 days). H&E. x 400



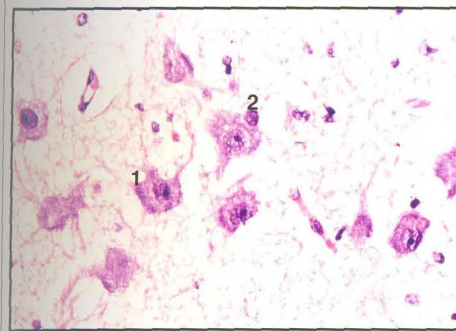
- 1. Unipolar neurons
- 2. Eccentric nucleus

Fig. 173 C.S.of the mesencephalon showing mesencephalic nuclei of trigeminal nerve (81 days). H&E. x 100



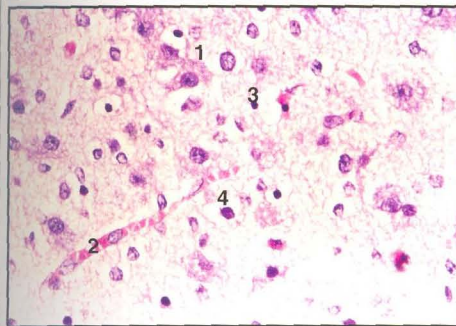
- 1. Neurons
- 2. Vesicular nucleus
- 3. Neuroglia

Fig. 174 C.S.of the red nucleus (76 days). H&E. x 400



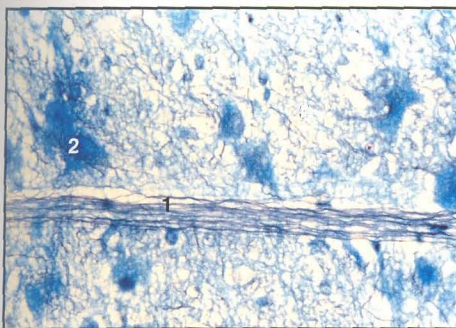
- 1. Multipolar neurons
- 2. Perineuronal satellite

**Fig.175 C.S.of the red nucleus showing magnocellular part (81 days).  
H&E. x 400**



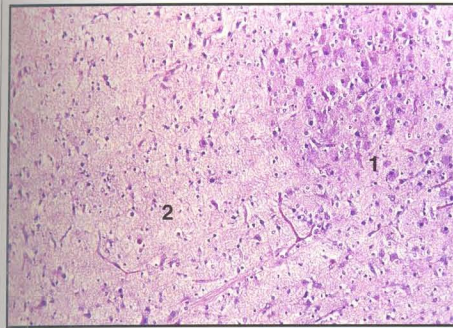
- 1. Neurons
- 2. Capillary
- 3. Oligodendrocyte
- 4. Protoplasmic astrocyte

**Fig. 176 C.S.of the red nucleus showing parvocellular part (81 days).  
H&E. x 400**



- 1. Oculomotor nerve bundle
- 2. Neurons

**Fig. 177 C.S.of the red nucleus showing the oculomotor nerve traversing through it (81 days). Holme's silver nitrate luxol fast blue method x 400**



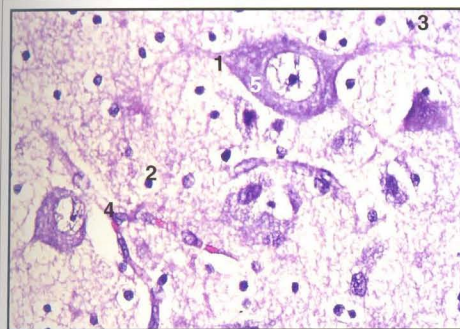
- 1. Substantia nigra
- 2. Crura cerebri

**Fig. 178 C.S.of the crura cerebri showing the substantia nigra (81 days).  
H&E. x 100**



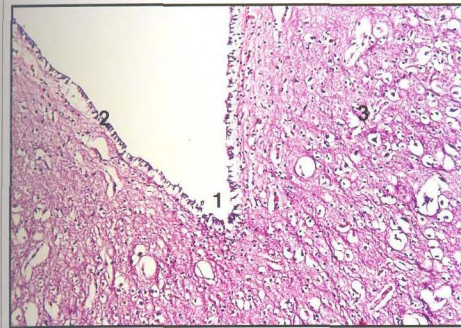
- 1. Unipolar neurons
- 2. Eccentric nucleus
- 3. Oligodendrocyte
- 4. Axons
- 5. Astrocyte
- 6. Capillary

**Fig. 179 C.S.of the tegmentum of mesencephalon showing mesencephalic nucleus of trigeminal nerve (101 days). H&E. x 400**



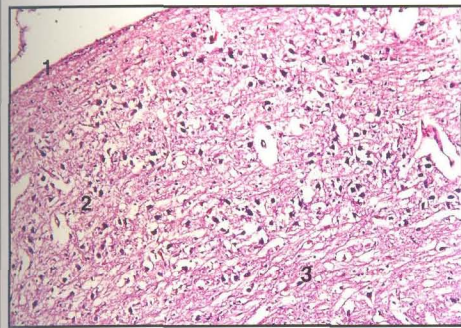
- 1. Multipolar neuron
- 2. Oligodendrocyte
- 3. Microglia
- 4. Capillaries
- 5. Neurofibrils

**Fig. 180 C.S.of the red nucleus showing large multipolar neurons (101 days).  
H&E. x 400**



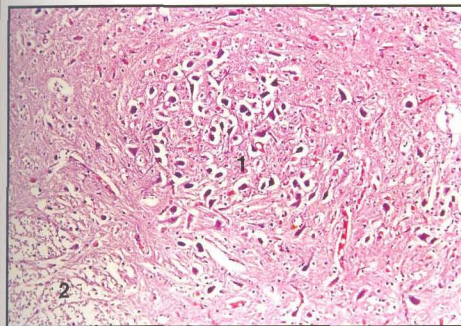
1. Lateral angle of aqueduct
2. Ependymal lining
3. Periaqueductal gray matter

**Fig. 181 C.S. of the mesencephalon (144 days). H&E. x 100**



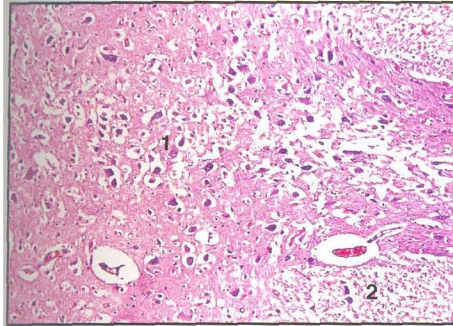
1. Stratum zonale
2. Stratum cinerium
3. Stratum opticum

**Fig. 182 C.S. of the rostral colliculus (144 days). H&E. x 100**



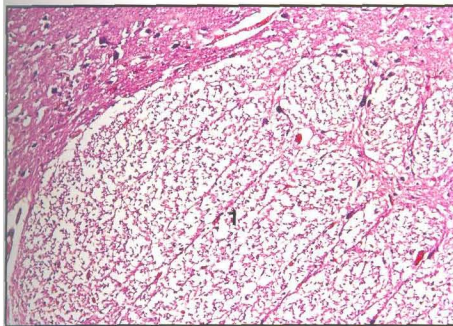
1. Red nucleus
2. Fibre bundle

**Fig. 183 C.S. of the mesencephalic tegmentum showing red nucleus (144 days). H&E. x 100**



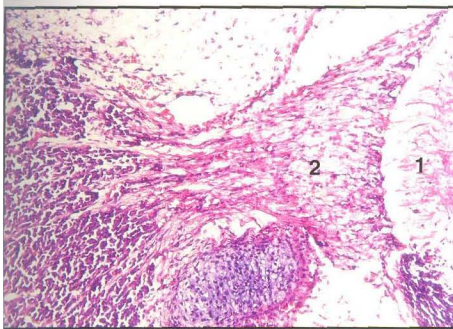
- 1. Interpeduncular nucleus
- 2. Corticospinal tract

**Fig. 184 C.S.of the mesencephalic tegmentum showing interpeduncular nucleus (144 days) x 100**



- 1. Corticospinal tract

**Fig. 185 C.S.of the mesencephalon showing corticospinal tract (144 days). H&E. x 100**



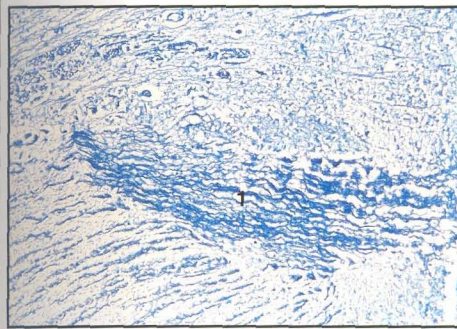
- 1. Pons
- 2. Trigeminal nerve
- 3. Semilunar ganglion

**Fig. 186 L.S.of the pons showing the emergence of trigeminal nerve and semilunar ganglion (48 days). H&E. x 100**



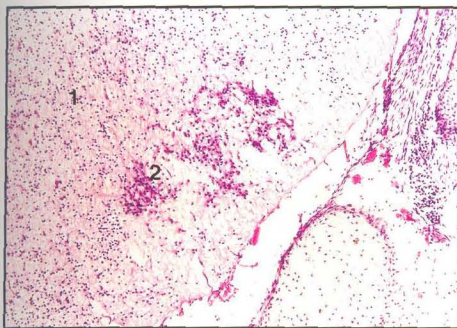
1. Fourth ventricle
2. Pons
3. Sulcus limitans
4. Ependymal layer

Fig. 187 C.S.of the pons showing the sulcus limitans (76 days). H&E. x 100



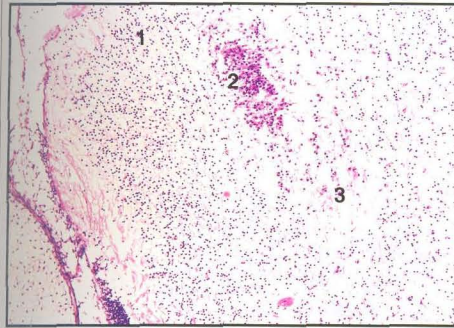
1. Nerve fibre bundle

Fig. 188 C.S.of the pons showing trigeminal nerve fibres emerging from the lateral aspect (81 days). Holme's silver nitrate luxol fast blue method x 100



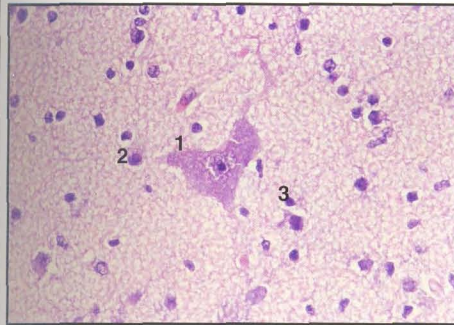
1. Pons
2. Pontine nuclei

Fig. 189 C.S.of the pons showing pontine nuclei (48 days). H&E. x 100



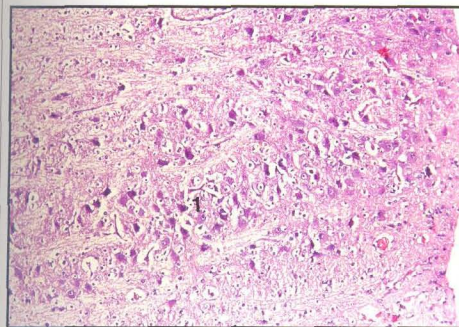
- 1. Alar plate of pons
- 2. Pontine nuclei in alar plate
- 3. Migrating neurons

**Fig. 190 C.S.of the pons showing migrating alar plate neurons (48 days). H&E. x 100**



- 1. Multipolar neuron
- 2. Protoplasmic astrocyte
- 3. Oligodendroglia

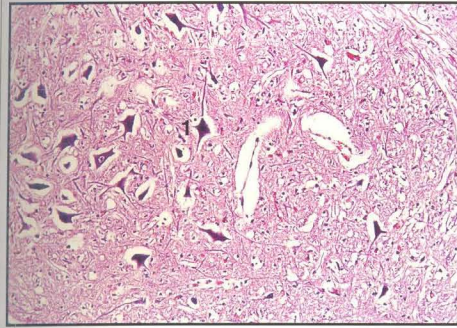
**Fig. 191 C.S.of the pons showing a multipolar motor neuron of trigeminal nerve (76 days). H&E. x 400**



- 1. Pontine nuclei

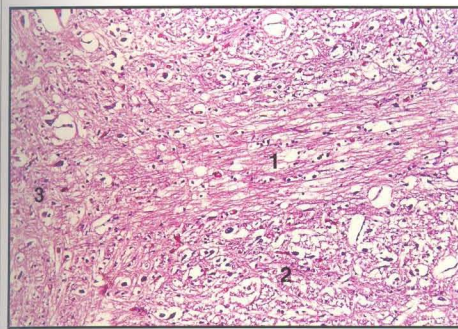
**Fig. 192 C.S.of the ventral portion of the pons showing the pontine nuclei (81 days). H&E. x 100**





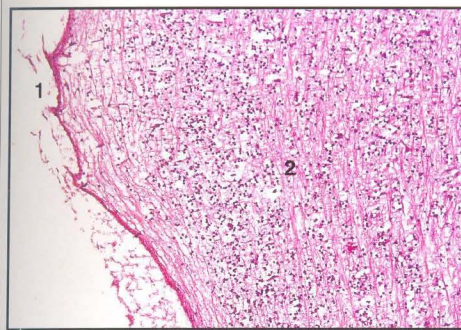
- 1. Neurons of the pontine nuclei

**Fig. 193 C.S.of the pons showing pontine nuclei (144 days). H&E. x 100**



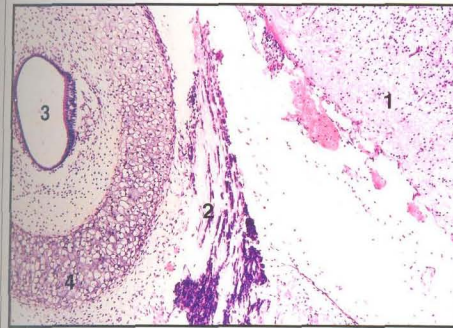
- 1. Median raphe
- 2. Medial lemniscus
- 3. Trapezoid body

**Fig. 194 C.S.of the pons showing median raphe (144 days). H&E. x 100**



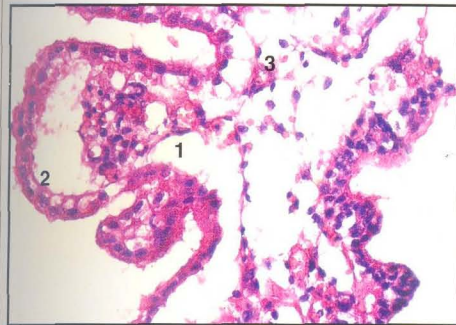
- 1. Trapezoid body
- 2. Medullary reticular formation

**Fig. 195 C.S.of the medulla oblongata showing trapezoid body and reticular formation (48 days). H&E. x 100**



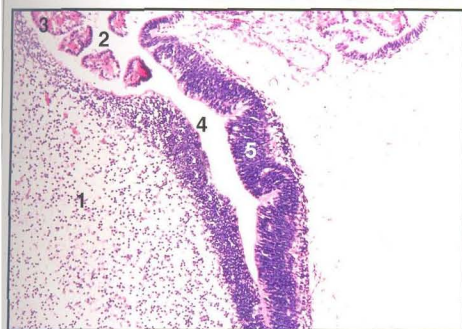
- 1. Medulla oblongata
- 2. Facial nerve
- 3. Endolymph duct
- 4. Petrous temporal bone

Fig. 196 C.S.of the medulla oblongata showing the facial nerve and endolymph duct (48 days). H&E. x 100



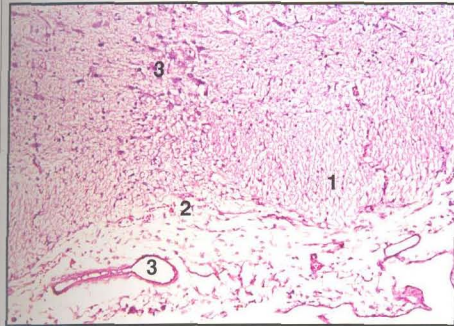
- 1. Primary fold of the plexus
- 2. Choroid epithelium
- 3. Connective tissue of pia mater

Fig. 197 Choroid plexus of the fourth ventricle (40 days). H&E. x 400



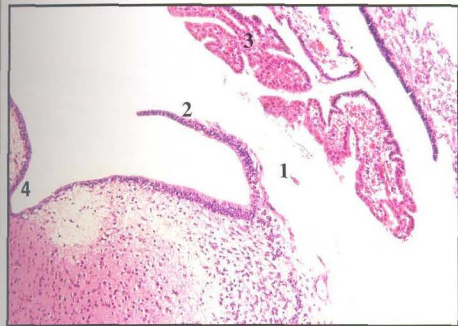
- 1. Medulla oblongata
- 2. Fourth ventricle
- 3. Choroid plexus
- 4. Central canal of spinal cord
- 5. Circumventricular organ

Fig. 198 L.S.of the medulla oblongata showing the fourth ventricle and circumventricular organ (48 days). H&E. x 100



- 1. Medullary pyramid
- 2. Ventral median fissure
- 3. Basilar artery
- 4. Median raphe

Fig. 199 C.S.of the medulla oblongata showing medullary pyramids (81 days). H&E. x 100



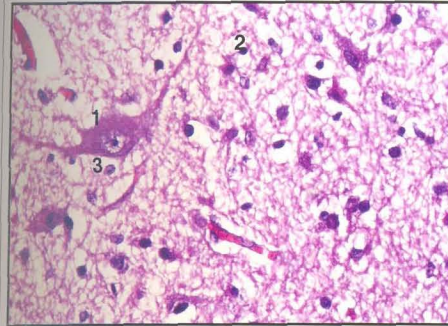
- 1. Foramen of Lushcka
- 2. Caudal medullary velum
- 3. Choroid plexus
- 4. Sulcus limitans

Fig. 200 C.S.of the medulla oblongata showing foramen of Lushcka and caudal medullary velum (76 days). H&E. x 100



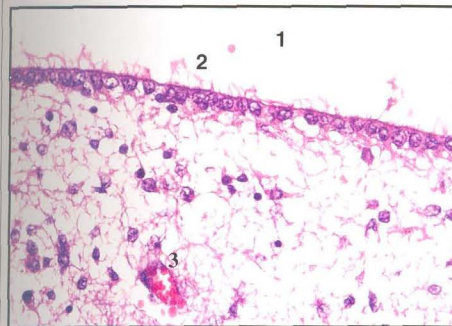
- 1. Central canal
- 2. Ventral median raphe

Fig. 201 C.S.of the caudal part of medulla oblongata (76 days). H&E. x 100



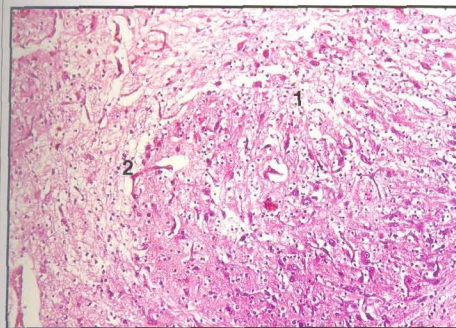
1. Multipolar neuron
2. Oligodendrocyte
3. Protoplasmic astrocyte

Fig. 202 C.S. of the reticular formation of medulla oblongata showing a large neuron of nucleus reticularis gigantocellularis (81 days). H&E. x 400



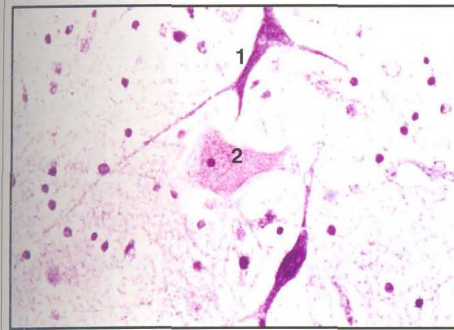
1. Fourth ventricle
2. Co-arctation of cilia
3. Blood vessel

Fig. 203 C.S. of the medulla oblongata showing single layered ependyma (101 days). H&E. x 400



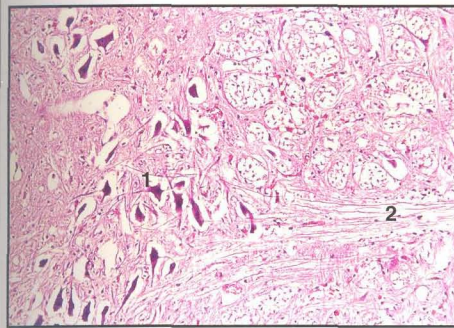
1. Chief olivary nucleus
2. Capsule

Fig. 204 C.S. of the medulla oblongata showing chief olivary nucleus (101 days). H&E. x 100



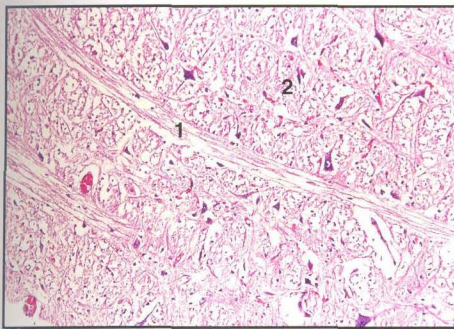
- 1. Neuron with Nissl granules
- 2. Neuron without Nissl granules

**Fig. 205 C.S.of the mesencephalon (101 days). PTAH. x 400**



- 1. Vagal nucleus
- 2. Vagal nerve fibres

**Fig. 206 C.S.of the medulla oblongata showing vagal nucleus and vagus nerve (144 days). H&E. x 100**



- 1. Hypoglossal nerve
- 2. Medial lemniscus

**Fig. 207 C.S.of the medulla oblongata showing hypoglossal nerve (144 days).**

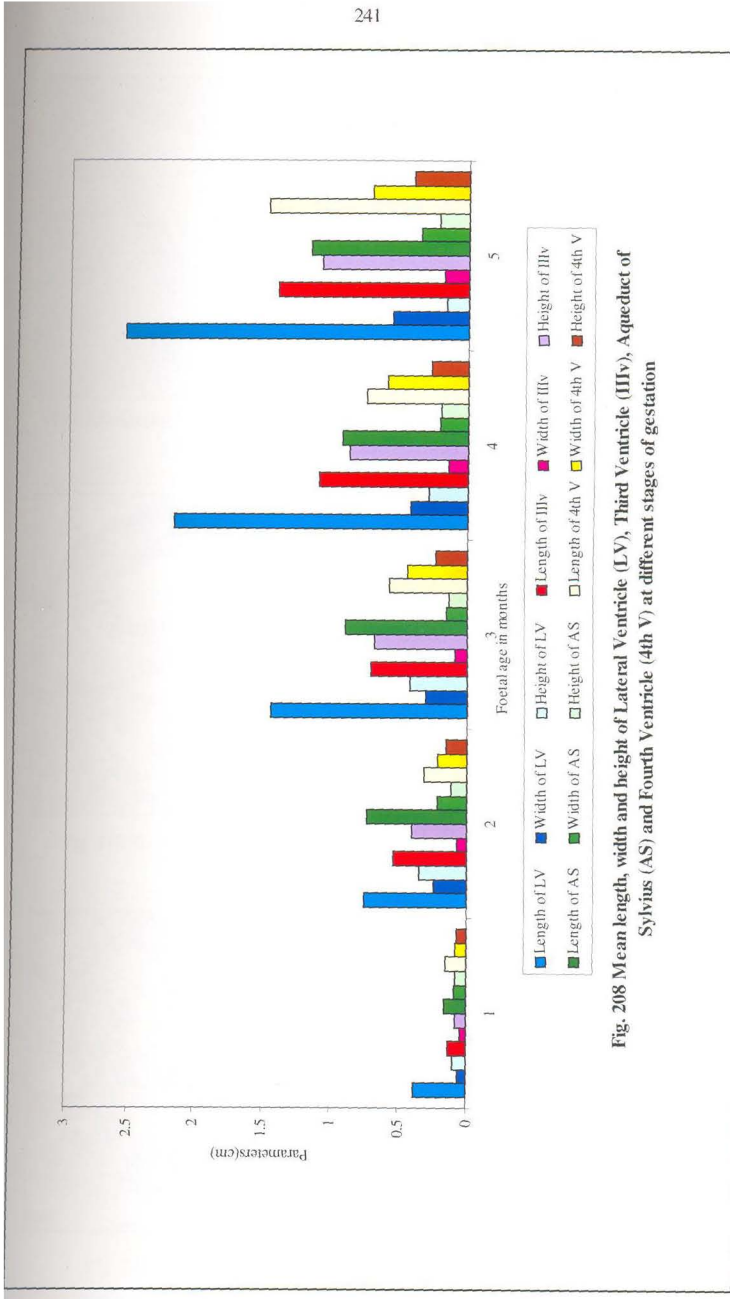
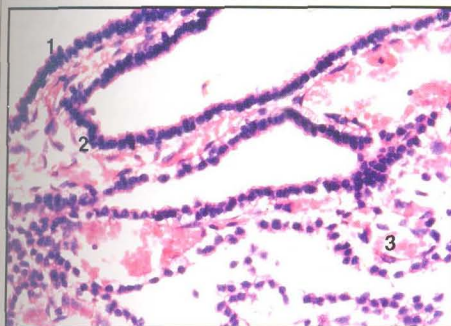


Fig. 208 Mean length, width and height of Lateral Ventricle (LV), Third Ventricle (IIIv), Aqueduct of Sylvius (AS) and Fourth Ventricle (4th V) at different stages of gestation



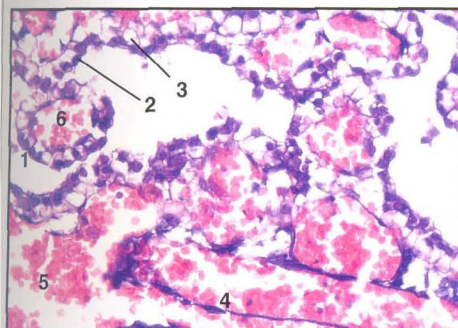
1. Choroid plexus
2. Caudate nucleus
3. Hippocampus
4. Velum interpositum
5. Pia mater
6. Thalamus
7. Lateral ventricle

Fig. 209 Section of the brain showing choroid fissure and the stalk of choroid plexus of lateral ventricle (48 days). H&E. x 100



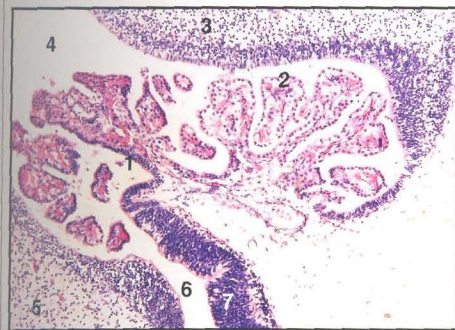
1. Choroid epithelium
2. Pial membrane
3. RBC and loose mesenchyme

Fig. 210 Stalk portion of the choroid plexus of lateral ventricle (48 days). H&E. x 400



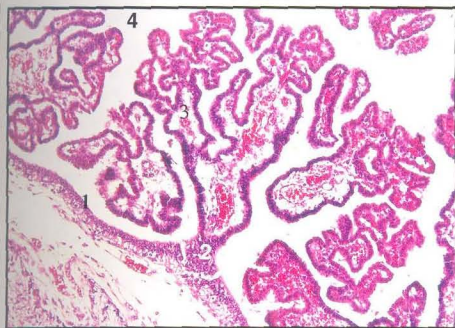
1. Choroid epithelium
2. Nucleus
3. Vacuolated cytoplasm
4. Fenestrated capillary endothelium
5. Erythrocytes
6. Tubule

Fig. 211 Choroid plexus of lateral ventricle (48 days). H&E. x 400



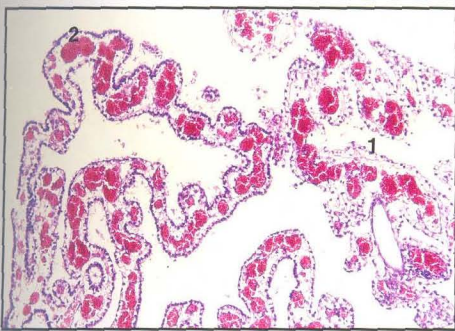
1. Stalk of the plexus
2. Simple columnar epithelium with vacuolated cytoplasm
3. Cerebellum
4. Fourth ventricle
5. Medulla oblongata
6. Central canal of spinal cord
7. Circumventricular organ

Fig. 212 T.S.of the brainstem through the fourth ventricle (48 days). H&E. x 100



1. Caudal medullary velum
2. Stalk of choroid plexus
3. Secondary and tertiary folds
4. Fourth ventricle

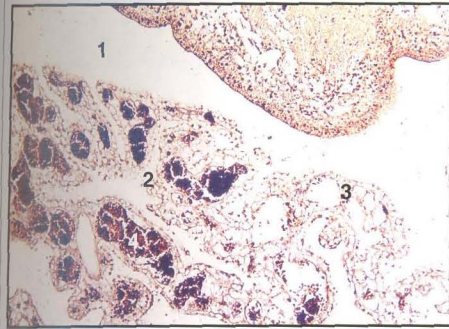
Fig. 213 T.S.of the brainstem through the fourth ventricle (76 days). H&E. x 100



1. Choroid epithelium showing vacuolated cytoplasm
2. Erythrocyte aggregations

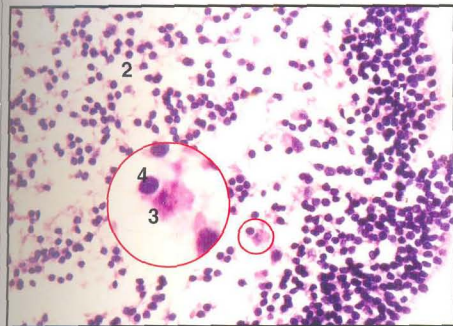
Fig. 214 Choroid plexus of the lateral ventricle (76 days). H&E. x 100





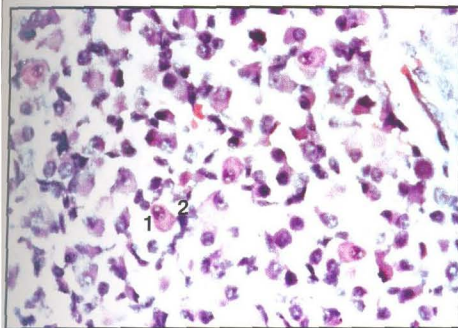
- 1. Lateral ventricle
- 2. Choroid plexus
- 3. Choroid epithelium
- 4. Cluster of RBCs

**Fig. 215** Choroid plexus of the lateral ventricle (80 days). Sevier-Munger silver impregnation method x 100



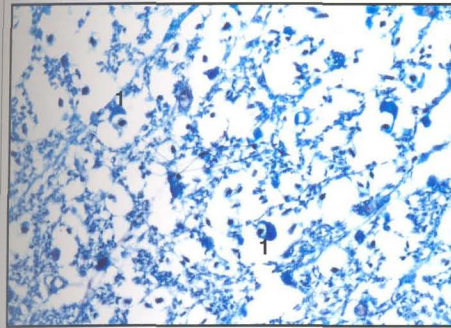
- 1. Ependymal layer
- 2. Mantle layer
- 3. Primitive multipolar neurons
- 4. Spongioblasts

**Fig. 216** Section of the medulla oblongata (40 days). H&E. x 400



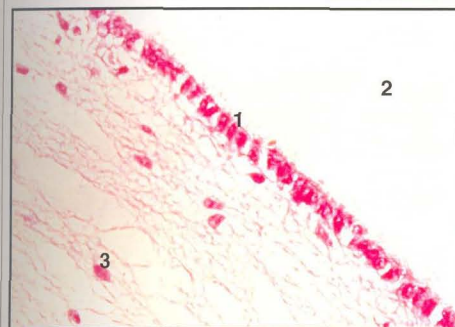
- 1. Unipolar neurons
- 2. Satellite cell

**Fig. 217** Section of the semilunar ganglion (76 days). H&E. x 400



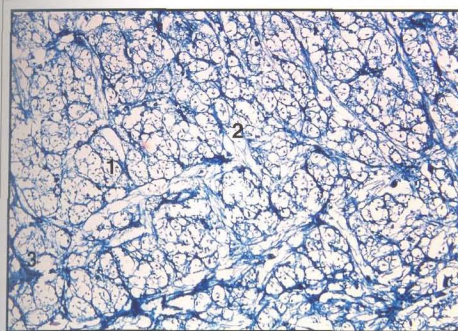
1. Axon surrounded by oligodendroglia

**Fig. 218 C.S. of the mesencephalon showing corticospinal tract (144 days).  
Holme's silver nitrate luxol fast blue method x 400**



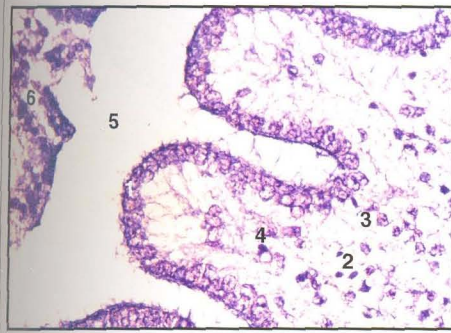
1. Ependyma with cilia
2. Lateral ventricle
3. Astrocyte

**Fig. 219 Ependymal lining of lateral ventricle (124 days).  
Best's carmine method x 400**



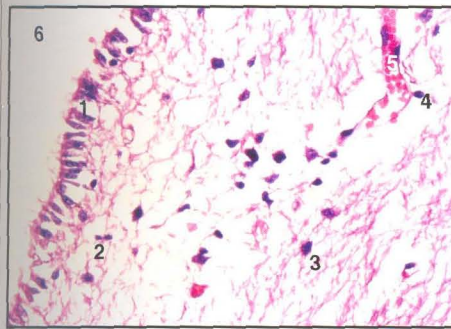
1. Astrocyte
2. C.S. of axon
3. Neuron

**Fig. 220 C.S. of the medullary reticular formation (144 days).  
Holme's silver nitrate luxol fast blue method x 100**



1. Ependyma
2. Microglia
3. Astrocytes
4. Oligodendrocytes
5. Fourth ventricle
6. Choroid plexus

Fig. 221 L.S. of cerebellum showing glial cells (101 days). PTAH. x 400



1. Ependyma
2. Microglia
3. Astrocytes
4. Oligodendrocytes
5. Capillary
6. Lateral ventricle

Fig. 222 Section of the cerebrum showing glial cells in the subependymal region (144 days). H&E. x 400



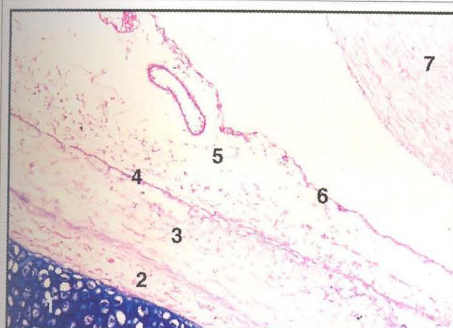
1. Dura mater
2. Subdural space
3. Subarachnoid space
4. Blood vessel
5. Pia mater
6. Cerebrum

Fig. 223 Section through the meninges (58 days). H&E. x 100



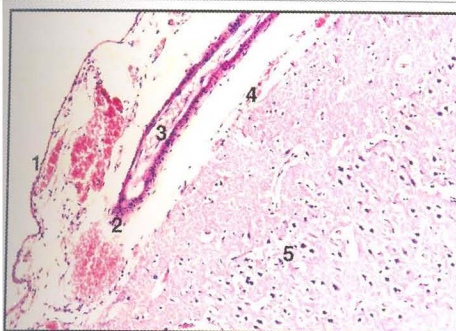
- 1. Cartilaginous cranial vault
- 2. Endosteal layer of dura
- 3. Meningeal layer of dura
- 4. Great petrosal sinus
- 5. Subarachnoid space

**Fig. 224 C.S. of the cranial vault showing venous sinus of the cranial dura (58 days). H&E. x 100**



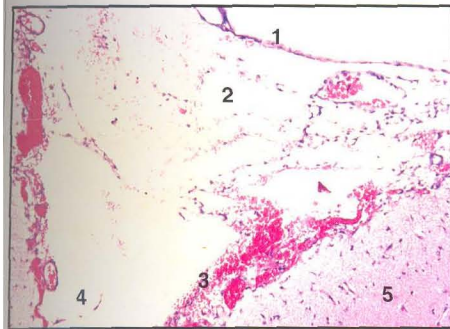
- 1. Cartilaginous cranial vault
- 2. Dura mater
- 3. Subdural space
- 4. Arachnoid
- 5. Subarachnoid space
- 6. Pia mater
- 7. Diencephalon

**Fig. 225 Section through the meninges (58 days). Aldehyde-thionine PAS method x 100**



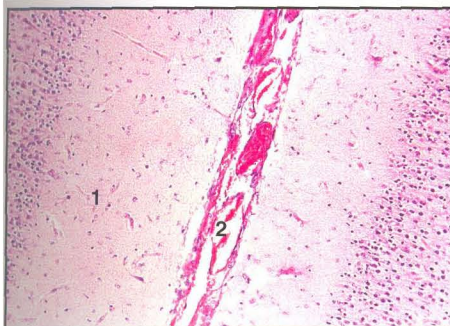
- 1. Arachnoid
- 2. Subarachnoid space
- 3. Blood vessel
- 4. Pia mater
- 5. Cerebral cortex

**Fig. 226 Section through the meninges and cerebral cortex (144 days). H&E. x 100**



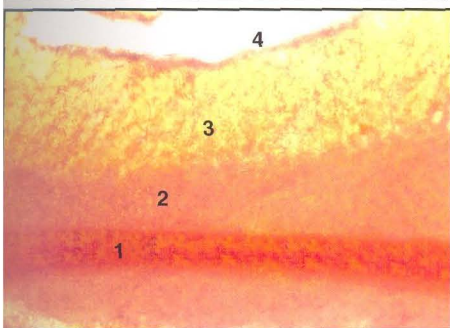
- 1. Arachnoid
- 2. Subarachnoid space
- 3. Pia mater
- 4. Sulcus
- 5. Cerebral cortex

**Fig. 227 Section through the meninges and cerebral cortex (124 days). H&E. x 100**



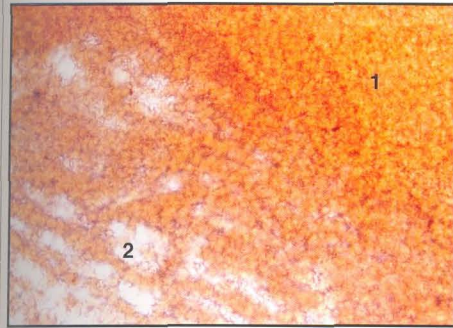
- 1. Cerebral cortex
- 2. Pia mater extending into the sulcus

**Fig. 228 Section of cerebral cortex showing pia mater extending into the sulcus (124 days). H&E. x 100**



- 1. White matter
- 2. Inner granular layer
- 3. Outer molecular layer
- 4. External granular layer

**Fig. 229 Section of cerebellum showing myelination of the white matter (Full term). Oil Red O method x 100**



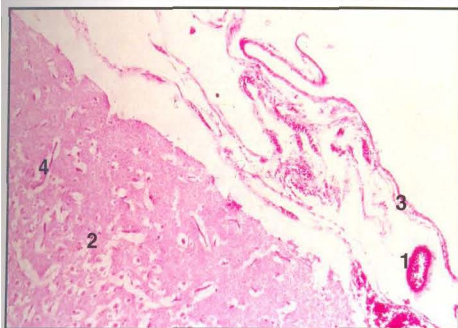
1. Cortex
2. Medulla

Fig. 230 L.S. of the pineal gland (Full term). Oil Red O method x 100



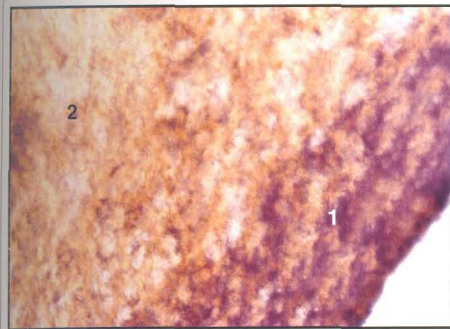
1. Myelinated fibres in the habenular commissure
2. Pineal gland

Fig. 231 L.S. of the habenular commissure and pineal gland (Full term). Oil Red O method x 100



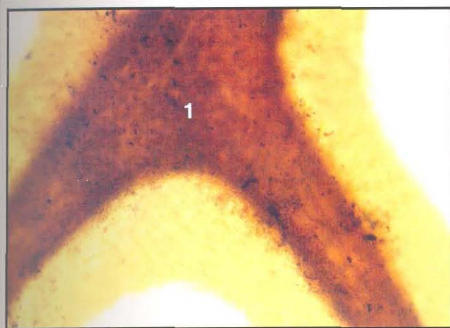
1. Blood vessel of pia-arachnoid
2. Cerebral cortex
3. Epithelia of arachnoid
4. Capillaries

Fig. 232 Section of the cerebral cortex (144 days). PAS. x 100



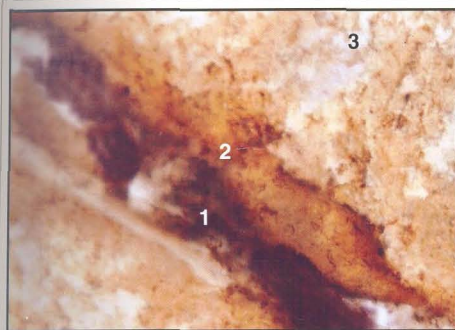
- 1. Outer plexiform layer
- 2. Cerebral cortex

**Fig. 233 C.S. of the cerebral cortex (Full term).  
Gomori's method for alkaline phosphatase x 100**



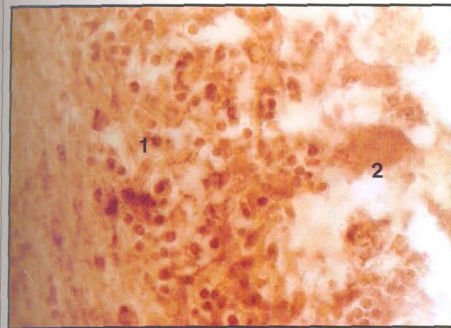
- 1. White matter

**Fig. 234 Sagittal section of cerebellum (Full term).  
Gomori's method for alkaline phosphatase x 100**



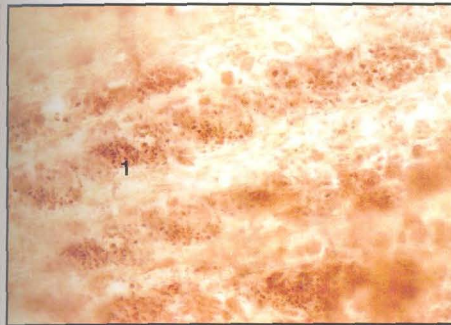
- 1. Pia mater
- 2. Outer plexiform layer
- 3. Cerebral cortex

**Fig. 235 Section of cerebral cortex (Full term).  
Gomori's method for alkaline phosphatase x 100**



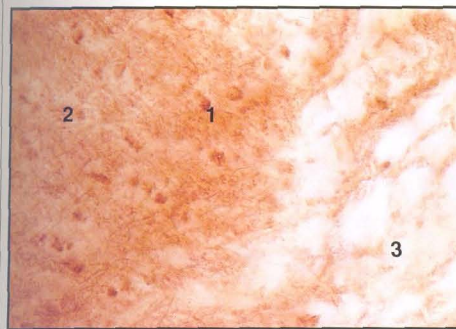
- 1. Granule cells
- 2. Purkinje cells

**Fig. 236** Sagittal section of cerebellum (Full term).  
Gomori's method for acid phosphatase x 400



- 1. Positive reaction in the glial cells of white matter

**Fig. 237** Sagittal section of cerebellum (Full term).  
Gomori's method for acid phosphatase x 400



- 1. Pinealocytes
- 2. Cortex
- 3. Medulla

**Fig. 238** L.S. of pineal gland (Full term).  
Gomori's method for acid phosphatase x 400



## *Discussion*

---

## 5. DISCUSSION

### 5.1 DEVELOPMENT OF THE NEURAL TUBE IN THE FIRST MONTH

#### 5.1.1 Brain Vesicles

The dilated cephalic end of the neural tube is the primordium of brain. The three-vesicle stage of brain is short lived. In this study, goat embryos of 24 days of age with a crown rump length (CRL) of 1.4cm showed the five brain vesicles, viz., telencephalon, diencephalon, mesencephalon, metencephalon and myelencephalon. Sadler (2004) made similar observations in human embryos and established that the signals for segregation of brain into forebrain, midbrain and hindbrain regions were derived from homeobox genes expressed in the notochord, prechordal plate and neural plate.

Patten (1948) and Huettner (1967) reported that the brain vesicles started to differentiate in the pig embryos of 7.0mm CRL and were well established between 9.0mm and 12.0mm stage. In human embryos of about 3.0mm CRL (early fourth week), the forebrain was subdivided into its components (Arey, 1957; Truex and Carpenter, 1969). At 8.0mm stage, the hindbrain also divided. After detailed studies on the development of canine brain, Jenkins (1978) concluded that the embryonic growth of neural tube was inherently influenced by a phenomenon called cephalization. Harper and Maser (1975) in their studies on the brain of American plain buffalo found that this cephalization was based on lateral expansion.

The ballooning of early embryonic brain resulted primarily from an increase in the cavity size and not from tissue growth. Walls of the brain vesicles were thin with a wide lumen in 24 days-old embryos. The rapid expansion of brain vesicle was thought to be due to positive fluid pressure against the wall of neural tube. A similar observation was made by Gilbert (1997) in chick embryo. Arey (1957) reported that this fluid was actively secreted by the ependymal layer of neural tube, which bulged at the thinner regions while the more resistant parts remained as constrictions.

##### 5.1.1.1 Morphogenesis

In the first month of gestation, the transverse distance of telencephalon was greater than its vertical distance. A similar observation was made by Shrivastava *et al.* (1987) in goats. Lateral walls were the thickest followed by the ventral and dorsal

walls. In 24 days-old subjects, the cavities of the telencephalic vesicles were broadly continuous with the lumen of the neural tube. By 26 days of age, the expansion of cerebral vesicles had commenced. At the age of 27 days, the lateral ventricles communicated with the third ventricle through the paired interventricular foramina of Monro. Keith (1947) reported that in human embryos the expansion of cerebral vesicles commenced by the end of sixth week. According to Arey (1957), the telencephalon of vertebrates was a product of alar plates. Basal and floor plates were lacking, and the roof plate was chiefly concerned with the formation of choroid plexus.

The olfactory pits lined with thickened ectodermal epithelium were developed by 24 days of age on either side of the telencephalon. Similar observations were made by Arey (1957) in pig embryos. Each pit was bordered by a lateral and medial nasal processes.

Wall of the diencephalon showed thicker lateral walls and a thin dorsal wall at 24 days of age. Diencephalon developed exclusively from alar and roof plates as observed by Huettner (1967) and Sadler (2004) in vertebrate embryos.

The third ventricle was relatively broad in 24 days-old embryos. By 26 days, the ventrolateral walls started thickening, which compressed the lumen. The median ventral trough-like diverticulum represented the infundibulum. Just below the infundibulum, Rathke's pouch was present. Sadler (2004) reported the presence of Rathke's pouch in three weeks-old human embryos as an evagination of the stomodeum, which subsequently grew toward the infundibulum. By the end of second month it lost its connection with the oral cavity and was then in close contact with the infundibulum. In this study, by 24 days of gestation itself, the Rathke's pouch had lost its connection with the stomodeum.

By 24 days of gestation, the junction between telencephalon and diencephalon was demarcated by the optic stalks. The optic cups were attached to the diencephalon by the optic stalks. The optic cups consisted of a thick inner layer that developed into the nervous elements of retina and a thin outer layer that formed the pigmented layer. The lens vesicle was separated distinctly from the overlying corneal ectoderm. Similar observations were made in pig embryos by Patten (1948). In human embryos, the developing eye appeared at 22<sup>nd</sup> day of gestation (Sadler, 2004).

Out of the three original embryonic divisions, mesencephalon was the only one that did not subdivide during the period of growth and differentiation, as reported by Jenkins (1978) in dog embryos. It was somewhat circular in cross section at 24 days of age. Total width was slightly more than its height. The lumen also showed the same pattern. Distinct basal and alar plates representing the motor and sensory areas were found on each side of the midline and were united by the floor and roof plates, respectively. Sulcus limitans marked the boundary between the alar and basal laminae. De Lahunta (1983) reported that in domestic animals rostral to the region of mesencephalon, the sulcus limitans was no longer evident in the primitive neural tube. The diencephalon and telencephalon were considered to be developed from the alar plate tissues.

The metencephalon, similar to the mesencephalon, was characterised by basal and alar plates. In 24 days-old subjects, the wall of metencephalon bore prominent scalloping neuromeres. Sadler (2004) reported that the hindbrain in human embryo showed eight rhombomeres. A sharply defined epithelial sac, the otocyst, that was a convenient landmark in identifying ganglia and nerves, demarcated the junction between metencephalon and myelencephalon. Cavity of the metencephalon, the fourth ventricle, was wide at this stage. Thickness of the basal plate greatly increased by 26 days of age and a bundle of nerve fibres (of trigeminal nerve) could be observed in the basal plate. The semilunar ganglion of the trigeminal nerve was another important landmark situated at the pontine flexure of the metencephalon. Most of the cranial ganglia and nerves were developed in embryos of 24 days of age. Reports in goat embryos on this aspect are not available for comparison.

Wall of the myelencephalon as in the case of metencephalon, showed the typical arrangement of longitudinal alar plates and basal plates and the sulcus limitans. Ghosh (2002) reported that in domestic animals, the myelencephalon was fairly comparable to their homologue in the spinal cord. Stretching of roof plate to form the thin roof of fourth ventricle was not commenced in the first month of gestation in goat embryos. The choroid plexus of the ventricles of the brain were also not developed. Diamond-shaped lumen of the myelencephalon in 24 days-old subjects became narrower with the growth of basal and alar plates. By 26 days of age, the lumen became coffin-shaped and at the age of 27 days the lumen was slit-like. Froriep's ganglion of the spinal accessory nerve was seen on either side of the

myelencephalon by 24 days itself. In pig embryos, Patten (1948) noticed that the Froriep's ganglion usually disappeared in the adult and the nerve was left without ganglia. Reports on this aspect are not available in goat foetus for comparison.

Jenkins (1978) studied the relation of gray and white matter and found that the spinal cord retained the original neural tube relationship of gray substance and white substance. In the medulla and the rest of the brainstem, this relationship was lost, so that there was more of an intermingling of gray and white matter.

#### ***5.1.1.2 Histogenesis***

In 24 days-old goat embryos, wall of the neural tube at the anterior end was already organised so that three concentric zones could be distinguished, viz., the ependymal, mantle and marginal layers. The neural tube wall was bounded on the inner and outer surfaces by internal and external limiting membranes, respectively. Arey (1957) made similar observation in human foetus in the sixth week of development. Chrisman (1991) noticed that the astrocytes formed a complete membrane on the external surface of the adult brain. They were reported to fuse with ependymal glial processes and formed the internal glial limiting membrane.

Inner ependymal layer was the thickest of all and composed of neuroepithelial or primitive medullary epithelial cells arranged radially in a pseudostratified manner. These cells possessed elongated nucleus and indistinct cell boundaries. Germinal cells with large spherical nucleus were located towards the luminal surface. Similar observations were made in vertebrates by De Lahunta (1983) who found that the cell membrane of each cell was connected to both sides of the neural tube and position of the nucleus changed depending on the mitotic stages. During interphase, the nucleus was located on the external surface of the tube. As it entered mitosis it migrated to the luminal surface. The nuclei of daughter cells again migrated to the external surface.

Middle mantle layer derived from the proliferation of innermost cells was distinguishable only in the ventral wall of developing brain in 24 days-old embryos. The present results confirmed the earlier observations of Harrison (1978) in vertebrates who stated that the region of the formation of neuroblasts was mainly the ventral aspect of neural tube. From 26 days onwards, the entire neural tube wall showed all the three layers. In the region of myelencephalon, the mantle layer was the thickest layer in basal plate region at the age of 26 days. Arey (1957) noticed that the

basal plate of the myelencephalon differentiated a little earlier than the alar plate. In vertebrates, Gilbert (1997) reported that the mantle layer became progressively thicker as more cells were added to it from the germinal neuroepithelium. In the alar plate of myelencephalon, the ependymal layer was thicker than the mantle layer. In the floor plate, only two layers were seen, the ependymal and marginal layers. The mantle layer was absent. Roof plate was the thinnest, formed of a single layer of ependymal cells as observed by Arey (1957) in pig embryos.

The cells of mantle zone were differentiated into two types, the neuroblasts and the spongioblasts by 24 days. Neuroblasts were less in number, possessed large pale vesicular nucleus with peripheral condensation of chromatin and a small dark staining nucleolus. Neuroblasts developed cellular processes and were converted into primitive neurons or multipolar neuroblasts by 27 days of age. Harrison (1978) reported that germinal cells initially differentiated into apolar neuroblasts. These cells then pushed out two processes at opposite poles of the cell to become bipolar neuroblasts and then lost one of these processes to become unipolar neuroblasts. Finally several processes were pushed out as dendrites, thus forming the multipolar neuroblast, which resembled an adult neuron. The original single process grew and formed the axon of the neuron. Neurons developed before the formation of neuroglia. Large neurons developed earlier than the small neurons. In human embryos, Keith (1947) reported the presence of scattered series of differentiated nerve cells in the wall of neural tube during the second month. It was concluded that the earliest nerve tract to appear in brain arose in connection with these centres.

Spongioblasts were more in number and possessed smaller and darker nucleus without a nucleolus. Their processes formed a network at 26 days. Patten (1948) noticed that in the neural tube of pig embryos, the neuroblasts and spongioblasts could be differentiated from each other by the fact that the neuroblasts developed large nuclei while the nuclei of the spongioblasts were small. The formation of supporting tissue from the spongioblasts took place by the development of exceedingly slender and irregular cytoplasmic processes.

From 24<sup>th</sup> day onwards, scattered nucleated erythrocytes were noticed in both the ependymal and mantle layers. Blood channels lined by endothelium also appeared. The outer acellular marginal layer was the thinnest, composed of growing processes of neurons in the mantle layer. This layer was limited by the external

limiting membrane. In 24 days-old embryos, the ventral wall was more organised with all the three layers, whereas the dorsal wall showed only two layers as reported by Arey (1957) in man. This was the general appearance of the neural tube wall in the first month of gestation.

Condensation of the mesenchymal cells and nucleated red blood cells surrounding the neural tube was more distinct towards the ventral wall by 24 days of age. In 26 days-old embryos, the primitive pia mater fully encircled the neural tube. Keith (1947) reported that in human embryos, even before the cephalic part of the neural tube was closed, mesenchymal cells spread in between it and the surrounding mesoderm, supplying a primitive covering for the tube. He opined that the differentiation of membranes of the brain and spinal cord was closely related to the establishment of a cerebrospinal fluid system.

Moore *et al.* (1987) noticed that the neurulation was accompanied by changes in the shape of cells of the neuroepithelium. Cells of the neuroepithelium were classified according to the shape of their profiles as rectangular, round and tapered. This method of cell shape analysis may be useful for the quantification of differences between normal and abnormal neurulation and for the analysis of cellular mechanisms, which are disturbed in neural tube malformation.

### **5.1.2 Brain Flexures**

By 24 days of gestation, all the three brain flexures appeared namely, the cephalic, cervical and pontine flexures. Mc Ewen (1957) observed that in porcine embryos, the cephalic flexure made its appearance at 13-somite stage and shortly thereafter, the cervical and pontine flexures were also underway. In dog embryos, the cephalic flexure appeared at 17<sup>th</sup> day and the cervical flexure at 18<sup>th</sup> day of development while the pontine flexure was visible at 21<sup>st</sup> day (Houston, 1968; Jenkins, 1978).

Arey (1957), Jenkins (1978) and Sadler (2004) reported that in vertebrate embryos, these flexures developed as a result of unequal growth process. Cephalic flexure developed ventrally in the midbrain region, cervical flexure at the caudal end of rhombencephalon and the pontine flexure in the rostral area of rhombencephalon in an opposite direction. The cervical flexure was not so pronounced in the goat foetus

when compared to that of bipedal animals as reported by Jenkins (1978) in canine embryos.

## 5.2 DEVELOPMENT OF PARTS OF BRAIN FROM SECOND MONTH TO TERM

### 5.2.1 Encephalometry

#### 5.2.1.1 *Relationship between Age and Brain Parameters*

##### 5.2.1.1.1 Weight of the Brain

Relatively low body weight gains were recorded up to mid gestation. Weight of the brain showed an increasing trend with the advancement of age. From 10<sup>th</sup> week onwards, a rapid increase was observed in the body weight and brain weight. A spurt in growth was noticed between fourth and fifth month. A similar trend was seen in the concentration of total protein and acetylcholine esterase activity in the developing goat foetal brain by Adejumo (1992). The coincidence of rapid foetal growth and increased acetyl choline esterase activity during late foetal life was reported to indicate slow morphological development in early foetal life associated with a low level of physiological activities while increased foetal development after mid gestation was accompanied by higher level of physiological activity.

Brain weighed  $1.108 \pm 0.163$ g,  $5.914 \pm 0.835$ g,  $14.462 \pm 0.136$ g and  $40.728 \pm 2.986$ g during second, third, fourth and fifth month of gestation, respectively. Malik *et al.* (2000) cited that the mean weight of brain in dogs, pigs, ox, horses and elephants were 60-70g, 125g, 500g, 650g and 3675g, respectively. In the present study, brain weight increased 76-fold from 0.700g (40 days) to 53.540g (150 days). This is in accordance with the findings of Mc Intosh *et al.* (1979) in sheep foetuses where the brain weight increased from 0.264g (40 days) to 52.740g at 150 days. In sheep, the increase in brain weight occurred in two phases; up to 90 days and a more rapid and larger increase thereafter. These two phases appeared to reflect an increase in neuroblast multiplication followed by neuroglial multiplication and myelination, respectively. Turley *et al.* (1996) observed that weight of the brain in sheep increased 32-fold between 90 days of gestational age and 17 days post partum.

In the present study, about 50 percent of foetal body weight and brain weight were attained by 18-19 weeks of gestation. Adejumo (1992) reviewed that the pig foetus attained about 50 percent of its final body weight and brain weight by 10 weeks. This differential growth rate could be due to the fact that growth events in



foetal life may be species specific. Another possible reason could be the relatively longer gestation period of the goat when compared to that of pig. Adejumo (1992) also reported that a critical period existed during brain development during which vital activities that determined the final biological fate of the animal are determined. This critical period usually occurred between mid and late foetal life and coincided with the period during which the brain underwent remarkable physical and chemical development.

#### 5.2.1.1.2 Volume of the Brain

Brain volume increased from second month to term. Mean values were slightly more than the corresponding values of the brain weight in all the groups studied. This could be due to the folding of the brain surface in order to accommodate the brain tissue in the limited space of the cranium.

#### 5.2.1.1.3 Size of the Brain

Length, width and thickness of the brain increased with the advancement of age. Brain length increased from 1.300cm at 40 days to 7.700cm in full term foetus. Similarly the width and thickness increased from 0.700cm and 0.600cm to 5.190cm and 3.300cm, respectively. In all age groups, length of the brain was more than its width followed by the thickness. Malik *et al.* (2000) reported that the brain of eight-year-old elephant measured 36.000cm, 30.000cm and 11.000cm its greatest length, width and thickness, respectively. In male calves of one to two months of age, the brain measured  $16.160 \pm 0.610$ cm and  $10.780 \pm 0.190$ cm in length and width, respectively (Parmar *et al.*, 2000). In the present study, length of brain and its various components showed more significant correlation with the age when compared to that of the body weight.

#### 5.2.1.1.4 Cerebrum

The cerebral hemispheres were much wider caudally than rostrally and showed definite pattern of gyri and sulci identical to those of an adult in the terminal stages of pregnancy. Percentage contributions of cerebral hemispheres to the total brain weight were 59.04, 66.97, 70.14 and 74.16 percent during second, third, fourth and fifth month of gestation, respectively. These values showed a sharp and steady increase throughout gestation and in full term foetuses, the mean weight of the two cerebral hemispheres was 19.290g. Truex and Carpenter (1969) reported that the telencephalon contributed 83.10 percent of the brain weight in human beings. They

opined that there is a correlation between the size of a particular part of animal's brain and its importance in the life of that animal. The vertebrate brain has evolved by a gradual "cephalic shift" of function from lower brainstem to the higher cerebral cortex in mammals.

Length, width and thickness of cerebrum consistently increased during prenatal period. Thickness of cerebrum exceeded its width throughout the period of study. Contrary to this, Shrivastava *et al.* (1987) reported that the transverse distance of cerebrum was greater than its vertical distance at early, mid and later stages of gestation in foetal goat. Percentage contributions of cerebral length to total brain length were 90.98, 64.35, 70.39 and 72.87 percent during second, third, fourth and fifth month, respectively. The greater value in the second month could be due to the fact that the entire brain was folded by the presence of cephalic flexure at the midbrain region and as a result, the total brain length remained less during this period. Higher percentage increase of cerebral length (240.38 percent) was recorded than the cerebral width (144.12 percent). This indicated the lengthening of cerebral convolutions and as a whole reflected the linear lengthwise body growth as reported by Parmar *et al.* (2000) in calves. Percentage lengths of cerebrum to cerebellar lengths were 315.00, 322.09, 260.71 and 217.08 percent during second, third, fourth and fifth month, respectively. Parmar *et al.* (2000) reported that in one to two months-old calves, percentage length of cerebral hemisphere was 75.80 percent to the total brain length and 237.86 percent to the cerebellar length. Fox (1963) and Pampiglione (1963) found that in dog at two weeks of age, the superficial flexures of the cerebral hemispheres resembled the adult brain. Mature patterns in relation to length: width ratios and relative sizes of different lobes of the cortex were adult like by six weeks of postnatal age and the adult brain weight was attained by 12 weeks.

Right cerebral hemisphere was found to be slightly heavier (0.88 percent) than the left one. Similarly the values for length, width and thickness also exceeded the corresponding values for the left hemisphere. Ganong (2003) noticed that there are anatomical and chemical differences between the two hemispheres that may correlate with the functional differences. Accordingly, in 91 percent of the human population, the left hemisphere was larger than the right and controlled most language functions as well as the preferred right hand. Animals showed little capability for such functions.

#### 5.2.1.1.5 Cerebellum

Weight, length, width and thickness of the cerebellum increased consistently during gestation. Mean weight of the cerebellum increased about five times from  $0.059 \pm 0.007$ g to  $0.310 \pm 0.050$ g from second to third month of gestation. The increase was about two times from third to fourth month. During fifth month, the weight increased by six folds. Percentage contribution of cerebellum to the total brain weight was 6.21, 6.73, 7.67 and 9.43 percent, respectively during second, third, fourth and fifth month. Upto the fourth month, the cerebellar weight increased gradually and thereafter, a spurt in growth was noticed. In the full term foetus, the cerebellum weighed 5.980g. This observation supports the findings of Done and Hebert (1968) in pig foetus. They found that the increase in cerebellar weight and whole brain weight with increasing age was small, although linear, between sixth and ninth weeks after conception; but after nine weeks there was a sharp increase in the rate of brain growth and that too was found to be linear.

Cerebellar length, width and thickness were highly correlated with foetal age. A sharp increase was evident in all these parameters towards the terminal stage of pregnancy. The spectacular growth spurt of cerebellum is interesting and its teratological implications have been well established. Studies by Done and Hebert (1968) on the brain of foetal pig has confirmed its vulnerability for neurological changes during this rapid phase of growth. Nutritional deficiencies and diseases during the growth period can cause permanent damage to the cerebellum, because maturation continues in spite of growth suppression.

#### 5.2.1.1.6 Brainstem

Unlike in the case of cerebrum and cerebellum, percentage contribution of brainstem to total brain weight decreased from second month to fifth month. Diencephalon was the heaviest component in most of the age groups. Mesencephalon was proportionately large and elongated in early age groups. But later its growth rate declined due to faster growth of other brain components. In human foetus, Keith (1947) reported that by the end of third month, the mesencephalon became overshadowed by the prepondering growth of forebrain and hindbrain. When compared to other divisions of brain, brainstem was noted to be a slow growing region. Klekamp *et al.* (1987) reported that fast growing areas were more susceptible to undernutrition than other parts.

### 5.2.1.2 Relationship between Body Weight and Brain Parameters

Weight of the brain was positively correlated with the body weight. A spurt in growth was noticed in the mean weight of brain between fourth and fifth month. Interference with a growth spurt by malnutrition or noxious agents may leave permanent damage because maturation continues in spite of growth suppression (Smith and Jansen, 1977). Monterde *et al.* (1998) reported that in kids, when compared to the age, live weight exerted significant influence on all morphometric brain parameters except hemisphere width and length.

The growth curve plotted using individual values of brain weight in goat foetuses was curvilinear, but can be expressed as linear by considering each curve as two straight segments with a sharp change in the rate of growth becoming apparent at 19 weeks. About 50 percent of the foetal body weight and brain weight were attained by this age. Prediction equations derived from it can be used to calculate normal values of brain weight from the body weight to assess cases of hypoplasia. Done and Hebert (1968) reported that in foetal pig absolute and relative growth curves determined for the cerebellum and whole brain from 45 days of gestation to term were curvilinear, with a sharp change in the rate of growth becoming apparent between nine and ten weeks.

The percentage contribution of brain weight to body weight showed a decreasing trend during prenatal period. The mean values were 9.81, 7.89, 5.23 and 2.74 percent during second, third, fourth and fifth month of gestation, respectively. This is in accordance with the findings of Tumbleson (1973) who noticed that the mean brain weight in swine as a function of body weight decreased from 12 weeks of gestation to four weeks postpartum. The increase in brain weight was linear from eight weeks of gestation until 13 weeks after birth with a decline in the rate of increase thereafter. In the present study, the brain weight was 1.86 percent of the body weight in the full term foetus. In sheep foetuses, Mc Intosh *et al.* (1979) noticed that the ratio of brain weight to body weight decreased from 6.70 percent (40 days) to 1.50 percent (150 days). The relative maturity of brain at birth justifies the classification of goats along with sheep as prenatal brain developer, as reported by Mc Intosh *et al.* (1979). But in dogs (Fox, 1963) and cats (Smith and Jansen, 1977), brain development occurred rapidly until six weeks after birth and by 12 weeks of age, the brain assumed adult morphologic characteristics. Towe and Mann (1992b) found that

in rats, major surge in brain growth occurred in the first three postnatal weeks. In human beings, growth of brain continued as long as two years of postnatal life (Smith and Jansen, 1977).

All the brain parameters showed an increasing trend with increase in the body weight. But more significant correlation was noticed between the body weight and brain weight. Klekamp *et al.* (1987) in their study on the brain of human beings reported that each area of brain had its own growth period. During these vulnerable periods, each area was susceptible to undernutrition. In man two growth phases have been distinguished. The first involved neuronal development and migration during early pregnancy, the other related to neuronal maturation, glial proliferation, and myelination. The second growth period started in the second half of pregnancy and lasted until the second postnatal year which contributed the largest volume increase in brain development. Stress in early pregnancy have led to neuronal deficiencies, whereas that during late pregnancy or early life caused glial and myelination deficits. It is also reported that volume deficits due to undernutrition during vulnerable periods cannot be compensated completely by optimal nutrition in later life.

#### ***5.2.1.3 Relationship between Other Body Parameters and Brain Parameters***

The weight, volume, length, width and thickness of brain showed significant positive correlation with body parameters at one percent level of significance. These are in accordance with the findings of Hubbert *et al.* (1974) in bovine. Among these parameters, maximum correlation was noticed between brain weight and total body length. Towe and Mann (1992a) reported that in rodents, the cranial capacity was directly proportional to body length within the species. They also found that cranial capacity could be estimated as accurately from body length as from body weight, and that body length was better if any differences in habitus were involved (because body length is relatively insensitive to habitus). Therefore, body length may serve as the primary variable in brain paleoallometry. Regression coefficients were calculated for various brain parameters on body parameters and prediction equations were computed to facilitate the prediction of brain weight and brain size from various body parameters during prenatal period. Ulinski (1997) identified a relationship between the size of an animal's brain and its body size. Mammals and birds possessed longer brains per unit body weight than other group of vertebrates. It was also reported that bigger animals had larger brains.

## 5.2.2 Craniometry

### 5.2.2.1 Head Parameters

Head constituted almost one-half of the curved crown rump length during second month. This agreed with the findings of Langman (1981), who reported that the head constituted approximately one-half of the CRL in human foetus at the beginning of the third month of gestation. All the head parameters showed an increasing trend with the advancement of age. Curved length of cranium was greater than that of the face in all the age groups. This may be due to the caudodorsal curvature of the head than the face. Langman (1981) opined that this was caused by the virtual absence of the paranasal sinuses and the small size of jawbones. Craniofacial ratios were 3.4:1, 2.6:1, 2.3:1 and 2.1:1 during second, third, fourth and fifth month, respectively. Parmar *et al.* (1997) reported that the approximate craniofacial length ratio was 2:1 during early, middle and later stages of gestation in goat foetuses. A growth rate of 845.7 percent was recorded for cranial length during prenatal period. The corresponding value for facial length was 341.4 percent. This indicates faster growth of cephalic region than the face during the foetal life. Transverse distance between lateral canthi was 1.2-1.4, 1.5-2.1, 1.7-2.3, 3.1-3.3 and 6.2-8.5 times of the distance between bases of ears, cornual buds, medial canthi, supraorbital foramina and nostrils, respectively during prenatal period. This was in accordance with the observations made by Parmar *et al.* (1997) in foetal goat. Highly significant positive correlation was noticed between brain and body parameters. This revealed symmetrical growth of head and face regions. Regression equations derived from these can be used to predict the brain parameters from the head parameters during gestation. Thus it is possible to assess the normal growth rate of brain. Curved and straight head lengths showed maximum correlation with brain length.

Unlike brain parameters, all the head parameters showed a greater increase during early gestation than in later stages. This is in agreement with the findings of Parmar *et al.* (1997) in goat foetuses. A similar trend in growth was reported for different body measurements in the foetal goat (Malik *et al.*, 1989). The variation in growth rate during the developmental stages resulted in a symmetrical and proportionate growth of different structures of the head that are responsible for moulding the head into a wholesome normal shape and size and is species dependent (Parmar *et al.*, 1997). Percentage contributions of curved head length to CRL

(curved) were 46.12, 42.03, 40.05 and 35.66 percent during second, third, fourth and fifth month of pregnancy, respectively. The gradual decrease in these data is due to a faster growth of trunk in comparison to the head in order to accommodate the rapidly growing viscera. All the head parameters showed highly significant correlation with CRL (curved) and total bent length of foetus. This shows that different head parameters contributed towards the body length and maintained the body symmetry. Parmar *et al.* (1997) found that the maximum symmetry of the body especially of the head was attained in mid- gestation period, in goat.

Eventhough all the head parameters showed a greater increase during early gestation, the whole brain, cerebrum and cerebellum showed a spurt in their growth during the terminal stages of pregnancy. This explains the highly convoluted pattern of cerebral and cerebellar cortices in the animal. The convoluted cortex allows increased surface area so that more brain tissue can be accommodated in the available space.

#### **5.2.2.2 Skull Parameters**

All the skull parameters showed a progressive increase during gestation. Significant positive relationship existed between the various parameters except the cephalic index and cranial index as reported by Sandhu and Dhingra (1986) in camel. Skull length was highly correlated with skull width, neurocranial length, facial length and interorbital distance. This agreed with the findings of Gupta and Sharma (1990) in bovines who noticed that the length of the skull had significant positive linear relationship with the cranial length and skull width. According to them, the facial length did not show significant relationship with any of these parameters. The difference may be due to the fact that these measurements are taken in the adult ox where the paranasal sinuses are well developed. Facial region constituted almost one-third of the total skull length during gestation. Sarma *et al.* (2004) in their craniometrical studies on the skull of New Zealand White rabbit noticed that the neurocranium was much longer than the splanchnocranium. In the present study, cranial height and width were almost equal. Contrary to this, Sarma *et al.* (2004) reported that cranial height was more than double the cranial width in rabbit. The cranial cavity length was much less than cranial length indicating a roomy cranial cavity in the rabbit.

Calculated cephalic indices were  $60.78 \pm 1.91$ ,  $55.60 \pm 0.82$ ,  $50.85 \pm 0.54$  and  $53.92 \pm 0.57$  percent during second, third, fourth and fifth month of gestation, respectively. This shows that in the first half of pregnancy, the foetal head was relatively short with a short facial region. In the second half, low cephalic indices indicated a comparatively narrower and relatively longer head. Gupta and Sharma (1990) reported that the cephalic index of adult bovine skull was  $52.14 \pm 3.10$  percent. In adult rabbit, the value was  $54.89 \pm 0.62$  percent (Sarma *et al.*, 2004), whereas in adult Indian yak, the cephalic index was  $64.12 \pm 3.77$  percent indicating a longer head of the species (Archana *et al.*, 1998). Skull length showed significant positive correlation with the weight, volume, length, width and thickness of brain. The difference between thickness of the brain and cranial height increased with gestational age. This is in agreement with the findings of Sandhu and Dhingra (1986) in camels, Malik *et al.* (1989) in adult goats, Sharma and Gupta (1990) in horses and Gupta and Sharma (1992) in dogs. However, in adult bovines Gupta and Sharma (1990) reported that the cranial capacity was found to be not affected with any of the parameters of the skull or orbit. They opined that large size of the bovine cranium was due to the great extent of the frontal sinuses and it did not affect the size of the cranial cavity. Archana *et al.* (1998) noticed that in the yak, the length of the skull reflected length of the cranial cavity but not the cranial capacity. However, the skull width and intercornual distance affected the length as well as cranial capacity of the yak. Dyce *et al.* (1996) found that the closest relation between the external contours and the cranial cavity was found in the newborn of all species. Among adults this agreement was best retained in cats and dogs. In adult animals, the form and extent of the cranial cavity could not be easily predicted from the external inspection since the paranasal sinuses, horns, bony ridges and other projections of the skull, and the temporal muscles contributed significantly to the conformation of this part of the head.

### **5.2.2.3 Skull Bones**

The shapes of cranium and face changed progressively in all the three dimensions. Cartilaginous cranial vault developed by 40 days of age. Boundaries of the skull bones became identifiable by 54 days. Mandible was found to be the longest among the skull bones in all the age groups. Among the cranial bones, frontal bone was the largest during foetal stage in goat. A highly significant positive correlation



existed among length of brain and medial length of frontal and parietal bones. Cranium showed a marked expansion as a result of proportionate growth of the frontal, parietal, interparietal and supraoccipital bones that formed the roof and walls. Length of nasal bone also increased markedly from 0.860cm to 3.500cm from second month to fifth month. Measurements of all the cranial bones showed a marked increase between fourth and fifth month. Young (1959) suggested that the intracranial pressure resulting from expansion of cranial contents was translated into tensile forces in surrounding tissues, influencing their orientation, and stimulating their proliferation, thereby producing compensatory expansion of the cranial capsule in rats. In the present study, a spurt in growth noticed during this period is supportive to the above findings.

Base of the cranium, formed by the basioccipital, sphenoid and ethmoid bones, showed only a slow growth rate when compared to the bones forming the wall and the roof. Similar observations were made in rats by Young (1959). Changes in the cranial contents led to compensatory modification in size and spatial arrangement of functionally related tissues like meninges, bones and muscles. The cranial vault was highly influenced; the cranial base was affected to a lesser degree and facial skeleton remained unaltered. The rapid increase in cranial contents was associated with a rise in intracranial pressure. Intracranial changes alter the size and shape of cranial capsule. Thus the volume and shape of cranial contents, dural fibre systems and the skull base all must be taken into account in analysing cranial morphogenesis and all these are species dependent. The accurate measurement of shape is critical in understanding the mechanisms involved in normal and abnormal craniofacial growth (Trenouth, 1984).

### **5.2.3 Cerebrum**

#### **5.2.3.1 Morphogenesis**

##### **5.2.3.1.1 Development in the Second Month**

The cerebral hemispheres appeared as bilateral evaginations of lateral wall of telencephalon by 26 days of gestation in goat embryos. During the second month, the surface of cerebral hemispheres was smooth without much differentiation. Keith (1947) reported that until the fifth month the surface of cerebral vesicle was comparatively smooth in human foetus. They enlarged and grew rostrally, dorsally and caudally to cover the diencephalon. The cavity of each vesicle became the lateral

ventricle, which communicated with the third ventricle through the interventricular foramen. The cavity followed the arching growth, thus accounting for the complicated curved shape of the lateral ventricles. Since the diencephalon remained stationary as a pivot point, the telencephalon including the hippocampus and fornix arched around it. Similar observations were made in domestic animals by De Lahunta (1983).

The basal portion of the telencephalon increased in thickness more rapidly than the rest and formed the basal nuclei, by 40 days of gestation. The thin walled upper portion was the pallium. Medially, along the zone of attachment to the roof of diencephalon, the pallial wall on either side became very thin by retarded development and pushed into the corresponding lateral ventricles as the tela choroidea. Tela choroidea was composed of pia mater and ependymal cells. The line of infolding known as the choroid fissure, appeared at the level of interventricular foramen by 40 days. The tela and the capillaries associated with it became the choroid plexus of the lateral ventricle. The choroid plexus first appeared at 40 days of gestation in the goat foetus. Truex and Carpenter (1969) reported that the telencephalic choroid plexus became visible in human foetus in the seventh week of gestation. The plexus in the goat foetus filled almost half of the lumen of the lateral ventricle during the seventh week. It extended more towards the dorsal portion. Sadler (2004) found that the region of choroid fissure failed to develop neuroblasts and remained very thin in human foetus.

In the present study, height of each cerebral hemisphere was more than its maximum width in the second month of gestation. Contrary to this, Shrivastava *et al.* (1987) reported that the transverse distance of cerebrum was greater than its vertical distance throughout gestation, in goat foetuses. Lateral wall of the cerebrum was the thickest followed by dorsal, ventral and medial walls. This agreed with the findings of Shrivastava *et al.* (1987).

#### 5.2.3.1.2 Development in the Third Month

At the beginning of the third month of gestation, the cerebral surface was agyric. By 69 days of age, the cerebral hemispheres showed gyri and sulci. Similar observation has been reported in goat foetus by Shrivastava *et al.* (1987). In bovine foetus, Louw (1989) noticed that until day 58, the cerebrum was smooth. In general, gyri appeared only after the formation of grooves. The rhinal sulcus demarcated

neocortex from paleocortex on the basal surface. A faint triangular depression at the junction between rostral and middle third of lateral surface indicated the Sylvian sulcus. Suprasylvian sulcus also appeared on the dorsolateral surface at this stage. The hippocampal fissure appeared on the medial aspect of the cerebral hemispheres above and parallel to the choroid fissure. Danko (1999) reported that in foetal sheep, the hippocampal and Sylvian fissures were observed at 42 - 43 days and 60 - 61 days, respectively.

By the age of 76 days, both the coronal and marginal sulci made their appearance. The coronal sulcus appeared as a linear impression parallel to the great longitudinal fissure over the frontal pole. The marginal sulcus developed on the caudodorsal aspect near the dorsal longitudinal fissure. At 83 days of age, cruciate fissure also became apparent. The sequence of sulci formation was similar to that of other vertebrates in general (Patten, 1948; Arey, 1957; Smart, 1982; Louw, 1989; Danko, 1999).

#### 5.2.3.1.3 Development in the Fourth Month

During fourth month, the cerebral surface showed more gyri and sulci. At 93 days of age (18.3cm CRL), the ansate, endomarginal and callosal sulci appeared. Ansate or post cruciate sulcus appeared just caudal to the cruciate fissure and it did not reach up to the great longitudinal fissure. Rostrally the ansate sulcus was bounded by the posterior sigmoid gyrus. Jenkins (1978) reported that in carnivores, the anterior and posterior sigmoid gyri, in front of and behind the cruciate sulcus constituted motor cortex. Endomarginal sulcus appeared medial to the marginal sulcus on the caudodorsal aspect of the cerebral surface. However, Shrivastava *et al.* (1987) reported that the endomarginal sulcus was seen only in foetuses above 20.0cm CRL. Callosal fissure demarcated the corpus callosum from the cingular gyrus on the medial surface.

By 101 days of gestational age, the marginal sulcus further elongated. Diagonal, presylvian, ectosylvian and rostral and caudal endogenual sulci started appearing towards the middle of fourth month. This agreed with the findings of Shrivastava *et al.* (1987) in goat foetuses.

#### 5.2.3.1.4 Development in the Fifth Month

In goat foetuses of 124 days of age, the cerebral surface showed most of the gyri and sulci. Overgrown cerebrum and cerebellum fully concealed the midbrain. The deepest and most prominent sulcus on the dorsolateral side of the hemisphere was the combined rostral, middle and caudal suprasylvian sulci. The rostral branch of sylvian fissure was continuous with the presylvian sulcus. The presylvian sulcus did not establish contact with the lateral rhinal sulcus but ran parallel to it. In equines, it joined the lateral rhinal sulcus (Dellmann and Mc Clure, 1975). The coronal sulcus limited the coronal gyrus and was continuous caudally with the ansate sulcus that reached up to the great longitudinal fissure. The ansate sulcus in turn was continuous with the suprasylvian sulcus. Oblique sulcus was located between the ectosylvian and middle suprasylvian sulci. The cingular gyrus was the only constant gyrus on the medial surface of the neopallium limited by the corpus callosum and the genual sulcus. Similar observations were made in large ruminants by Dellmann and Mc Clure (1975).

At this age, the marginal sulcus was a deep fissure that subdivided the caudal part of the cerebral hemisphere into two unequal parts namely the ectomarginal gyrus and the medial marginal gyrus. The ectomarginal sulcus was absent. Similar findings were made in adult goats by Dellmann and Mc Clure (1975). Contrary to this, Shrivastava *et al.* (1987) reported that the ectomarginal sulcus appeared in the middle of gestation in goat foetuses. In full term foetus (41.5cm CRL), numerous secondary and tertiary sulci appeared dividing the cortical surface into numerous small gyri and the cerebral surface attained the adult pattern. Cerebral gyri appear to have evolved independently in different mammalian lineages, and there is no general model of gyrogenesis. Different species arrived at a gyral configuration in different ways and folding have been related to various patterns of organisational changes within the evolving nervous systems (Jenkins, 1978). The process of prosencephalisation led to an increase in the size of cerebral hemispheres with increasing complexity of integrating mechanisms.

### 5.2.3.2 *Histogenesis*

#### 5.2.3.2.1 Development in the Second Month

Wall of the cerebral hemisphere showed ependymal, mantle and marginal layers up to 40 days of gestation. Sadler (2004) reported that in human embryos, the cerebral hemispheres began to develop in the fifth week of development. In goat foetus, during the sixth week, continued proliferation of cells in the mantle layer of the evaginating wall of telencephalon adjacent to the thalamic area of diencephalon produced a bulge into the lateral ventricle, the embryonic basal nuclei.

A septum pellucidum appeared as a well-developed partition between the two lateral ventricles by 58 days of gestation. This was made up of fibre bundles with very few cells. On either side, it was lined by elongated ependymal cells. At this stage, the cilia first appeared in these ependymal cells. According to Truex and Carpenter (1969), in human beings, the septum pellucidum was made up of two thin plates of neural tissue, the laminae of septum pellucidum each of which consisted of fibres covered superficially by a layer of gray matter. Between the two laminae there was a space of variable extent, the cavum pellucidum. Similar laminae could not be identified in the present study.

As described in the first month of gestation, wall of the cerebrum showed the inner ependymal, middle mantle and outer marginal layers at 40 days of gestation. But towards the middle of the second month, migration of neuroblasts to form an outer cortical layer commenced. Cells of the ependymal layer migrated outwards through the mantle layer into the marginal layer thereby forming a superficial primordial gray cortex. This is in accordance with the observations made in human foetus by Arey (1957), Kappers *et al.* (1967) and Harrison (1978). The gray matter therefore came to occupy the marginal zone of the neural tube and the nerve fibres to which its cells gave origin passed centripetally instead of centrifugally as in the spinal cord. A similar process occurred in the cerebellum also. These are in accordance with the findings in various domestic animals by Ghosh (2002).

The middle zone formed the white medullary mass of cerebral hemispheres. This white matter showed many radiating fibres and was traversed by neuroblasts and spongioblasts migrating from the matrix zone to the more superficial layer. In some areas wavy lines of neuroblasts could be seen. Thus the position of gray and white

substances of the spinal cord were largely reversed in this region of brain. According to Arey (1957), such changing relations through mass migration of neuroblasts to new locations was accomplished by the cell bodies moving closer to the source from which they received their messages. Such a directed and oriented response has been named as neurobiotaxis. It would presumably proceed under the influence of some unknown attracting and orienting forces. He also reported that the primordial cerebral cortex was formed in the human foetus early in the third month of gestation. Some neuroblasts did not participate in this migration and constituted scattered deep nuclei in the mantle layer.

According to Gilbert (1997), these migrating neurons moved radially along the glial processes after their final mitosis. Like the cerebellar cortex, those neurons with the earliest 'birthdays' formed the layer closest to the ventricle. Subsequent neurons travelled greater distance to form the more superficial layers of the cortex. This formed an 'inside-out' gradient of development. A single cell in the ventricular layer could produce neurons and glial cells in any of the cortical layers. But how these cells enter a particular layer is not known. He found that about 80 percent of cells migrated radially. But about 12 percent of cells migrated laterally from one functional region of the cortex into another. Once the cells arrived their final destination, it is thought that they elaborate particular adhesion molecules that organised them together as brain nuclei.

In 48 days-old subjects, the outer zone or cortical plate showed two distinct layers. The outer marginal layer was composed mostly of fibres and became the molecular or plexiform layer. The inner cellular layer represented the future layers II to VI of the fully developed cortex. Neurons of this layer were small cells with dark compact nuclei and inconspicuous cytoplasm. Similar observations were made in goat foetuses by Shrivastava *et al.* (1987). They reported that the neurons of cerebral cortex in early and mid gestation were undifferentiated cells of small size with dark compact nuclei and inconspicuous cytoplasm. Neurons of cerebral cortex towards term were small to medium sized, more differentiated and with distinct neuronal configuration.

Towards the end of second month, cortical migration of neuroblasts was very much pronounced so that thickness of cerebral cortex greatly increased. Correspondingly thickness of the outer molecular layer also increased. Stratification

of the granular layer into various zones was not evident in this stage. White matter showed large number of migrating neuroblasts and they migrated along the glial processes. This is in accordance with the observations made in vertebrates by Gilbert (1997).

#### 5.2.3.2.2 Development in the Third Month

During initial stages of third month (61 days of gestation), the cortical plate showed only two layers, viz., the outer molecular layer and the inner cellular layer. By the middle of third month, the inner cellular layer showed stratification. Thus at the age of 76 days (12.0cm CRL), the cerebral cortex revealed four layers, viz., the outer molecular layer, superficial granular layer, intermediate granular layer and the deep granular layer. According to Larsell (1951), this happened in human embryos during the fourth and fifth month of gestation. Contrary to this, Shrivastava *et al.* (1987) reported that the cerebral cortex was differentiated into four layers in goat foetuses of 2.7cm to 44.0cm CRL. Cerebral cortex was thicker at the top of the crown of gyrus and the thickness gradually diminished towards the floor of the sulcus. Mean thickness of the molecular layer at the floor of the sulcus exceeded that at the top of the gyrus. Similar observations have been reported in human foetus by Kappers *et al.* (1967). The reasons for these variations were explained to be mechanical. Differences in the compression or stretching of the various layers, viz., the compression of the outer layer towards the base of the fissure and stretching of the inner layer could be the reason for these variations. At the top of the gyrus a condition just opposite to this happened.

White matter revealed the migrating neuroblasts and the spongioblasts as noticed during the second month. Width of ependymal layer gradually diminished but the cells were non-ciliated. Deeper layers were more vascular compared to the outer layers. Hence it could be inferred that the superficial layers are mainly nourished by the pial vessels.

#### 5.2.3.2.3 Development in the Fourth Month

Histological picture of the cerebral mantle was same as that observed during the third month, but the width of various layers increased. Vasculature of the cerebral cortex greatly increased. Kappers *et al.* (1967) reported that in human foetal brain, vascularization of the superficial layers (I to IV) was more or less independent of that

of the deeper layers, and that the blood supply to the deep granular layer VI was especially rich. They suggested that this layer was the chief matrix in which proliferation occurred in the organisation of the cortex. Pyramidal cells of the cerebral cortex were not differentiated during the fourth month.

Unlike in the third month, white matter did not reveal waves of migrating neuroblasts and spongioblasts. This indicated that cortical migration of ependymal layer already came to an end by about 12 weeks of gestation and the cortical cells might be undergoing differentiation during the fourth month. Width of white matter further increased. Another feature noticed was that the inner ependymal layer became extremely thin by 101 days of age and was pseudostratified with ciliated columnar ependymal cells. Reports on this aspect are not available for comparison.

#### 5.2.3.2.4 Development in the Fifth Month

Mean cortical thickness was  $1274.667 \pm 79.644 \mu\text{m}$  and  $1120.000 \pm 212.466 \mu\text{m}$  at the top of the gyrus and bottom of the sulcus respectively during fifth month of gestation. Thickness of the cerebral cortex decreased when compared to that in the fourth month. Decrease in cortical thickness might be associated with the increase in number of gyri and sulci that will help for a better vascularisation of the cortical tissue through the blood vessels in the pia mater. Larsell (1951) reported that the average cortical thickness in the human beings was 2.500mm and about two-thirds of the total area of the cortex was hidden in the folds of sulci and fissures. Truex and Carpenter (1969) noticed that the cortex was always thickest over the crest of a convolution and thinnest in the depth of a sulcus.

During fifth month, the neocortex could be divided into six layers as in adults, viz., the molecular, external granular, external pyramidal, internal granular, internal pyramidal and the fusiform cell layers. This pattern was evident from 124 days of gestation. Contrary to this, Shrivastava *et al.* (1987) described the cerebral cortex of foetal goat as heterogenetic type that did not reveal six distinct layers. Dellmann and Eurell (1998) reported that in domestic animals, layering of neocortex was evident only in thick sections and the prominence of individual layers varied from region to region. Ferrer *et al.* (1986) compared the sixth layer of cerebral cortex in carnivores, Artiodactyla and primate brains and observed a basic structural uniformity in all these species.



The molecular layer was the thickest layer formed mainly of fibre plexuses with relatively few cells. Truex and Carpenter (1969) reported that this contained the terminal dendritic ramifications of the pyramidal and fusiform cells from the deeper layers. The molecular layer constituted 27 percent and 39 percent of the total width of cerebral cortex on the top of the gyrus and at the bottom of the sulcus, respectively. Similar observations have been made in goat fetuses by Shrivastava *et al.* (1987). Mean thickness of the molecular layer increased from  $80.000 \pm 3.578 \mu\text{m}$  to  $344.000 \pm 50.045 \mu\text{m}$  from second month to fifth month on the top of the gyrus.

The external granular layer consisted of numerous closely packed small cells. Dendritic processes of pyramidal and fusiform cells passed through it to reach the molecular layer. External pyramidal layer was composed mainly of typical pyramidal neurons of two categories. The larger cells measured  $18.8 \mu\text{m}$  at 144 days and the corresponding value for smaller cells was  $15.0 \mu\text{m}$ . The internal granular layer was composed of closely packed stellate cells. Internal pyramidal layer consisted principally of large pyramidal neurons that measured  $37.5 \mu\text{m}$  at 144 days with a nucleus measuring  $15.0 \mu\text{m}$ . Dellmann and Eurell (1998) reported that in domestic animals the cells of internal pyramidal layer were extremely larger than that of the external pyramidal layer. The fusiform cell layer contained spindle-shaped cells whose long axes were perpendicular to the cortical surface. Dellmann and Eurell (1998) opined that in animals, the functional unit of cerebral cortex is a vertical column (about 0.5mm diameter) extending from the white matter to the cortical surface. Though the individual cortical columns are not histologically evident, physiologically, all neurons within a column become active in response to a certain feature of a stimulus and become inactive in the absence of that feature. The pyramidal neuron forms the anatomic basis for the vertical columnar organisation.

The white matter filled in the space between cortex, ventricle and basal nuclei, and formed the medullary core of the various convolutions. Afferent and efferent projection fibres arose from the whole extent of the cortex and entered the white substance, where they formed the radiating mass of fibres, the corona radiata, converging toward the brainstem. The short association fibres curved around the floor of each sulcus transversely to the long axis of the sulcus, thus connecting adjacent convolutions. The cingulum seen on the medial surface of the cerebral hemisphere was made up of long association fibres. Similar observations were made

in domestic animals by King (1987). Mean thickness of the corpus callosum increased from  $0.176 \pm 0.009$  cm to  $0.249 \pm 0.088$  cm from fourth to fifth month. Stromston (1947) reported that corpus callosum was about 1 mm in thickness and 3 cm in width in adult cat. No sex difference was detected in the shape of splenium of corpus callosum at any stage of gestation in goat foetuses. Bell and Variend (1985) noticed sex differences in the shape of splenium of corpus callosum in adult human beings but not in the children. The corpus callosum represented the cross commissural fibres that reciprocally interconnected the neopallial cortex of the two cerebral hemispheres as reported in human beings by Truex and Carpenter (1969).

### **5.2.3.3 Olfactory Bulb and Olfactory Pathways**

#### 5.2.3.3.1 Morphogenesis

##### *5.2.3.3.1.1 Development in the Second Month*

The olfactory bulb was well developed at 48 days of gestation. It projected cranioventrally from the frontal pole of cerebral hemisphere. Larsell (1951) reported that the olfactory lobe appeared in the sixth week of gestation in human foetus. The lateral ventricle could be seen extending into the olfactory bulb. Towards the end of the second month, there was a decline in the size of the cavity due to the growth and differentiation of the neural tube wall.

##### *5.2.3.3.1.2 Development in the Third Month*

In the third month, size of the olfactory bulb gradually increased. By the age of 81 days, the olfactory peduncle was divided into medial and lateral olfactory striae separated by the olfactory trigone. The lateral stria merged with the rostral portions of the piriform area and the medial one with the subcallosal area. Similar findings were made in the sheep by Wischnitzer (1993).

##### *5.2.3.3.1.3 Development in the Fourth Month*

The olfactory bulbs did not project beyond the frontal pole of the cerebral hemispheres. All other features were similar to that of the third month. Jenkins (1978) reported that the olfactory bulbs in dogs were very large and projected beyond the cerebral hemispheres. In the foetal elephant, the olfactory bulbs were flat, oval and large (Mariappa, 1985). Smuts and Bezuidenhout (1987) found that in the adult dromedary, olfactory bulb was exceptionally small.

#### *5.2.3.3.1.4 Development in the Fifth Month*

During fifth month, the mean length of olfactory bulb doubled and reached the rostral end of the frontal pole of cerebral hemisphere but did not project beyond it. Unlike during the fourth month, the mean width was more than the mean height. Lumen of olfactory bulb greatly reduced due to thickening of its wall. In human foetus, the olfactory lobe became solid by the end of third month of gestation and elongated into a tubular stalk (Truex and Carpenter, 1969). Jenkins (1978) observed that the olfactory bulbs in dogs were very large when compared with those in man. Crosby and Schnitzlein (1982) noticed that the rhinencephalon in all ungulates was well developed and occupied a good proportion of the ventral part of the brain. The olfactory bulbs and stalks were short and stocky, extending slightly beyond the frontal pole of the brain.

#### *5.2.3.3.2 Histogenesis*

##### *5.2.3.3.2.1 Development in the Second Month*

Histologically the olfactory bulb showed the three layers of the neural tube wall, viz., ependymal, mantle and marginal layers. A stratum similar to the cortical layer formed by the migration of cells of the ependymal layer in the neocortex region at 48 days could not be seen in the olfactory bulb. The olfactory bulb was united with the frontal pole of cerebral hemisphere by the olfactory peduncle. Cranial to the olfactory bulb, the olfactory nerve fibres were seen running towards the bulb from the olfactory mucosa. Arey (1957) reported that the olfactory bulb in mammals was constituted by the termination of olfactory nerve fibres. Towards the end of second month, the cortical migration of neuroblasts was evident. But the thickness of the cortical layer was less when compared to the neocortical regions. Crosby and Schnitzlein (1982) reported that the olfactory bulb in all ungulates presented the same concentric lamination as found in other mammals.

##### *5.2.3.3.2.2 Development in the Third Month*

During the third month, cortical migration of neuroblasts continued but stratification of the cortex was not evident. Similar observations were made in human foetuses by Harrison (1978).

#### 5.2.3.3.2.3 *Development in the Fourth Month*

Unlike in the third month, the cortical tissue showed stratification. It showed the outer molecular layer, superficial granular layer, internal granular layer and deep granular layer as in the cerebral cortex. Studies on this aspect in goat foetuses are not available for comparison.

#### 5.2.3.3.2.4 *Development in the Fifth Month*

Microscopically the wall of the olfactory bulb showed the following layers from anterior to posterior direction: layer of olfactory nerve fibres, the glomerular layer formed by the synapses of olfactory nerve fibres with dendrites of mitral cells, the mitral cell layer, internal granular layer consisting of small granule cells and the white substance formed by axons of mitral cells. A similar structure has been reported in vertebrates by Kappers *et al.* (1967). But the internal and external plexiform layers were not so distinct. The white substance constituted the olfactory striae. Truex and Carpenter (1969) reported that in man this consisted principally of secondary olfactory fibres from cells of the bulb. In the olfactory trigone area, the olfactory tubercle appeared as a cluster of cells. Truex and Carpenter (1969) reported that in macrosmatic animals, especially those with well-developed muzzles; this area was marked by a prominent elevation, the olfactory tubercle. This region received fibres from olfactory bulb, anterior olfactory nucleus and the amygdaloid nuclear complex.

#### 5.2.3.4 *Piriform lobe and Hippocampus*

##### 5.2.3.4.1 Morphogenesis

##### 5.2.3.4.1.1 *Development in the Second Month*

Immediately above and parallel to the choroid fissure, the medial wall of cerebral hemisphere thickened forming the hippocampus, which appeared in the sixth week and developed a distinct elevation in the seventh week. Towards the terminal stage of second month, thickness of hippocampus greatly increased with some structural differentiation. According to Ghosh (2002), in domestic animals, hippocampus developed from the medial wall of telencephalic vesicle and remained in close association with the choroid fissure.

The hippocampus was separated from the thalamus by a cleft that was lined by a double layer of pia mater with many blood vessels and was filled with loose mesenchyme, the velum interpositum. This cleft constituted the most rostral

extension of the transverse cerebral fissure as reported in the human foetus by Truex and Carpenter (1969). This pia projected into the lateral ventricle as the choroid plexus. The lower pial layer of this fissure formed the roof of diencephalon and became invaginated as the choroid plexus of the third ventricle. This is in accordance with the observations made by Sadler (2004) in human foetus.

#### *5.2.3.4.1.2 Development in the Third Month*

Piriform lobe appeared as a distinct convexity on the base of brain in the beginning of third month. Laterally this was marked by the caudal part of the rhinal sulcus; medially, by the hippocampal sulcus which separated the paleocortex from the archicortex. Similar observation has been reported in the adult dog by Jenkins (1978).

The hippocampus invaginated into the lateral ventricle through the hippocampal sulcus by 62 days of age. This sulcus separated the caudomedial parahippocampal gyrus (or subiculum) from the rostrolateral dentate gyrus and the fimbria. The dentate gyrus was narrow without any indentations. Dellmann and McClure (1975) reported that the dentate gyrus lacked indentations in ruminants. At the age of 81 days, the rostrolateral fimbria was characterised by a rather thin, cutting edge to which was attached the choroid plexus of the lateral ventricle. The more medial parahippocampal gyrus was a rather smooth uniform structure, which was continuous with the medial portion of the caudal part of the piriform lobe and neopallial cortex.

#### *5.2.3.4.1.3 Development in the Fourth Month*

A gradual increase in all the parameters of piriform lobe and hippocampus was noticed during the fourth month. Larsell (1951) reported that the cerebral cortex showed its earliest differentiation in the hippocampus. In human embryo at 12mm stage, cells were found to migrate in the dorsomedial walls of the hemisphere from the mantle zone into the marginal zone. These became the cells of the hippocampal cortex, being the first to appear and was designated as the archicortex.

#### *5.2.3.4.1.4 Development in the Fifth Month*

The piriform lobe was elongated. The hippocampus formed a rounded eminence on the floor of the temporal horn of the lateral ventricle and arched caudodorsally and rostrally on the ventricular floor. The fimbria continued rostral to

the corpus callosum to become the fornix. Similar observations were made in the hippocampus of adult domestic animals by Jenkins (1978).

#### 5.2.3.4.2 Histogenesis

##### *5.2.3.4.2.1 Development in the Second Month*

At 48 days, histologically the hippocampus showed the same histological picture as that of the cerebral cortex. The neuroblasts in the mantle layer started developing into pyramidal neurons. Many cells migrated through the marginal layer to the outer aspect forming the cortex. Towards the end of second month, wall of the hippocampus showed an internal ependymal layer, a layer of fibres containing migrating neuroblasts, a cellular layer that was continuous with the cerebral cortex and an outer molecular layer. The cellular layer showed developing pyramidal neurons. Harrison (1978) reported that among the parts of cerebral hemisphere in vertebrates, the first to differentiate was the hippocampus since it was the most primitive part of the pallium. A band of fibres converged from the hippocampus ventrally as the fimbria. Ependymal cells lined the luminal surface of fimbria. The free border of the fimbria was directly continuous with the epithelium of the choroid fissure, which lay immediately above it.

##### *5.2.3.4.2.2 Development in the Third Month*

By 76 days of age, ventricular surface of the hippocampus was covered by a white layer, the alveus. Truex and Carpenter (1969) reported that the alveus in vertebrates was composed of axons from cells of the hippocampus. These fibres converged on the medial face of the hippocampus to form the already described fimbria. Fibres from the alveus entering the fimbria constituted the beginning of the fornix system. At the age of 81 days, hippocampus showed four layers, viz., inner ependymal layer, the alveus, a cellular layer containing some developing pyramidal neurons and undifferentiated neurons and the outer molecular layer.

##### *5.2.3.4.2.3 Development in the Fourth Month*

Unlike the cerebral cortex, more pyramidal neurons appeared in the cellular layer of hippocampus at 101 days as reported by Larsell (1951) in human embryos.

#### *5.2.3.4.2.4 Development in the Fifth Month*

In goat foetuses of 144 days of age, the hippocampus showed the following layers from the lateral ventricular surface to the interior namely the ependymal layer, stratum alveus, stratum oriens, stratum pyramidale and stratum lacunosum-moleculare. A similar histological pattern was reported in the hippocampus of the sheep by Rao (1991). Stratum alveus was located beneath the ependymal layer and was made up of white matter. The stratum oriens revealed a layer of polymorphous cells varying in their shape. Round, oval and stellate neurons were found.

Stratum pyramidale consisted chiefly of large pyramids (37.5 $\mu$ m) with small pyramids (18.5 $\mu$ m) scattered among them. Pyramidal cells of the inferior fold of hippocampus were larger than those of the superior fold. Double pyramidal cells also could be located in the hippocampus. Larsell (1951) reported that the two series of large dendritic processes, directed in opposite directions, the one into stratum oriens and other into the stratum lacunosum-moleculare, gave rise to the term "double-pyramids" frequently applied to the neurons of the pyramidal layer. The pyramids of the inferior fold deviated more and more from the typical pattern as they approached the hilus of the dentate gyrus; their processes became shorter and more widely spread out with an uneven appearance. It was difficult to recognise stratum lacunosum-moleculare separately as reported by Rao (1991) in the sheep.

The dentate gyrus histologically revealed three laminae at 144 days of age, viz., an outer molecular layer, a granular layer in the form of a 'U', the hilus of which was directed toward the fimbria and a polymorph layer. Larsell (1951) reported that the dentate gyrus might be regarded as the modified margin of the hippocampus that has been folded into the hippocampal fissure whose extreme margin was continuous with the fimbria.

#### *5.2.3.5 Basal Nuclei*

##### *5.2.3.5.1 Morphogenesis*

###### *5.2.3.5.1.1 Development in the Second Month*

Basal nuclei appeared as a gray mass in the wall of cerebral hemisphere near the thalamus by 40 days of gestation. In transverse sections, this region had a striated appearance due to alternate arrangement of gray and white substance (corpus

striatum). These are in accordance with the observations made in human embryos by Sadler (2004).

The medial-most gray mass of the basal nuclei was the caudate nucleus. Large number of nerve fibres ventrolateral to this formed the internal capsule, which separated the caudate nucleus from the rest of the gray substance during the sixth week. During the seventh week, the lenticular nucleus also appeared as a narrow elongated mass of cells that was separated from the outer gray matter by a thin external capsule. Studies on this aspect are not available in goat foetus for comparison.

The corpus striatum was in line with the thalamus and was closely related to it. It was separated from the thalamus by a deep groove in early stages. Later the two structures enlarged and they appeared like a continuous mass towards the seventh week of gestation. In human foetus this occurred at the beginning of fourth month (Arey, 1957). The corpus striatum was thus anchored; it did not share greatly in the displacements experienced by the rest of the expanding hemisphere. On the contrary, it served as a fixed area from which the cerebral expansion was produced.

#### *5.2.3.5.1.2 Development in the Third Month*

During the third month, vascularity of the basal nuclei further increased. Largest among the vessels were seen in the caudate nucleus. Dyce *et al.* (1996) reported that the brain, particularly its gray substance, had very high metabolic requirements and the arterial supply was adequate with this, amounting to some 15 to 20 percent of the cardiac output. The middle cerebral artery supplied the largest area of the brain surface. The lenticulostriate arteries arising from the middle cerebral artery to supply the lenticular nucleus and internal capsule area are extremely important. At 62 days of age, the two divisions of the lenticular nucleus were not distinct. By 76 days, the globus pallidus and putamen started differentiating. Victor *et al.* (1979) reported that in rabbit foetus, cellular components of neostriatum (caudate nucleus and putamen) originated between days 15 to 18 from a layer of proliferating matrix cells that lay on the floor of the anterior part of the lateral ventricle.

#### *5.2.3.5.1.3 Development in the Fourth Month*

A notable feature of basal nuclei during the fourth month was that, the claustrum appeared by 101 days of gestation. This was separated from putamen by



external capsule and from insular cortex by the extreme capsule. Extreme capsule is reported to be primarily a cortical association bundle interconnecting frontal, insular, and temporal cortex (Truex and Carpenter, 1969).

#### 5.2.3.5.1.4 *Development in the Fifth Month*

Width of various components of basal nuclei greatly increased during the fifth month. Jenkins (1978) reported that in domestic animals, the caudate nucleus and putamen increased in size proportionately with the development of the cerebral cortex and increased in size to a greater extent than did the globus pallidus. The internal capsule separating the caudate nucleus from the lenticular nucleus was convex internally and concave externally. According to Dellmann and Mc Clure (1975) internal capsule in the domestic animals showed rostral, middle and caudal parts.

Clastrum showed a thin dorsal part and a slightly thicker ventral part. Crosby and Schnitzlein (1982) found that the claustrum in ungulates consisted of dorsal and ventral parts and in sheep, the two parts were connected by a slender band of loosely arranged cells that was not present in goats. Claustrum was separated from the amygdaloid body by the extreme capsule. The amygdaloid body was an almond shaped structure situated ventrolateral to the corpus striatum within the caudal part of the piriform lobe.

#### 5.2.3.5.2 Histogenesis

##### 5.2.3.5.2.1 *Development in the Second Month*

In the caudate nucleus, neuroblasts were more in number than the glial cells. These neuroblasts were of two categories, viz., larger cells and smaller cells, however both were not fully differentiated. These might be the precursors of large and small neurons that were normally seen in the sections of caudate nucleus. Late differentiation might be due to the fact that the caudate nucleus and putamen are phylogenetically newer components of the basal nuclei, the neostriatum. The lenticular nucleus showed comparatively less number of cells than the caudate nucleus. Internal capsule was formed of nerve fibres passing in both directions between the thalamus and cerebral cortex and these were arranged in a radiating fashion. Apart from that, the internal capsule showed radiating columns of migrating neurons destined to become the cerebral cortex. Larger cells were more frequent in the infero-external region as reported by Nin *et al.* (1978) in the cat.

#### *5.2.3.5.2.2 Development in the Third Month*

In the caudate nucleus, dense aggregation of neuroblasts and spongioblasts was noticed, but the neuronal differentiation was incomplete. The lenticular nucleus was composed of islands of cells separated by fibre bundles. In some regions, the caudate and lenticular nuclei were interconnected by transverse cellular bands crossing the internal capsule. Jenkins (1978) reported that this connection was primarily between the caudate nucleus and putamen, which were similar phylogenetically and developmentally and differed from the phylogenetically older globus pallidus.

#### *5.2.3.5.2.3 Development in the Fourth Month*

Clastrum was made of a thin layer of gray matter similar to that of putamen. Truex and Carpenter (1969) reported that in man the claustrum is regarded as a detached portion of the putamen.

#### *5.2.3.5.2.4 Development in the Fifth Month*

Caudate nucleus showed large multipolar neurons scattered among small stellate cells. Nissl granules appeared in the large cells by 144 days of age. Buchanan (1957) reported that in man the stellate cells sent their axons to the putamen and globus pallidus of the lenticular nucleus. Axons of large multipolar cells were distributed exclusively to the globus pallidus. Truex and Carpenter (1969) reported that the ratio between small and large neurons was 20:1. The globus pallidus contained large multipolar neurons and spindle shaped neurons. Large number of nerve fibres were also seen. Globus pallidus is reported to be the main efferent centre of the basal ganglia (Buchanan, 1957). This region is considered as the phylogenetically oldest part of the entire basal nuclei (Dellmann and Mc Clure, 1975). Putamen contained small triangular and large multipolar neurons similar to that of the caudate nucleus. Buchanan (1957) noticed that the smaller neurons participated in internuclear connections between putamen, caudate nucleus and globus pallidus. Long axons of the larger neurons contributed to the efferent pathways from the lenticular nucleus.

Jenkins (1978) and King (1987) opined that most of the activities of basal nuclei were applied to the cerebral cortex and brought about the complicated automatic actions by which an animal performed every day of its life whilst changing

its posture, walking, feeding and defending itself. These purposive movements are commonly called as the instinctive responses. The young one of Equidae and other fleet-footed herbivores run with their mother within a few hours of birth and rely on this to escape from predators. Presumably their basal nuclei would have been fully programmed genetically at birth itself.

## 5.2.4 Cerebellum

### 5.2.4.1 *Morphogenesis*

#### 5.2.4.1.1 Development in the Second Month

Roof of the metencephalon formed the cerebellum. Towards the middle of second month, the metencephalic alar plates were greatly enlarged and presented a striking contrast to the thin roof of the myelencephalon. Bilateral dorsal growths or rhombic lips expanded medially and fused in the midline to completely cover the roof of the fourth ventricle in the rostral part. Moustafa (1996) noticed that the rhombic lips developed in canine embryos ranging from 10 to 15mm CRL. This transverse plate demonstrated a small midline portion (vermis) and two lateral portions (cerebellar hemispheres). Sadler (2004) reported that in human embryos, the vermis and lateral hemispheres appeared in a 12-week embryo and the cerebellum assumed a dumb-bell form. The cranial and caudal portions of the thin metencephalic roof plate formed the rostral and caudal medullary vela. Height of the vermis was half of that of the cerebellar hemispheres in 48 days-old subjects. But towards the end of second month (58 days), height of vermis greatly increased and reached almost the same level as that of the lateral hemispheres.

#### 5.2.4.1.2 Development in the Third Month

Fissures of various depth subdivided the entire cerebellar surface into a considerable number of folia. Cerebellar folia started developing by 62 days (8.6cm CRL). This is in accordance with the observations made by Shrivastava *et al.* (1986) who noticed that the cerebellum showed fissures of variable depth in 8.5cm goat foetus. At 76 days lobulations further increased. Height of vermis exceeded that of the lateral hemispheres at this age.

#### 5.2.4.1.3 Development in the Fourth Month

Increase in cerebellar weight and whole brain weight with increasing age was gradual up to the fourth month, thereafter a spurt in growth was noticed. The

spectacular growth rate of cerebellum is important in its teratological implications. Done and Hebert (1968) suggested that the foetal CNS was most vulnerable while growing most rapidly. Cerebellar surface showed more gyri and sulci during the fourth month. The primary fissure separated the cerebellum into rostral and caudal lobes. Far caudally, the caudolateral fissure separated the caudal lobe from the flocculonodular part, phylogenetically the oldest part of the cerebellum. Similar findings were made in man by Truex and Carpenter (1969) and in domestic animals by Jenkins (1978) and Dyce *et al.* (1996). At the age of 101 days, instead of the nine classical lobules, six were well developed, viz., the lingula, the central lobule, the culmen, the combined declive, folium and tuber, a single mass of pyramid and uvula, and the nodulus. Secondary and tertiary branches were also present. In the kids that walk within an hour after birth, cerebellar gyri and sulci were more numerous than in the cerebral cortex. Earlier appearance of cerebellar gyri and sulci might be one of the reasons attributed to the earlier attainment of muscular co-ordination. Cerebellum was connected to other parts of CNS by rostral, middle and caudal cerebellar peduncles.

#### 5.2.4.1.4 Development in the Fifth Month

Cerebellum was partly covered by the occipital poles of cerebral hemispheres from the beginning of fifth month onwards and the tentorium cerebelli formed a fibrous partition between them. Cerebellum in turn covered the caudal part of the mesencephalon and lateral sides of the medulla oblongata. The median vermis became prominent and was clearly separated from the lateral hemispheres. Similar observations were made in adult small ruminants by Dellmann and Mc Clure (1975). They opined that as the maintenance of equilibrium became more complicated in higher vertebrates, the proprioceptive impulses became more important for equilibrium and orientation; thus the median part of cerebellum and its afferent fibres increased considerably in size or number.

Cerebellum contributed 9.43 percent of the total brain weight. In the adult buffalo, it contributed 8.62 percent of the brain mass (Khatra and Roy, 1980) and in the adult goat, it was 10 percent (Roy and Khatra, 1982). Yeh *et al.* (1982) found that the average weight of cerebellum in Chinese buffalo was  $44.917 \pm 1.950$ g. They also observed that the posterior part of the culmen of the vermis was more developed.

In the present study, percentage length and width of cerebellum in comparison to the total length and width of brain were 33.57 percent and 63.35 percent, respectively. Parmar *et al.* (2000) reported that the percentage length and width of cerebellum in male calves of one to two months of age was 31.86 percent and 57.05 percent of the brain length and width, respectively. Length and width of cerebellum increased more in comparison to the corresponding parameters of cerebrum. At the beginning of fifth month itself, all the nine classical lobules appeared. They were the lingula, central lobule, culmen, declive, folium, tuber, pyramid, nodulus and the uvula in the vermis region. In the full term foetus, cerebellum acquired the characteristic adult appearance.

#### **5.2.4.2 Histogenesis**

##### **5.2.4.2.1 Development in the Second Month**

Wall of metencephalon showed the original three layers of the neural tube wall, viz. ependymal, mantle and marginal layers up to the sixth week of gestation. By the seventh week, a superficial population of proliferating neuroepithelial cells appeared. This external granular layer or external germinal layer was unique to the cerebellum. Keith (1947) noticed that this layer appeared in the third month of gestation in human foetus. Sadler (2004) reported that progenitors of this population arose in the inner ependymal layer of the rhombic lips, and then spread over the entire roof of the cerebellum. Cells of this layer retained their ability to divide and formed a proliferative zone on the surface of the cerebellum. They gave rise to cerebellar cortical neurons. Thickness of external granular layer varied in different areas of cerebellum. On an average, the thickness was 13.0 $\mu$ m and was composed of three to four layers of cells. The closely packed cells were of uniform appearance and possessed dense oval nucleus. The cytoplasmic margins were not clear. Clustering of cells was more intense in the superficial part of this layer than in the deeper parts. These are in accordance with the observations made in foetal rabbit by Smith (1960). Gilbert (1997) reported that at the outer boundary of the external germinal layer (one to two cells thick) the neuroblasts proliferated. The inner compartment contained post mitotic neuroblasts that were the precursors of the granule cells. These pregranular neurons migrated back towards the white matter to produce granule cells of the internal granular layer.

Neuroepithelial cells occupying the dorsal aspect of mantle zone differentiated into the primitive Purkinje cells towards the end of second month. In human foetus, Keith (1947) reported that the Purkinje cells although not fully differentiated even after birth, took up their stations at third month. Andreoli *et al.* (1973) determined the time of origin of Purkinje cells and their final location in various lobes of the cerebellum in mice. Cells formed on 11 and 12 days of gestation appeared in all lobes of vermis but those formed on day 13 became restricted mainly in the anterior lobe. Beneath the primitive Purkinje cell layer, the wall of cerebellum exhibited a wide zone containing uniformly distributed cells. Towards its deeper portion, large neurons appeared that later formed the basal cerebellar nuclei in the white matter. The internal granular layer and the white matter were not differentiated at 48 days of gestation. But towards the end of second month, migrating cells from the external granular layer aggregated just beneath the primitive Purkinje cell layer to form the internal granular layer. Deeply the white matter of the cerebellum started developing. But these two layers were not demarcated. These are in accordance with the findings of Shrivastava *et al.* (1986) in goat foetus who reported that inner granular layer imperceptibly diffused into medulla in early and mid-gestation, whereas the separation between the two layers was slightly more appreciable in the late gestation. Thus, towards the end of second month the cerebellum showed the following layers from outer to inner: the external granular layer, molecular layer, primitive Purkinje cell layer, internal granular layer and the white matter. Thickness of the inner ependymal layer greatly reduced.

#### 5.2.4.2.2 Development in the Third Month

Histological structure was the same as that in the second month up to the middle of the third month. Thickness of the external granular layer increased. White matter started separating from the internal granular layer by 81 days of age. As reported by Dyce *et al.* (1996) in domestic animals, the arrangement of gray and white substance was in sharp contrast to that found in the spinal cord and in medulla oblongata. In the cerebellum, bulk of the gray substance was arranged as an external cortex that enclosed the white substance. The medulla of cerebellum arose from the peduncles and radiated through the various lobes, lobules and folia forming a branching structure with some resemblance to a tree (*arbor vitae*).

#### 5.2.4.2.3 Development in the Fourth Month

During the fourth month, all layers of the adult cerebellum could be clearly distinguished. Mean thickness of the external granular layer ( $42.667 \pm 3.373 \mu\text{m}$ ) was maximum at this stage. In foetal calf, the external granular layer appeared at around 57 days of gestation and reached maximum thickness at around 183 days (De Lahunta, 1983). Gabr *et al.* (1991) found that in camel, the external granular layer reached its maximum thickness at 51cm CRL, and then it decreased to about one to two cells in thickness at 125cm CRL. Outer molecular layer was more fibrous in nature and showed two types of neurons. The outer stellate cells, located in the outer two-thirds of the molecular layer had small cell bodies. The basket cells were situated in the vicinity of the Purkinje cell bodies but the cell body was not clear. Purkinje cells were arranged as a definite layer at 101 days. It has been estimated that human cerebellar cortex contains 15 million Purkinje cells (Truex and Carpenter, 1969). The inner granular layer showed closely packed chromatic nuclei. The cell boundary of these was not clear. The naked appearance of granule cells is said to be due to the complete absence of discrete Nissl granules and the thinness of rimming cytoplasm (Truex and Carpenter, 1969). Irregular scattered spaces seen at random constituted the cerebellar islands or glomeruli, which were not fully developed. According to Truex and Carpenter (1969), the cerebellar glomerulus was formed of a single mossy fibre rosette in the centre surrounded by granule cell dendrites and Golgi axon terminals to which it formed synapses. The inner granular layer also showed Golgi cells that were twice larger than the granule cells. They were more in the upper part of the granular layer. In man, it has been estimated that there is one Golgi cell for every 10 Purkinje cells (Truex and Carpenter, 1969). Deep in the white matter, the cerebellar nuclei were well developed. Ependyma lining the roof of fourth ventricle was pseudostratified and ciliated.

#### 5.2.4.2.4 Development in the Fifth Month

At the beginning of fifth month (124 days of age), thickness of the outer granular layer was  $32.0 \mu\text{m}$ . By 144 days this became very thin and was made up of one or two layers of cells. In full term foetus, this layer was almost single layered. This might be one of the reasons attributed to the fact that the kids could walk immediately after birth. Smith and Downs (1978) opined that there was a parallel relationship between the differentiation of the cerebellar cortex and development of

co-ordination in cats. Lamina granularis externa was reported to be well developed in the newborn. Changes in the external granular layer thickness and in the morphology of the granule cell neurons as they migrated through the molecular layer into the granular layer occurred within the first two weeks postnatally. In calves, foals and other species that walk within an hour after birth, the cerebellum was found to be much more developed at birth. In rabbit, the external granular layer was 8-10 cells thick at birth and attained its mature form by two months of age (Smith, 1960). In calf, the external granular layer reached two cells thick by two months postnatally, and completely disappeared by six months of age (De Lahunta, 1983).

The molecular and internal granular layers increased in thickness greatly during the fifth month. This increase was at the expense of external granular layer as suggested in camel foetus by Gabr *et al.* (1991). A remarkable feature was that the Nissl granules started appearing in the cytoplasm of Purkinje cells during initial stages of fifth month of gestation (at 124 days) and by the age of 144 days these were concentrically arranged as reported by Truex and Carpenter (1969) in man. Each cell gave rise to an elaborate dendritic tree that spread in a fanlike manner in a plane at right angles to the long axis of the folium. The dendritic tree arose from the neck of the cell as two or three large primary dendrites, which divided repeatedly. The morphometric characteristics of Purkinje cell perikarya and dendritic trees were evaluated in man, cat and rat by Ruela *et al.* (1980). Size of Purkinje cell perikaryon, number of synapses and the synaptic surface per Purkinje cell were significantly greater in man than in cat and rat. Gilbert (1997) opined that a typical Purkinje cell in vertebrates might form as many as 1,00,000 synapses with other neurons, more than any other neuron studied. Each Purkinje neuron also gave rise to a slender axon, which was connected to other cells in the deep cerebellar nuclei. No intraneuronal pigment could be identified during foetal stage. Vyas and Nanda (1984) reported that intraneuronal pigment in Purkinje cells first appeared after the age of two and a half years in goat and there was no trace of extra neuronal pigment around them.

The granule cell layer also showed all the features of adult cerebellum during the fifth month. The granule cells have been reported to possess the smallest cell bodies in the CNS (Jenkins, 1978). Cerebellar glomeruli appeared as clusters of fibres among the cells of the granular layer. Truex and Carpenter (1969) reported that the glomerulus is basically a cluster in which two types of presynaptic fibres enter



into a complex relationship with one postsynaptic element. White matter was highly vascular. Deep cerebellar nuclei were well developed and the ependymal layer showed a single layer of ciliated columnar cells.

## **5.2.5 Brainstem**

### **5.2.5.1 Diencephalon**

#### **5.2.5.1.1 Morphogenesis**

##### **5.2.5.1.1.1 Development in the Second Month**

Diencephalon is the rostral most division of brainstem that remained in the midline after the telencephalic vesicles grew out from the forebrain. Caudally this was continuous with the mesencephalon. Lumen of the diencephalon was in communication with each lateral ventricle by interventricular foramen. Similar observations were made in domestic animals by Ghosh (2002). The symmetric development of the lateral walls of the neural tube in the diencephalon reduced the width of the neural canal during the sixth week. In the seventh week, the two thalami grew into approximation so that the third ventricle became a slit-like cavity. The two thalami united across the midline by a bridge-like massa intermedia or interthalamic adhesion, which obliterated the central region of third ventricle into a small dorsal component and a larger ventral component. These are in accordance with the observations made in pig embryos by Mc Ewen (1957), in bovine embryos by Junge (1976), in dog by Salazar *et al.* (1989) and in man by Sadler (2004). The total width of diencephalon was more than its height and the diencephalon became largely concealed by the greater expansion of the cerebral hemispheres.

A hypothalamic groove on the lateral wall of diencephalon divided the lateral plate into upper thalamic and lower hypothalamic regions during the seventh week of gestation. Arey (1957) reported that in human foetus, wall of diencephalon in the second month of gestation showed three main regions namely the epithalamus dorsally, thalamus in the middle and hypothalamus ventrally. The roof plate became the thin ependymal lining of the tela choroidea of this region. Blood vessels growing into this folded area formed the choroid plexus, which invaginated into the third ventricle during the sixth week of gestation. By the end of the second month, the choroid plexus almost entirely filled the triangular dorsal portion of the third ventricle. A large venous sinus could be seen on the roof of the third ventricle. Far caudad, the epiphysis or pineal body developed during the seventh week as a conical

evagination. Pineal body appeared at 48 hours of incubation in the fowl (Spiroff, 1958) and in the sixth week of gestation in the human foetus (Sadler, 2004).

Hypothalamus was narrower than the thalamus and its floor was trough-like. From the floor of diencephalon, a small diverticulum (the infundibulum) developed, which formed the stalk and posterior lobe of pituitary gland by the age of 48 days. The anterior lobe developed from the Rathke's pouch that was evident in the first month itself. In third week human embryo, Rathke's pouch appeared as an evagination of the oral cavity and by the end of second month, it lost its connection with the oral cavity and was in close contact with the infundibulum (Sadler, 2004). Towards the end of second month the pituitary gland was almost completely differentiated.

Far cranially, the hypothalamus showed the optic chiasma during the seventh week, which was 278.00 $\mu$ m thick at 48 days of age. Towards the end of second month, its thickness increased to 910.00 $\mu$ m. The optic nerve emerged out of the cranial cavity through the wide optic foramen between the body and wings of presphenoid bone. Lumen of the third ventricle extended towards the optic chiasma as the optic recess. Decussation of the optic chiasma was evident more towards the ventral aspect. Magras and Karamanlidis (1971) investigated the extent of decussation in the optic chiasma in domestic animals. Non-crossing fibres in the optic chiasma constituted 12 percent in horse, 15 percent in cattle and 11 percent in sheep. But in pig there were 28 percent of non-crossing fibres suggesting a broad field of vision in this species. Mariappa (1985) reported that in elephants the optic nerves, optic chiasma and the optic tracts were slender suggesting a poorly developed "visual system" in this species.

#### *5.2.5.1.1.2 Development in the Third Month*

Thalamus, the largest unit of diencephalon was clearly subdivided into a number of nuclei in this stage. Line of attachment of the ependyma of the third ventricle formed a ridge, the taenia thalami by 76 days of age. Taenia thalami formed the medial boundary of the upper surface of each thalamus. Choroid plexus of the third ventricle extended across the mid plane between the two taeniae. Laterally the superior surface was separated from the caudate nucleus by the sulcus terminalis. Similar reports are not available in goat foetus for comparison.

The pineal gland lay in the depression between the rostral colliculi. The base was attached to the taeniae thalami and habenular and posterior commissures by a shallow stalk into which extended the pineal recess of the third ventricle. The stalk was divided into a dorsal lamina continuous with the dorsal commissure, and a ventral lamina, continuous with the posterior commissure. This supports the findings of Larsell (1951) in vertebrates who reported that the pineal body appeared as an ependymal outgrowth from the roof of diencephalon.

#### *5.2.5.1.1.3 Development in the Fourth Month*

Diencephalon contributed 42.70 percent of the brainstem weight and 7.34 percent of the total brain weight during the fourth month. As in the third month, the width of diencephalon exceeded the height and length and the corresponding dimensions of the hypothalamus. The mamillary body appeared as a distinct entity on the basal surface of hypothalamus. Dellmann and Mc Clure (1975) reported the presence of a very shallow furrow that subdivided the ventral surface of mamillary body into symmetric halves in small ruminants. Such a furrow could not be distinguished at this age.

#### *5.2.5.1.1.4 Development in the Fifth Month*

Mean weight of diencephalon increased about three times from fourth month to fifth month. Width of diencephalon was more than its height and length throughout the prenatal period. On the ventral surface of diencephalon, the infundibulum appeared as a hollow stalk in the samples from which the pituitary was removed. Infundibulum in turn was connected to the tuber cinerium, which had an irregular surface. Dellmann and Mc Clure (1975) reported that in small ruminants the tuber cinerium was not uniform in appearance as in large ruminants and was characterised by four spherical elevations.

### 5.2.5.1.2 Histogenesis

#### *5.2.5.1.2.1 Development in the Second Month*

The choroid plexus of the cavity of diencephalon appeared in the sixth week of gestation in goat foetus. Alar plates of diencephalon showed three zones as in the neural tube wall. During the second month, width of the ependymal layer was greatly reduced. Towards the middle portion of thalamus, the ependymal layer was comparatively wider. Middle or mantle zone was the thickest layer, which

contributed most of the thickness of the wall. The outer marginal layer was thin. Proliferation of neuroblasts in localised regions of the mantle layer led to aggregation of cell bodies. These masses or aggregations of gray substance were subdivided by ingrowing nerve fibres into several parts. These nuclei first appeared in the goat foetuses in the seventh week of gestation. Arey (1957) reported that such massing of nerve cells and fibres led to regional thickenings of brain wall and was one of the chief agencies through which the brain took form and acquired its characteristic internal organisation. According to Harrison (1978), thalamus in vertebrate embryos was a collection of nerve cells, which later became divided into separate nuclei connected with spinal cord and other parts of CNS. Primitive neurons in such aggregations were of small size with dark compact nucleus and inconspicuous cytoplasm. Numerous blood channels lined with endothelial cells were seen in this area. In general, cellular density was more towards the dorsal aspect of thalamus than its ventral regions and the hypothalamus. Similar reports are not available in goat foetus for comparison.

By 48 days of age, the pars distalis of the pituitary showed cords of cells without much differentiation. Towards the end of second month, the parenchyma showed chromophils and chromophobes. The chromophils included acidophilic and basophilic cells. Numerous capillaries were seen between these cords. Pars nervosa showed numerous nerve fibre bundles supported by neuroglia. Similar observations were made in goat foetus by Singh and Dhingra (1979).

The region of interthalamic adhesion did not contain any nerve fibre. This is in accordance with the observations made by Harrison (1978) in vertebrate embryos. On either side of massa intermedia, bundles of nerve fibres could be seen.

In the hypothalamus also bundles of nerve fibres and aggregation of neurons were noticed during the seventh week of gestation. Keith (1947) reported that in the human foetus, during the second month, a scattered series of nerve cells differentiated in the hypothalamus into anterior, middle and posterior ill-defined groups. It was also reported that the earliest nerve tracts to appear in the brain arose in connection with these centres.

The developing eyeball demarcated the area of diencephalon. The different tunics were developed by 48 days of gestation. Different layers of cornea, viz., the

anterior epithelium, corneal substance proper and the caudal endothelium could be distinguished at this stage. The sclera was formed of bundles of collagen fibres and cells. In human foetus at the end of fifth week, the eye primordium was completely surrounded by loose mesenchyme from which developed the choroid and sclera (Sadler, 2004). Thickness of vascular tunic increased towards the rostral aspect. Retina was thickest at its caudal part. It was made up of an outer pigmented layer and an inner neural layer at the age of 48 days. Layer of rods and cones, the ganglion cell layer and the optic nerve fibre layer started developing towards the end of second month. The lens was very large and strongly eosinophilic, and the anterior epithelium that was multilayered in the first month became single layered at this stage. The primary lens fibres reached the anterior wall of the lens vesicle occluding its lumen at 40 days of age. In human embryos this occurred by the end of seventh week (Sadler, 2004). Anterior and posterior chambers were not developed.

At the junction between diencephalon and mesencephalon, immediately beneath the posterior commissure, on the dorsal surface of aqueduct of Sylvius, the ependymal cells were highly modified to form the subcommissural organ (SCO). It was in the form of a sharply curved plate of cells. The cells were columnar in shape and possessed elongated or oval nuclei and were named as the tanocytes. Unlike the ependymal cells, they had no cilia. Talanti (1959) investigated various stages of development of SCO in bovine foetus from three months of gestation to term. The secretory material was already present in the SCO at the age of three months which increased in amount up to the seventh month. The results suggested that the SCO of the bovine foetus was functionally active at least by third month of intrauterine life. Jenkins (1978) reported that functionally this organ is implicated in the secretion of aldosterone. Perdomo *et al.* (1985) reported that SCO appeared in the second month of intrauterine life in human beings. Maximum development was seen in 45mm embryo, and exhibited the characteristic high columnar epithelium.

#### 5.2.5.1.2.2 *Development in the Third Month*

Thin layers of white matter covered the dorsal and lateral surfaces of the thalamus by 76 days of age. White matter on the dorsal surface formed the stratum zonale and that on the lateral surface was the external medullary lamina. At the age of 81 days, a vertical plate of white substance, the internal medullary lamina, extended into the thalamus from the stratum zonale dividing it into medial and lateral

portions. The medial nuclei occupied the dorso-medial portion of the central half of the thalamus. Wedged between this and the ventral nuclei caudally was the centromedian nucleus, the largest of the intralaminar nuclei. The internal medullary lamina partially surrounded this nucleus. Truex and Carpenter (1969) recorded similar observations in adult human diencephalon. Differentiation of neurons was not complete. Cilia appeared on the free surface of ependymal cells at 76 days of gestational age.

A thin connective tissue capsule covered the pineal gland by 76 days of age. The parenchymal cells were arranged in a cord-like manner. There was a small central lumen. The lining cells were columnar in shape with basally located round nucleus and eosinophilic cytoplasm. The neuroglial cells were scattered through the parenchyma from which they could be distinguished by their smaller and darker nuclei. The pinealocytes were not differentiated into light and dark types in the third month of gestation. Number of pinealocytes was more than that of the glial cells. Reiter (1981) distinguished three phases during the development of pineal gland in rat. The morphogenetic phase was considered to begin at about the 12<sup>th</sup> embryonic day and extended until the young are delivered. The cellular proliferation phase commenced on the 16<sup>th</sup> embryonic day and terminated within several days after birth. The cellular hypertrophy and differentiation phase began roughly at birth and ended 9 to 12 weeks postpartum. Kumar *et al.* (1995a) described the topography and histology of pineal gland in young goat. According to them, the parenchyma was formed of pinealocytes, glial cells, fine blood capillaries and nerve fibres.

Column of the fornix divided the hypothalamic nuclei into medial and lateral nuclear groups. In vertebrates, Truex and Carpenter (1969) reported that the fornix represented one of the largest afferent systems to the hypothalamus that arose from the hippocampal formation in the temporal lobe of the cerebral hemisphere.

At 76 days, the posterior commissure appeared as a rounded bundle of fibres that crossed the mid plane beneath the stalk of the pineal body at the junction between diencephalon and mesencephalon. Larsell (1951) reported that the posterior commissure connected the rostral colliculi with each other and fibres of the pretectal region of one side to the other side. Just beneath the posterior commissure was the subcommissural organ, which was lined by several layers of non-ciliated, elongated tanyocytes as seen in the second month. Talanti (1959) investigated various stages of

development of SCO in the bovine foetus and the results suggested that the SCO of the bovine foetus was functionally active at least by third month of intrauterine life. Perdomo *et al.* (1985) reported that maximum development of SCO was seen in 45mm human embryo, and exhibited the characteristic high columnar epithelium.

#### *5.2.5.1.2.3 Development in the Fourth Month*

The ependymal lining of the third ventricle was pseudostratified during fourth month. Free surface showed cilia. Rajtova (1999) noticed in the third ventricle of sheep and goat foetuses, three to four layered ependyma between 40 and 50 days of development. This changed through a pseudostratified epithelium (upto day 130) into the typical one-layered ependyma. Another feature noticed during this period was that the neurons appeared in most of the thalamic and hypothalamic nuclei. Supraoptic nucleus of the hypothalamus showed long spindle shaped cells. Most of these were bipolar cells. Presence of bipolar neurons in the supraoptic nucleus has been reported by Truex and Carpenter (1969) in adult human brain. Paraventricular nucleus also started developing during the fourth month.

#### *5.2.5.1.2.4 Development in the Fifth Month*

Dorsomedial nucleus of the thalamus showed a rostral magnocellular portion consisting of large polygonal deeply staining cells and a caudal parvocellular portion made up of small pale staining cells by 144 days of age as reported by Truex and Carpenter (1969) in adult human brain. Nissl granules appeared in the cytoplasm of neurons of the diencephalon at 144 days.

Supraoptic and paraventricular nuclei of hypothalamus were composed mostly of bipolar cells and peripherally distributed Nissl substance. Paramasivan and Sharma (2001), in their studies on the hypothalamus of Gaddi sheep found that the preoptic nucleus was composed of spindle shaped medium-sized neurons located rostrocaudal to the optic chiasma. Paraventricular nucleus was triangular with densely grouped neurons placed as a vertical plate along the wall of the third ventricle. Truex and Carpenter (1969) reported the presence of colloidal material in these cells indicating its secretory activity. Both these nuclei sent fibres to the neurohypophysis. The supraoptic and paraventricular nuclei were interconnected by scattered cells that formed an incomplete bridge between the two.

The pineal gland was elongated or oval in shape located in the central depression at the caudal end of the thalamus in between the rostral colliculi of corpora quadrigemina. Kumar *et al.* (1995b) reviewed the anatomy of pineal gland in domestic animals and found that the gland was conical in shape in cattle, round to oval in sheep, goats and buffaloes, fusiform or ovoid in horses, elongated cone shaped in pigs, lancet shaped in dogs and conical in cats. They also reported the occurrence of an accessory pineal gland in buffaloes on the posterior margin of the main gland, which could not be located in the goat foetuses.

Histologically the pineal gland acquired the adult characteristics towards the terminal stages of pregnancy. At 144 days of age, a fibrous capsule covered it. Simple ciliated columnar ependymal cells covered the surface facing the third ventricle. From the capsule, connective tissue septae penetrated the gland dividing the parenchyma into small lobules as reported by Kumar *et al.* (1995a) in young goats, Pawar and Ramakrishna (2000) in adult Indian donkeys and Saggar *et al.* (2001) in adult sheep. The parenchyma consisted of pinealocytes and glial cells scattered throughout in the fibrous network of interstitial tissue, fine blood vessels and nerve fibres. Towards the central portion, the cells were loosely arranged when compared to the periphery. Lalitha and Seshadri (1986) reported that in buffalo calves, the pineal gland showed a diffuse narrow peripheral zone and syncytium-like central arrangement. The small central lumen that appeared during third month of gestation disappeared later.

The pinealocytes were of two types namely the light and dark cells. The round to oval irregular nuclei of light pinealocytes had fine chromatin localised more towards the periphery. The dark cells showed uniform distribution of chromatin. Similar observations were made in young goats by Kumar *et al.* (1995a). The parenchyma showed a greater population of pinealocytes than glial cells. Four types of glial cells could be identified based on nuclear morphology, viz., glial cells with round, oval or cone-shaped nucleus, smaller glial cells with round or oval strongly basophilic nuclei, glial cells with elongated nuclei closely associated with the blood capillaries and a few cells with large nuclei. Similar observations were made in adult buffaloes by Prasad and Sinha (1984), in goats by Kumar *et al.* (1995a) and in sheep by Saggar *et al.* (2001). The nerve fibres were distributed irregularly adjacent to the pinealocytes. Pigmented cells and corpora arenacea were not observed at this stage.



Saigal *et al.* (1976) and Calvo *et al.* (1988) observed pigment cells in the adult goat and the dog, respectively.

### **5.2.5.2 Mesencephalon**

#### 5.2.5.2.1 Morphogenesis

##### *5.2.5.2.1.1 Development in the Second Month*

The mesencephalon was limited by the mamillary bodies in front and isthmus behind and lay exposed under the crown of head up to the middle of second month of gestation. The cephalic flexure lay in the ventral aspect of midbrain as a sharp bend even during this stage. Thickness of the wall of mesencephalon gradually increased and the lumen was typically diamond-shaped in the seventh week of gestation. In cross section the wall showed three regions, the tectum, tegmentum and crura cerebri. The alar plates now developed into the primordium of corpora quadrigemina or the tectum. A conspicuous roof plate that was present in early stages lost its separate identity. In human foetus this happened at two months of gestation (Arey, 1957).

Microscopically the rostral colliculus could be distinguished from the caudal colliculus by 48 days of age. Keith (1947) reported that in human foetus, the quadrigeminal plate developed during the third month. Roof of the midbrain first thickened on each side of the midline to form two longitudinal elevations. Later a transverse constriction appeared so that four bodies of corpora quadrigemina were formed. Wenisch *et al.* (1997) noticed that the rostral colliculus was clearly differentiated in bovine embryos of 4.5cm CRL and reached adult structure at 80cm CRL.

In the seventh week, the basal plates gave rise to two regions, the upper tegmentum and lower crura cerebri. Towards the end of second month, the cerebral peduncles bulged conspicuously on the ventral surface of brain as two rounded masses. The intercrural fossa with many blood vessels constituted the caudal perforated substance. The primitive neural cavity gradually became narrow to form the aqueduct. Similar reports are not available in goat foetuses for comparison.

##### *5.2.5.2.1.2 Development in the Third Month*

Relative size of the mesencephalon gradually declined during this period. This observation supports the findings of Wenisch *et al.* (1997) in cattle. The cerebral aqueduct passing through the mesencephalon became narrow at 76 days of gestational

age. Symmetrical proliferation of the wall of the neural tube in the mesencephalon reduced size of the neural canal to a narrow tube, the mesencephalic aqueduct as reported by Wenisch *et al.* (1997) in bovine foetus. Pseudostratified ciliated ependymal cells lined it. At the age of 81 days, the ependymal layer consisted of a single layer of ciliated columnar cells.

#### *5.2.5.2.1.3 Development in the Fourth Month*

The average weight, length, width and height of mesencephalon increased gradually during the fourth month. As noticed in the diencephalon, width of mesencephalon exceeded the length and height, which was an indication of differential growth of midbrain by lateral expansion rather than by dorsoventral expansion. Mesencephalon contributed 37.07 percent of the brainstem weight and 6.38 percent of the total brain weight. Both these parameters showed a decreasing trend as age advanced as reported by Keith (1947) in the human foetus. Average distance from ventral longitudinal groove to the aqueduct was about four times greater than that from the dorsal longitudinal groove. This may be due to the rapid growth of tectum and tegmentum on the floor of aqueduct.

#### *5.2.5.2.1.4 Development in the Fifth Month*

Grossly, the mesencephalon acquired adult characteristics during the fifth month of pregnancy. Weight of mesencephalon almost doubled from fourth month to fifth month. Mesencephalon contributed 25.51 percent of the total length of brainstem during fifth month. Truex and Carpenter (1969) reported that the mesencephalon was the smallest and least differentiated of the five brain divisions in human beings.

#### *5.2.5.2.2 Histogenesis*

##### *5.2.5.2.2.1 Development in the Second Month*

A section across the mesencephalon in goat foetus at the beginning of second month of gestation revealed the same three zones of the neural tube wall. However, the lumen became narrow and thickness of wall increased during the sixth week. During the seventh week, the primordial quadrigeminal plate appeared. The neuroblasts invaded the dorsal marginal zone of tectum to form the rostral and caudal colliculi. Histomorphogenesis of mesencephalon was studied by Keith (1947) in man, Mc Ewen (1957) in pigs and Wenisch *et al.* (1997) in cattle. Wenisch *et al.* (1997)

reported that in bovine embryos up to 3.4cm CRL, the primordium of tectum exhibited a trilaminar pattern namely the ventricular, intermediate and marginal zones. At 4.5cm CRL, formation of the specific tectal layers was marked by the origin of stratum profundum and intermedium.

#### 5.2.5.2.2.1.1 Tectum

The cellular concentration was comparatively more in the tectal area when compared to the tegmentum or crura cerebri. The ependymal layer was thicker than that of the basal plate region. Mantle layer showed scattered small neuroblasts. The marginal layer was composed of fibres and a few cells. Surrounding this the migrated collicular cells were seen. Sadler (2004) opined that the colliculi were formed by waves of neuroblasts migrating into the overlying marginal zone and later organised to form stratified ganglionic layers which were comparable to cortical layers of cerebrum; the deeper cell masses corresponded to the cerebellar nuclei. Towards the basal plate, the ependymal layer was very thin with two to three layers of cells. Ependymal cells had developed cilia.

#### 5.2.5.2.2.1.2 Tegmentum

In the basal plate, neuroblasts aggregated to form nuclei during the seventh week of gestation. This is in accordance with the observation made by Arey (1957) in man who found that the motor nuclei of the third and fourth cranial nerves appeared early in the second month. Tegmentum contained network of fibres and cells representing the reticular formation. Larger multipolar neurons of the red nucleus started appearing in the seventh week. Similar reports are not available in goat foetus for comparison.

#### 5.2.5.2.2.1.3 Crura Cerebri

The crura cerebri started developing in the seventh week of gestation and enlarged to form large spherical masses by the end of second month. According to Harrison (1978), on the ventral aspect of tegmentum, certain nerve tracts appeared one after another, these tracts placed various parts of the brain in communication with each other. The development of mesencephalon was dependent on the differentiation of various parts of brain. Most of the tracts developed and passed up or down from different levels of CNS, through the ventral aspect of midbrain. The first nerve tract

to become associated with the tegmentum in this way was the medial longitudinal fasciculus, an association tract connecting cranial nerve nuclei.

#### *5.2.5.2.2.2 Development in the Third Month*

Histological pattern was similar to that in the second month until the middle of third month. By 76 days of gestation, the mesencephalon revealed numerous nuclear masses. Mesencephalic nucleus of trigeminal nerve, nuclei of oculomotor and trochlear nerves, tegmental nuclei, red nuclei and the substantia nigra were the main nuclei. This is in agreement with the observations of Truex and Carpenter (1969) in man and Jenkins (1978) in dogs.

##### *5.2.5.2.2.2.1 Tectum*

The colliculi of both sides were separated by a median longitudinal groove, in the rostral portion of which lay the pineal body. Each colliculus was connected to the thalamus by fibre bundles. The caudal colliculi were ovoid in shape and whiter than rostral colliculi. This compares favourably with the findings of Dellmann and McClure (1975) in small ruminants.

Mesencephalic nucleus of trigeminal nerve appeared in the lateral margin of the central gray of the aqueductal region by 81 days of gestational age. This was not capsulated. Truex and Carpenter (1969) reported that in vertebrates, this nucleus extended from the rostral margin of medulla oblongata to the level of rostral colliculi. This was primarily composed of large unipolar neurons. They appeared as small islands of cells arranged in a flower-like manner. They possessed eccentric vesicular nucleus. Truex and Carpenter (1969) noticed that the unipolar neurons were characteristic to the cerebrospinal ganglia and mesencephalic nucleus of the trigeminal nerve. However, unlike the ganglion cells, those lying within the CNS were not encapsulated. Pannese (1974) opined that the nuclear eccentricity and wrinkling of the nuclear surface were indicative of a marked synthetic activity. Eccentric nucleus was characteristic to the intermediate neuroblast. In the mature neuron, nucleus was central in position.

##### *5.2.5.2.2.2.2 Tegmentum*

Tegmentum lay between the substantia nigra and the cerebral aqueduct. By 81 days of age, the magnocellular and the parvocellular parts of the red nucleus could be distinguished. Axons of these cells formed the rubrospinal tract. Numerous fibre

bundles including the oculomotor fibres traversed the red nucleus. In man, Truex and Carpenter (1969) reported that the spreading of the root fibres through and around the red nucleus is an expression of intraradicular expansion of the red nucleus during embryonic development.

In addition to the red nucleus, tegmentum showed a number of smaller aggregations of cells collectively called the tegmental nuclei. A number of fibre tracts also ascended and descended through it, and there were several decussations. The nuclei of the oculomotor and trochlear nerves appeared as masses of nerve cells ventral to the aqueduct close to the mid plane at 81 days of age, which are in agreement with the findings of Dyce *et al.* (1996) in the adult brain of domestic animals.

#### 5.2.5.2.2.2.3 Crura Cerebri

The white substance of the crura was made up of fibre bundles predominantly. Jenkins (1978) found that these were the descending fibres of the cerebral cortex to the pons, medulla and spinal cord. The substantia nigra appeared by 81 days of age with undifferentiated neurons.

#### 5.2.5.2.2.3 Development in the Fourth Month

Histological picture did not change much during the fourth month. Size and number of neurons and glial cells increased during this period. Klekamp *et al.* (1987) in their study on human brain reported that later stages of brain growth were related to neuronal maturation, glial proliferation, and myelination.

##### 5.2.5.2.2.3.1 Tectum

Length of rostral colliculus exceeded its width, but the situation was reverse in the caudal colliculus. According to Dellmann and Mc Clure (1975), the caudal colliculi of small ruminants were comparatively smaller than those of large ruminants.

##### 5.2.5.2.2.3.2 Tegmentum

Cells of the red nucleus were the largest among the neurons that could be seen in the entire brain during the fourth month. King (1987) reported that the rubrospinal tract arising from the red nucleus is a major pathway of the extrapyramidal system and of particular importance in domestic animals in postural control and locomotion.

#### 5.2.5.2.2.3.3 Crura Cerebri

The cerebral peduncle increased in thickness during this period. King (1987) reported that cerebral crus in domestic animals was composed of descending fibres belonging to pyramidal system.

#### 5.2.5.2.2.4 Development in the Fifth Month

Neurons of the mesencephalon were differentiated by 144 days of gestation. The nerve cell distribution was diffused rather than focal. Cytoplasm of these neurons showed basophilia. Myelination also began. All these indicated that development of midbrain was almost completed towards the terminal stage of pregnancy. The principal vessels supplying the midbrain were the caudal cerebral, rostral cerebellar, caudal communicating branch and rostral choroidal arteries as reported in domestic animals by Dellmann and Mc Clure (1975). Ependyma lining the aqueduct was adult-like during fifth month.

#### 5.2.5.2.2.4.1 Tectum

The rostral colliculi were almost hemispherical separated by a deep furrow, which opened into a wide subpineal fossa. The caudal colliculi extended laterally beyond the rostral ones, they were spherical in shape, and whitish with a prominent point that was directed dorsocaudolaterally. A similar observation was made in adult small ruminants by Dellmann and Mc Clure (1975).

Each colliculus showed a laminated structure consisting of alternating gray and white matter. The outermost layer, stratum zonale was made up of fine nerve fibres. Truex and Carpenter (1969) reported that in man these fibres originated mainly from the occipital cortex and passed through the brachium of the rostral colliculus. Stratum cinerium or superficial gray layer consisted of small cells and the corticotectal fibres and most of the optic fibres terminated here (Larsell, 1951). Stratum opticum was composed mainly of nerve fibres from retina and lateral geniculate body. The remaining layers or stratum lemnisci were composed of gray and white matter. Similar observations were made in wild boar by Szalak and Stefan (1977).

#### 5.2.5.2.2.4.2 Tegmentum

Various nuclei of the midbrain tegmentum increased progressively in size. Periaqueductal gray appeared as distinct entity and showed fusiform and stellate

neurons. Similar observations were made in young cats by Herrera *et al.* (1988). All the nuclei constituting midbrain architecture, were well developed by 144 days of age. In the rapheal region of the ventral tegmentum was the interpeduncular nucleus, a collection of medium-sized, multipolar cells. Truex and Carpenter (1969) reported that this nucleus was prominent in most mammals, but comparatively small in man.

#### 5.2.5.2.2.4.3 Crura Cerebri

The corticospinal tract appeared as a compact bundle of nerve fibres at the caudal level of mesencephalon. Truex and Carpenter (1969) reported that the corticospinal tract constituted the largest descending fibre system in human beings. The fibres converged in the corona radiata and passed downward through the internal capsule, crura cerebri, pons and medulla oblongata.

### 5.2.5.3 Pons

#### 5.2.5.3.1 Morphogenesis

##### 5.2.5.3.1.1 Development in the Second Month

The pons was interposed between the medulla oblongata caudally and the crura cerebri rostrally and developed by the enlargement of basal plate. It formed part of the floor of the fourth ventricle. Motor nuclei of origin for cranial nerves V, VI and VII started developing in the seventh week of gestation. The trigeminal nerve and semilunar ganglion were also well developed. Immediately beneath the fourth ventricle was the tegmental portion of the pons, which made a thick floor to the cavity of the metencephalon. Below this was the more conspicuous basilar portion of the pons. The floor plate formed a raphe as mentioned in the mesencephalon. The basilar artery was located on the floor of the pons. Similar observations were made in domestic animals by Ghosh (2002).

##### 5.2.5.3.1.2 Development in the Third Month

Pons occupied the central portion of the brainstem. It contributed 21.87 percent of the total length of the brainstem. Transverse distance of the pons was more than the dorsoventral distance during first, second and third month of gestation. The ventral midline enclosed a shallow indentation in direct continuation of the ventral median fissure of the medulla oblongata at 76 days and this groove lodged the basilar artery. Similar findings were made in domestic animals by Dyce *et al.* (1996).

#### *5.2.5.3.1.3 Development in the Fourth Month*

Gross features were similar to that in the third month. Unlike in the earlier age groups, the dorsoventral distance exceeded the transverse distance. Similar reports are not available in goat foetus for comparison.

#### *5.2.5.3.1.4 Development in the Fifth Month*

Mean weight of pons increased three and half times during the fifth month. As noticed during the fourth month, the height of pons exceeded its width. The rostral border of pons was straight as reported by Dellmann and Mc Clure (1975) in small ruminants. According to them, in large ruminants, the rostral border was convex and slightly indented at midline. So also, the transition between the ventral surface and caudal edge of the pons was gradual. Dellmann and Mc Clure (1975) found that this was more abrupt in large ruminants than in small ruminants.

#### *5.2.5.3.2 Histogenesis*

##### *5.2.5.3.2.1 Development in the Second Month*

Up to the sixth week of gestation, the pons showed the three original layers of the neural tube wall. In the seventh week, nuclei started appearing in the mantle layer. These were the motor nuclei of origin for cranial nerves V, VI and VII as reported in human foetus by Sadler (2004). Some alar plate neurons migrated ventrally from the lateral wall to the basal plate to form the pontine nuclei. The marginal layer expanded and formed a thick layer of nerve fibres. Sadler (2004) noticed that in human foetus, this layer made a bridge for nerve fibres connecting the cerebral and cerebellar cortices with the spinal cord and hence it is named as pons that means 'bridge'.

##### *5.2.5.3.2.2 Development in the Third Month*

Sensory nucleus of the trigeminal nerve could be seen in the alar plate region near the lateral margin of the central gray surrounding the fourth ventricle. Jenkins (1978) opined that this nucleus functioned as a typical sensory ganglion and was an exception to the rule that sensory neurons of peripheral nerves have their cell bodies located in a ganglion. Large motor neurons of the trigeminal nerve were seen in the alar plate. Ventral portion of pons was made of longitudinal and transverse fibres interspersed with irregular masses of gray substance, the pontine nuclei. According to Larsell (1951), the longitudinal fibres entered the pons rostrally from the crura cerebri



as a large compact bundle, which became broken up into fascicles of varying sizes by the transverse fibres and the nuclear masses.

#### *5.2.5.3.2.3 Development in the Fourth Month*

Histological structure of pons did not change much during the fourth month. The dorsal longitudinal fasciculus became a sharply defined round bundle, which lay close to the raphe below the gray matter on the floor of the fourth ventricle. This is in accordance with the findings of Dellmann and Mc Clure (1975) in ox.

#### *5.2.5.3.2.4 Development in the Fifth Month*

The pons was divided into a dorsal or tegmental part and a basilar part. Transverse fibres of the pons were divided into superficial and deep fibres according to their position with reference to the longitudinal fibres. At the dorsolateral aspect of the pons was the large rounded section of the rostral cerebellar peduncle. De Lahunta (1983) and Ghosh (2002) reported that in domestic animals, the transverse fibres had their origin in the pontine nuclei, crossed the midplane and converged laterally, augmented by uncrossed fibres, and formed, on each side, a large compact bundle, the brachium pontis which passed dorsally and medially into the medullary substance of the cerebellum.

### **5.2.5.4 Medulla Oblongata**

#### **5.2.5.4.1 Morphogenesis**

##### *5.2.5.4.1.1 Development in the Second Month*

Medulla oblongata (MO), the caudal most segment of the brainstem, extended from the level of first pair of cervical nerves to the caudal edge of pons and lay on the cartilaginous basioccipital. By 40 days, the roof plate region of the embryonic rhombencephalon expanded extensively instead of being displaced by the proliferating alar plates as occurred in the rostral portions of the brainstem. As a result, the entire alar and basal plates of the neural tube moved to a lateral and ventral position. Arey (1957) compared this to an opened book whose hinge was the floor plate. This enlarged the lumen of the central canal of the spinal cord to form the fourth ventricle, which was covered dorsally by the thin, single layer of ependyma, the anterior and posterior medullary vela. The sulcus limitans present on the ventrolateral wall of the fourth ventricle provided the plane of division of the medulla

into a ventromedial basal plate and a dorsolateral alar plate. Similar observations were made in dog fetuses by Jenkins (1978).

Choroid plexus of the fourth ventricle developed on its roof during the sixth week of gestation. Keith (1947) reported that the choroid villi developed on the ventricular surface of the caudal medullary velum at eight weeks in the human foetus and CSF was being produced during the third month. The rhombic lip, ridge where the tela joined the alar plate was made up of 3-4 layers of cells. Harrison (1978) reported that the cells of rhombic lip were actively mitotic and provided large number of neuroblasts, which migrated cephalad into the ventral aspect of the hindbrain where they formed the pontine nuclei and the olivary nuclear complex.

#### *5.2.5.4.1.2 Development in the Third Month*

Main changes noticed during the third month were that the medullary pyramids and the trapezoid body appeared on the ventral surface of the medulla. The medullary pyramids could be distinguished from 81 days of gestation and were in the form of longitudinal ridges on either side of the ventral median fissure, but they were not widely separated in the rostral portion. These agree with the findings of Dellmann and Mc Clure (1975) in small ruminants. However, in cattle the pyramids were widely separated at the point of emergence from the caudal aspect of pons.

Dorsal surface of the medulla that formed the floor of fourth ventricle was marked by a deep median sulcus, which became shallower rostrally. On either side of the median sulcus were the medial eminences, the intermediate eminences and the lateral eminences as observed by Truex and Carpenter (1969) in man and Dyce *et al.* (1996) in domestic animals.

Width of medulla oblongata was more than its height throughout gestation. The trapezoid body was clearly demarcated. Dellmann and Mc Clure (1975) reported that the trapezoid body was more clearly demarcated in small ruminants than in cattle.

#### *5.2.5.4.1.3 Development in the Fourth month*

The medulla oblongata contributed 17.57 percent of the brainstem weight and 3.02 percent of the total brain weight. Length and width of medullary pyramids increased 15.03 percent and 93.04 percent, respectively. More increase in width corresponds to growth of cerebrum since these fibres have their origin in the cerebral cortex.

#### *5.2.5.4.1.4 Development in the Fifth Month*

Grossly medulla oblongata was adult-like by the terminal stages of pregnancy. Trapezoid body was clearly demarcated from the pons. Mean weight of medulla oblongata increased three-fold during fifth month. Corresponding changes were also noticed in the length, height and width of medulla oblongata. Ventral median fissure was flanked by the pyramids. Similar observations were reported in adult domestic animals by Dellmann and Mc Clure (1975).

#### *5.2.5.4.2 Histogenesis*

##### *5.2.5.4.2.1 Development in the Second Month*

Up to the sixth week of gestation the myelencephalon showed the same basic structural pattern of the neural tube wall. Proliferation of neuroblasts in localised regions of mantle layer lead to aggregation of cell bodies that were functionally alike. These masses of gray substance were called the nuclei. Such nuclei were evident at 48 days of gestation. Nerve fibres crossing in every direction broke up the gray substance into a mixture of gray and white known as the reticular formation. Arey (1957) opined that such massing of nerve cells and fibres led to regional thickenings of brain wall and were one of the chief agencies through which the brain took form and acquired its characteristic internal organisation.

During the second month of gestation, differentiation of neurons and formation of nuclei occurred earlier in the brainstem than in the cerebrum and cerebellum. In the cerebrum, hippocampal region was an exception where the pyramidal neurons started developing towards the middle of the second month. This could be due to the early phylogenetic origin of these regions.

##### *5.2.5.4.2.2 Development in the Third Month*

Arrangement of gray and white substances in the medulla oblongata showed a much more complex pattern during the third month when compared to the spinal cord. The main difference from spinal cord was that a sharp demarcation between gray and white substances disappeared. The remainder of the gray substance was broken up into cell groups widely distributed throughout with numerous oblique and transverse bundles of nerve fibres passing among them constituting the extensive reticular formation. Medullary reticular formation was a wealth of cells of various sizes and types, arranged in diverse aggregations and enmeshed in a complicated fibre network.

Truex and Carpenter (1969) opined that it constituted a matrix within which specific nuclei and tracts were embedded. The reticular area located medial and dorsal to the rostral half of inferior olivary nucleus was occupied by the nucleus reticularis gigantocellularis composed of characteristic large cells as well as medium and small cells. The medullary pyramids consisted of large bundles of nerve fibres. Lateral to these were the inferior olivary nucleus, which appeared as a folded bag with the hilus directed medially and composed of small rounded or pear-shaped cells at 81 days.

The median raphe extended in the median plane from the subventricular gray to the pyramids, dividing the medulla into bilaterally symmetrical halves. Periaqueductal gray could be seen ventral to the median fissure at dorsal aspect of the raphe. As reported by Larsell (1951) in man, the medulla oblongata contained the nuclei and fibre tracts associated with cranial nerves V to XII and also ascending and descending tracts between higher centres of brain and spinal cord.

#### *5.2.5.4.2.3 Development in the Fourth Month*

Ependyma lining the fourth ventricle became single layered in most regions. Each cell had 15.00 $\mu$ m length, 7.50 $\mu$ m width with a nucleus of 6.60 $\mu$ m diameter. The cilia measured 15.00 $\mu$ m in length. The cilia were very thick and long. Externally a capsule surrounded the chief olivary nucleus. This supports the findings of Larsell (1951) in man. The median lemniscus was seen on either side of the median raphe towards the ventral aspect. In man, Larsell (1951) found that the median lemniscus was made up of fibres arising from the nuclei of the posterior funiculus and running to the thalamus.

#### *5.2.5.4.2.4 Development in the Fifth Month*

The arrangement of gray and white substances in the medulla oblongata had a much more complex pattern than the simple relations found in the spinal cord. This agreed with the findings of Truex and Carpenter (1969) in human beings and Jenkins (1978) in domestic animals. Medullary pyramids were well developed and most of the fibres were myelinated at this stage.

Nuclei and fibre tracts associated with cranial nerves V to XII were located at different levels. The hypoglossal nucleus was located on the medial aspect of medulla oblongata at the dorsomedial angle on either side of median raphe beneath the floor of the fourth ventricle. Hypoglossal nerve rootlets left the ventral surface of the nucleus,

passed ventrally, lateral to the median lemniscus and emerged on the surface along the ventrolateral sulcus, between the pyramid and the olivary nucleus. Similar reports are available for domestic animals (Dellmann and Mc Clure, 1975; Jenkins, 1978; King, 1987).

### 5.3 VENTRICLES OF BRAIN

The dilated cavities of the brain vesicles were the forerunners of the ventricular system. They underwent extensive alterations as a result of future cellular proliferation, growth and brain flexures. This supports the observations made by Larsell (1951) in human brain and Arey (1957) in domestic animals. At 24 days of gestation (1.4cm CRL), the embryonic lumen of the neural tube at the rostral end was divided into five regions, viz., telocoele, diacoele, mesocoele, metacoele and myelocoele.

#### 5.3.1 Lateral Ventricles

Lateral ventricles appeared as a distinct entity at 27 days (1.7cm CRL) of gestation. They communicated with each other and with the third ventricle through the interventricular foramina or Foramina of Monro. Mean height of lateral ventricle increased from first to third month. Thereafter the height gradually decreased due to the thickening of the cerebral walls. At full term, the lateral ventricles measured 2.743cm in length and 0.576cm in width. Malik *et al.* (1978) reported that the average greatest length and width of lateral ventricles were  $5.460 \pm 0.580$ cm and  $1.250 \pm 0.080$ cm respectively in the adult goat. From the present study it was concluded that the lateral ventricles attained almost half of its length and width towards term. Height of the lateral ventricles was less than their width. According to Malik *et al.* (2000), the plan of ventricular system was similar in elephants, horses, goats, pigs and buffaloes. But the height of lateral ventricles was more than its width.

The lateral ventricles followed the development of cerebral hemispheres and extended into four pairs of their lobes by 48 days (4.0cm CRL) of gestation. The choroid plexus did not extend into these horns. The roof of the ventricle was formed by the corpus callosum and the medial wall by the septum pellucidum. The floor was formed by the caudate nucleus in front and hippocampus caudally separated by the choroid fissure as observed by Dellmann and Mc Clure (1975) in domestic animals.

Kii *et al.* (1997) observed that sex and body weight had no correlation with lateral ventricle symmetry in dogs.

### 5.3.2 Third Ventricle

Third ventricle was an unpaired, cleft-like space lying between the two thalami and extending downward into the hypothalamus. During initial stages of pregnancy, the third ventricle was relatively broad as reported by Arey (1957) in domestic animals. By 48 days (4.0cm CRL), the two thalami grew into approximation so that the third ventricle became a slit-like cavity. At the roof portion, the third ventricle widened to form a triangular space, which was almost completely filled with choroid plexus. There was only roof plate along the median plane over the small dorsal portion of the third ventricle. Similar findings were made in human foetuses by Truex and Carpenter (1969).

The third ventricle showed three recesses. The funnel-like infundibular recess extended into the infundibulum, the optic recess projected ventrally in front of the optic chiasma and posteriorly, the pineal recess that extended between the habenular and posterior commissures into the stalk of the pineal body. This supports the findings made by Lignereux *et al.* (1991) in the ewe. The third ventricle appeared adult-like towards the terminal stages of pregnancy.

### 5.3.3 Aqueduct of Sylvius

The space enclosed by the mesencephalon, the mesocoele was relatively large during the initial stages of pregnancy. It became gradually narrow by the enlargement of the corpora quadrigemina and the basal plate as reported by Larsell (1951) in human foetuses. The aqueduct became narrow in 76 days-old subjects. The transverse diameter exceeded the vertical diameter throughout gestation. Increase in the length of aqueduct was in accordance with the growth of mesencephalon. The aqueduct was narrow at its initial portion; the diameter increased at the level of rostral colliculi and the greatest width was recorded at the level of the caudal colliculi. Similar observation was made in domestic animals by Dellmann and Mc Clure (1975). The cranial part was at a higher level than the caudal portion. Lignereux *et al.* (1991) observed that the conformation of the fourth ventricle, the bending of mesencephalic aqueduct and the inclination of the general axes of the cerebrum and mesencephalon in the ewe were similar to those of the cow.

Wall of the aqueduct was lined by ciliated ependymal cells, which were multilayered upto 62 days of age. By 76 days, this was pseudostratified and at 81 days, single layer of ciliated columnar cells appeared. Typical adult-like ependyma could be noticed at 144 days. These observations support the studies conducted in the foetal sheep and goats by Rajtova (1999).

#### **5.3.4 Fourth Ventricle**

Lumen of the hindbrain (metacoele and myelocoele) was diamond-shaped in cross section at 24 days of gestation (1.4cm CRL). Due to the thickening of the basal plates, the lumen was coffin-shaped by 26 days. By the age of 27 days, it was slit-like except at the region of the sulcus limitans. Reports on this aspect are not available in goat foetus for comparison.

Stretching of the roof plate to form thin roof of the fourth ventricle commenced at 40 days of gestation. Ventrolateral wall of this cavity was demarcated by the sulcus limitans into a ventromedial basal plate and dorsolateral alar plate. Similar observations were made in the dog foetus by Jenkins (1978). During the third month of gestation, dorsal surface of the brainstem that formed floor of the fourth ventricle was marked by a deep median sulcus that became shallower rostrally as reported by Dyce *et al.* (1996) in domestic animals.

During fifth month, the fourth ventricle was adult-like and was bounded by the rhomboid fossa ventrally, cerebellar peduncles laterally and rostral and caudal medullary vela and cerebellum dorsally which corresponded to the reports made earlier in domestic animals during postnatal life (Stromston, 1947; Dellmann and Mc Clure, 1975; Jenkins, 1978; Dyce *et al.*, 1996). Ventricular system communicated with the subarachnoid space by the foramina of Luschka. The median foramen of Magendie could not be located which is in accordance with the findings of Dellmann and Mc Clure (1975) in domestic animals, Malik *et al.* (1978) in goat and Malik *et al.* (2000) in elephant. Knowledge on the developmental pattern of the ventricular system and their measurements may be useful in studying the developmental anomalies associated with it.

#### **5.3.5 Choroid Plexus**

In the present study, the choroid plexus could be located for the first time in 2.5cm CRL goat foetus (40 days of gestation). Plexus of the fourth ventricle showed

more number of primary convolutions than that in the anterior regions which indicated that the choroid plexus of the fourth ventricle appeared a little earlier than in the other two ventricles. These agree with the findings of Rugh (1964) in the pig and Shuangshoti and Netsky (1966) and Truex and Carpenter (1969) in human foetus. According to Rugh (1964), the anterior choroid plexus appeared in the roof of the third ventricle at 2.4cm stage pig embryo and the posterior choroid plexus developed earlier in the roof of fourth ventricle. Truex and Carpenter (1969) noticed that the primordia of all choroid plexuses developed during the second month of gestation in man. Myelencephalic plexus appeared in six weeks embryo, telencephalic plexus in the seventh week and in the diencephalic area at eight weeks (Shuangshoti and Netsky, 1966). Contrary to this, Malik *et al.* (1992) found that in goat fetuses, primordium of telencephalic plexus developed in 5.0cm CRL fetuses followed by diencephalic and myelencephalic plexuses, respectively.

The originally flat surface of the caudal medullary velum became wrinkled and invaginated into the fourth ventricle by the blood vessels of pia mater. As a result of disproportionate growth of various parts of the ventral wall of the cerebral hemisphere, the choroid plexus protruded into the lateral ventricle along the choroid fissure. The horizontal cleft that persisted between the cerebral vesicle above and the diencephalon below was lined by a double layer of pia mater with many blood vessels and filled with loose mesenchyme. Upper layer of this protruded into the lateral ventricle and the lower layer formed the roof of the diencephalon and became invaginated as the choroid plexus of the third ventricle. Thus choroid plexus of the third ventricle was continuous with that of the lateral ventricle through the interventricular foramen and along the line of vesicle evagination. Similar observations were made in the human foetus by Truex and Carpenter (1969). Each primordium enlarged, became lobulated and each lobule later demonstrated secondary and tertiary branches. Histologically choroid plexus consisted of dilated blood vessels, connective tissue remnants of pia mater and a layer of ependymal cells as reported by Davis *et al.* (1973) in foetal pig.

In the lateral ventricle, stalk of the choroid plexus was double layered, each layer showed inner pial membrane and outer layer of ependymal cells. The ependymal layer was tall and pseudostratified in the initial stages. That portion of the ependymal lining of the ventricle which was originally reflected from the fornix to the dorsal



surface of the thalamus across the choroid fissure, was carried into the third ventricle with the choroid plexus and thus formed its ependymal covering. Dyce *et al.* (1996) cited that in domestic animals the choroid plexus of lateral and third ventricle, which merged within the interventricular foramen, developed within an invagination of pia that became entrapped between the expanding telencephalic vesicles and the roof of the diencephalon.

By 48 days (4.0cm CRL) the choroid plexus branched several times but did not fill the cavity. Towards the stalk portion, the cells were pseudostratified with eosinophilic cytoplasm. The portions of choroid plexus away from the stalk region were lined by single layer of low columnar cells. The spherical nucleus was seen towards the apical portion of the cell. Basal part of the cell was clear and vacuolated. This could be due to the dissolution of glycogen in the fixative as reported by Shuangshoti and Netsky (1966) in man. Sturrock (1979) observed both light and dark cells from 14 days of gestation in mice. There was no significant difference in the structure of choroid plexus of the three ventricles as noticed by Davis *et al.* (1973) in the foetal pig. There was a gradual decrease in the height of these cells as age advanced. Among the three ventricles, epithelium of lateral ventricles showed maximum height followed by third and fourth ventricles.

Lumen of the plexus showed dilated blood channels filled with non-nucleated erythrocytes. Fletcher. (1993) reported that the plexus capillaries were atypical because they possessed a fenestrated epithelium. Numerous tubules were formed by folding of the surface epithelium into the stroma during the differentiation of the plexus as reported by Shuangshoti and Netsky (1966) in human beings. Number of tubules increased at the same rate as the number of lobules of the plexus. Ventricles showed accumulation of secretion from the middle of second month. By 58 days (7.6cm CRL), almost two-third portion of the lateral ventricle was filled with the choroid plexus. In the third ventricle, the plexus filled the triangular roof portion. In the fourth ventricle, the primordium showed numerous secondary folds at the age of 48 days. By the end of second month, the plexus greatly enlarged and filled almost half of the ventricle.

In 76 days-old foetus, the branching pattern was more complex in the fourth ventricle. The epithelium was pseudostratified towards the stalk portion but simple low columnar in the remaining regions. In the lateral ventricle, the choroid plexus

reached its maximum size at the beginning of the third month. The plexus filled about three-fourth of the ventricle reaching up to the anterior levels. At the age of 76 days, the plexus epithelium was mostly simple low columnar and vacuolation of the cytoplasm was more evident. By 80 days (13.0cm CRL), entire choroid epithelium of lateral ventricle showed vacuolated cytoplasm. In the fourth ventricle also, the choroid epithelium showed glycogen granules during third month. Shuangshoti and Netsky (1966) reported that the glycogen content of cells of the myelencephalic plexus was greater than in the diencephalic plexus; but it was much less than in the telencephalic plexus. During fourth month also the same pattern was seen.

In every specimen examined, the epithelium was simple low columnar type, but areas of stratification and pseudostratification could always be identified. The epithelium was also pseudostratified at the stalk of the plexus. These findings indicated that the choroid epithelium was of multiple type, although largely simple low columnar at this stage. Towards term, the cells were typically cuboidal in shape with centrally placed nucleus and eosinophilic cytoplasm and no glycogen granules could be located at this stage. This is in accordance with the observations made by Evans *et al.* (1974) in foetal sheep. Truex and Carpenter (1969) reported that in human foetuses between 29 weeks and full term, the cytoplasm of these cells lost the glycogen content. Once removed, the glycogen never reappeared as a normal constituent of the adult choroid epithelium. They suggested that such disappearance of glycogen after birth, or at the beginning of aerobic oxidation, might be due to the fact that the developing nervous tissue uses energy, which is released by the anaerobic metabolism of glycogen. Mesenchymal elements were replaced by large amounts of connective tissue fibres, predominantly collagen fibres. Maximum amount of secretory tissue was seen in the lateral ventricles followed by the third and fourth ventricles. In goat, Malik *et al.* (1992) reported that this indicated the rostrocaudal decrease in the secretory activity of the ventricular system.

## 5.4 NEURONS AND NEUROGLIA

### 5.4.1 Neurons

At 1.4cm CRL (24 days of gestation), neuroepithelial cells were arranged radially in a pseudostratified manner in the inner ependymal layer of the neural tube wall. The middle mantle layer showed two types of cells, viz., the larger cells or neuroblasts and the smaller cells or the spongioblasts. Gilbert (1997) opined that the

neuroepithelial cells of the ependymal layer could give rise to the precursors of neurons and glial cells, which depends largely on the environment that they enter. Cortical migration of neuroblasts in the cerebrum and cerebellum commenced towards the middle of the second month. Gilbert (1997) found that about 80 percent of the young neurons migrated radially along the glial processes from the ventricular zone into the cortical plate and about 12 percent migrated laterally from one functional region of the cortex into another.

Aggregations of neuroblasts, the nuclei, first appeared during the seventh week in the brainstem. Gilbert (1997) reported that once the neuroblasts arrived at their final destination, they elaborated particular adhesion molecules that organised them together as brain nuclei.

Primitive Purkinje cells ( $11.3\mu\text{m}$ ) were differentiated by 58 days of gestation. Neurons of the deep cerebellar nuclei appeared at 76 days of age. The cytoplasm showed neurofibrils but the Nissl granules were not developed at this stage. In the cell body the neurofibrils interlaced but in the processes they ran straight. Neurofibrils have been reported to be characteristic of the nerve cells (Truex and Carpenter, 1969). In the red nucleus also, similar kinds of neurons appeared at this stage. At 81 days these neurons ( $37.5\mu\text{m}$ ) were typically multipolar with an axon and several dendrites. Multipolar motor neurons of the trigeminal nucleus ( $41.3\mu\text{m}$ ) appeared in the pons at 76 days. Unipolar neurons of the mesencephalic nucleus of the trigeminal nerve were arranged in a flower-like manner with eccentric nucleus by 81 days of age. Truex and Carpenter (1969) reported that unipolar sensory neurons were characteristic of the cerebrospinal ganglia and mesencephalic nucleus of the trigeminal nerve.

Granule cells of the cerebellum could be distinguished during the fourth month. During fifth month, these cells measured 3.8 to  $4.1\mu\text{m}$ . These are reported to be the smallest neurons of the brain (Truex and Carpenter, 1969). They found that the dimension of the cell body is proportional to the length, thickness, richness of branching and terminal arborization of its dendrites and axon. Golgi cells of the inner granular layer of the cerebellum appeared during the fourth month and were twice larger than that of the granule cells.

Most of the neurons of the thalamus and hypothalamus developed during the fourth month. Bipolar neurons appeared in the supraoptic nucleus of the

hypothalamus during the fourth month. Presence of bipolar neurons in the adult hypothalamus has been reported by Truex and Carpenter (1969) in human beings and Paramasivan and Sharma (2001) in the sheep. Multipolar neurons of the magnocellular part of the red nucleus measured  $52.5\mu\text{m}$  during the fourth month, which were one among the largest neurons of the entire brain measured during that period.

Pyramidal neurons of the cerebral cortex appeared during the fifth month. Double pyramidal cells also could be located in the hippocampus. Larsell (1951) reported that two series of large dendritic processes, directed in opposite directions, one into stratum oriens and the other into the stratum lacunosum-moleculare, gave rise to the term "double-pyramids" frequently applied to the neurons of the pyramidal layer.

Nissl granules started appearing in the cytoplasm of some of the neurons in the middle of fourth month. In the Purkinje cells these granules appeared during the initial stages of fifth month and at the age of 144 days, these were concentrically arranged. Towards term, the Nissl granules appeared in most of the neurons of the brain. These granules extended into the dendrites also. According to Truex and Carpenter (1969), Nissl bodies were coarser and more abundant in large neurons, especially motor neurons, and small and scarce in small neurons. The naked appearance of granule cells is said to be due to the complete absence of discrete Nissl granules and the thinness of rimming cytoplasm (Truex and Carpenter, 1969). They were usually absent from the most peripheral region of the perikaryon, axon hillock as well as the axis cylinder. Nissl bodies were reported to be part of a mechanism for synthesis of cytoplasmic proteins. Nucleus of most of the neurons appeared vesicular and centrally placed with a deeply staining nucleolus. Truex and Carpenter (1969) reported that small aggregates of deoxyribonucleic acid were scattered in a somewhat homogeneous nucleoplasm and accounted for the pale appearance of the nucleus. In the granule cells of the cerebellum, the nucleus was chromatic and non-vesicular.

#### **5.4.2 Neuroglia**

Neuroglia developed from the precursors, the spongioblasts. The nuclei of the spongioblasts were smaller and darker without a nucleolus unlike that of neuroblasts that possessed larger vesicular nucleus with a prominent nucleolus. Similar

observations were made in pig embryos by Patten (1948), in human embryos by Arey (1957) and Langman (1981). Towards the middle of second month, migration of spongioblasts along with the neuroblasts to form the outer cortical layer of the cerebrum commenced. By 58 days of gestation, the spongioblasts started differentiating into astrocytes and oligodendrocytes.

#### ***5.4.2.1 Astrocytes***

These were the largest among the glial cells. The astrocytes with their processes formed a delicate frame work in which the neural elements were suspended. The protoplasmic astrocytes were most numerous in the gray matter and the nucleus was finely granular, ovoid and pale. According to Buchanan (1957), scattered chromatin in small amounts and absence of nucleoli distinguished them from nuclei of nerve cells. In the white matter, fibrous astrocytes with long thin processes were numerous. Presence of glycogen granules also helped to distinguish them from the oligodendroglia and microglia. Hirano and Zimmerman (1967) noticed an increase in glycogen in both ependyma and astrocytes in response to injury in the rat. Truex and Carpenter (1969) reported that astrocytes manifested changes like hypertrophy in response to a variety of brain injuries. They also formed the glial limiting membrane as reported by Dellmann and Eurell (1998) in domestic animals.

#### ***5.4.2.2 Oligodendrocytes***

These were characterised by round nucleus and were smaller than that of the astrocytes. They were numerous both in the gray and white matter. Some of them were closely apposed to neuronal cell bodies. Buchanan (1957) reported that in the brain of human beings, most of the perineuronal satellites were oligodendrocytes but a few microglial cells were similarly situated. Interfascicular cells appeared in rows between the nerve fibres in the white matter. Truex and Carpenter (1969), Angevine (1975) and Sadler (2004) made similar observations in human embryos and found that they formed the myelin sheath. Oligodendrocytes also appeared throughout the gray and white matter in the form of perivascular satellites. Buchanan (1957) noticed that under pathological conditions these cells considerably increased in number.

#### ***5.4.2.3 Microglia***

These were distinguished from oligodendrocytes by smaller, denser and ovoid or elongated nuclei. These appeared at a later stage (76 days) when compared to other

types. Their number was comparatively less. Schultz *et al.* (1957) in their study on the brain of rats found that the microglia appeared in full numbers only after birth. Truex and Carpenter (1969) reported that they entered the nervous system as perivascular mesenchymal cells along with the neural blood vessels and has long been considered as the scavengers of the nervous system. They were located in the gray matter as juxtaneuronal cells. In the telencephalon they could be located in the subependymal regions of the lateral ventricles as reported by Trautwein *et al.* (1996) in the brain of bovines.

#### **5.4.2.4 Ependyma**

Ependymal cells also developed from the spongioblasts. Those which retained their attachment to the internal limiting membrane developed into adult ependymal cells and lined the ventricles of brain. During the first month, the inner ependymal layer was very thick. As age advanced, the thickness gradually reduced and by the end of second month, this layer was very thin with two to three layers of cells and they developed cilia on their luminal surface in the brainstem region. By the middle of third month, those lining the third ventricle, aqueduct and fourth ventricle acquired the adult features except for pseudostratification. In the lateral ventricle region, these changes were noticed at a later stage (101 days). These are in accordance with the findings of Rajtova and Kacmarik (1998) in small ruminants. They noticed that the ependymal surface was regionally differentiated by the end of first half of prenatal development. At 101 days, they were simple and co-arctation of cilia could be noticed on the surface. Presence of cilia throughout the ependymal surface of brain ventricles in adult goat has been reported by Kumar *et al.* (1997). Ependymal cells showed glycogen granules during third and fourth month and in the first half of fifth month of gestation as reported by Hirano and Zimmerman (1967) in the rat.

Choroid plexus of the lateral ventricle was lying closely adherent to the inner ependymal layer during third month. Hirano and Zimmerman (1967) noticed close relationship between some ependymal cells and blood vessels in rat brain. According to them, the astrocytes and ependymal cells were intimately related to the blood vessels, and, the tanycytes were considered as an intermediate form between these two.

Glial fibres, as a whole, formed a supportive framework throughout the brain. Dellmann and Eurell (1998) reported that the neuroglia provided structural support, formed CNS boundary, ensheathed and insulated axons, maintained a narrow extracellular space with proper ionic milieu, and, in the event of injury, phagocytosed debris and produced 'scar' tissue.

## 5.5 MENINGES

The meninges arose as condensation of the neighbouring mesenchyme. The pia mater started differentiating at 24 days (1.4cm CRL) of age. Externally, the dura mater started developing at 40 days (2.5cm CRL). The arachnoid developed in between these two at 48 days (4.0cm CRL). Arey (1957) reported that the dura mater developed in the human foetus by eight weeks. Studies on the morphogenesis of the hypophyseal meninges in the goat by Singh and Dhingra (1978) revealed that the hypophyseal dura mater started differentiating in embryos of 2.48cm CRL at caudodorsal surface of the primordium of neurohypophysis. The formation of arachnoid was evident in embryos of 5.55cm CRL. It assumed a typical fibrous structure at 13.50cm CRL. Pia mater encapsulated the whole primordium in 1.20cm CRL embryos.

### 5.5.1 Dura Mater

Dura mater started differentiating at 40 days and was a distinct entity by 48 days of gestation. It was made up of two layers, which were closely adherent except in regions of cranial venous sinuses. Thickness of dura varied greatly at different locations. It was the thickest among the three meninges as reported by Jenkins (1978) in domestic animals. The inner layer folded itself to form several partitions that projected into the cranial cavity, viz., falx cerebri, tentorium cerebelli and diaphragma sellae. Similar observations were made in domestic animals by Dellmann and McClure (1975), Jenkins (1978) and Dyce *et al.* (1996).

### 5.5.2 Arachnoid

Arachnoid was very thin and appeared by 48 days of age. Connective tissue fibres of the arachnoid formed an outer surface parallel to the inner surface of the dura mater and was covered on either side by simple squamous epithelium as noticed by King (1987) in domestic animals. From the arachnoid, strands of fibres formed a loose reticulum across the subarachnoid space, which were attached to the pia mater.

Thus the subarachnoid space contained a loose sponge-like tissue with spaces filled with cerebrospinal fluid (CSF). King (1987) reported that the arachnoid was a very thin membrane in domestic animals, which pressed against the dura mater by the pressure of CSF. Arachnoid followed the infoldings of the dura mater but it did not follow the sulci of cerebrum and cerebellum and bridged over them. Similar observations were made in domestic animals by Dellmann and Mc Clure (1975). In some regions, the subarachnoid spaces were of considerable depth constituting subarachnoid cisterns, viz., cisterna magna, cisterna fossa lateralis and cisterna pontis.

### **5.5.3 Pia Mater**

The pia mater started differentiating at the age of 24 days. Fine connective tissue fibres, mesenchymal cells and erythrocytes constituted the pia. At 27 days, the pia appeared as a continuous layer. Pia mater was highly vascularised and extended deep into the sulci of cerebrum and cerebellum. It was thicker than the arachnoid but thinner than the dura mater as reported by King (1987) in domestic animals. Depending on the vascularity, thickness of the pia varied over the surface of different regions of brain and in different age groups. In the regions of brainstem and cerebellum, thickness was maximum towards the end of second month as noticed by Morse and Low (1972) in rats and Shrivastava *et al.* (1989) in foetal goats. But on the cerebral surface, it showed maximum development during fifth month. It is suggested that the variation in the regional thickness of pia mater might be based on the regional vascularity since pia mater served as a pathway for blood vessels supplying different parts of the brain. Choroid plexus of lateral and third ventricles, which merged within the interventricular foramen, developed within an invagination of pia that became entrapped between the expanding telencephalic vesicles and the roof of the diencephalon. The plexus of the fourth ventricle developed separately within the pia over the caudal medullary velum as reported by Dyce *et al.* (1996) in domestic animals.

## **5.6 HISTOCHEMISTRY**

### **5.6.1 Lipids and Myelin**

Myelination in the foetal brain of goats began during third month. In the initial stages only a mild reaction was noticed. During the fifth month, most of the fibres were myelinated. In the telencephalon, myelinated fibres could be



demonstrated in the white matter, olfactory pathways, hippocampal fibres and in the internal capsule. Myelination was initially observed in the olfactory pathways and hippocampus. Clark (1965) and Kappers *et al.* (1967) reported that in vertebrates, myelination coincided approximately with the order in which the tracts have become developed phylogenetically. The first fields that medullated were those in which sensory impulses were located. They also found that the process of myelination was associated with the establishment of normal function. The optic chiasma and optic nerve fibres were also myelinated during the third month. On the other hand, in human foetus eventhough the myelination began at fourth month, these fibres did not become mature till the time of birth (Clark, 1965; Langman, 1981). In the cerebellum, the white matter showed a strong positive reaction for the lipids. A moderate reaction was noticed in the molecular layer. No lipids could be demonstrated in the external granular layer, Purkinje cell layer and the internal granular layer. According to Truex and Carpenter (1969), the mossy fibres as they entered from white matter into the internal granular layer of human cerebellum, they lost their myelin sheath. In the brainstem region, myelinated fibres could be demonstrated throughout the extent from the third month. But the medullary pyramids gave a positive reaction at a later stage (fifth month) as noticed in the human foetus by Clark (1965).

Lipid granules were also demonstrated in the pineal gland and tanocytes of the subcommissural organ. This confirms the observations made by Saigal *et al.* (1976), Kumar *et al.* (1996) and Kumar *et al.* (1998) in the goat. The epithalamo-epiphyseal tract fibres of the pineal gland showed intense reaction. The habenular commissure to which the pineal stalk was attached showed a strong positive reaction indicating heavy myelination of the commissural fibres. Towards term, degree of myelination was much more advanced. This is associated with the functional maturity of the kid at birth. The same pattern was observed in sheep brain by Clark (1965) but he noticed a relative absence of myelinated fibres in the newborn rat.

### **5.6.2 Carbohydrates**

Glycogen granules could be located in the neurons, ependymal cells lining the ventricles of brain and in astrocytes, which helped in distinguishing them from oligodendrocytes and microglia (Buchanan, 1957). Kumar *et al.* (1995b) reported that the abundance of glycogen in these cells played a role in the mediation of nutrition

from blood to nervous tissue proper. Modified ependymal cells of the choroid plexus of brain ventricles also showed a positive reaction from the middle of second month of gestation. But towards term the glycogen granules disappeared from these cells. Similar observations were made in the human foetus by Shuangshoti and Netsky (1966) and Truex and Carpenter (1969). They found that between 29 weeks and full term, the cytoplasm of these cells lost the glycogen. Once removed, the glycogen never reappeared as a normal constituent of the adult choroid epithelium. They suggested that such disappearance of glycogen after birth, or at the beginning of aerobic oxidation, might be due to the fact that the developing nervous tissue uses energy, which is released by the anaerobic metabolism of glycogen. Blood vessels of pia-arachnoid, choroid plexus and the brain tissue showed a PAS-positive reaction. The simple squamous epithelial covering on either side of the arachnoid was also positive as reported by Prasad and Sinha (1983) in buffaloes. The cerebral and cerebellar cortices showed a mild positive reaction as noticed by Manocha and Shantha (1969) in vertebrates. PAS-positive granules were also observed in the parenchyma of pineal gland and subcommissural organ, which supports the findings of Kumar *et al.* (1998) in goats. Neurons of supraoptic and paraventricular nuclei of hypothalamus gave a positive reaction. Presence of  $\beta$ -glucuronidase has been reported in these cells by Manocha and Shantha (1969).

### 5.6.3 Phosphatases

In the cerebral cortex, the outer plexiform layer gave a more intense reaction for alkaline phosphatase (ALP) than other layers. This is due to the abundance of synaptic regions in this layer as reported by Manocha and Shantha (1969) in vertebrate brains. Electron microscopical studies have proved that the synaptic junctions were rich in mitochondria and synaptic vesicles. White matter of the cerebrum also showed a positive reaction. The neurons and glial cells were negative. But the nucleoli of neurons gave a positive reaction due to the presence of ribonucleic acid (Manocha and Shantha, 1969). The tunica intima of blood vessels both in the gray and white matter showed a strong positive reaction. Kumar *et al.* (1998) in their studies on pineal gland of the goat reported that the blood capillaries presented a strong affinity for the enzyme indicating its significant role in the process of absorption and transport across the membranes. In the cerebellum, the white matter and granule cells showed a positive reaction. In the brainstem, ALP activity was

noticed in the blood vessels and neuropil. Activity was particularly strong in the hypothalamus especially in the highly vascularised supraoptic and paraventricular nuclei. Manocha and Shantha (1969) found a distinct correlation between ALP activity and increase in ribonucleic acid associated with the differentiation of hypothalamic neuroblasts. Choroid plexus of the ventricles and pia-arachnoid gave a strong positive reaction. Ependymal cells lining the ventricles and tanocytes of the subcommissural organ showed a positive reaction, which supports the findings of Talanti (1959) in the bovine foetus and Kumar *et al.* (1997) in the goat. A mild reaction for ALP was noticed in the pineal gland. Contrary to this, no definite reaction for ALP could be localised in the parenchyma of pineal gland in the adult goat by Kumar *et al.* (1998). This could be because ALP levels reached maximum before birth (Tam and Kwong, 1987).

Acid phosphatase (ACP) activity was less pronounced in the foetal brain when compared to that of ALP. This supports the findings of Tam and Kwong (1987) in the brain of mice who found that ALP activity reached highest levels before birth whereas the activity of ACP increased sharply after birth. The reaction was particularly strong at the site of production of lipofuscin pigment, which is an ageing pigment (Manocha and Shantha, 1969).

In general, ACP activity was noticed in the cytoplasm of all neurons and glial cells. In the white matter of brain, ACP activity could be noticed in the glial cells as reported by Manocha and Shantha (1969). Among the various neurons of the brain, the Purkinje cells, pyramidal neurons and cranial nerve nuclei showed more activity indicating a higher rate of metabolism in these cells. The granule cells of cerebrum and cerebellum showed only mild activity. This is due to the fact that these cells have only a thin rim of cytoplasm encircling the nucleus and have fewer mitochondria. The variability in the degree of positive activity indicated that individual neurons undergo a series of phasic activities in which the enzyme content of that cell increases or decreases depending on the functional status of the cell (Manocha and Shantha, 1969). Neispodziewanski (1964) in the studies on developing cerebellum in pigs noticed that localization of phosphatases was not stable; initially they predominated in the nucleus, and later in the nuclear and cellular membranes and in the cytoplasm. The ependymal cells reacted positively for ACP and ALP. The strong reaction for phosphatases in these cells was related to the energy cycle needed for differential permeability of the membranes as explained by Manocha and Shantha (1969) in

vertebrates. Histoenzymic studies on the pineal gland revealed a moderate ACP reaction in pinealocytes and glial cells as uniformly distributed granules, which supports the findings of Kumar *et al.* (1995a) in the goat.

It was concluded that in the goat foetus, even though the head parameters showed a greater increase during early gestation, the encephalometric parameters showed a spurt in growth during terminal stages, which is important in its teratological implications. Foetal CNS is most vulnerable when it is growing rapidly and nutritional deficiencies and diseases during the growing period can cause permanent damage. In the kids that walk within an hour after birth, cerebellar gyri and sulci were more numerous than in the cerebral cortex. The phylogenetically older brainstem developed more extensively at first and was then overtaken by the phylogenetically recent parts like cerebrum and cerebellum. The process of prosencephalization led to an increase in the size of cerebral hemispheres with increasing complexity of integrating mechanisms. Towards term, all parts of the brain were well developed and the relative maturity of the brain in goats at birth justifies the classification of goat as a prenatal brain developer.

## *Summary*

---

## 6. SUMMARY

Prenatal development of the brain in goats was studied using 52 fetuses ranging from 1.4cm CRL (24 days of gestation) to 41.5cm CRL (full term). Based on the age, the fetuses were divided into five groups representing five months of gestation. At 24 days of age, dilated cephalic end of the neural tube showed five brain vesicles, viz., telencephalon, diencephalon, mesencephalon, metencephalon and myelencephalon. Expansion of the cerebral vesicles commenced at 26 days of age and this ballooning resulted primarily from an increase in the cavity size. Thickening of the ventrolateral walls of the diencephalon compressed the relatively broad lumen of the third ventricle. The median ventral trough-like diverticulum represented the infundibulum. Wall of the three caudal brain vesicles showed the typical arrangement of longitudinal alar and basal plates marked by the sulcus limitans.

Histologically wall of the neural tube at 24 days of age showed an inner ependymal, middle mantle and outer marginal layers bounded by the inner and outer limiting membranes. Inner ependymal layer was the thickest of all, composed of proliferating neuroepithelial cells. These cells differentiated into neuroblasts and spongioblasts that occupied the middle mantle layer. The outer non-cellular marginal layer was the thinnest, composed of growing processes of the neuroblasts.

Differential growth of the rostral end of the neural tube gave rise to the brain flexures, viz., cephalic, cervical and pontine flexures. All these had developed in 24 days-old embryos.

Weight, volume, length, width and thickness of the brain showed an increasing trend with the increase in body weight and advancement of age. Among these parameters, more significant positive correlation was noticed between the body weight and brain weight. A rapid increase in both the parameters was noticed in the second half of gestation with a spurt in growth between fourth and fifth month of age. The percentage contribution of brain to body weight showed a decreasing trend during prenatal period. Among the other body parameters, maximum positive correlation was noticed between the brain weight and total body length.

In all age groups, length of the brain was more than its width followed by the thickness. Length of the brain and its various components showed more significant correlation with the age than with the body weight. Percentage contributions of

cerebral hemispheres to the total brain weight showed a sharp and steady increase during gestation. Right cerebral hemisphere was slightly heavier (0.88 percent) than the left one. This could be explained by the fact that the left hemisphere, which is larger than the right in human beings, controls most language functions and animals show little capability for such functions. Cerebellar parameters showed a spectacular growth spurt towards the terminal stage of pregnancy, which is interesting in its teratological implications. Unlike in the case of cerebrum and cerebellum, percentage contribution of brainstem to total brain weight decreased during gestation. The phylogenetically older brainstem developed more extensively in the first half of gestation.

Head constituted almost one-half of the curved crown rump length during second month. All the head and skull parameters showed an increasing trend with the advancement of age. Percentage increase for cranial and facial length were 845.7 and 341.4, respectively from second to fifth month, which indicated faster growth of the cephalic region than face. This could be due to the intracranial pressure exerted by the rapidly expanding brain. Highly significant positive correlation was noticed between brain parameters and some body parameters. Regression equations derived from these can be used to predict the brain parameters during gestation from known body parameters of the foetus. Thus one can assess the normal growth rate of brain and also cases of hypoplasia and other disorders. All the head parameters showed a greater increase during early gestation than in later stages. But the whole brain, cerebrum and cerebellum showed a spurt in growth during terminal stages of pregnancy, which explains the highly complex structural pattern of the cerebral and cerebellar cortices. The convoluted cortex allows increased surface area so that more brain tissue can be accommodated in the available space. Percentage contribution of head length to curved crown rump length showed a gradual decrease during gestation, which can be attributed to the faster growth of the body in comparison to the head to adapt viscera for specific postnatal physiological needs. Calculated cephalic indices showed that in the first half of pregnancy, the foetal head was relatively short whereas, in the second half, it was long and narrow.

Even though the cartilaginous cranial vault appeared by 40 days of gestation, boundaries of the skull bones became identifiable by 54 days. A highly significant positive correlation existed among brain length and medial length of frontal and

parietal bones. A spurt in brain growth and growth of the cranial bones was noticed during fifth month. Bones forming the base of cranium showed a slower growth rate than those forming the sides and roof.

During second month, the surface of the cerebral hemispheres was almost smooth. Lateral wall was the thickest followed by dorsal, ventral and medial walls. Gyri and sulci started developing by 69 days of age. The rhinal sulcus, Sylvian sulcus, suprasylvian sulcus and hippocampal fissure appeared at this stage. By 76 days, the coronal and marginal sulci appeared. At 83 days, the cruciate fissure also made its appearance.

During the fourth month, the ansate, endomarginal, callosal, diagonal, presylvian, ectosylvian and endogenual sulci started appearing. At the beginning of the fifth month, the cerebral surface showed most of the gyri and sulci. The ectomarginal sulcus was absent. By term, numerous secondary and tertiary sulci appeared dividing the cortical surface into numerous small gyri and the cerebral surface attained the adult pattern.

In the cerebrum towards the middle of second month, neuroblasts and spongioblasts of the inner ependymal layer migrated outwards through the mantle layer into the marginal zone thereby forming a superficial gray cortex. Thus the position of gray and white substances of the spinal cord were largely reversed in this region of brain. By 48 days, this cortical plate showed an outer molecular and inner cellular layers. White matter showed many radiating fibres and migrating cells. By 76 days, the cerebral cortex revealed four layers, viz., outer molecular, superficial granular, intermediate granular and deep granular layers.

Unlike in the third month, the white matter did not reveal waves of migrating cells during fourth month, which indicated that the cortical migration already came to an end by about 12 weeks of gestation and the cortical cells, were undergoing differentiation during the fourth month. In the fifth month, the neocortex was divided into six layers, viz., the outer molecular, external granular, external pyramidal, internal granular, internal pyramidal and the fusiform cell layers. The cerebral cortex was thicker at the top of the gyrus and the thickness gradually diminished towards the floor of the sulcus. Average thickness of the cerebral cortex decreased from the fourth to the fifth month. This could be associated with the increase in the number of



gyri and sulci so that the cerebral cortical tissue will be more vascularised by the pia mater that closely invests the cortical tissue. The white matter filled in the space between cortex, ventricles and the basal nuclei and formed the medullary core of the various convolutions.

The olfactory bulb was well developed by 48 days and the lateral ventricle extended into it, which projected cranioventrally from the frontal pole of the cerebral hemisphere. At 81 days, the olfactory peduncle was divided into medial and lateral olfactory striae separated by the olfactory trigone. In the fifth month, the wall showed a laminar organisation with mitral cells and granule cells.

Hippocampus appeared as a thickened area on the medial wall of cerebral hemisphere immediately above and parallel to the choroid fissure by 48 days of gestation. It was separated from the thalamus by a cleft filled with the velum interpositum. During the fifth month, hippocampus formed a rounded eminence in the floor of the temporal horn of the lateral ventricle and arched caudodorsally and rostrally in the ventricular floor. Histologically, the hippocampus revealed an inner ependymal layer, middle mantle layer with developing pyramidal neurons and outer marginal layer at 48 days of age. Cortical migration of cells also started. A band of fibres converged from the hippocampus ventrally as the fimbria, to which attached the choroid plexus of the lateral ventricle. At 76 days, the ventricular surface of the hippocampus was covered by the alveus. By 144 days the hippocampus revealed an ependymal layer, stratum alveus, stratum oriens, stratum pyramidale and stratum lacunosum-moleculare in cross section.

Basal nuclei appeared as a gray mass in the floor of cerebrum near the thalamus at 40 days of gestation. The internal capsule separated the caudate nucleus from the rest of the gray substance in the sixth week. The lenticular nucleus and the external capsule appeared during the seventh week. By 62 days, two divisions of the lenticular nucleus, viz., the globus pallidus and the putamen started differentiating. The claustrum was demarcated from the insular cortex by the extreme capsule at 101 days. The amygdaloid body appeared as a distinct entity during the fifth month.

Histologically, the neuroblasts outnumbered the glial cells in the caudate nucleus by 58 days and these neuroblasts were of two types; large and small cells. The lenticular nucleus showed islands of cells separated by fibre bundles during third

month. In some regions, caudate and lenticular nuclei were interconnected by transverse cellular bands crossing the internal capsule. In the fifth month, caudate nucleus and putamen showed large multipolar neurons scattered among small stellate cells. The globus pallidus contained large multipolar neurons and spindle-shaped neurons.

Cerebellum developed from the roof of the metencephalon. The rhombic lips expanded medially and fused in the midline by the seventh week and showed the small midline portion, the vermis and two lateral portions, the cerebellar hemispheres. Cerebellar folia started developing at 62 days. By 101 days, of the nine classical lobules, six were well developed. The declive, folium and tuber appeared as a single mass. Similarly the pyramid and uvula were also not subdivided. Cerebellar gyri and sulci were more numerous than in the cerebral cortex. Cerebellum contributed 9.43 percent of the total brain weight during the fifth month and all the nine classical lobules appeared. In the full term foetus, cerebellum acquired the characteristic adult appearance.

Histologically, wall of metencephalon showed the original three layers of the neural tube wall. By the seventh week the external granular layer containing proliferating neuroepithelial cells, unique to the foetal cerebellum, appeared. Neurons of the deep cerebellar nuclei started appearing by 48 days. Primitive Purkinje cells, the internal granular layer and the white matter appeared towards the end of second month. During the fourth month, all layers of cerebellum, viz., external granular, molecular, Purkinje cell layer, internal granular layer and the white matter could be clearly distinguished. Mean thickness of the external granular layer was maximum at this stage. Outer molecular layer showed the outer stellate cells and inner basket cells. Purkinje cells were arranged as a definite layer by 101 days. Inner granular layer showed Golgi cells in addition to the granular cells. By term, thickness of the external granular layer greatly reduced indicating functional maturity. This might be one of the reasons attributed to the fact that the kids could walk immediately after birth.

Walls of diencephalon thickened much and the two thalami grew into approximation so that the third ventricle became a slit-like cavity by 48 days. The thalami united across the midline by a massa intermedia. Pineal body developed during the seventh week as a conical evagination from the roof of diencephalon at the posterior aspect. From the trough-like floor of hypothalamus the infundibulum

developed during seventh week. Optic chiasma also appeared at 48 days. Towards the end of second month, all components of pituitary were greatly enlarged. The supraoptic nucleus also started developing. Grossly the mamillary body appeared as a distinct entity on the basal surface of hypothalamus during the fourth month. The width of the diencephalon was more than its height and length throughout the prenatal period.

Cellular aggregations, the nuclei, first appeared in the brain of goat foetuses during the seventh week, in the diencephalon. Tunics of eyeball started differentiating by 48 days and they could be clearly distinguished towards the end of second month. The subcommissural organ developed immediately beneath the posterior commissure during second month and was lined by tanocytes. During third month, stratum zonale, external medullary lamina, internal medullary lamina and medial, centromedian and ventral nuclei started developing. By 76 days, the pineal gland showed pinealocytes and glial cells. During fourth month, neurons were differentiated in the thalamic and hypothalamic nuclei. The supraoptic nucleus showed spindle-shaped and bipolar neurons. During fifth month, the diencephalon showed most of the nuclei including the reticular nucleus. At 144 days, the pineal gland showed light and dark pinealocytes and four types of glial cells.

Width of mesencephalon was more than its height during prenatal period. Wall of the mesencephalon was thickened and showed three regions; the tectum, tegmentum and crura cerebri by 48 days. The alar plates developed into the primordium of corpora quadrigemina and the rostral colliculus was separated from the caudal colliculus by a groove. The crura cerebri bulged conspicuously towards the end of second month. The cephalic flexure was no longer visible during the third month. The aqueduct became narrow in 76 days-old subjects and the ciliated ependymal lining was single layered at 81 days. In general, growth rate of mesencephalon was less in the second half of gestation indicating a cephalic shift of function from phylogenetically older brainstem to the higher cerebral and cerebellar cortices.

Histologically, the primordial quadrigeminal plate developed by the invasion of neuroblasts in the dorsal marginal zone. Reticular formation of the tegmentum appeared during seventh week. Multipolar neurons of the red nucleus made their presence by 48 days. Mesencephalic nucleus of trigeminal nerve, nuclei of

oculomotor and trochlear nerves, tegmental nuclei and substantia nigra appeared by mid gestation. Mesencephalic nucleus of trigeminal nerve showed flower-like arrangement of unipolar neurons in the lateral margin of central gray of the aqueductal region by 81 days. At the same time, the red nucleus showed magnocellular and parvocellular parts. Each colliculus showed stratum zonale, cinerium, opticum and stratum lemnisci from outer to inner. The corticospinal tract appeared as a compact bundle of myelinated nerve fibres at caudal levels of mesencephalon during the fifth month.

Basal plate of metencephalon greatly enlarged to form the pons at the floor of the fourth ventricle. Pons occupied approximately the central portion of the brainstem. A fibrous protuberance developed on the ventral aspect of the pons by 76 days, which continued into the middle cerebellar peduncles. Rostral border of the pons was straight.

Histologically, motor nuclei of origin for cranial nerves V, VI and VII and the pontine nuclei started appearing in the mantle layer of pons by 48 days. Some alar plate neurons migrated ventrally from the lateral wall to the basal plate to form the pontine nuclei. Motor neurons of the trigeminal nerve were larger than the sensory neurons. During fourth month, dorsal longitudinal fasciculus became a sharply defined spherical bundle, which lay close to the raphe below the gray matter of the floor of the fourth ventricle. During fifth month, the pons was divided into a dorsal tegmental part and a basilar part.

Medulla oblongata extended from the level of first pair of cervical nerves to the caudal edge of pons. By 40 days of gestation, the roof plate region of the rhombencephalon expanded enormously and as a result the entire alar and basal plates of the neural tube were displaced laterally and ventrally which can be compared to opening a book. The expanded lumen became the fourth ventricle, which was covered dorsally by the cerebellum and the thin anterior and posterior medullary vela. The trapezoid body started developing by 48 days. The medullary pyramids appeared on the ventral surface by 81 days of age. Grossly medulla oblongata was adult-like by the terminal stages of pregnancy.

Histologically, the myelencephalon showed the same basic pattern of the neural tube wall up to the sixth week. Proliferation of neuroblasts in localised regions

of mantle layer led to formation of nuclei that were evident at 48 days. Nerve fibres crossing in different directions broke up the gray substance into a mixture of gray and white known as the reticular formation. The main difference from spinal cord was that a sharp demarcation between the gray and white substances disappeared. The floor plate region was replaced by the midline raphe that extended into the pons and mesencephalon. Lateral to the medullary pyramids, the inferior olivary nucleus appeared by 81 days as a folded bag with the hilus directed medially. Nuclei and fibre tracts associated with cranial nerves V to XII were located at different levels of medulla oblongata.

The dilated cavities of the brain vesicles were the forerunners of the ventricular system of brain. They underwent extensive alterations as a result of cellular proliferation, growth and development of brain flexures. Lateral ventricles appeared as a distinct entity by 26 days. They communicated with each other and with the third ventricle through the foramina of Monro. Length and width of lateral ventricles increased from first month to fifth month. But the mean height first increased and from fourth month onwards the height gradually decreased due to the thickening of the cerebral walls.

Third ventricle was an unpaired, cleft-like space lying between the two thalami. Towards the end of second month, the triangular wide portion at the roof was almost completely filled with choroid plexus. Third ventricle showed the infundibular, optic and pineal recesses from the second month onwards. Cilia appeared on the surface of ependymal cells in the middle of second month and acquired their adult characteristics towards the terminal stages of pregnancy.

Mesocoele was relatively broad during initial stages and the aqueduct became narrow in 76 days-old subjects. Aqueduct was relatively narrow at its beginning portion; the diameter increased at the level of rostral colliculi and the greatest width was recorded at the level of the caudal colliculi. Wall of the aqueduct was lined by multilayered ciliated ependymal cells during second month. By 76 days, this was pseudostratified and typical adult-like ependyma could be noticed towards the terminal stage.

Cavity of rhombencephalon expanded to the sides by stretching of the roof plate to form the fourth ventricle at 40 days of gestation. During third month, dorsal

surface of brainstem that formed floor of the fourth ventricle was marked by a deep median sulcus. During fifth month, the fourth ventricle was adult-like and communicated with the subarachnoid space by the foramina of Luschka. The median foramen of Magendie could not be located. Knowledge on the developmental pattern of the ventricular system and their measurements may be useful in studying the developmental anomalies associated with it.

Choroid plexus first appeared in brain ventricles at 40 days of gestation. Plexus of the fourth ventricle showed more number of primary convolutions than in the anterior regions, which indicated that the choroid plexus of the fourth ventricle appeared a little earlier than in the other two ventricles. Each primordium enlarged, became lobulated and each lobe later demonstrated secondary and tertiary branches. Histologically, choroid plexus consisted of dilated blood vessels, connective tissue remnants of pia mater and a layer of ependymal cells. In every specimen examined, the epithelium was simple low columnar type, but areas of stratification and pseudostratification could always be identified. There was a gradual decrease in the height of these cells as age advanced. Among the three ventricles, epithelium of lateral ventricle showed maximum height followed by the third and fourth ventricles. Choroid plexus of the lateral ventricle reached its maximum size at the beginning of the third month. Maximum amount of secretory tissue was seen in the lateral ventricles followed by the third and fourth ventricles. During second month, cytoplasm of the lining epithelium was eosinophilic with central nucleus. Ventricles showed accumulation of secretion from the middle of second month. During third month, the entire choroid epithelium showed vacuolated cytoplasm due to the presence of glycogen granules and the nucleus was seen towards the apical portion of the cell. Towards term, the cells were cuboidal with eosinophilic cytoplasm and centrally placed nucleus and no glycogen granules could be demonstrated at this stage.

Primitive neurons could be clearly distinguished from spongioblasts at 40 days. Aggregation of neuroblasts, the nuclei, first appeared in the seventh week in the thalamus, mesencephalic tegmentum, pons and medulla oblongata. Multipolar neurons showed neurofibrils in the cytoplasm towards the middle of gestation. But the Nissl granules appeared in the middle of fourth month. Most of the neurons of the brain differentiated during fourth month. Nuclei of most of the neurons were

vesicular, centrally placed with dark staining nucleoli. In the granule cells of cerebellum, the nuclei were chromatic and non-vesicular.

The spongioblasts started differentiating into astrocytes and oligodendrocytes by 58 days of gestation. Microglia appeared at a later stage (76 days of gestation). Astrocytes were the largest among the glial cells. Their nuclei were finely granular, ovoid and pale. Presence of glycogen granules also helped to distinguish them from oligodendrocytes and microglia. Oligodendrocytes were characterised by round nucleus of smaller diameter and were numerous both in gray and white matter. Microglia were distinguished from oligodendrocytes by smaller, denser and ovoid or elongated nuclei and were less in number. Those spongioblasts that retained their attachment to the internal limiting membrane developed into adult ependymal cells and lined the ventricles of brain. During first month, the inner ependymal layer was very thick and stratified. As age advanced, thickness gradually reduced and by the second month, they developed cilia on their luminal surface. By the middle of gestation, they acquired the shape of adult ependyma but were pseudostratified and co-artation of cilia could be noticed on the surface. By 81 days, it was single layered in the aqueductal region.

The meninges arose as condensation of neighbouring mesenchyme. The pia mater started differentiating by 24 days of age and the dura at 40 days. Cartilaginous cranial vault also appeared by 40 days. The arachnoid developed at 48 days of age. The thickest one, the dura mater was made up of two layers that were closely adherent except in regions of cranial venous sinuses. The dura was generally thicker in the ventral aspect of brain when compared to the sides and top. Arachnoid, the thinnest of the three, followed the infoldings of the dura but it did not follow the sulci of cerebrum and cerebellum but bridged over them. From the arachnoid, strands of fibres formed a loose reticulum across the subarachnoid space. Pia was highly vascularised and extended deep into the sulci. Depending on the vascularity, thickness of the pia mater varied over different regions and at different ages. In the brainstem and cerebellum, thickness was maximum towards the end of second month. But on the cerebral surface it showed maximum development during fifth month.

Histochemical studies revealed that the myelination began in the foetal brain during third month. During fifth month, most of the fibres were myelinated. This is associated with functional maturity of the kid at birth. Lipid granules were also

demonstrated in the cells of pineal gland and tanocytes of subcommissural organ. Glycogen could be demonstrated in the neurons, ependyma, astrocytes and choroid plexus epithelium. Alkaline phosphatase reaction could be located in the outer plexiform layer of cerebral cortex, white matter, hypothalamus, blood vessels, choroid plexus, pia-arachnoid and ependyma. In general, acid phosphatase activity was less pronounced in the foetal brain. Activity was noticed in the cytoplasm of all neurons and glial cells. Among these, the Purkinje cells, pyramidal neurons and cranial nerve nuclei showed more activity indicating a higher rate of metabolism in these cells.

It was concluded that in the goat foetus, even though the head parameters showed a greater increase during early gestation, the encephalometric parameters showed a spurt in growth during terminal stages, which is interesting in its teratological implications. Towards term, all parts of the brain were well developed and the relative maturity of the brain in goats at birth justifies the classification of the goat as a prenatal brain developer.



## *References*

---

## REFERENCES

- Adejumo, D.O. 1992. Gestational changes in foetal development, acetyl choline esterase activity and total protein concentration in the developing goat foetal brain. *Int. J. Anim. Sci.* 7: 31-34
- Allen, D.J. and Low, F.N. 1973. The ependymal surface of the lateral ventricle of the dog as revealed by scanning electron microscopy. *Am. J. Anat.* 137: 483-490
- Andreoli, J., Rodier, P. and Langman, J. 1973. The influence of a prenatal trauma on formation of Purkinje cells. *Am. J. Anat.* 137: 87-102
- Angevine, J.B. 1975. The nervous tissue. *A Text Book of Histology* (eds. Bloom, W. and Fawcett, D.W.). W.B.Saunders Company, Philadelphia, pp.333-385
- Archana, Sudhakar, L.S., Sharma, D.N. and Bhardwaj, R.L. 1998. Craniometry in yak (*Bos grunniens*). *Indian J. Vet. Anat.* 10: 1-8
- Arey, L.B. 1957. *Developmental Anatomy*. Sixth edition. W.B.Saunders Company, Philadelphia, p.676
- \*Baer, S., Hummeg, G. and Goller, H. 1985. Ultrastructure of the hippocampus of cattle, sheep and goats. *Anat. Histol. Embryol.* 14: 242-261
- Bancroft, J.D. and Stevens, A. 1977. *Theory and Practice of Histological Techniques*. Churchill Livingstone, Edinburgh, p. 436
- \*Barone, R. and Dowcet, J. 1964. Morphology and topography of the gray matter in the medulla oblongata in cattle. *Ann. Biol. Anim. Biochem. Biophys.* 4: 307-343
- \*Beery, F. 1962. Development of motility and histological differentiation in the feline cerebellum during the first week of life. *Schweizer Arch. Tierheilk.* 104: 701-721
- Bell, F.R. and Lawn, A.M. 1956. Delineation of motor areas in the cerebral cortex of the goat. *J. Physiol.* 133: 159-166

- Bell, A.D. and Variend, S. 1985. Failure to demonstrate sexual dimorphism of the corpus callosum in childhood. *J. Anat.* 143: 143-147
- Bhaskaran, G. 2001. Brain dynamics: Neural correlates of mental activities. *Curr. Sci.* 80: 1372-1373
- Blinderman, E. and Brown, W.J. 1966. Maturation and water composition of murine cerebrum, cerebellum, brainstem and spinal cord. *Anat. Rec.* 154: 753-758
- Boya, J., Calvo, J. and Prado, A. 1979. The origin of microglial cells. *J. Anat.* 129: 177-186
- Bradley, O.C. 1948. *Topographical Anatomy of the Dog*. Fifth edition. Oliver and Boyd, Edinburgh, p. 319
- Brizzee, K.R. and Jacobs, L.A. 1959. The glia to neuron index in the submolecular layers of the motor cortex in the cat. *Anat. Rec.* 134: 97-105
- Buchanan, A.R. 1957. *Functional Neuroanatomy*. Third edition. Lea and Febiger, Philadelphia, p. 362
- \*Bujak, A. 1967. Development of the nucleus interpositus of the cerebellum in the pig. *Polskie Archwm Wet.* 10: 693-704
- Calvo, J., Boya, J., Maurino, J.E.G. and Carbonell, A.L. 1988. Structure and ultrastructure of the pigmented cells in the adult dog pineal gland. *J. Anat.* 160: 67-73
- Cammermeyer, J. 1966. Morphologic distinctions between oligodendrocytes and microglia cells in the rabbit cerebral cortex. *Am. J. Anat.* 118: 227-248
- Card, J.P. and Rafols, J.A. 1978. Tanycytes of the third ventricle of the neonatal rat: A Golgi study. *Am. J. Anat.* 151: 173-190
- \*Choi, B.H. and Lowell, W.L. 1980. Evolution of Bergmann glia in developing human foetal cerebellum: A Golgi, electron microscopic and immunofluorescent study. *Brain Res.* 190: 369-384

- Chrisman, C.L. 1991. *Problems in Small Animal Neurology*. Second edition. Lea and Febiger, Philadelphia, p.526
- Clark, W.E.L. 1965. *The Tissues of the Body*. Fifth edition. Oxford University Press, London, p.423
- Crosby, E.C. and Schnitzlein, H.N. 1982. *Comparative Correlative Neuroanatomy of the Vertebrate Telencephalon*. Mac Millan Publishing Company, New York, p.522
- \*Danko, J. 1999. The development of the sulcus hippocampi of the sheep. *Folia Vet.* 43: 147-148
- Davis, D.A., Lloyd, B.J. and Milhorat, T.H. 1973. A comparative ultrastructural study of the choroid plexus of the immature pig. *Anat. Rec.* 176: 443-453
- De Lahunta, A. 1983. *Veterinary Neuroanatomy and Clinical Neurology*. Second edition. W.B. Saunders Company, Philadelphia, p.471
- Dellmann, H.D. and Eurell, J.A. 1998. *Textbook of Veterinary Histology*. Fifth edition. Lippincott Williams and Wilkins, Philadelphia, p.380
- Dellmann, H.D. and Mc Clure, R.G. 1975. Central nervous system. *Sisson and Grossman's The Anatomy of the Domestic Animals*. Fifth edition. (ed. Getty, R.). W.B. Saunders Company, Philadelphia, pp.1065-1080
- \*Deutsch, K. 1973. An electron microscopical study of the cerebral cortex of the calf. 1. The normal calf. *Zentbl. Vet. Med.* 20: 434-439
- Done, J.T. and Hebert, C.N. 1968. The growth of the cerebellum in foetal pig. *Res. Vet. Sci.* 9: 143-148
- Dyce, K.M., Sack, W.O. and Wensing, C.J.G. 1996. *Textbook of Veterinary Anatomy*. Second edition. W.B. Saunders Company, Philadelphia, p. 856
- \*Eustachiewicz, R. and Luszczewska, I. 1999. The morphology and topography of *formatio hippocampi* in the polar fox (*Alopex lagopus*). *Medna Vet.* 54: 33-45

- Evans, C.A.N., Reynolds, J.M., Reynolds, M.L., Saunders, N.R. and Segal, M.B. 1972. The development of blood brain barrier and choroid plexus function in immature foetal sheep. *J. Physiol.* 224: 15-16
- Evans, C.A.N., Reynolds, J.M., Reynolds, M.L., Saunders, N.R. and Segal, M.B. 1974. The development of blood brain barrier mechanism in foetal sheep. *J. Physiol.* 238: 371-386
- Ferrer, I., Fabregues, I. and Condom, E. 1986. A Golgi study of the sixth layer of the cerebral cortex. II. The gyrencephalic brain of Carnivores, Artiodactyla and Primates. *J. Anat.* 146: 87-104
- Ferrer, I., Fabregues, I. and Condom, E. 1987. A Golgi study of the sixth layer of the cerebral cortex. III. Neuronal changes during normal and abnormal cortical folding. *J. Anat.* 152: 71-82
- \*Fleischhauer, K. and Angelika, V. 1979. Cell densities in the various layers of the rabbit striate area. *Anat. Embryol.* 156: 269-282
- Fletcher, T. F. 1993. Nervous system. *Textbook of Veterinary Histology*. Fourth edition. (ed. Dellmann, H.D.). Lea and Febiger, Philadelphia, pp. 87-107
- Fox, M.W. 1963. Gross structure and development of the canine brain. *Am. J. Vet. Res.* 24: 1240-1247
- \*Gabr, M. A., El Din, M.A.A., Abdel, M.M.E. and Hassan, S.A.S. 1991. Histogenesis of the cerebellar cortex in camel. *Assiut Vet. Med. J.* 25(50): 27-38
- Ganong, W. F. 2003. *Review of Medical Physiology*. Twenty-first edition. Mc Graw Hill, Boston, p. 912
- Geelen, J.A.G. and Langman, J. 1977. Closure of the neural tube in the cephalic region of the mouse embryo. *Anat. Rec.* 189: 625-640
- \*Geurts, F.J., Timmermans, J.P., Shigemoto, R. and De Schutter, E. 2001. Morphological and neurochemical differentiation of large granular layer interneurons in the adult rat cerebellum. *Neuroscience* 104: 499-512

- Ghosh, R. K. 2002. *Essentials of Veterinary Embryology*. Medical Book Company, Kolkatta, p.127
- Gilbert, S.F. 1997. *Developmental Biology*. Fifth edition. Sinauer Associates, Sunderland, p.473
- \*Gruetze, I. 1978. On the nuclei of the mamillary body and the fibre connections of the mamillary body of cattle. *Z. Mikrosk. Anat. Forsch.* 92: 317-339
- Gupta, S.K. and Sharma, D.N. 1990. Biometry of the bovine skull. *Indian J. Anim. Res.* 24: 110-114
- Gupta, S.K. and Sharma, D.N. 1992. Canine encephalometry. *Haryana Vet.* 31: 192-195
- Harper, J.W. and Maser, J.D. 1975. A microscopic study on the brain of bison (*Bison bison*), the American plain buffalo. *Anat. Rec.* 184: 187-202
- Harrison, R. G. 1978. *Clinical Embryology*. Academic Press, London, p. 250
- Herrera, M., Campo, F.S.D., Ruiz, A. and Agreda, V.M. 1988. Neuronal relationships between the dorsal periaqueductal nucleus and the inferior colliculus (Nucleus commissuralis) in the cat. A Golgi study. *J. Anat.* 158: 137-145
- Hirano, A. and Zimmerman, H.M. 1967. Some new cytological observations of the normal rat ependymal cell. *Anat. Rec.* 158: 293-302
- \*Houston, M. L. 1968. The early brain development of the dog. *J. comp. Neurol.* 134: 371-384
- Hubbert, W. J., Hughes, D.E., Stalheim, O.H.V. and Booth, G.D. 1974. Weight changes of rhombencephalon and eye lens in the developing bovine foetus. *Am. J. Vet. Res.* 35: 769-772
- Huettner, A.F. 1967. *Fundamentals of Comparative Embryology of the Vertebrates*. Second edition. The Mac Millan Company, New York, p. 309

- Humason, G. L. 1972. *Animal Tissue Techniques*. Third edition. W. H. Freeman and Co., San Fransisco, p.641
- \*Inouye, M. and Ichi, S.O. 1980. Strain-specific variations in the folial pattern of the mouse cerebellum. *J. comp. Neurol.* 190: 357-362
- Ito, T. and Matsushima, S. 1969. A quantitative morphological study of the postnatal development of the pineal body of the mouse. *Anat. Rec.* 165: 447-452
- Jacobson, A.G. and Tam, P.P.L. 1982. Cephalic neurulation in the mouse embryo analyzed by SEM and morphometry. *Anat. Rec.* 203: 375-396
- Jain, K.K. and Koranne, S.P. 1976. Some observations on pineal organ of *Bos indicus* and *Sus vittatus*. *J. anat. Soc. India.* 25: 12-15
- \*Jastrzebski, M. 1973. Development of the myelin sheaths of the cranial nerves in the bovine medulla oblongata. *Zentbl. Vet. Med.* 2: 221-228
- Jenkins, T.W. 1978. *Functional Mammalian Neuroanatomy*. Second edition. Lea and Febiger, Philadelphia, p.480
- \*June, S.K. 1978. Development and cytoarchitecture of cerebral cortex in insular gyri of normal Korean foetus. *Seoul J. Med.* 19: 211-223
- \*Junge, D. 1976. Topographico-cytoarchitectonic studies on the diencephalon of female cattle (*Bos Taurus var domesticus*). *Arch. exp. Vet. Med.* 30: 867-879
- Kappers, C.U.A., Huber, G.C. and Crosby, E.C. 1967. *The Comparative Anatomy of the Nervous System of Vertebrates Including Man*. Hafner Publishing Company, New York, p.1239
- Keith, A. 1947. *Human Embryology and Morphology*. Sixth edition. Williams and Wilkins, Baltimore, p.690
- Khatra, G.S. and Roy, K.S. 1980. A biometrical study on the brain of the Indian buffalo (*Bubalus bubalis*). *J. Res.* 17: 321-325

- \*Kii, S., Uzuka, Y., Taura, Y., Nakaichi, M., Takeuchi, A., Inokuma, H. and Onishi, T. 1997. Magnetic resonance imaging of the lateral ventricles in Beagle-type dogs. *Vet. Radiol. Ultrasound* 38: 430-433
- King, A.S. 1987. *Physiological and Clinical Anatomy of the Domestic Mammals*. Oxford University Press, New York, p.325
- Klekamp, J., Reidel, A., Harper, C. and Kretschmann, H.J. 1987. A quantitative study of Australian Aboriginal and Caucasian brains. *J. Anat.* 150: 191-210
- \*Kotter, B., Kressin, M., Hummel, G. and Goller, H. 1992. Early development and cell differentiation of the nucleus parasympatheticus nervi vagi et glossopharyngei in cattle. Light and electron microscopic observations. *Berl. Munch. tierarztl. Wschr.* 105: 61-66
- Kozlowski, G.P., Scott, D.E. and Murphy, J.A. 1972. Scanning electron microscopy of the lateral ventricles of sheep. *Am. J. Anat.* 135: 561-566
- Kumar, P., Kumar, S. and Singh, Y. 1995a. Topography and histomorphology of pineal gland in young goat. *Indian J. Anim. Sci.* 65: 633-635
- Kumar, P., Kumar, S. and Singh, Y. 1995b. Anatomy of the pineal gland in domestic animals. *Indian J. Vet. Anat.* 7: 1-10
- Kumar, P., Kumar, S. and Singh, Y. 1996. Histochemical studies on the subcommissural organ of goat. *Indian J. Anim. Sci.* 66: 877-880
- Kumar, P., Kumar, S. and Singh, Y. 1997. Microarchitecture of the subcommissural organ of goat. *Indian J. Anim. Sci.* 67: 1036-1039
- Kumar, P., Kumar, S. and Singh, Y. 1998. Histochemical and histoenzymatic studies on the pineal gland of goat. *Indian J. Anim. Sci.* 68: 640-642
- \*Kumar, P., Nagpal, S.K., Kumar, S. and Gupta, A.N. 1999. Histomorphology of the subcommissural organ of camel. *J. Camel Pract. Res.* 6: 311-316



- \*Lakomy, M. 1970. Cytoarchitectonics of the lobus piriformis in the cow. *J. Hirnforsch.* 12: 185-194
- Lalitha, P.S. and Seshadri, V.K. 1986. Studies on the microscopical structure of pineal gland of the Indian buffalo (*Bubalus bubalis*) parenchymal cells. *Cheiron* 15: 37-43
- Langman, J. 1981. *Medical Embryology*. Fourth edition. Williams and Wilkins, Baltimore, p.384
- Larsell, O. 1951. *Anatomy of the Nervous System*. Second edition. Appleton Century Crofts, New York, p.520
- Lavail, J.H. and Wolf, M.K. 1973. Postnatal development of the mouse dentate gyrus in organoleptic cultures of the hippocampal formation. *Am. J. Anat.* 137: 47-66
- \*Lignereux, Y., Regodon, S., Marty, M.H., Franco, A. and Bubein, A. 1991. Encephalic ventricles of the ewe (*Ovis aries*); conformation, relations and stereotaxic topography. *Acta Anat.* 141: 82-84
- \*Lindberg, L.A., Sukura, A. and Talanti, S. 1991. Morphology of the ependymal cells of the bovine area prostroma. *Anat. Histol. Embryol.* 20: 97-100
- \*Louw, G.W. 1989. The development of the bovine cerebral hemispheres. *Anat. Histol. Embryol.* 18: 246-264
- Luna, L.G. 1968. *Manual of Histological Staining Methods of the Armed Forces Institute of Pathology*. Third edition. Mc Graw-Hill Book Company, New York, p.258
- \*Magras, J. and Karamanlidis, A. 1971. Quantitative study of the optic nerve fibres and the extent of decussation in the chiasma of the horse, ox, sheep and pig. *Scient. Yr Bk Vet. Fac. Thessaloniki* 12:181-194
- Malik, M.R., Shrivastava, A.M. and Jain, N.K. 2000. A note on encephalometry of Asian elephant. *Indian J. Vet. Anat.* 12: 103-104

- Malik, M.R., Shrivastava, A.M. and Parmar, M.L. 1978. Cerebral ventricles of goat. *Indian J. Anim. Sci.* 48: 194-197
- Malik, M.R., Taluja, J.S. and Parmar, M.L. 1992. Histogenesis and mode of growth of choroid plexus in goat. *Indian J. Anim. Sci.* 62: 1157-1159
- Malik, M.R., Taluja, J.S., Rao, K.C. and Shrivastava, A. M. 1989. Skull parameters as an index to endocranial volume in goat. *Indian J. Anim. Sci.* 59: 669-671
- Manocha, S.L. and Shantha, T.R. 1969. Enzyme histochemistry of the nervous system. *The Structure and Function of Nervous Tissue.* (ed. Bourne, G.H.). Academic Press, New York, pp.137-193
- Mariappa, D. 1985. *Anatomy and Histology of the Indian Elephant.* Indira Publishing House, USA, p.209
- Mc Ewen, R.S. 1957. *Vertebrate Embryology.* Fourth edition. Henry Holt and Company, New York, p.701
- \*Mc Intosh, G.H., Baghurst, K.I., Potter, B.J. and Helzel, B.S. 1979. Foetal brain development in the sheep. *Neuropath. appl. Neurobiol.* 5: 103-114
- \*Milart, Z. 1964. Morphogenesis of the brain in domestic cattle. II. Mid and forebrain. *Arch. exp. Vet. Med.* 18:1139-1150
- Moliner, R.E. 1960. A statistical analysis of the dendritic distribution in the cerebral cortex of the cat. *Anat. Rec.* 136: 262
- Monteiro, R.A.F. 1983. Do the Purkinje cells have a special type of oligodendrocyte as satellite? *J. Anat.* 137: 71-83
- \*Monterde, J.G., Gonzalez, A.J., Galisteo, A.M. and Aguera, E. 1998. The influence of age, live weight and gender on the morphometrical aspects of the goat brain during early postnatal development. *Acta Vet. Brno.* 67:145-151
- Moore, W.J. 1981. *The Mammalian Skull.* Cambridge University Press, Cambridge, p. 394

- Moore, D.C.P., Stanisstreet, M. and Evans, G.E. 1987. Morphometric analysis of changes in cell shape in the neuroepithelium of mammalian embryos. *J.Anat.* 155: 87-99
- Mori, Y., Takeuchi, Y., Shimada, M., Hayashi, S. and Hoshino, K. 1990. Stereotaxic approach to hypothalamic nuclei of the Shiba goat with radiographic monitoring. *Jap. J. Vet. Sci.* 52: 339-349
- Morse, D.E. and Low, F.N. 1972. The fine structure of the pia mater of the rat. *Am. J. Anat.* 133: 349-368
- \*Moustafa, M.N.K. 1996. Histogenesis of the cerebellar cortex of dog during the prenatal life and suckling period. *Assiut Vet. Med. J.* 35: 22-41
- \*Niespodziewanski, M. 1964. Histochemical activity of non-specific phosphatases in the developing cerebellum of the domestic pig. 1. Cerebellar hemispheres. *Medna Vet.* 19: 1-10
- \*Nin, V.G.H., Donati, O., Echeverria, O., Martinez, D. and Roig, J.A. 1978. Neuronal distribution in caudate nucleus and reticular-caudate pathways. *Brain Res. Bull.* 3: 419-424
- \*Norita, M. 1980. Neurons and Synaptic patterns in the deep layers of superior colliculus of the cat: A Golgi and electron microscopic study. *J. comp. Neurol.* 190: 29-48
- Ommer, P.A., Paily, L., Radakrishnan, K. and Padmanabhan, V. 1971. Convolutions of the cerebral cortex of the Indian buffalo (*Bubalus bubalis*)-a preliminary study. *Kerala J. Vet. Sci.* 2: 25-28
- Padmanabhan, R. and Singh, S. 1982. Postnatal development of the olfactory bulb in rat. *Indian J. Anim. Sci.* 52: 1075-1081
- Paily, L. and Salam, A. 1983. The red nucleus of the buffalo (*Bubalus bubalis*). I. Morphology and cytoarchitecture. *Kerala J. Vet. Sci.* 14: 45-56

- Paily, L. and Salam, A. 1984. The red nucleus of the buffalo (*Bubalus bubalis*). II. Quantitative studies on the neurons. *Kerala J. Vet. Sci.* 15: 61-68
- Pampiglione, G. 1963. *Development of Cerebral Function in the Dog*. Butterworth and Co. Ltd, New York, p.68
- Pannese, E. 1974. *The Histogenesis of the Spinal Ganglia*. Springer-Verlag, New York, p.75
- Paramasivan, S. and Sharma, D.N. 2001. Cytomorphological and cytochemical studies on the neurosecretory cells of the hypothalamus of Gaddi sheep (*Ovis aries*). *Indian J. Vet. Anat.* 13: 62-69
- Parmar, M.L., Malik, M.R. and Taluja, J.S. 2000. Morphometry of the brain and spinal cord of calves. *Indian J. Vet. Anat.* 12: 99-100
- Parmar, M.L., Malik, M.R. Taluja, J.S. and Arora, J.S. 1997. Growth dynamics of head in prenatal goat. *Indian J. Anim. Sci.* 67: 872-873
- Patten, B.D. 1948. *Embryology of the Pig*. Third edition. The Blakiston Company, Philadelphia, p.352
- \*Patterson, D. S. P., Sweasey, D. and Hebert, C.N. 1971. Changes occurring in the chemical composition of the central nervous system during foetal and postnatal development of the sheep. *J. Neurochem.* 18: 2027-2040
- Paula, B.M.M., Amelia, T.M., Ruela, C. and Barroca, H. 1983. The distribution of stellate cell descending axons in the rat cerebellum: a Golgi and a combined Golgi-electron microscopic study. *J. Anat.* 137: 757-764
- Pawar, A. and Ramakrishna, V. 2000. Histology of the pineal gland in the Indian donkey (*Equus asinus*). XV Convention of Indian Association of Veterinary Anatomists and National Symposium on Indispensable Anatomy- A Dispensing Tool in Veterinary Science, 23-25 December 2000. Department of Anatomy, Madras Veterinary College, Chennai. *Abstract*: 46

- Pease, D.C. and Schultz, R.L. 1958. Electron microscopy of rat cranial meninges. *Am. J. Anat.* 102: 301-322
- Perdomo, A.C., Meyer, G. and Torres, R.F. 1985. The early development of the human subcommissural organ. *J. Anat.* 143: 195-200
- Prasad, J. and Sinha, R.D. 1983. Histology and histochemistry of the epi-pineal saccular pia-arachnoid in buffalo. *Indian J. Anim. Sci.* 53: 437-440
- Prasad, J. and Sinha, R.D. 1984. Histological and histochemical study on the pineal and accessory pineal bodies in buffalo. *Indian J. Anim. Sci.* 54: 45-49
- \*Rajtova, V. 1997. Choroid plexus in sheep and goat: a scanning electron microscopic study of the foetuses. *Acta Vet. Brno.* 66: 199-202
- \*Rajtova, V. 1999. The foetal ependyma of cerebral ventricles in sheep and goat. The third cerebral ventricle in the light and scanning electron microscope. *Acta Vet. Brno.* 68: 241-245
- \*Rajtova, V. and Kacmarik, J. 1998. Foetal ependyma in sheep and goat. A scanning electron microscopy study. *Anat. Histol. Embryol.* 27: 131-134
- \*Ramakrishna, V. and Saigal, R.P. 1986. Histomorphology of the subcommissural organ in buffalo (*Bubalus bubalis*). *Acta Vet. Hung.* 34: 3-9
- Ramakrishna, V. and Saigal, R.P. 1987. Carbohydrate, protein and lipid histochemistry of buffalo subcommissural organ. *Indian J. Anim. Sci.* 57: 391-397
- \*Rangelov, P. 1966. Central subcortical nuclei of the telencephalon in pigs. II. The amygdaloid complex. *Nauchni Trud. Vissh. Vet. Med. Inst.* 16: 205-216
- Rao, G.S. 1991. Ovine hippocampus. *Indian J. Anim. Sci.* 61: 168-169
- Rao, G.S. and Sharma, V.K. 1974. Morphological study on the brain of the Indian buffalo (*Bubalus bubalis*) with particular reference to the sulci. *Indian J. Anim. Sci.* 44: 178-182

- Reiter, R.J. 1981. The mammalian pineal gland: structure and function. *Am. J. Anat.* 162: 287-313
- Richard, L. and Angevine, J.B. 1962. Autoradiographic analysis of time of origin of nuclear versus cortical components of mouse telencephalon. *Anat. Rec.* 142: 326-327
- Roy, K.S. and Khatra, G.S. 1982. A biometrical study on the brain of goat (*Capra hircus*). *J. anat. Soc. India.* 31: 91-95
- \*Ruela, C., Matis, L.L., Sorbinho, S. and Paula, B.M.M. 1980. Comparative morphometric study of cerebellar neurons: 2. Purkinje cells. *Acta Anat.* 106: 270-275
- Rugh, R. 1964. *Vertebrate Embryology - The Dynamics of Development.* Harcourt, Brace and World, New York, p. 600
- \*Ruhrig, S., Hummel, G. and Goller, H. 1994. Origin and neurogenesis of the nuclei of the cranial nerve VIII in cattle. *Anat. Histol. Embryol.* 23: 1-11
- \*Ryszard, E. 1979. Cytoarchitectonics of the cortex of the lobus piriformis of the sheep. *Polskie Archwm Wet.* 21: 405-416
- Sadler, T.W. 2004. *Langman's Medical Embryology.* Ninth edition. Lippincott Williams and Wilkins, Philadelphia, p.534
- Saggar, D., Kumar, P., Kumar, S. and Gupta, A.N. 2001. Histology and histochemistry of pineal gland of sheep. *Indian J. Vet. Anat.* 13: 58-61
- Saigal, R.P., Nanda, B.S., Nagpal, S.K. and Roy, K.S. 1976. Epiphysis cerebri of ageing goats. *J. anat. Soc. India.* 25: 51
- \*Salazar, I., Ruiz, P.P., Fernandez, A.P. and Cifuentes, J.M. 1989. The thalamus of the dog: a tridimensional and cytoarchitectonic study. *Anat. Anz.* 169: 101-103

- Sandhu, P.S. and Dhingra, L.D. 1986. Cranial capacity of Indian camel. *Indian J. Anim. Sci.* 56: 870-872
- Sarma, K., Devi, J. and Sarma, P. 2004. Craniometrical studies on the skull of New Zealand White rabbit. *Indian Vet. J.* 81: 179-182
- \*Scala, G., Mirabella, N., Paino, G. and Pelagalli, G.V. 1994. Microvascularization of the lateral ventricle of the goat choroid plexus. *Anat. Histol. Embryol.* 23: 93-101
- Schultz, R.L., Maynard, E.A. and Pease, D.C. 1957. Electron microscopy of neurons and neuroglia of cerebral cortex and corpus callosum. *Am. J. Anat.* 100: 369-408
- \*Sharma, D.N. and Gupta, S.K. 1990. Equine encephalometry. *Centaur* 6: 86-89
- Sharma, D.N., Singh, Y. and Dhingra, L.D. 1978. Arteries of the brain of goat (*Capra hircus*). *Indian J. Anim. Sci.* 48: 187-193
- Shrivastava, A.M., Mehrotra, T.N. and Malik, M.R. 1986. Morphogenesis of cerebellum of goat. *Indian J. Anim. Sci.* 56: 916-919
- Shrivastava, A.M., Mehrotra, T.N. and Malik, M.R. 1987. Morphogenesis of cerebrum in goat. *Indian J. Anim. Sci.* 57: 666-670
- Shrivastava, A.M., Mehrotra, T.N. and Malik, M.R. 1989. Histometry of pia mater in foetal goat. *Indian J. Anim. Sci.* 59: 951-952
- Shuangshoti, S. and Netsky, M.G. 1966. Histogenesis of choroid plexus in man. *Am. J. Anat.* 118: 283-316
- Singh, Y. and Dhingra, L.D. 1978. Morphogenesis of the hypophyseal meninges in goat. *Indian J. Anim. Sci.* 48: 741-745
- Singh, Y. and Dhingra, L.D. 1979. Morphogenesis of the hypophysis cerebri in goat. 4. Pars distalis and pars infundibularis adenohypophysis. *Indian J. Anim. Sci.* 49: 1057-1075

- Singh, Y. Sharma, D.N. and Dhingra, L.D. 1979. Morphogenesis of the testis in goat. *Indian J. Anim. Sci.* 49: 925-931
- Singh, U.B. and Sulochana, S. 1996. *Handbook of Histological and Histochemical Techniques*. Premier Publishing House, Hyderabad, p.111
- Sinha, B.P. 1970. Cytoarchitectonic and ontogenic study of the occipital lobe of puppy less than a month old. *J. anat. Soc. India.* 19: 67-70
- Smart, I.H.M. 1982. Development of cerebral convolutions in the ferret. *J. Anat.* 135: 844
- Smart, I.H.M. 1985. Differential growth of the cell production systems in the lateral wall of the developing mouse telencephalon. *J. Anat.* 141: 219-229
- Smart, I.H.M. and Mc Sherry, G.M. 1986. Gyrus formation in the cerebral cortex in the ferret. 1. Description of the external changes. *J. Anat.* 146: 141-152
- Smith, K.R. 1960. An electron microscopic study of maturation of the cerebellar cortex of the rabbit. *Anat. Rec.* 136: 280
- Smith, D.E. and Downs, I. 1978. Postnatal development of the granule cell in the kitten cerebellum. *Am. J. Anat.* 151: 527-538
- Smith, B.A. and Jansen, G.R. 1977. Brain development in the feline. *Nutr. Rep. int.* 16: 487-495
- Smuts, M.M.S. and Bezuidenhout, A.J. 1987. *Anatomy of the Dromedary*. Clarendon Press, Oxford, p.188
- Snedocor, G.W. and Cochran, W.G. 1985. *Statistical Methods*. Seventh edition. The Iowa State University Press, USA, p. 313
- Spiroff, B.E.N. 1958. Embryonic and post-hatching development of the pineal body of the domestic fowl. *Am. J. Anat.* 103: 375-401
- Stanley, J. 1968. The molecular layer of the sensimotor cortex of the albino rat. *Anat. Rec.* 160: 371



- \*Steinbach, W., Hummel, G. and Goller, H. 1980. Light and electron microscopical studies of the cerebellar cortex in cattle, sheep and goat. *Anat. Anz.* 147: 354-370
- \*Stormer, R., Hummel, G., Hild, A. and Goller, H. 1985. Structure of the parasympathetic nucleus of the ninth and tenth cranial nerves in sheep and goat. *Tierarztl. Umsch.* 40: 904-907
- Stromston, F.A. 1947. *Davison's Mammalian Anatomy with Special Reference to the Cat*. Seventh edition. The Blakiston Company, Philadelphia, p.387
- Sturrock, R.R. 1979. A morphological study of the development of the mouse choroid plexus. *J. Anat.* 129: 777-793
- Sturrock, R.R. 1988. An ultrastructural study of the development of the leptomeningeal macrophages in the mouse and rabbit. *J. Anat.* 156: 207-215
- \*Szalak, M. and Stefan, H. 1977. Tectum mesencephali of the wild boar (*Sus scrofa*). *Polskie Archwm Wet.* 20: 165-172
- Takeda, H., Nakamura, K. and Yamadori, T. 1960. Comparative anatomical study of the cerebellum. *Anat. Rec.* 136:288
- Talanti, S. 1959. Studies on the subcommissural organ of the bovine foetus. *Anat. Rec.* 134: 473-490
- Tam, P.P.L. and Kwong, W.H. 1987. A study on the pattern of alkaline phosphatase activity correlated with observations on silver impregnated structures in the developing mouse brain. *J. Anat.* 150: 169-180
- Tanaka, D. and Alexander, B. 1978. An electron microscopic study of the caudate nucleus in the neonatal dog. *Anat. Rec.* 190: 623-624
- Todd, P.H. 1982. Gross morphology and the geometry of cell production in the early development of the mouse cerebral vesicle. *J. Anat.* 135: 830

- \*Towe, A.L. and Mann, M.D. 1992a. Brain size to body length relations among myomorph rodents. *Brain Behav. Evolut.* 39: 17-23
- \*Towe, A.L. and Mann, M.D. 1992b. Relation between brain and body growth in allied rats. *Growth Dev. Agg.* 56: 159-166
- \*Trautwein, M., Krueger, N., Urban, K. and Trautwein, G. 1994. Immunohistochemical localization of glial and neuronal cell markers in the developing bovine brain. *Anat. Histol. Embryol.* 23: 154-165
- Trautwein, M. and Schulthesis, G. 1994. Lecithin labelling of amoeboid and ramified microglial cells in the telencephalon of ovine foetuses with the B4 isolectin from *Griffonia simplicifolia*. *J. comp. Path.* 111: 21-31
- \*Trautwein, M., Schulthesis, G. and Trautwein, G. 1996. Demonstration of amoeboid and ramified microglial cells in pre- and postnatal bovine brains by lectin histochemistry. *Ann. Anat.* 178: 25-31
- Trenouth, M.J. 1984. Shape changes during human foetal craniofacial growth. *J. Anat.* 139: 639-651
- Truex, R.C. and Carpenter, M.B. 1969. *Human Neuroanatomy*. Sixth edition. The Williams and Wilkins, Baltimore, p.673
- Tumbleson, M.E. 1973. Brain weight, as a function of age in miniature swine. *Growth* 37: 13-17
- \*Turley, S.D., Burns, D.K., Rosenfield, C.R. and Dietschy, J.M. 1996. Brain does not utilize low-density lipoprotein-cholesterol during foetal and neonatal development in the sheep. *J. Lipid Res.* 37: 1953-1961
- Ulinski, P.S. 1997. Vertebrate nervous system. *Comparative Physiology* (ed. Dantzler, W.H.). Oxford University Press, New York, pp.17-30
- \*Urban, K. Trautwein, M. and Trautwein, G. 1997. Development of myelination in the bovine foetal brain: an immunohistochemical study. *Anat. Histol. Embryol.* 26: 187-192

- \*Victor, F., Bravo, H., Kuljis, R. and Fuentes, I. 1979. Autoradiographic study of the development of the neostriatum in the rabbit. *Brain Behav. Evolut.* 16: 113-128
- Vyas, K.N. and Nanda, B.S. 1984. Quantitative distribution of the lipofuscin (ageing) pigment in the brain cortices and ventral spinal root horn of the ageing goat (*Capra hircus*). *Indian Vet. J.* 61: 750-756
- \*Wenisch, S., Jost, K. and Hummel, G. 1997. Morphology and histology of the colliculus rostrales in cattle. *Anat. Histol. Embryol.* 26: 281-287
- Wischnitzer, S. 1975. *Atlas and Laboratory Guide for Vertebrate Embryology*. McGraw-Hill Book Company, New York, p. 157
- Wischnitzer, S. 1993. *Atlas and Dissection Guide for Comparative Anatomy*. W.H. Freeman and Company, New York, p. 157
- Worthington, W.C. and Cathcart, R.S. 1963. Ependymal cilia: Distribution and activity in the adult human brain. *Science* 139: 221-222
- \*Yeh, L.S., Guang, L.D., Xing, L.H. and Fa, T.S. 1981. Anatomy of the central nervous system of the Chinese buffalo. I. A macroscopic study on the cerebrum with special reference to the sulci and gyri. *J. South China agric. Coll.* 2: 45-56
- \*Yeh, L.S., Guang, L.D., Xing, L.H. and Fa, T.S. 1982. Anatomy of the central nervous system of the Chinese buffalo. II. A macroscopic study on the cerebellum and brainstem. *J. South China agric. Coll.* 3: 70-82
- Young, R.W. 1959. The influence of cranial contents on postnatal growth of the skull in the rat. *Am. J. Anat.* 105: 383-415
- \*Originals not consulted

**PRENATAL DEVELOPMENT OF BRAIN  
IN GOATS (*Capra hircus*)**

By  
**K. M. LUCY**

**Abstract of the thesis submitted in partial fulfilment of the  
requirement for the degree of**

**Doctor of Philosophy  
in  
Veterinary Anatomy**

**Faculty of Veterinary and Animal Sciences  
Kerala Agricultural University, Thrissur**

**2005**

**Department of Anatomy  
COLLEGE OF VETERINARY AND ANIMAL SCIENCES  
MANNUTHY, THRISSUR-680651  
KERALA, INDIA**

## ABSTRACT

Studies on the prenatal development of brain in goats were conducted using 52 foetuses of varying gestational ages ranging from 24 days of gestation (1.4cm CRL) to full term (41.5cm CRL). The project was undertaken to trace the developmental pattern of brain and its relationship with age, body weight, cranial size and other body parameters. After recording the body measurements and craniometry, the material was fixed in 10 percent neutral buffered formalin. Then the encephalometry was recorded and standard procedures were adopted for histoarchitectural and histochemical studies.

At 24 days, dilated cephalic end of the neural tube showed the five brain vesicles, viz., telencephalon, diencephalon, mesencephalon, metencephalon and myelencephalon. Histologically, wall of the neural tube showed an inner ependymal, middle mantle and outer marginal layers bounded by the inner and outer limiting membranes. The thickest inner ependymal layer was composed of proliferating neuroepithelial cells that gave rise to the neuroblasts and spongioblasts.

All the head parameters showed a greater increase during early gestation but the encephalometric parameters showed a spurt in growth during terminal stages which explains the highly convoluted pattern of cerebral and cerebellar cortices. Cephalic region of head grew faster than the face. Cartilaginous cranial vault developed by 40 days and boundaries of skull bones could be identified by 54 days. A highly significant positive correlation existed among brain length and medial length of frontal and parietal bones. Among the body parameters, maximum correlation was noticed between the body weight and brain weight and also between the brain weight and total body length. Regression equations were derived from significantly correlated brain and body parameters that could be used to predict brain parameters during gestation from known body parameters of the foetus. Thus one can assess the normal growth rate of brain and cases of hypoplasia and other disorders. Contributions of cerebral hemispheres and cerebellum to the total brain weight showed a sharp and steady increase indicating a gradual "cephalic shift" of function from phylogenetically older brainstem to the higher cerebral and cerebellar cortices. Right cerebral hemisphere was slightly heavier (0.88 percent) than the left one.

During second month, surface of the cerebral hemisphere was almost smooth. By 69 days, gyri and sulci started developing and at the beginning of fifth month, most of them appeared. By term, the cerebral surface attained adult pattern. Histologically, towards the middle of second month, neuroblasts and spongioblasts of the inner ependymal layer of the cerebral wall migrated outwards giving rise to a superficial gray cortex. By 76 days, the cortex revealed four layers, viz., outer molecular, superficial granular, intermediate granular and deep granular layers. Cortical migration came to an end by about 12 weeks of gestation and the cells were undergoing differentiation during the fourth month. During the fifth month, the neocortex was divided into six layers. Cortex was thicker at the top of the gyrus and the mean thickness decreased from fourth to fifth month leading to a better vascularisation of the cortical tissue by the pial vessels. Hippocampus appeared at 48 days and was well developed towards term. Basal nuclei started developing by 40 days and all the components developed as a distinct entity towards term.

Cerebellum developed from rhombic lips of the roof of the metencephalon and formed the midline vermis and two lateral hemispheres by 48 days. Folia started developing at 62 days and by 101 days of age, six lobules were identified. By 124 days, all the nine classical lobules appeared. During the seventh week, the external granular layer unique to the foetal cerebellum appeared. Neurons of the deep cerebellar nuclei were visible by 48 days. Primitive Purkinje cells, the internal granular layer and the white matter started differentiating towards the end of second month. All the layers were well developed during the fifth month and the external granular layer became very thin by term indicating the functional maturity.

Cellular aggregations, the nuclei, first appeared in diencephalon during seventh week. Pineal body, optic chiasma, infundibulum and subcommissural organ developed during the same period. Mesencephalon showed tectum, tegmentum and crura cerebri by 48 days. Reticular formation of the tegmentum and multipolar neurons of the red nucleus appeared during seventh week. Basal plate of metencephalon developed into the pons, which showed motor nuclei of origin for cranial nerves V, VI and VII and the pontine nuclei at 48 days. During fifth month, pons was divided into tegmental and basilar parts.

By 40 days of gestation, the roof plate of rhombencephalon expanded enormously and as a result the entire alar and basal plates were displaced laterally and

ventrally. The main difference of the medulla oblongata from the spinal cord was that a sharp demarcation between the gray and white substances disappeared in this region. Nuclei appeared at 48 days and nerve fibres crossing in different directions broke up the gray substance into a mixture of gray and white known as the reticular formation.

The dilated cavities of the brain vesicles were the forerunners of the ventricular system. Lateral ventricles appeared as a distinct entity by 27 days and extended into lobes of cerebral hemispheres at 48 days. The roof of third ventricle was triangular and wide. The three recesses of third ventricle were evident from the second month. Cavity of hindbrain expanded to the sides to form the fourth ventricle at 40 days and communicated with the subarachnoid space by the foramina of Luschka. Choroid plexus first appeared in brain ventricles at 40 days.

Primitive neurons could be clearly distinguished from spongioblasts at 40 days. Nissl granules appeared in some neurons by the middle of fourth month and towards term, most neurons showed Nissl granules. Astrocytes and oligodendrocytes started differentiating by 58 days but the microglia appeared at 76 days. Ependyma developed cilia on their luminal surface in the second month. Pia mater started differentiating by 24 days, dura by 40 days and the arachnoid by 48 days of age.

Histochemical studies revealed that the myelination began in the foetal brain during third month. In the fifth month, most of the fibres were myelinated. Glycogen could be demonstrated in the neurons, ependyma, astrocytes and choroid plexus epithelium. Alkaline phosphatase reaction was noticed in the outer plexiform layer of cerebral cortex, white matter, hypothalamus, blood vessels, choroid plexus, pia-arachnoid and ependyma. In general, acid phosphatase activity was less pronounced in the foetal brain.